Structural and functional mapping of the vertebrate centromere

Susana Abreu Ribeiro

A thesis presented for the degree of Doctor of Philosophy

University of Edinburgh | April 2010

Declaration

I hereby declare that this thesis is composed entirely by myself and that the work presented in it is my own, except where explicitly stated otherwise.

Susana Abreu Ribeiro

May 10, 2010

ACKNOWLEDGMENTS

I would like to express my gratitude to Professor Kenneth Murray and the Darwin Trust of Edinburgh for the generous funding that I received.

I thank:

My supervisor, Bill Earnshaw, for all the support through the years and for giving me the opportunity to pursue my research interests. Thanks for all the freedom and opportunities to broaden my horizons. Thanks for telling me to walk on my own! It made me believe (a bit more) in myself.

Paola Vagnarelli for being a great mentor. I will never forget your enthusiasm and dedication to science. I am deeply indebt for all that you have taught me. Above all, thanks for the friendship, kindness and patience.

Cristina Flors for the great project that we built up together. It was very enjoyable to learn and work with you. This collaboration, for me, was also a life-long seeded friendship.

All present lab members of the Earnshaw group for making work in the lab pleasant: Mar Carmena, Melpi Platani, Kumiko Samejima, Hiromi Ogawa, Jan Bergman, Shinya Ohta, Laura Wood, Diana Papini, Zhenjie Xu. Also to past members, especially Mafalda Tadeu, Daniel Roth and Tina Freisinger but also to Fiona MacIsaac, Sandrine Ruchaud, Gonzalo Fernandez Miranda, Damien Hudson, ZuoJun Yue, Sasha Ageichick and Stefano Cardinale for help and support.

A special thanks to the following people, who were directly involved in the work presented in this thesis, for their help and support throughout, and invaluable contribution: Paola, Cristina, Hiromi, Kumiko, Melpi, Laura, Mar and Allison Pidoux.

Ted Salmon for the great time I spent in your lab. I am deeply grateful. It was an honor to work with you. Thanks for letting me participate and understand how Science can be fundamentally great and how discussion can be fruitful. Thanks to everyone in his lab: Jay Gatlin, Ajit Joglekar, Tom Maresca and Lisa Cameron.

The Physiology Course 2008! A special thanks to the directors: Tim Mitchison and Ron Vale and to everyone that I met there! Impossible to explain how important these 7 weeks were for me! This was the most rewarding experience of my life. Thank you all.

Ron Vale for the incredible experience that I had working in your lab. Thanks to all the Vale lab members, especially Eric Griffis, Sabine Petry, Sarah Goodwin, John James and Thomas Huckaba.

The portuguese mafia: Ana, Ricardo, Claudia and Vanessa - thanks for being my family in Edinburgh!

To the friends that I made here and will never forget: Alessia, Jan, Alba, Erwan, Nathalie, Thomas, Mafalda, Ricardo, Ana, Claudia, Bruno, Cristina Flors, Tina, Daniel Roth, Gonzalo, Sasha, Nadia, Dave Kelly, Paola & Arthur, Mar, Melpi.

To my friends in Portugal, Carla and Rui for never forgetting my existence, even when I am barely present, and for always supporting my wildest dreams! Also to Joana Prata, Mafalda, Isabel, Sofia, Toni, Paula and Silvia thanks for all the great moments and support!

To Martin… A special Thanks to a special Friend. I am glad that our paths crossed!

To Claudia! Difficult to write down this list… too long! THANKS! You made this lovely (or awesome)! Many thanks! (One day we will say: "When I was in grad school…").

To my brothers: Milo, obrigada por me ouvires, por me chamares a atenção e por seres um apoio como mais ninguém. Petuca, obrigada pelo suporte, por me entenderes e apoiares. Paulo, obrigada por servires de exemplo de luta, e por engrandeceres os meus parcos achievements! Aos meus sobrinhos: Pedro, João, Kiko, António, Carlota, Ângela e Zé mesmo sem se aperceberem vocês deram-me muita força!

Last but not the least… Aos meus pais! Obrigada por TUDO. Por ser quem sou, por me apoiarem, por me darem sábios conselhos, por me tentarem entender, por me ajudarem sempre e sem questionar, neste percurso!

PUBLICATIONS

The work presented in this dissertation has led to the following publications:

1 | Ribeiro SA, Gatlin JC, Dong Y, Joglekar A, Cameron L, Hudson DF, Farr CJ, McEwen BF, Salmon ED, Earnshaw WC, Vagnarelli P. Condensin regulates the stiffness of vertebrate centromeres. Mol Biol Cell. 2009 May; 20(9): 2371-80.

2 | Vagnarelli P, Ribeiro SA, Earnshaw WC. Centromeres: old tales and new tools. FEBS Lett. 2008 Jun 18; 582(14): 1950-9. Epub 2008 Apr 22.

3 | Vagnarelli P, Hudson DF, Ribeiro SA, Trinkle-Mulcahy L, Spence JM, Lai F, Farr CJ, Lamond AI, Earnshaw WC. (2006) Condensin and Repo-Man-PP1 co-operate in the regulation of chromosome architecture during mitosis. Nat Cell Biol, 8(10): 1133-42.

4 | Ribeiro SA, Vagnarelli P, Dong Y, Hori T, McEwen BF, Fukagawa T, Flors C, Earnshaw WC. A super-resolution map of the vertebrate centromere. PNAS (accepted).

TABLE OF CONTENTS

I. Abstract

ABSTRACT

Mitosis is the shortest phase of the cell cycle but visually the most outstanding. The key goal of mitosis is to accurately drive chromosome segregation. On one hand, DNA has to be condensed into characteristically shaped chromosomes. On the other hand, a very specialized structure needs to be built to conduct segregation, the mitotic spindle which is composed of microtubules organized into an antiparallel array between the two poles. The interaction between microtubules and chromosomes occurs at the kinetochore, a macromolecular complex assembled in mitosis at the centromere. The centromere/kinetochore monitors proper spindle microtubule attachment to each of the chromosomes, aligning them at the metaphase plate and also ensuring that chromosome segregation happens in perfect synchrony. Although centromeres are present in all eukaryotes, their basic structure and chromatin folding are still poorly understood.

One of the aims of my work was to understand the function of the condensin complex specifically at the centromere during mitosis. Condensin I and II are pentameric protein complexes that are among the most abundant components of mitotic chromosomes. I have shown that condensin is important to confer stiffness to the inner-centromeric chromatin once spindle microtubules interact with kinetochores in metaphase. Labile inner-centromeric regions delay mitotic progression by altering microtubule-kinetochore attachments and/or dynamics with a consequent increase in levels of Mad2 checkpoint protein bound to kinetochores. In the absence of condensin, kinetochores perform prominent “excursions” toward the poles trailing behind a thin thread of chromatin. These excursions are reversible suggesting that the centromeric chromatin behaves like an elastic polymer.

During these excursions I noticed that only the inner centromeric chromatin was subjected to reversible deformations while the kinetochores (inner and outer plates) remained mostly unaltered. This suggested that the centromeric chromatin part of the inner kinetochore plate was organised differently from the subjacent chromatin. I went on to investigate how the centromeric chromatin is organised within the inner kinetochore domain.

Super-resolution analyses of artificially unfolded centromeric chromatin revealed novel details of the vertebrate inner kinetochore domain. All together, the data allowed me to propose a new model for the centromeric chromatin folding: CENP-A domains are interspersed with H3 domains arranged in a linear segment that forms planar sinusoidal waves distributed in several layers. Both CENP-A and H3 arrays face the external surface, building a platform for CCAN proteins. CENP-C binds to more internal CENP-A blocks thereby crosslinking the layers. This organization of the chromatin explains the localisation and similar compliant behaviour that CENP-A and CENP-C showed when kinetochores come under tension. Other kinetochore proteins (the KMN complex) assemble in mitosis on top of the CCAN and bind microtubules. KMN binding may confer an extra degree of stability to the kinetochore by crosslinking CENP-C either directly or indirectly.

My work and the testable model that I have developed for kinetochore organization provide a fundamental advance in our understanding of this specialized chromosomal substructure.

II. INTRODUCTION

1. The Cell cycle

Cell division is a universal process performed by all multiplying cells. From a simplistic view, four events must be completed: cell growth, DNA replication, chromosome segregation into two identical sets, and cell division. In the eukaryotic cell cycle, these events reside in one of two fundamental parts: interphase, which spans the greater part of the cell cycle, and mitosis, which is very short and ends with the division of the cell. From here, the cell cycle can be further divided into four discrete phases (Fig. 1).

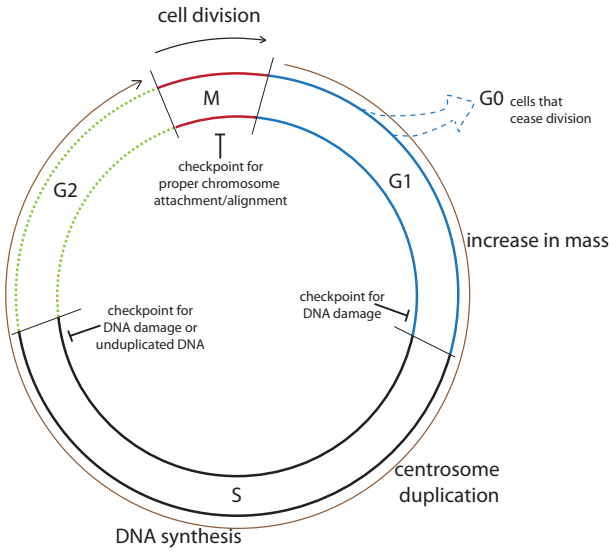

Figure 1 | Eukaryotic cell cycle diagram. Each phase (represented by a different color) has a different length reflecting the relative duration. Checkpoints operating in each phase are indicated. Interphase that comprises G1, S and G2 is shown in brown.

In the middle of interphase, DNA synthesis takes place in S phase where it is preceded by a gap termed G1 and followed by a second gap, G2. Subsequently, G2 cells proceed to M phase, otherwise known as mitosis (Murray and Hunt, 1993). In some situations there is a phase known as G0 where cells can exit the cell cycle from G1 and enter a quiescent state. However, when certain conditions are met, cells may return to G1 and proceed through the cell cycle.

The cell cycle is unidirectional, spatially ordered and tightly regulated. These features are maintained through two key classes of cell cycle regulators: cyclins and cyclin-dependent-kinases (CDKs). Cyclins form the accessory subunits, while CDKs comprise the catalytic subunits of the activated heterodimer. Although cyclins have no catalytic activity, CDKs remain in an inactive state in the absence of a partner cyclin (Evans et al., 1983; Lohka et al., 1988; Nash et al., 1988; Hadwiger et al., 1989). This is important as

CDKs are constitutively expressed in cells, whereas distinct cyclins are synthesised at specific stages of the cell cycle in response to various molecular signals, and destroyed by ubiquitin-mediated proteolysis (Glotzer et al., 1991; Hershko and Ciechanover, 1998). For example, there are cyclins associated with G1 (cyclin D), S phase (cyclins E and A) and mitosis (cyclin B and A). Temporal activation through this mechanism is therefore able to promote directionality and drive cell cycle progression in an irreversible manner.

A key regulator of the eukaryotic cell cycle is the APC/C (anaphase promoting complex/cyclosome). APC/C is a multibunit E3 ubiquitin ligase that targets proteins for proteasome mediated destruction by attaching polyubiquitin chains to them. APC/C is essential to separate sister chromatids in anaphase, for exit from mitosis and division into two daughter cells, and to initiate the steps that are necessary for DNA replication later in S phase (Peters, 2006). APC/C was initially discovered as an ubiquitin ligase essential to degrad cyclins in mitosis (Irniger et al., 1995; King et al., 1995; Sudakin et al., 1995). APC/C activity is strictly dependent on one of several co-activator proteins that associate with APC/C during specific periods of the cell cycle. The best studied of these are Cdc20 and Cdh1 (Visintin et al., 1997; Fang et al., 1998). APC/C^{Cdc20} is thought to be assembled in prophase and initiates the degradation of cyclin A already in prometaphase. Proteolysis of cyclin B and the separase inhibitor securin also depends on APC/C^{Cdc20} but is delayed until metaphase by the spindle-assembly checkpoint (SAC). During anaphase and telophase, APC^{Cdh1} is activated, contributes to the degradation of securin and cyclin B, and mediates the destruction of additional substrates such as Polo-like kinase-1 (Plk1) and Cdc20, which leads to the inactivation of APC/C^{Cdc20}. In G1 phase, APC/C^{Cdh1} mediates the destruction of the ubiquitin conjugating (E2) enzyme UBCH10, and thereby allows for the accumulation of cyclin A, which contributes to the inactivation of APC/C^{Cdh1} at the transition from G1 to S phase. This inactivation is essential for the accumulation of APC/C substrates such as cyclins that are required for the initiation of DNA replication in S phase.

To further ensure that cell cycle events progress in the correct order and coordinate with cell cycle progression, the cell has developed a series of checkpoint controls. In interphase, the DNA damage and replication checkpoints ensure DNA repair and full genome replication are complete before entering mitosis (Painter and Young, 1980; Weinert and Hartwell, 1988). In mitosis, however, the spindle assembly checkpoint ensures the fidelity of chromosome segregation. This is achieved by delaying anaphase

onset until all chromosomes are properly attached to spindle microtubules (Sluder, 1979; Sluder and Begg, 1983; Rieder et al., 1995).

2. Mitosis

During the cell cycle, highly impressive morphological changes take place when the cell separates its duplicated genome and divides into two cells. Not surprisingly this process has fascinated cell biologists for more than a hundred years. Until 1970 the main approach used to study mitosis was based on light microscopy observations and descriptive analysis. Supported by these early observations, mitosis was divided into six stages (Fig. 2): prophase, prometaphase, metaphase, anaphase, telophase and cytokinesis.

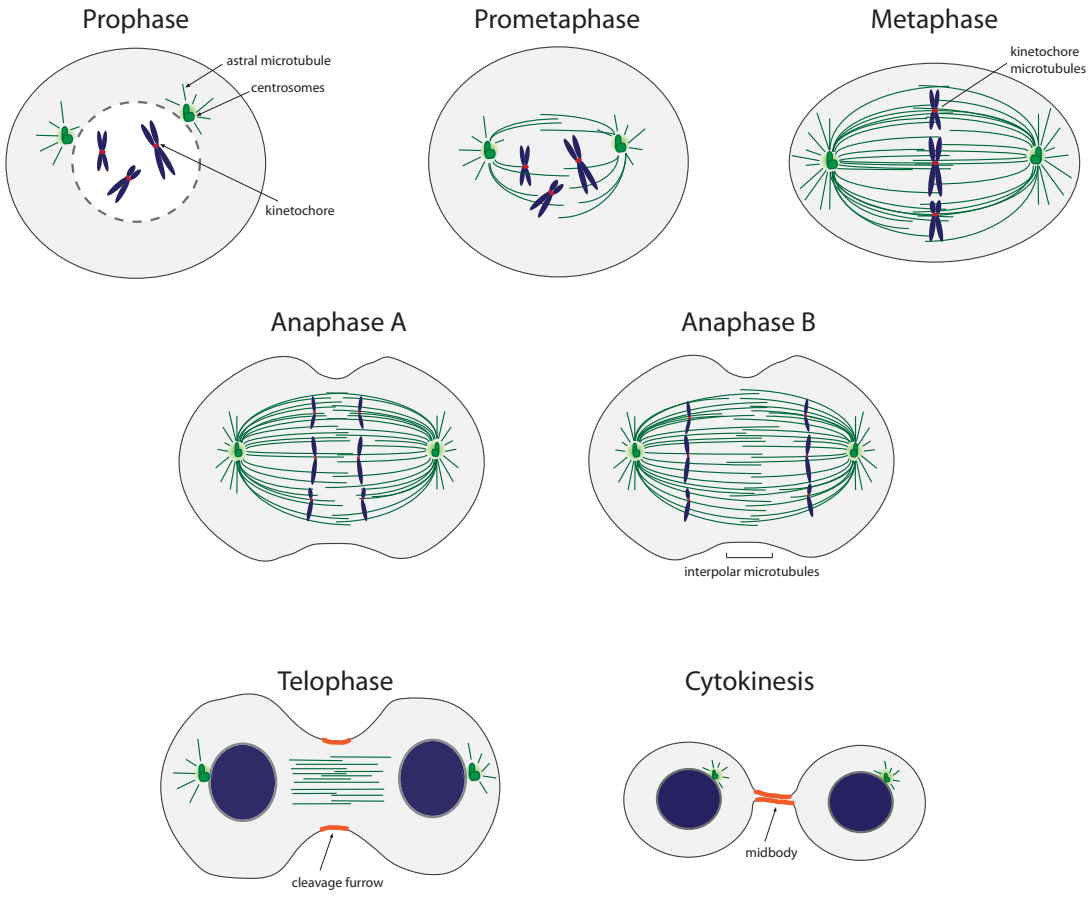

Figure 2 | Schematic representation of mitotic phases. The major morphological changes involve DNA (in blue) and microtubules (in green).

In prophase, chromatin starts condensing, the nucleoli disassemble and nuclear permeability changes along with nuclear pore disassembly. Importantly, chromosomes condense into distinct paired chromatids. These are termed sister chromatids and are held together by cohesin. In the cytoplasm, the extensive microtubule network re-organises into two radial arrays of short filaments surrounding each centrosome. Nuclear envelope breakdown finally defines the transition into prometaphase, during which microtubules grow from the centrosomes and a bipolar microtubule-based spindle assembles. Microtubules then start attaching to the kinetochores, which form a laminar structure on the surface of the centromeric region of each chromatid. The attachment of each sister kinetochore to microtubules emanating from opposing spindle poles ultimately leads to the alignment of all chromosomes along the middle of the spindle; defining the metaphase plate and metaphase itself. This is a very dynamic stage that results in several different types of microtubule-kinetochore attachments: amphitelic, monotelic, merotelic and syntelic attachments (detailed discussed in section 3.4.3). To proofread these attachments, (i.e., sister kinetochore attachment to microtubules from opposite poles) the spindle checkpoint is active, and only once it has been satisfied will anaphase initiate. In the first stage of anaphase (also designated anaphase A) cleavage of cohesin allows sister chromatids to separate. Sister chromatids are then pulled apart by shortening kinetochore microtubules and move toward the respective pole to which they are attached. Next, in anaphase B, the interpolar microtubules elongate, pulling the centrosomes to opposite ends of the cell, leading to an increase in the distance between the poles. In telophase, the nuclear envelope re-forms around the two masses of separated sister chromatids, which have already begun the process of decondensation. The cleavage furrow formed during cytokinesis then constricts the plasma membrane between the two nuclei, and the mitotic cell is finally divided into two daughter cells. In this process, the contraction of the cleavage furrow reduces the cytoplasm between the two daughter cells, enabling a thin intercellular bridge to form. This structure is designated the midbody and contains a dense array of microtubules. Eventually, the intercellular bridge must break to allow the two daughter cells to separate (Pollard and Earnshaw, 2007).

3. The Mitotic apparatus

3.1 Mitotic chromosome condensation

Condensation of mitotic chromosomes is essential for the successful segregation of sister chromatids during anaphase onset. One reason for this is that chromosomes must be significantly shorter than the distance that separates the spindle poles, otherwise they would extend to the middle of the cell and be cut during cytokinesis. Yet, chromosome condensation is not simply a linear compaction of DNA. One of the most important functions of condensation is to organize chromatin fibers so that tangles between sister chromatids, or different chromosomes, are effectively removed before anaphase (Holm et al., 1989; Holm, 1994).

In higher eukaryotic cells, chromosome condensation leads to a ~10,000 to 20,000-fold compaction of chromatin up to the metaphase stage. More importantly, the reorganization of the chromatin that occurs from interphase to mitosis and result in recognizable and distinct chromosomes is a long-standing question. Although condensed chromosomes were observed more than a century ago, the molecular basis driving chromosome condensation is still poorly understood. It has, however, been well established that double stranded DNA wraps around a set of four basic proteins called histones (H2A, H2B, H3 and H4). These proteins assemble into an octameric complex (2 copies of each histone) (Luger et al., 1997) and when found in association with DNA a structure designated the nucleosome is formed. In addition to the core histones, chromatin also contains linker histones (such as Histone H1), which bind to nucleosomes. Thus, the basic unit of chromatin is considered to be the nucleosome array. There are two classical models that describe mitotic chromosome structure: the hierarchical folding model and the radial loop (or scaffold) model. More recently a third model was proposed – a network model (Fig. 3).

In the hierarchical folding model it has been proposed that compaction is achieved through at least three levels of chromatin folding. Here, the coiling of 165 bp of DNA around the basic histone octamer generates nucleosomes and constitutes the first level of compaction. This, together with the folding of regularly spaced nucleosomes into ~30 nm chromatin fibers, accounts for a ~40:1 compaction ratio. Finally, these 10- and 30-nm chromatin fibers are postulated to fold progressively into larger fibers that coil to form the metaphase chromosomes. This event accounts for a ~500-fold compaction, where

DNA-DNA interactions and protein-DNA interactions between neighbouring fibers potentially play important roles (Sedat and Manuelidis, 1978; Zatsepina et al., 1983; Belmont et al., 1987; Belmont and Bruce, 1994).

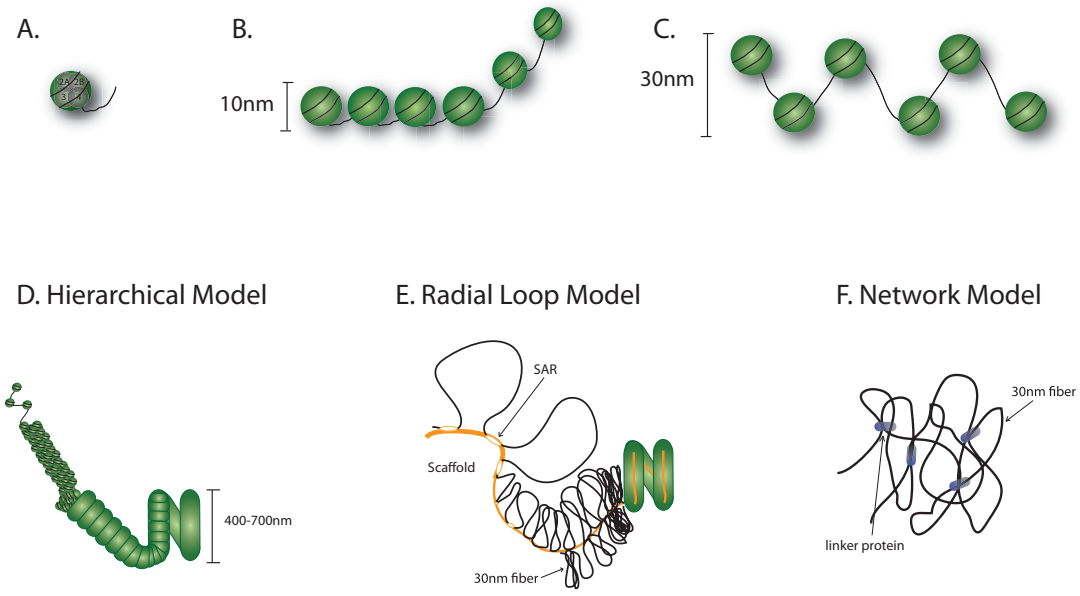

Figure 3 | Different models for mitotic chromosome condensation. A. The basic block of chromatin - nucleosome array, composed by the core histones (2 copies of each H2A, H2B, H3 and H4) arranged in an octamer **B.** The nucleosome fiber is the basic unit of chromatin and consists of double-stranded DNA (in black) wrapped around a histone octamer (green sphere), leading to a 6-7 fold compaction. **C.** The chromatin fiber, corresponds to another 6-7 fold compaction and is formed by folding of the 10nm fiber into a solenid, zig-zag or crossed fiber. **D.** Hierarchical folding model, the 30nm fibers is folded and/or coiled into a higher-order structure that can fold into larger structures. **E.** Radial loop model, folding of the chromatin into loops mediated by proteins in the chromosome scaffold (orange line) and SARs (scaffold attachemnt regions - white oval). **F.** Network model proposes that shape, structural and mechanical properties depend on DNA integrity. The 30-nm fiber (black lines) form a network-type structure held by proteins that crosslink chromatin originating chromatin higher-order structure (adapted from Swedlow and Hirano, 2003; Poirier and Marko, 2002).

The radial loop model, by comparison, is based on earlier studies which showed that histone-depleted chromosomes retain the shape of a highly expanded chromosome with a halo of DNA loops 50-100 Kb in length surrounding a chromosome-shaped substructure designated the scaffold (Paulson and Laemmli, 1977; Laemmli et al., 1978). The radial loop model postulates that chromatin folding above the level of the 30-nm chromatin fiber is guided by non-histone scaffold proteins which form interactions with specific DNA sequences. The original model hypothesised that an interconnected protein structure may exist (Mirkovitch et al., 1984); however, subsequent electron microscopy observations in which topoisomerase II was shown to localize to discrete foci in

hypotonically swollen chromosomes, suggested that regions of scaffold proteins could function by anchoring local clusters of radial loops (Earnshaw and Heck, 1985).

Meanwhile, a third model was proposed based on micromanipulation of chromosomes. The network model suggests that mitotic chromosome integrity is dependent on the DNA itself as nuclease treatment leads to changes in the mechanical properties of chromosomes, arguing against a primary structural role for a contiguous protein scaffold network embedded within the chromosome (Poirier and Marko, 2002). Also, mechanical stretching experiments revealed that elastic extension of metaphase chromosomes to several times their normal length does not result in obvious changes in diameter, or to the sequential uncoiling of different folding levels; as would be predicted in hierarchical model (Poirier et al., 2000). This model proposes that chromosomes are best described as a polymer-network that crosslinks 30-nm fibers. Nevertheless, these experiments do not rule out the possibility that a dynamic protein assembly could drive chromatin folding of chromosomes into a defined shape. Nor do they yet distinguish between a network model in which rare, specific protein crosslinks are used, from a model where chromosomes are held together by distributed chromatin fiber–fiber interactions (Belmont, 2002).

The different approaches, and the data described for the three models, demonstrate the complex nature of this subject. Both biological and biophysical approaches have revealed several key pieces of information that need to be taken in account when trying to establish a model that must integrate various parameters. In theory, the mechanisms regulating chromatin condensation *per se* might be different from the one leading to chromatin architecture; or molecular requirements for chromatin elasticity and integrity might be different than the requirements for chromatin compaction.

3.1.1 Condensin role in chromosome condensation

Two major protein components of the non-histone fraction of chromosomes were designated ScI and ScII (Lewis and Laemmli, 1982). Later, ScI was identified as Topoisomerase II (TopoII) (Earnshaw et al., 1985; Gasser and Laemmli, 1986). Topo II is an ATP-dependent DNA-strand passing enzyme that cleaves one strand of DNA, passes a second strand of DNA through the break, and then reseals the break (Wang and Eastmond, 2002). This activity is required for the individualization of chromosomes, a process in which catenated strands of DNA between different chromosomes are resolved and each chromosome is converted into an individual mobile unit. RNAi depletion studies in *Drosophila* cells and a conditional knockout in human cells showed that TopoII is not essential for chromosome condensation (Chang et al., 2003; Carpenter and Porter, 2004). Both studies found chromosome congression defects with chromosome arms extruding form the metaphase plate towards the spindle poles. A hypothesis proposed was that a pool of centrosomal Topo II could have a role in enabling the arms of metaphase chromosomes to detach from centrosomes (Chang et al., 2003). So far, the exact role of topo II in this process remains to be determined as genetic, biochemical, and pharmacological disruptions of topo II function in different organisms produce highly variable chromosome morphologies (Uemura et al., 1987; Hirano and Mitchison, 1993; Gimenez-Abian et al., 1995; Vagnarelli et al., 2006).

The second abundant non-histone scaffold protein to be identified, ScII, is the SMC2 (*s*tructural *m*aintenance of *c*hromosome, originally named *s*tability of *m*ini *c*hromosomes) subunit of condensin I and II complexes (Saitoh et al., 1994). Condensin I and condensin II are two large pentameric complexes sharing the SMC2/4 subunits and differing in the non-SMC subunits: CAP-H/CAP-H2, CAP-G/CAP-G2 and CAP-D2/CAP-D3 (Fig. 4). The architecture of SMC proteins reveals two halves of a nucleotide binding domain, known as Walker A and B motifs, that are located at opposite ends of the protein and flanking a long coiled-coil motif. In previous studies, it has been demonstrated that a single SMC monomer is able to fold back on itself through antiparallel coiled-coil interactions, creating an ATP-binding head domain and with a hinge domain at the opposite end (Saitoh et al., 1994; Melby et al., 1998). In turn, SMC2 and SMC4 monomers associate with each other at the hinge domain to form a V-shaped molecule. Unlike the hinge-hinge interaction, which is very strong and ATP-independent, the head-head

engagement is dynamically regulated by ATP hydrolysis (Hirano, 2002). In regard to the non SMC subunits CAP-G/CAP-G2 and CAP-D2/CAP-D3, HEAT (Huntingtin-elongantion-A subunit TOR) repeats, that are also present in a number of other chromosomal proteins, are thought to mediate protein-protein interactions (Neuwald and Hirano, 2000). In addition, CAP-H/CAP-H2 belongs to kleisins family of proteins, they bridge SMC2/SMC4 heads and recruit the remaining non-SMC subunits (Schleiffer et al., 2003) (Fig. 4).

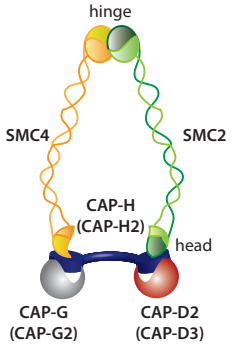

Figure 4 | Schematic diagram of Condensin I and II complexes. Both condensin I and II are pentameric complexes that share SMC2/4 subunits (green and yellow) the non-SMC subunits differ between condensin complexes (condensin II subunits are depicted inside brackets). Each SMC subunit forms dimers that self-fold by antiparallel arrangement to form a hinge region in one end and an ATP-binding head on the onter end. The head domains associate with CAP-H, or CAP-H2 in condensin I and II, respectively. Separate pairs of HEAT repeat-containing proteins associate with condensin I (CAP-D2 and CAP-G) or II (CAP-D3 and CAP-G2). (adapted from Nasmyth, K. and Haering, C.H. 2005; Hirano, T. 2006).

Condensin I and II have different temporal and spatial localizations throughout the cell cycle. For instance, condensin II is predominantly nuclear, while condensin I is sequestered in the cytoplasm during interphase (Hirota et al., 2004; Ono et al., 2004). Only after nuclear envelope breakdown in prometaphase is Condensin I capable of binding chromosomes; although, both condensins still display an alternating localization along the chromosome axis (Ono et al., 2003).

The SMC2/SMC4 dimer seems to bind dsDNA in a cooperative manner, independently of ATP (Yoshimura et al., 2002; Stray and Lindsley, 2003). However, the SMC2 complex was shown to have DNA supercoiling activity *in vitro* in an ATP dependent manner (Kimura and Hirano, 1997; Kimura et al., 1999; Bazett-Jones et al., 2002). It was also clear from experiments in *Xenopus laevis* cell free systems that condensin function is required for the establishment and maintenance of chromosome condensation (Hirano and Mitchison, 1994). Thus, it was proposed that condensin was partly responsible for the mechanism underlying the compaction of chromatin fibers in mitosis. A proposed model based on current data postulates that condensin interacts with chromatin in a closed

conformation. This interaction then triggers ATP hydrolysis opening the arms and establishing ATP-driven head-to-head engagement between different condensin complexes. Alternatively, individual complexes could drive DNA looping by intramolecular head-to-head engagement (Hirano, 2006). Besides condensin's supercoiling activity, it has also been proposed that condesin complex has re-annealing activity (Sutani and Yanagida, 1997; Sakai et al., 2003). Based on assays conducted in purified condensin complexes from fission yeast it was proposed that the DNA annealing activity could be required for the recovery from unwound duplex DNAs. Complementary DNA strands in chromosome are thought to be always spontaneously associated but, in certain situations, the DNA reannealing reaction might have to be positively supported.

All members of the condensin complexes have been shown to be essential for cell and organism viability (Swedlow and Hirano, 2003). Additionally, subsequent studies of condensin function in *C. elegans* (Hagstrom et al., 2002), *D. melanogaster* (Steffensen et al., 2001; Coelho et al., 2003) and chicken DT40 cells (Hudson et al., 2003; Vagnarelli et al., 2006) demonstrated that condensin has a limited role in the formation of condensed mitotic chromosome morphology *in vivo*. This was clearly shown in the chicken DT40 SMC2 knockout cell line where condensin-depleted chromosomes achieved near-normal levels of compaction (Hudson et al., 2003), with only a 40% decrease in chromosome arm lateral compaction (Vagnarelli et al., 2006). Curiously, although chromosomes did condense, their higher-order structure was compromised: topo II was distributed along the chromosome rather than restricted to the chromosome axial core. Other non-histone proteins were also mislocalized, for example, INCENP and the chromokinesin Kif4. Importantly, condensin-depleted chromosomes were found to be highly fragile *in vitro*. In an attempt to develop an assay to examine morphological perturbations, chromosomes were exposed to a low-salt buffer containing EDTA. In this buffer DNA unravels (by chelating the cations resulting in an unbalanced negative net charge), but following addition of Mg^{2+}, chromosomes are able to refold and their morphological appearance returns to near normal. Curiously, in the absence of condensin the refolding does not occur, showing that there is a compromised structure and revealing condensin as an essential organizer of chromosome architecture. In DT40 cells lacking both condensin I and II, chromosomes still condense, exhibit normal sister chromatid cohesion, and initiate segregation correctly. However, while still moving in anaphase the chromatids abruptly lose their organized structure and display massive chromatin bridges (Hudson et al.,

2003). The same phenotype is observed in several other systems (Saka et al., 1994; Steffensen et al., 2001; Hagstrom et al., 2002).

3.1.2 Condensin-independent mechanism of chromosome condensation

The chicken DT40 KO system allowed a more thorough dissection of additional factors that could work with condensin to contribute to mitotic chromosome formation (Vagnarelli et al., 2006).

The sudden loss of chromosomal integrity in anaphase indicates that other mechanism(s) are involved in driving chromosome condensation and stabilizing the condensed chromosome architecture when condensin is absent.

In fact, the loss of chromosome integrity observed in condensin-depleted cells can be rescued by preventing the PP1γ (protein phosphatase 1, γ isoform) targeting subunit of Repo-Man from recruiting PP1 to chromatin at anaphase onset. PP1 association is mediated by a RVXF binding motif in Repo-Man and is blocked if this motif is mutated to RAXA. The Repo-Man-RAXA mutant is still targeted to chromatin in anaphase, but PP1 is not recruited to the chromosome periphery. In condensin-depleted cells, targeting of Repo-Man-RAXA to the anaphase chromosomes rescues the characteristic anaphase bridge phenotype. This study revealed the existence of an activity termed RCA (Regulator of Chromosome Architecture), which is negatively regulated by PP1. The data suggests that phosphorylated RCA can stabilize the condensed mitotic chromosome structure and that in normal mitosis condensin acts to stabilise this state after RCA is inactivated by Repo-Man/PP1 early in anaphase (Vagnarelli et al., 2006).

3.2 Centromeres

In mitosis, the replicated chromatin is condensed into characteristically shaped chromosomes composed of two sister chromatids held together at a specialised chromosomal region: the centromere. The centromeric region is also where kinetochores assemble during mitosis. The centromere/kinetochore directs a series of key tasks in chromosome segregation: it is involved in sister chromatid cohesion and separation; acts as an attachment site for microtubules of the mitotic spindle; monitors microtubule attachment and correction by activating/deactivating the spindle assembly checkpoint; and it is the force generator driving chromosome movement (Przewloka and Glover, 2009).

Despite the central role of the centromere in some of the most important mechanisms in eukaryotic cell division, its underlying structure and specification are still poorly understood.

3.2.1. Centromere specification: beyond DNA

There are three different types of centromeres in eukaryotes: point, holocentric and regional centromeres (Pluta et al., 1995) (Fig. 5). Upon the discovery that point centromeres (*S. cerevisiae*) are rigorously specified by the underlying DNA sequence consisting of 125 bp of centromeric DNA packaged into a single nucleosome (Clarke and Carbon, 1980, 1985) that is enough to specify kinetochore formation (McAinsh et al., 2003; Meraldi et al., 2006; Westermann et al., 2007); a model for sequence-based centromere positioning in higher eukaryotes was also thought to hold true. However, all studies until now have failed to identify sequence elements sufficient to define centromeric regions in higher eukaryotes. Apart from budding yeast, centromeres are not specified simply by a DNA sequence, but rather chromatin composition and architecture may also contribute. Yet another type of centromeres described is the holocentric type (e.g. in *C. elegans*). In this case, centromeres are diffuse and distributed along the length of the chromosome (Maddox et al., 2004). Thus, kinetochore assembly must be epigenetically determined.

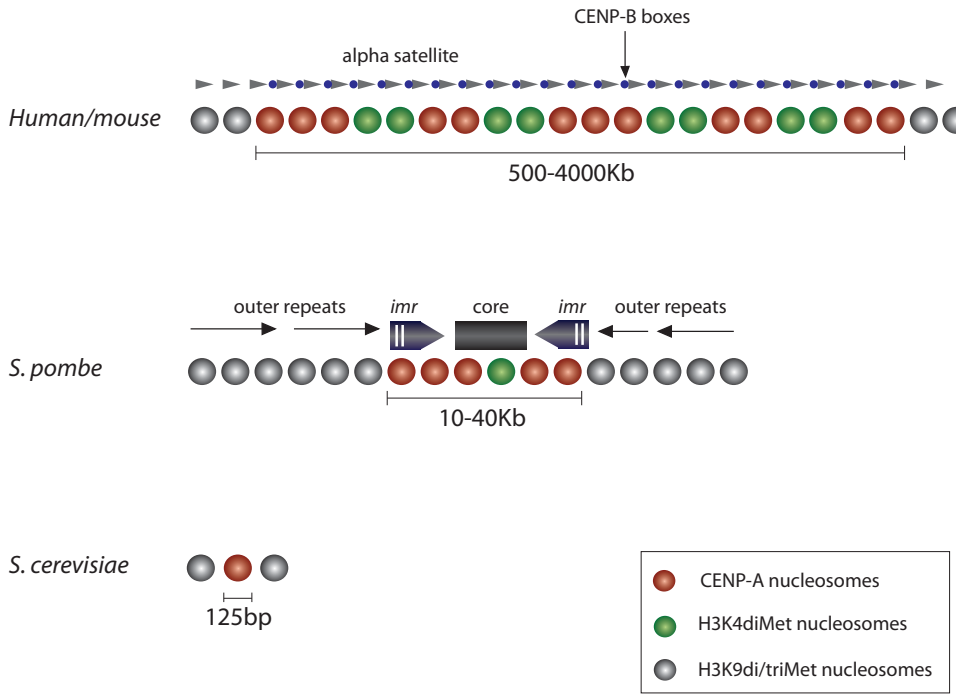

Figure 5 | Examples of organization of centromeric region in different organisms. Schematic representation of regional centromeres: human/mouse; and *S. pombe* and point centromere, *S. cerevisiae* (adapted from Allshire and Karpen, 2009)

The regional centromeres of fission yeast, plants, flies and humans can span 40-4000 Kb (Sullivan et al., 2001). In fission yeast, *Schizocaccharomyces pombe*, the centromere is composed of a central core element of 4-10 Kb, flanked by regions of inverted repeats: innermost (imr) sequences and the outer (otr) repeats. The centromere has an overall size of 30-110 Kb depending on the chromosome (Clarke et al., 1986; Nakaseko et al., 1986; Clarke, 1990). In contrast, centromeric DNA in higher eukaryotes is composed of highly repetitive tandem sequences. In general, human centromeric DNA consists of repeats of 171 bp of α-satellite DNA monomers arranged in a head-to-tail fashion (Willard, 1990) and can be subdivided into two types (Alexandrov et al., 1991; Ikeno et al., 1994). Type I α-satellite DNA forms higher order repeat arrays, while type II is monomeric and lacks regular higher order organization. Type I α-satellite is associated with kinetochore function and contains a 17 bp motif known as the CENP-B box which is the binding site for the centromeric protein, CENP-B (Earnshaw and Rothfield, 1985; Earnshaw et al., 1987; Masumoto et al., 1989). Type II α-satellite flanks the type I array and can be interrupted by interspersed elements (LINE, SINE, LTR) (Prades et al., 1996). Evidence for additional regulation of centromere activity, beyond the level of the DNA, came from the analysis of abnormal centromeres using classical cytogenetic and cell

biology techniques. This finding opened the field to a concept in which epigenetic regulation was perceived to be extremely important in centromeric specification and propagation. For example, certain human and fly chromosomes containing two separated blocks of centromeric DNA – dicentric chromosomes – segregate normally. This is because only one of these sites is able to recruit centromere proteins and assemble kinetochores, while the other is epigenetically inactivated (Earnshaw and Migeon, 1985; Merry et al., 1985). An exception to this rule, however, is CENP-B, which binds to both centromeres (Earnshaw and Migeon, 1985; Earnshaw et al., 1989; Sullivan and Schwartz, 1995; Warburton et al., 1997; Agudo et al., 2000).

The discovery of neocentromeres further confirmed that DNA *per se* is not sufficient to drive centromere assembly. Neocentromeres arise from chromosomal rearrangements in which a region of euchromatic DNA acquires the ability to function as a centromere, and assemble a kinetochore (Voullaire et al., 1993). These sites lack any sequence that is homologous to the normal centromere, but once established neocentromeres propagate and segregate normally (Williams et al., 1998; Choo, 2001; Lo et al., 2001b; Warburton, 2004; Alonso et al., 2007). Taken together, evidence from neocentromeres and dicentric chromosomes reveal that neither the specific DNA sequence, nor the DNA binding protein CENP-B, is essential or sufficient to determine centromere propagation. CENP-B is also not necessary for centromere function, because it is not associated with the alphoid region of chromosome Y (Earnshaw et al., 1991; Haaf et al., 1995). In addition, CENP-B knockout mouse cells are capable of assembling functional kinetochores (Hudson et al., 1998; Kapoor et al., 1998; Perez-Castro et al., 1998). In fact, recent data suggests that the main role of CENP-B is in the establishment, rather than the maintenance of centromeric chromatin, as it represses the formation of ectopic centromeres (Okada et al., 2007).

3.2.2 Centromere organization

Despite centromeric sequence divergence, important similarities in chromatin organisation are shared by all eukaryotic centromeres. All centromeres contain a centromere specific histone H3 variant, CENP-A (Earnshaw and Rothfield, 1985). The first human CENPs were identified using serum of patients with autoimmune disorders (Moroi et al., 1980; Earnshaw and Rothfield, 1985). Sera from these patients contain antibodies recognizing two other centromeric proteins, named CENP-B and CENP-C (Earnshaw and

Rothfield, 1985; Earnshaw et al., 1986). In concert with a number of other polypeptides, these proteins form the foundation of the kinetochore, and remain associated with the centromere throughout the cell cycle (Moroi et al., 1981). CENP-A, in particular, has been studied extensively. One distinguishing property of CENP-A is that it is a variant of histone H3 (Palmer and Margolis, 1987; Palmer et al., 1989; Palmer et al., 1991). Indeed, human CENP-A, which is 17 kDa in length, shares 57% identity with histone H3. This homology is restricted to the C-terminal histone fold and does not extend to the N-terminal domain, which is highly divergent between species (Sullivan et al., 1994).

From yeast to mammals, homologues of CENP-A have been identified and named accordingly: *Schizosaccharomyces pombe,* cnp-1; *Saccharomyces cerevisiae,* cse4; *Caenorhabditis elegans,* HCP-3; *Drosophila melanogaster,* CID; highlighting the existence of an evolutionary link between widely divergent DNA sequences. Furthermore, CENP-A is recruited to all active centromeres in stable dicentric chromosomes (Earnshaw and Migeon, 1985). CENP-A is also found at neocentromeres lacking α -satellite repeats (Warburton et al., 1997; Amor et al., 2004). Studies of CENP-A knockouts in *C. elegans* (Oegema et al., 2001), mouse (Howman et al., 2000) and DT40 cells (Regnier et al., 2005), and depletion by siRNA in human cells, (Goshima et al., 2003) have shown that CENP-A is required for centromeric function. These observations place CENP-A at the foundation of the centromere, playing major roles both in the structural and functional maintenance of centromeric chromatin.

Nucleosomes can be assembled *in vitro* from purified CENP-A and histones H2A, H2B and H4 (Yoda et al., 2000), indicating that CENP-A can replace both copies of H3. It has also been shown that nucleosomes containing CENP-A and H4 are biochemically and structurally more compact, with a more rigid conformation than the corresponding H3-H4 tetramers (Black et al., 2004). However, *in vivo* analysis has brought to light some intriguing results. In budding yeast, the Cse4 nucleosome were claimed to possess an unusual composition; H2A and H2B were replaced by one molecule of Scm3 (Camahort et al., 2007; Mizuguchi et al., 2007; Stoler et al., 2007). This result implies that budding yeast centromeric nucleosomes consist of a hexamer containing two copies of Cse4, Scm3 and H4. However, a more recent paper argues convincingly that Cse4 nucleosomes contain a canonical histone octamer with two copies of Cse4 (Camahort et al., 2009). 'Nucleosomes' containing Scm3 may be assembly intermediates. Another recent study on *Drosophila* centromeric chromatin organization using cross-linking experiments followed by protein

purification analysis, showed that in interphase cells Cid/CENP-A nucleosomes are composed of heterotypic tetramers termed hemisomes, which consist of one molecule of Cid, H2A, H2B and H4 (Dalal et al., 2007). However, in another study where a tagged version of CENP-A was introduced into HeLa cells and used to isolate centromeric nucleosome arrays, 85% of nucleosomes were octameric homotypic (i.e., lack H3); whereas, only 15% were heterotypic nucleosomes (contained both CENP-A and H3) (Foltz et al., 2006). More recently, it has been shown that Cid/CENP-A nucleosomes reconstituted from *Drosophila* histones produce right-handed wrapping of the DNA around the histone core, instead of the canonical negative supercoil observed in histone H3 nucleosomes (Furuyama and Henikoff, 2009). *In vivo* analysis is supportive of this finding as CENP-A induces positive supercoiling when using a budding yeast minichromosome system (Furuyama and Henikoff, 2009).

Regardless of the structure and composition of CENP-A nucleosomes, which is still controversial, these nucleosome arrays are essential for establishing the structural foundation of the kinetochore.

Eukaryotic centromere regions are broadly classified into domains encoding: a) centromeric chromatin and b) heterochromatin (Choo, 2001; Pidoux and Allshire, 2004). Centromeric chromatin is a unique type of chromatin containing CENP-A and is flanked on one or both sides by large blocks of heterochromatin. On one hand centromeric chromatin is essential for kinetochore assembly and therefore acts as a site for microtubule attachment and spindle assembly checkpoint activation. On the other hand, heterochromatin contributes to sister chromatid cohesion. Even though CENP-A replaces one or both copies of H3 in centromeric nucleosomes, not every centromeric nucleosome contains CENP-A. An early study by Zinkowski *et al*, (Zinkowski et al., 1991) demonstrated that in mechanically stretched chromosomes CENP antibodies stained blocks of CENP interspersed with regions where the signal was absent. Later, regions of CENP-A were shown to co-localise with blocks of canonical H3 nucleosomes (Blower et al., 2002). This unique pattern was first described in human and *Drosophila* centromeres, but was later observed in organisms from fission yeast to plants, and even found in neocentromeres (Nagaki et al., 2004; Cam et al., 2005; Alonso et al., 2007).

3.2.3 Assembly of centromeric chromatin

Once CENP-A is incorporated into centromeric chromatin it remains stably associated throughout the cell cycle. In terms of timing, it has been demonstrated that the loading of CENP-A into the replicated centromeres happens only in late mitosis for early fly embryos (Schuh et al., 2007) or early G1 in human cells (Jansen et al., 2007; Maddox et al., 2007) and not, as proposed initially, in G2 phase where a CENP-A mRNA expression peak is observed (Shelby et al., 1997).

A complex containing Mis18α, KNL-2 (also designated Mis18 Binding Protein, M18BP1) and the RbAp46/RbAp48 histone chaperones known as the Mis18 complex, is essential for CENP-A incorporation during mitotic exit. The Mis18 complex is specifically recruited to centromeres at anaphase and is released in G1, consistent with a role in CENP-A loading during mitotic exit (Hayashi et al., 2004; Fujita et al., 2007; Maddox et al., 2007). Although CENP-A loading is dependent on this complex, no direct interaction has been established. It has been suggested, however, that Mis18 might prime loading of new CENP-A in a process that possibly involves acetylation of centromeric chromatin (Fujita et al., 2007).

This chromatin-priming event is followed by CENP-A loading. Recently, this process has been clarified by isolating proteins that associate with pre-nucleosomal CENP-A, and not with histone H3 (Dunleavy et al., 2009; Foltz et al., 2009). Both studies identified a common CENP-A binding protein, known as HJURP (Holliday junction-recognition protein). This protein localizes to centromeres slightly after Mis18α, supporting the possibility that the Mis18 complex first primes the centromere for receiving CENP-A, while HJURP promotes CENP-A stability (rather than directly mediating CENP-A assembly), thereby regulating its incorporation into centromeres. The exact mechanism underlying CENP-A loading remains elusive, however. One possible candidate is the ATP-dependent remodeling and spacing factor (RSF) complex, which is recruited to the centromere in mid-G1 and is able to interact with CENP-A nucleosomes. At a functional level this complex could either mediate the assembly of CENP-A into chromatin, stabilize already assembled CENP-A nucleosomes by promoting incorporation of H2A/H2B or regulate nucleosome phasing (Perpelescu et al., 2009).

3.3 Kinetochore

3.3.1 Kinetochore structure

The kinetochore is a protein-based structure located on the surface of the chromosomes which interacts directly with spindle microtubules, and is responsible for chromosome movement. At the ultrastructural level, the mammalian kinetochore has been shown to be composed of a trilaminar disk in which two electron-dense plates are separated by an electron translucent middle region (Brinkley and Stubblefield, 1966; Jokelainen, 1967; Ris and Witt, 1981). The innermost layer is a disk of densely packed material designated the inner plate and is continuous with the surface of the centromeric chromatin underneath the kinetochore. This region is responsible for the assembly of a robust kinetochore, which must be capable of withstanding the forces imposed by the spindle microtubules. The outer plate is a dense structure that is typically 0.5 µm in diameter, 30-40 nm thick, and forms the primary point of attachment for spindle microtubules. Furthermore, between the two plates there is an interstitial space 15-35 nm thick. The typical trilaminar structure is only visible from late prophase until the end of mitosis, suggesting that the kinetochore undergoes cycles of assembly/disassembly (Roos, 1973; Brenner et al., 1981). Finally, the inner centromeric chromatin, which is found between the two sister kinetochores, functions as a support for the kinetochore (Fig. 6).

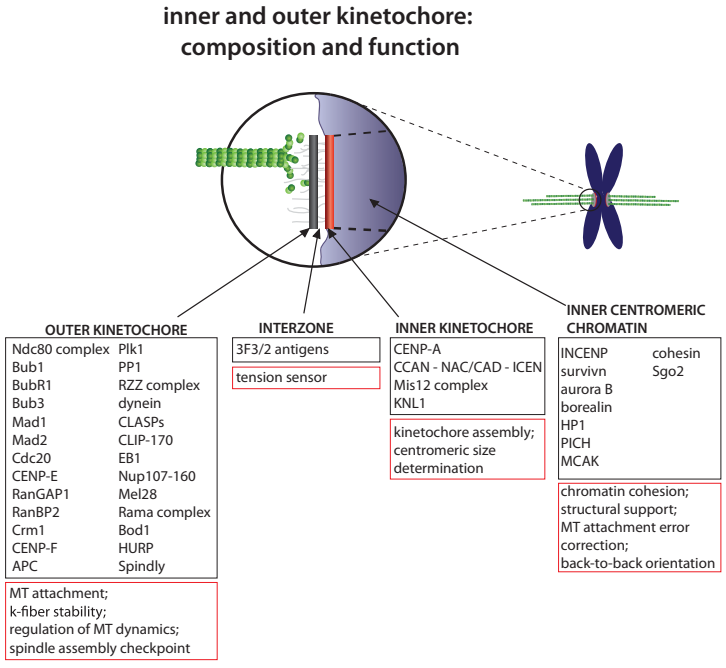

Figure 6 | Molecular composition of the kinetochore. During mitosis, the outer kinetochore proteins (grey plate) assemble on the centromeric region (red plate) allowing microtubule attachments. Black boxes contain known proteins that localize to each of the trilaminar structures or inner centromere. Red boxes show the functions achieved by each of the kinetochore components (adapted from Maiato *et. al.*, 2004)

More recently, EM analysis employing high-pressure freezing and freeze substitution instead of conventional chemical fixation, reveal a distinct kinetochore structure (McEwen et al., 1998). This study proposes that the trilaminar structure may be an artifact of chemical fixation and it was proposed that the kinetochore is composed of a thick mat of light-staining fibrous material that is directly connected with the more electron-opaque surface of the centromeric heterochromatin. This mat corresponds to the outer plate in conventional preparations, and individual connections to the microtubule end seem to be distinct in attached versus unattached kinetochores (Dong et al., 2007). This suggests an alteration in the kinetochore structure dependent on microtubule attachment.

In the past decade, genetic analysis and mass-spectrometry based proteomic studies have identified around 80 proteins that are associated at different times with the centromere/kinetochore (Foltz et al., 2006; Meraldi et al., 2006; Okada et al., 2006; Cheeseman and Desai, 2008). Although this is a large number, these proteins have been further grouped into subcomplexes, and their localization shown to be highly dynamic throughout the cell cycle. Some of these subcomplexes are found constitutively at the centromere and comprise the CCAN (Constitutive Centromere Associated Network), otherwise termed NAC/CAD (CENP-A nucleosomes associated complex and CENP-A distal) or ICEN (interphase centromere complex) (Obuse et al., 2004b; Foltz et al., 2006; Izuta et al., 2006; Meraldi et al., 2006; Okada et al., 2006; Hori et al., 2008). Unlike the constitutively localized proteins, outer kinetochore proteins are assembled on kinetochores at prophase and leave at the end of mitosis. One example is the KMN complex, which is formed from three highly conserved proteins, *K*NL-1/*M*is12 complex/*N*dc80 complex, and is involved in the interface between the kinetochore and microtubules. Other outer kinetochore proteins that have the same temporal mitotic localization are motor and regulatory proteins that take part in the fine-tuning of microtubule attachment (Cheeseman and Desai, 2008).

During mitosis a series of signaling proteins within the inner centromere control kinetochore functions, the fidelity of microtubule attachment, and even the cohesion of sister chromatids. Essential to keep sister chromatids held together is the cohesin complex. Cohesin is a multiprotein complex that mediates sister chromatid cohesion and its ring-shaped structure first suggested that it may perform this task by embracing the sister chromatids. The interaction of cohesin with chromatin is tightly regulated

throughout the cell cycle, with several different proteins contributing to cohesin loading and mobilization along DNA, establishment of cohesin-mediated cohesion, and the removal of cohesin during mitosis. Importantly, cohesin is released from chromosome arms at prophase, but maintained at the inner centromeric region by members of the Shugoshin family until anaphase onset where it is eventually cleaved by separase (Nasmyth and Haering, 2009).

3.3.2 CENP-C and the Constitutive Centromere-Associated Network (CCAN)

Although kinetochore structures are not visible in interphase, pre-kinetochore structures persist throughout the cell cycle, as shown by light microscopy with antibodies to kinetochore components (Moroi et al., 1981; Brinkley et al., 1984). One group of polypeptides that display this constitutive localization are the CCAN proteins (Cheeseman and Desai, 2008), otherwise termed the CENP-A NAC/CAD complex (CENP-A nucleosomes associated complex and CENP-A distal) (Foltz et al., 2006) and also designated ICEN (interphase centromere complex) (Obuse et al., 2004b).

The CCAN comprises of a group of 14 proteins: CENP-C, -H, -I K-U and -W (Obuse et al., 2004b; Foltz et al., 2006; Izuta et al., 2006; Meraldi et al., 2006; Okada et al., 2006; Hori et al., 2008). The alternative designation CENP-A NAC/CAD is based on biochemical isolation: NAC proteins (CENP-C, -H, -M, -N, -T and –U) were purified in association with CENP-A nucleosomes, while CAD proteins (CENP-I, -L, -K, -O, -P, -R and –S) were purified with NAC proteins (Foltz et al., 2006). Yet, another designation for these proteins exists – ICEN (interphase centromere complex) based in studies conducted in isolated interphase HeLa centromere complexes that contain CENP-A, CENP-B and CENP-C, using monoclonal antibodies against CENP-A (Ando et al., 2002). After purification of these DNA-protein complexes a proteomic analysis was carried out identified approximately 40 proteins (Obuse et al., 2004b; Izuta et al., 2006).

Within this network, CENP-C (Saitoh et al., 1992), CENP-I (Nishihashi et al., 2002; Liu et al., 2003) and CENP-H (Fukagawa et al., 2001) were characterized first. However, follow up studies show that CENP-C and CENP-T/W do not interact directly with CENP-A nucleosomes after full micrococcal nuclease (MNase) digestion, and instead interact with H3 (Hori et al., 2008). Moreover, CENP-C binds directly to DNA *in vitro* (Yang et al., 1996)

and from the remaining CCAN proteins only CENP-N has been shown to directly interact, *in vitro*, with CENP-A nucleosomes (Carroll et al., 2009) (Fig. 7).

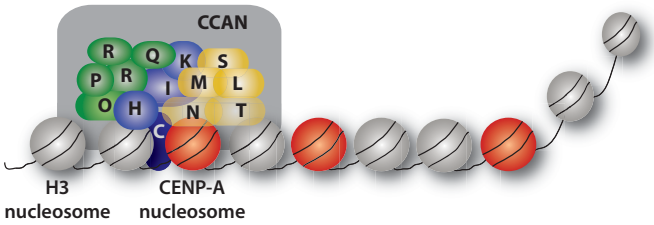

Figure 7 | The constitutive centromere associated network (CCAN) (adapted from Cheeseman and Desai, 2008).

CENP-C, in addition to forming a complex with CENP-A and CENP-B (Ando et al., 2002), also contains a DNA-binding domain that allows a direct interaction with the DNA (Sugimoto et al., 1994; Yang et al., 1996). However, attempts to identify specific CENP-C binding sequences have failed. In any case, depletion studies have clearly shown that CENP-C is required for the formation of a functional kinetochore structure and antibody injection mediated-depletion of CENP-C in interphase HeLa cells causes mitotic defects (Tomkiel et al., 1994). Kinetochores appear smaller, or longer and punctuated, and microtubule attachments are defective. These cells also arrest in metaphase, suggesting that spindle assembly checkpoint proteins are still able to localize properly to the defective kinetochores and detect microtubule attachment errors. Follow up studies support a model where CENP-C is located near the top of the kinetochore assembly pathway. In this case siRNA depletion of CENP-C in human cells results in a failure of some proteins, except the passenger protein Aurora B, to localize to the kinetochore (Liu et al., 2006). Among the mislocalized proteins are hMis12 (one of the components of the KMN network (see section 3.3.3), involved in the core interaction between kinetochores and microtubules); the checkpoint proteins BUB1 and BUBR1, which transiently localize to the kinetochore while sensing the establishment of correct microtubule attachments; the microtubule-depolimerize kinesin MCAK and the motor protein CENP-E. Based on this data, CENP-C could possibly be involved in specifying the compaction and dimension of the kinetochore plate. As CENP-C is involved in recruiting a number of different proteins, its loss would reduce the number of fully assembled unit modules (Liu et al., 2006).

Several studies have been undertaken to examine the interdependence of assembly of different components of the CCAN. Attempts have also been made towards

grouping these proteins in sub-complexes with different functions and roles. However, the resulting picture is very complex and far from being clear. A first definition came with the two biochemically distinct groups: NAC and CAD. Yet, this division might not predict any functional suborganization, since the exact role and function of these proteins is still under discussion. For instance, depletion of NAC and CAD proteins in human or chicken cells causes chromosome congression defects (Liu et al., 2003; Minoshima et al., 2005; Foltz et al., 2006; Okada et al., 2006). On the other hand, depletion of CAD protein CENP-O and NAC protein CENP-N causes failure in bipolar spindle assembly (McAinsh et al., 2006; McClelland et al., 2007). In regard to the interaction of CCAN proteins with the KMN network (described in the next section) there is also contradictory data. Data from some studies suggest that CCAN proteins are required for loading Mis12 and Ndc80 complexes onto the kinetochore (Hori et al., 2003; Liu et al., 2006; Kwon et al., 2007) while other studies did not find such an association (Foltz et al., 2006; McAinsh et al., 2006; McClelland et al., 2007). The exact subcomplexes and assigned roles of each of the CCAN proteins is still to be determined.

3.3.3. The KMN network

Unlike CCAN proteins, outer kinetochore proteins are assembled at the beginning of prophase and persist until the end of mitosis, forming subcomplexes that show different functions and/or binding stabilities. Three highly conserved protein complexes; KNL-1, Mis12 complex and the Ndc80 complex form the KMN network, that assembles within the outer kinetochore to produce core interactions with microtubules (Cheeseman et al., 2006; Deluca et al., 2006; Tanaka and Desai, 2008). The KNL-1/Mis12 complex/Ndc80 complex (KMN) network is conserved throughout eukaryotes and is essential for viability and kinetochore microtubule interactions in multiple organisms (Fig. 8).

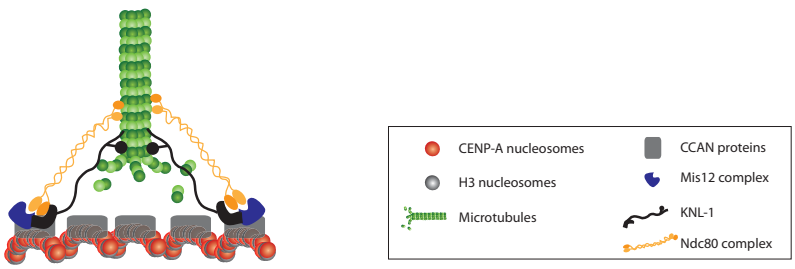

Figure 8 | The KMN network. KNL-1 is recruited to the kinetochore by Mis12 complex (Mis12, Nnf1, Nsl1 and Dsn1) and binds to one of its subunits, hDsn1. The Ndc80 complex is a tetramer composed of Ndc80 (or Hec1), Nuf2, Spc24 and Spc25, and while Ndc80/Nuf2 form a dimer that interacts with microtubules, Spc24/Spc25 dimers interact with KNL-1 (adapted from Cheeseman and Desai, 2008).

The Mis12 complex is the first to be recruited to centromeres, possibly by interacting with CENP-C (Goshima et al., 2003). However, there is also data suggesting that Mis12 complex interacts with heterochromatin protein 1 (HP1) (Obuse et al., 2004a). This complex is composed of four proteins: Mis12, Nnf1, Nsl1 and Dsn1 (Euskirchen, 2002; Nekrasov et al., 2003) and all are required for proper complex assembly (Kline et al., 2006). Depletion of components of the Mis12 complex compromises kinetochore assembly (De Wulf et al., 2003; Kline et al., 2006). The timing of recruitment of Mis12 complex components is not entirely established. Mis12 protein was initially reported to localize constitutively at the kinetochore throughout the cell cycle (De Wulf et al., 2003; Goshima et al., 2003). A later study showed that Nnf1 in HeLa cells is bound to kinetochore during most of the cell cycle excluding a brief period in telophase (McAinsh et al., 2006). In another study human Mis12 was shown to localize to kinetochores from late G2 to telophase (Kline et al., 2006).

In *C. elegans*, an RNAi-based screen led to the discovery of KNL-1 (Gonczy et al., 2000; Desai et al., 2003). Depletion of KNL-1 completely abolishes kinetochore-microtubule interactions (Nekrasov et al., 2003). The human homologue of KNL-1 was shown to localize to the kinetochore in late G2, before Ndc80 complex recruitment (Cheeseman et al., 2008). Furthermore, KNL-1 was shown to bind to Nsl1 and Dsn1 - components of the Mis12 complex (Cheeseman et al., 2006; Kiyomitsu et al., 2007). Both KNL-1 and the Mis12 complex cooperate in recruitment of the Ndc80 complex to the outer kinetochore. In support of this model, the Ndc80 complex has been shown to associate with KNL-1 and Mis12 protein in the KMN network (Cheeseman et al., 2004; Obuse et al., 2004a), as well as CENP-H of the CCAN (Mikami et al., 2005; Okada et al., 2006).

Several studies of the Ndc80 complex have shown that it is important for the fidelity of kinetochore-microtubule attachments (DeLuca et al., 2005; Cheeseman et al., 2006; Deluca et al., 2006). The four subunits of the complex (Hec1/Ncd80, Nuf2, Spc24 and Spc25) assemble into a tetrameric rod of around 570 Å in length, with two globular heads at each end (Wei et al., 2006). When microtubules attach to the kinetochore, the complex is oriented with the Ndc80/Nuf2 heads associated with microtubules, while the Spc24/Spc25 are directed toward the centromere (Ciferri et al., 2008). Microtubule cosedimentation assays have shown that the Ndc80/Nuf2 are responsible for the direct

interaction with microtubules (Cheeseman et al., 2006). Additionally, the binding of Ndc80/Nuf2 to the microtubules seems to be stabilized by KNL-1 and the Mis12 complex.

A key hallmark of the kinetochore-spindle interface is its ability to maintain stable associations while microtubules are polymerizing and depolymerizing. Such a feature is explained by an interaction surface composed of an array of intrinsically low-affinity binding sites. There are two such low-affinity binding activities within the KMN network: one intrinsic to the Ndc80 and Nuf2 subunits of the Ndc80 complex, and a second intrinsic to KNL-1. Such an array of low-affinity interactions allows attachments to remain dynamic in response to growing and shrinking microtubules, without resulting in microtubule detachment (Cheeseman et al., 2006). It has also been proposed that the Ndc80 arm can bend as a result of a kink inside the coiled-coil region of Ndc80/Hec1 (Ciferri et al., 2008; Wang et al., 2008; Wan et al., 2009). The flexibility provided by this kink could further contribute to the mechanical movement of Ndc80 complex in response to microtubule dynamics, without releasing microtubules.

In summary, the KMN network is a key component of the kinetochore. It directly binds to centromeres by yet unidentified interactions and to microtubules through a well-known mechanism. It is a platform that allows a variety of proteins to interact with kinetochore in a regulated manner.

3.4 The mitotic spindle

3.4.1 Assembly of mitotic spindle

Microtubule filaments are 25 nm cylindrical structures that assemble from heterodimers of α- and β-tubulin monomers. Both α- and β-tubulin bind GTP, but only β-tubulin has GTPase activity, which is stimulated upon incorporation of the heterodimer into the microtubule plus ends. Microtubule polymers are polar structures formed by head-to-tail arrangements of α/β heterodimers (Amos and Klug, 1974). The two ends of the filaments are denoted plus and minus according to their association and dissociation rates with tubulin heterodimers (the faster growing end is defined as the plus end) (Desai and Mitchison, 1997).

Microtubule protofilaments display a very interesting behaviour, coined dynamic instability. The first demonstration of this microtubule property was carried out by Mitchison and Kirschner (Mitchison and Kirschner, 1984) where it was shown that although a population of microtubules exhibits a steady state, a single microtubule never reaches a steady state length, but persists in prolonged states of polymerization (growth) and depolymerization (shrinkage) that interconvert occasionally. A conversion from growth to shrinkage is termed a catastrophe. Conversely, the switch from growth to shrinkage is named rescue. This non-equilibrium state is dependent on GTP binding at the nucleotide exchangeable site (E site) on β-tubulin during polymerization.

Microtubule assembly and dynamics are further regulated by other components, including microtubule assembly-promoting factors, microtubule stabilizing factors (e.g. microtubule associated proteins (MAPs)), microtubule destabilizing factors, microtubule severing proteins and microtubule-based motors of the dynein and kinesin families (Vale, 2003; Joglekar et al., 2010; Walczak et al., 2010).

During mitosis, a microtubule-based array nucleates mainly from the centrosome and functions to physically segregate sister chromatids. The centrosomes are the major microtubule-organizing centres in vertebrate cells. In electron microscopic images they appear as a focus of electron dense material consisting of two centrioles, surrounded by pericentriolar material (Vorobjev and Chentsov, 1980). Microtubule nucleation occurs in the pericentriolar material and requires the γ-tubulin complex, or γ-TuRC (Zheng et al., 1995). A large dynamic array is nucleated from the two centrosomes positioned on opposite poles of the cell, and is designated the mitotic spindle. Dynamic instability allows microtubules to search in a three-dimensional space for factors that bind and stabilise them, such as kinetochores. Thus, dynamic instability is a microtubule property essential to the formation of the mitotic spindle (Kirschner and Mitchison, 1986). In addition, microtubules can be nucleated independently of centrosomes and stabilized by a RanGTP gradient present around the chromosomes (Heald et al., 1996; Carazo-Salas et al., 2001; Wilde et al., 2001). Recently, it has been shown that in addition to the RAN gradient, the chromosomal passenger complex (CPC) can function in an alternative molecular mechanism that promotes microtubule assembly from the centromeric region (Maresca et al., 2009). The current accepted model for spindle assembly proposes that centrosome-dependent and chromatin-dependent pathways co-exist and cooperatively

assemble the mitotic spindle (O'Connell and Khodjakov, 2007). Very recently, a third pathway has been shown to further contribute to mitotic spindle maintenance by increasing the density of microtubules in a centrosome independent manner (Goshima et al., 2008; Meireles et al., 2009). Here, a complex that directly binds microtubules named augmin, recruits the γ-TuRC enabling further microtubule nucleation independently of the centrosome.

3.4.2 Establishing kinetochore-microtubule attachment – from initial attachment to congression

After nuclear envelope breakdown, kinetochores initially associate laterally with microtubules in such a way that the kinetochore outer plate is orientated parallel to the microtubule lattice (Hayden et al., 1990; Merdes and De Mey, 1990; Rieder, 1990). The exact trajectory of each chromosome during prometaphase is unique however the final goal is to achieve congression – the chromosome alignment at the spindle equator. This process involves both establishing a proper bipolar attachment and the alignment of chromosomes. There are multiple independent pathways involved in congression and whether chromosome congression promotes biorientation or biorientation is a requirement for congression is still unclear (Walczak et al., 2010). I will start by describing the mechanisms of laterally attached chromosome movement in prometaphase, and then will refer to the existing models for transition from mono- to bipolar attachment.

During prometaphase, the lateral interaction between kinetochores and microtubules is associated with the rapid poleward gliding that some chromosomes exhibit (Rieder and Alexander, 1990). Recently, was shown that lateral kinetochore-microtubule interaction is enough to position chromosomes at the spindle equator (Kapoor et al., 2006). This phenomenon is predominant in meiosis (Wignall and Villeneuve, 2009). In both cases, poleward gliding and chromosome congression without biorientation, kinetochore movement is dependent on forces generated by molecular motors bound to kinetochores (Kapoor et al., 2006; Yang et al., 2007). Both plus end- and minus end-directed motors, such as CENP-E and cytoplasmic dynein have been shown to be involved in the movement of chromosomes towards the spindle equator. Loss of CENP-E is associated with chromosome congression failure (Yen et al., 1991; Schaar et al.,

1997; Wood et al., 1997). Recently, CENP-E was directly implicated in the movement of mono-oriented chromosomes to the metaphase plate (Kapoor et al., 2006; Cai et al., 2009). Also the minus-end motor dynein has been shown to be required for the rapid poleward motion of attaching kinetochores. In this study, both by depleting ZW10 (that directly recruits dynein to the kinetochores (Starr et al., 1998)) and by dynein-antibody injection was possible to observe congression defects (Yang et al., 2007).

Several models have been proposed that may explain the transition from mono- to bipolar attachment of the chromosomes. In the classical search and capture model monotelic chromosomes remain close to the spindle pole that they are attached to until a microtubule from the opposite pole attaches to the free sister kinetochore. The key assumption of this model is that bipolar attachment is necessary for congression (Kirschner and Mitchison, 1986). The other proposed model argues that instead of centrosomal microtubules, k-fibers emanating from the kinetochores have a major role in congression. Both *in vitro* data, where microtubules were observed at chromosomes (Telzer et al., 1975) and *in vivo* analysis of microtubule recovery after washout of microtubule depolymerising drugs (Witt et al., 1980; De Brabander et al., 1986) support this model. Despite the difference in the source of microtubules, both models propose that bipolar attachment is necessary to achieve congression.

3.4.3 Types of kinetochore-microtubule attachments and error correction

After a kinetochore has been captured by the microtubule lattice, the chromosome becomes mono-oriented, a state also referred to as monotelic attachment. When its sister kinetochore attaches to microtubules from the opposite pole, the now bi-oriented chromosome (also know as amphitelic attachment) moves towards the spindle equator. When considering stochastic attachments, two other types of mis-attachments might occur; chromosomes with both kinetochores attached to microtubules from the same spindle pole (syntelic attachment), or one kinetochore attached to microtubules from both poles (merotelic attachment) (Fig. 9).

Monotelic attachment is very common in early mitosis and is normally converted into an amphitelic orientation before anaphase onset. The monotelic attachments

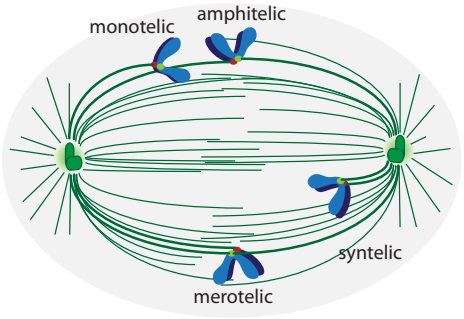

Figure 9 | Types of microtubule attachments. The two sister kinetochores (red and light green elipses) interact with spindle microtubules (green) during prometaphase and metaphase. Monotelic, merotelic and syntelic need to be corrected to achieve the amphitelic attachment before anaphase onset.

prevent spindle checkpoint satisfaction (Rieder et al., 1994; Rieder et al., 1995). In syntelic orientation both kinetochores are occupied by microtubules emanating from the same pole thus, although kinetochores exhibit full microtubule occupancy, the centromere is under reduced tension. This leads to mitotic delay, as tension is thought to play an important role in spindle checkpoint satisfaction. Finally, merotelic attachments, in which a single kinetochore is attached to microtubules from both spindle poles tather than just one, are not detected by the spindle checkpoint (Khodjakov et al., 1997; Wise and Brinkley, 1997; Cimini et al., 2002). Due to this geometry the kinetochores are under less tension than bipolar ones. Nevertheless, many of them are corrected before anaphase onset by an Aurora B-dependent mechanism as discussed below.

Kinetochores are involved in at least two related feedback mechanisms of error correction. The first mechanism coordinates the process of microtubule attachment with mitosis and is named the spindle assembly checkpoint (SAC) (Musacchio and Salmon, 2007). The second mechanism discriminates between correct and incorrect kinetochore-microtubule attachments (Pinsky and Biggins, 2005; Kelly and Funabiki, 2009).

The SAC is able to block anaphase onset by delaying the activation of the anaphase-promoting complex (APC/C) until all chromosomes have been properly bioriented. It is worth emphasizing that the SAC monitors attachments by remaining constitutively active from the beginning of spindle assembly, and only once all microtubules are attached to kinetochores can the SAC be satisfied (Khodjakov and Rieder, 2009). Unattached kinetochores act as the catalytic site for the production of the inhibitory signal. When microtubules capture both sister kinetochores the signal that was

preventing anaphase is silenced. Therefore, blocking the inhibitory signal leads to the activation of the APC/C (Ciliberto and Shah, 2009). The APC/C is an E3 ubiquitin ligase (King et al., 1995; Sudakin et al., 1995). To promote anaphase onset the APC/C is activated by its cofactor, Cdc20 (Fang et al., 1998), and ubiquitinates cyclin B and securin, targeting these substrates for proteasomal destruction (Glotzer et al., 1991; Zou et al., 1999). While decreasing the levels of cyclin B initiates mitotic exit through a reduction in cyclin-dependent kinase (Cdk1) activity (Evans et al., 1983), loss of securin releases the activity of separase where it is free to cleave cohesin, a complex that binds replicated sister chromatids at the inner centromeric region in metaphase (Ciosk et al., 1998; Uhlmann et al., 1999). The best studied components of the SAC pathway are Mad1, Mad2, BubR1, Bub1 and Bub3 (Hoyt et al., 1991; Li and Murray, 1991). Common to these proteins is their specific localization at unattached kinetochores (Chen et al., 1996; Li and Benezra, 1996). After microtubule attachment the SAC proteins need to be removed from the kinetochore. Using kinetochore-bound microtubules as tracks, the dynein engine removes several SAC proteins from kinetochores, including Mad1, Mad2, and components of the RZZ (Rod-Zw10-Zwilch) complex, creating a flow of these proteins towards the spindle pole (Howell et al., 2001; Wojcik et al., 2001; Basto et al., 2004).

It has been postulated that two inputs control the SAC: the kinetochore/microtubule attachment and the tension generated by stretched centromeric chromatin. Classic experiments have clearly shown using laser ablation studies that a single unattached kinetochore prevents the satisfaction of the SAC (Rieder et al., 1994). Furthermore, laser ablation experiments in PtK (Rat Kangaroo) cells demonstrated that mitotic delay was mediated by an inhibitory signal generated by the unattached kinetochore (Rieder et al., 1995). This work also indicated that lack of tension was not sufficient for generating the wait anaphase signal, because cells containing a mono-oriented chromosome in which the unattached kinetochore was ablated exited mitosis shortly after ablation. Therefore critics of the tension role in checkpoint propose that tension, at best, contributes to SAC satisfaction indirectly by stabilizing kinetochore-microtubule attachment. However, experiments carried out at the same time began pointing towards a role of tension in microtubule attachment. Clearly, microtubule-kinetochore attachments are destabilized under low kinetochore tension and stabilized when tension is high between sister kinetochores (Nicklas et al., 2001). How bipolarity is sensed remains poorly understood; however data from pioneering experiments directly

identified tension as the checkpoint signal: tension from a microneedle on a misattached chromosome leads to anaphase (Li and Nicklas, 1995). Further studies identified a link between a change in kinetochore chemistry when under tension: whether from a micromanipulation needle or from normal mitotic forces, tension causes dephosphorylation of the kinetochore proteins recognized by 3F3/2 antibody that detects phosphorylated kinetochore proteins (Gorbsky and Ricketts, 1993; Nicklas et al., 1995). Recently, tension and its impact in the SAC has been associated with intra-kinetochore stretch (Maresca and Salmon, 2009; Uchida et al., 2009). Both studies propose that stretching between inner and outer kinetochore promotes silencing of SAC. More specifically, low intrakinetochore stretch is associated with generation of a wait-anaphase signal, whereas increased intrakinetochore stretch correlated with SAC satisfaction. Whether tension and attachment represent two different pathways of SAC detection or whether lack of tension results in microtubule release is under debate.

The second mechanism of error correction relies on the ability to regulate the stability of microtubule attachments, and to recognize and correct attachments that otherwise fail to result in biorientation. The stability of attachments is controlled by the chromosomal passenger complex (CPC), of which Aurora B kinase is the key enzymatic component (Ruchaud et al., 2007).

The CPC, which contains Aurora B, INCENP, Surivin and Borealin (also know as Dasra), plays multiple roles at different places during mitosis (Ruchaud et al., 2007). During metaphase, the CPC localizes to the inner-centromeric region between sister kinetochores, where Aurora B destabilizes microtubule attachments by phosphorylating kinetochore substrates such as the Ndc80 complex (Cheeseman et al., 2006; Deluca et al., 2006) and the microtubule-depolimerize kinesin, MCAK (Andrews et al., 2004; Lan et al., 2004; Ohi et al., 2004).

The centromeric chromatin between sister kinetochores stretches in response to pulling forces from the kinetochore microtubules, which leads to an increase in interkinetochore distance in response to tension (Skibbens et al., 1993). This raised the possibility of a potential role for tension in correcting microtubule attachments. The first evidence of a protein complex involved in such mechanism came from budding yeast experiments. In this work was shown that Ipl1-Sli15 complex, the yeast ortholog of the

Aurora B-INCENP, played a role in the turnover of microtubules at the kinetochore in a tension dependent manner (Tanaka et al., 2002). Later, a mechanism linking tension to the phosphorylation of Aurora B substrates was established in human cells. In the absence of tension, kinetochore substrates are phosphorylated because they are in close proximity to Aurora B at the inner centromere. In comparison, tension exerted by bipolar attachments moves sister kinetochores in opposite directions, away from the inner centromere, so that kinetochore substrates are further away from the kinase. The net result is that they become dephosphorylated, leading to an increase in their affinity for microtubules and the stabilisation of attachments (Liu et al., 2009).

One proposed molecular mechanism for correcting merotelically-oriented kinetochores is based on the enrichment of the Aurora B complex at inner centromeric regions of mal-oriented kinetochores (Cimini et al., 2004; Cimini et al., 2006). Aurora B kinase promotes kinetochore-microtubule detachment by phosphorylating the N-terminus of the kinetochore protein, Hec1. When kinetochore-microtubules detach, the proximity of the centromeric depolymerase MCAK, promotes rapid depolymerization of the detached microtubule. As the kinetochore associates with microtubules from the correct pole and the centromere becomes stretched, kinetochore-microtubule attachment sites are pulled away from the inner centromere, Hec1 is no longer phosphorylated, and microtubule attachments become more stable.

Syntelic attachments, where both kinetochores are occupied by microtubules of the same pole, lack tension between kinetochores. It has been shown that in the presence of Aurora B inhibitors, such as Hesperadin, the cells enter anaphase in the presence of numerous syntelic and monoriented attachments. This data suggests two effects: that Aurora B is involved in correcting syntelic attachments and that it is required to generate unattached kinetochores (Tanaka et al., 2002; Hauf et al., 2003; Pinsky et al., 2006).

In summary, the mechanisms outlined above are interrelated: Aurora B destabilizes improper attachments and creates unattached kinetochores that in turn recruit checkpoint proteins. These then activate the SAC and prevent anaphase progression (Santaguida and Musacchio, 2009). Moreover, tension has emerged as an important aspect of both the spindle checkpoint and error correction, where the spatial separation of kinases and their substrates must be carefully modulated.

3.4.4 Forces exerted on chromosomes during mitosis

Chromosomes in mitosis are subjected to a large number of forces. When microtubules capture a kinetochore in prometaphase they move rapidly towards a spindle pole. When biorientation is achieved, microtubule plus ends become embedded in kinetochores. Bioriented chromosomes undergo oscillatory movements throughout metaphase (Skibbens et al., 1993) and the kinetochore controls microtubule growth and shrinkage (Hyman and Mitchison, 1990; Hunt and McIntosh, 1998). The forces at the kinetochore-microtubule interface are generated by microtubule motors (eg. dynein and dynactin) located in the outer plate and by the dissociation of the terminal tubulin subunits on the microtubule plus ends. The forces towards opposite spindle poles simultaneously impose tension across the centromeres and increase the separation between sister kinetochores.

At metaphase, an attached kinetochore moves poleward because of forces exerted through its associated microtubules. This stretches the centromere region from its rest length. Once the tension (stretch) on the centromere reaches critical levels, this switches the kinetochore into a neutral state that allows its transport back to the metaphase plate. In literature, a large number of forces have been proposed to govern these movements, but the ones considered significant enough to be taken in account are: 1) $F_{tension}$, elastic tension forces exerted by centromeric chromatin between sister kinetochores during metaphase and 2) F^{kt}_{dep} forces resulting from the antagonistic effect of plus and minus end directed motors, CENP-E and dynein, bound to the kinetochore and moving along microtubules toward the poles (Civelekoglu-Scholey et al., 2006). Mechanical studies using artificial micromanipulation of metaphase chromosomes were done in newt lung or grasshopper cells (Skibbens *et al.*, 1993; Houchmandzadeh *et al.*, 1997; Skibbens and Salmon, 1997; Poirier *et al.*, 2000). These studies showed that chromatin is highly elastic when extended up to 10 times, and that it displayed reversible stretch. For extreme stretching the chromosomes become permanently distorted. Elasticity indicates the nature and strength of the interactions holding materials together and thus can be used to understand the higher-order chromosome structure.

3.4.5 From congression to segregation

When all chromosomes are finally aligned and bioriented at the metaphase plate they do not remain stationary. Instead, chromosomes oscillate around an average position, first moving poleward and then in the reverse direction away-from-pole. This oscillatory behaviour is termed directional instability (Skibbens et al., 1993). After cohesin is degraded, anaphase starts and chromosomes travel to the poles with their movement driven by microtubules.

Several microtubule-associated proteins (MAPs), including EB1, CLASP, XMAP125, Clip170, Nde/Ndel1 and Lis1 are involved in microtubule stabilization; and the kinesin-13 Kif2a and MCAK, which do not have microtubule motor activity, but act as microtubule destabilizers. Together, these proteins are implicated in the regulation of kinetochore microtubule dynamics (Kline-Smith et al., 2005). However, none of the MAPs identified so far seems to be essential for forming end-on attachments (Cheeseman and Desai, 2008).

The current accepted model for metaphase kinetochore oscillation and anaphase A movement proposes that two types of microtubule dynamics are involved: 1) kinetochore based force generating mechanisms, coupled to depolymerization/polymerization of microtubule plus end attachment (PacMan mechanism) and; 2) poleward flux of kinetochore microtubules, i.e. the translocation of tubulin polymers poleward, coupled to minus end depolymerisation close to centrosomes (Maddox et al., 2003). Lower tension promotes the switch to microtubule depolymerisation and high tension promotes microtubule polymerization (Rieder and Salmon, 1994; Skibbens et al., 1995; Skibbens and Salmon, 1997). At metaphase, flux places the kinetochore under tension, resulting in persistent microtubule polymerization. When polymerization at the kinetochore is equal to the flux, the result is a stationary kinetochore. In this case, only small oscillations are observed due to the interchangeable balance of the referred two mechanisms. Initially, sister kinetochore separation at anaphase onset slows the polymerization of kinetochore microtubules and chromosomes start to move poleward. As resistive tension becomes lower, the kinetochore microtubules switch to a depolymerization state and increase the rate of anaphase A to greater than the flux. Therefore, chromosome velocity is the sum of the flux rate plus depolymerization at the kinetochores.

The dominance of the flux or pac-man mechanism appears to differ between cells. For example, embryonic cells seem to rely predominantly on flux activity (Desai et al., 1998; Brust-Mascher and Scholey, 2002; Maddox et al., 2003); whereas somatic cells appear to depend essentially on the pac-man mechanism to segregate their chromosomes (Mitchison and Salmon, 1992).

4. Thesis Outline

The data presented in this dissertation will describe the work I have completed in order to understand the specific role that condensin plays at centromeric chromatin (Chapter IV) and to map the structure and organization of the vertebrate centromere (Chapter V). Each chapter contains a Results section followed by a Discussion section. At the end of the last chapter there is a general Conclusion of the work which includes Future Perspectives and Final Remarks.

III. MATERIAL AND METHODS

1. Chemicals and common solutions

Unless otherwise stated, all chemicals used were purchased from Sigma. Fermentas provided all restriction enzymes, and Invitrogen supplied tissue culture solutions. Phosphate-buffered saline (PBS; 137 mM NaCl, 2.7 mM KCl, 10 mM Na_2KHPO_4 and 2 mM KH_2PO_4). Luria-Bertani medium (LB) is 1% (w/v) tryptone, 0.5% (w/v) yeast extract and 1% (w/v) NaCl pH 7.0.

2. Molecular Biology

2.1 Cloning

RNA was prepared from DT40 cells using TRizol (Invitrogen) and pellets were ressuspended in dH_2O. cDNA was synthesized from 1µg of total RNA using oligo(dT) primers according to the instructions supplied with Superscript First-Strand Synthesis kit (Invitrogen). Hec1 full or partial coding sequence was amplified from DT40 cDNA using appropriate primer pairs (Table 1). The PCR reaction typically contained 0.2 mM dNTPs, 1 mM $MgCl_2$, 0.2 µM primer and 2.5 U Taq Polymerase (Roche) with 1x the corresponding buffer and in 50 µl of final volume. Thermal cycling was performed as recommended by the manufacturer of the DNA polymerase. For linker-CENP-A and SBP, the coding sequence was amplified by PCR from vectors previously constructed in the lab (Hiromi Ogawa and Dr. Kumiko Samejima), using primer pairs (Table 1) with specific restriction. The PCR products were introduced into the appropriate vectors (pGEMT-Easy, Promega; pGEX, Pharmacia; pRSET, Invitrogen; mRFP – derived from pEGFPC1, Clontech) using the standard cloning techniques described below. All constructs were sequenced using ABI Big Dye reaction system (Applied Biosystems).

Table 1 – Cloning and amplification of coding sequences

Primer name	Coding sequence	Vector(s)	Primer sequence 5′ – 3′	Restriction Sites or comments
Hec1Fw Xho	ggHec1 full length	mRFP	Fw - ctc gag att tat agc tca gcc aca atg	XhoI/NotI
Hec1FL RV Age			Rv - acc ggt atg ctt tca gcc ttc ttt tt	
Hec1C BamHI	ggHec1 (483 – stop codon)	pGEMT and pGEX4T-1	Fw - gga tcc aaa gct act caa cgg aaa atg	BamHI/XhoI
Hec1C XhoI			Rv - ctc gag tca gct ttt cgg taa tta	
SBP Fw Nhe	SBP	GFP- linker-CENP-A	Fw - gct agc atg gac gag aag acc acc	NheI/AgeI
SBP Rv Age			Rv - acc ggt ccg ggc tcc cgc tg	
CENP-A fw	linker-CENP-A	pGEMT and Dronpa-C1	Fw - aga tcc gcc gct atc aga g	
CENP-A rv			Rv - gca ggt ctt tgg ggt aca gt	
SMC2 UTR5	5′ UTR SMC2 gene		Fw - ttc act gag ggc tcc ctt cg	Primers to verify insertion of SMC2 transgene
SMC2 Rv			Rv - aat ggc att gaa taa cgg	
tetO Fw	tetO specific primer		Fw - aat ggc att gaa taa cgg	Primers to check that tetO driven SMC2 gene copy was
SMC2 Rv			Rv - aat ggc att gaa taa cgg	

2.2 Electrophoresis of DNA

DNA fragments were separated on agarose gels containing 0.5µg/ml ethidium bromide in TAE buffer (40 mM Tris-acetate pH 8.0, 1 mM EDTA) and visualized on a UV transilluminator. For cloning, gel slices containing the appropriate DNA fragments were excised with a scalpel, and the DNA was purified using the QIAquick Gel Extraction kit (Qiagen).

2.3 Restriction digestion and DNA ligation

Plasmids and PCR fragments were digested with the appropriate restriction enzymes (FastDigest, Fermentas) for 15 min at 37°C. Plasmid DNA was incubated with 10 U of calf intestine phosphatase (New England Biolabs) for 1 h at 37°C. Ligation reactions

were carried out with a plasmid to insert ratio of 2:7 for 5 min with NEB QuickLigase (2000 U).

2.4 Preparation and transformation of competent *E. coli*

E. coli Top10 cells were grown in LB supplemented with 1M $MgSO_4$ at 37°C to an OD600 of 0.5, transferred to ice for 5 min, and pelleted at 3300 x g for 15 min at 4°C. Cells were ressuspended in 40 ml per 100 ml of bacterial culture TfbI (AcOH pH 5.8. 30 mM KAc, 100 mM $RbCl_2$, 10 mM $CaCl_2$, 50 mM $MnCl_2$, 15% (v/v) glycerol), pelleted, and ressuspended again in 4 ml per 100 ml bacterial culture TbfII (KOH pH 6.5, 10 mM MOPS, 10 mM $RbCl_2$, 75 mM $CaCl_2$, 50 mM $MnCl_2$, 15% (v/v) glycerol). All steps were carried out at 4°C and aliquots were snap frozen and stored at -80°C.

For transformations, 100 µl aliquots of competent cells were thawed on ice and mixed with ligation reactions containing up to 100µg of DNA. The mixture was incubated on ice for 20 min, heat shock treated at 42°C for 90 s and chilled on ice for 1 min. 400 µl of LB was added and the cells were incubated on a shaking platform at 37°C for 1h. After pelleting and ressuspending in 100 µl LB, cells were spread on agar plates containing the appropriate antibiotic.

3. SDS PAGE and Immunoblotting

Denaturing protein gel electrophoresis was carried out using the Tris-glycine buffer system described previously (Cleveland et al., 1977). Polyacrimide gels were prepared from a 30% (v/v) acrylamide/bisacrylamide mixture (Severn Biotech). Proteins were dissolved in sample buffer (150 mM Tris-HCl pH 8.8, 2 mM Na-EDTA, 15% (w/v) sucrose, 3% (w/v) SDS, 20 mM DTT) by sonication and boiling. Gels were run in vertical electrophoresis apparatus (BioRad) according to the manufacturer's instructions.

After SDS-PAGE, proteins were transferred to nitrocellulose membranes (Amersham Pharmacia) in transfer buffer (25 mM Tris-HCl pH 8.3, 192mM glycine, 20% (v/v) methanol)

in an electrophoretic transfer unit (BioRad). The membranes were rinsed with dH_2O, stained with Ponceau S to visualize transferred proteins and washed again thoroughly with dH_2O. Blocking was carried out with 5% low fat milk in PBS containing 0.05% (v/v) Tween-20 for 1h at room temperature, followed by incubation with primary antibodies (Table 3) in 3% milk/PBS/Tween-20 for 1h. After three washes with PBS/Tween-20 for 5 min each, the membranes were incubated with appropriate secondary antibodies conjugated to horseradish peroxidase (goat; Immunojackson) in 1% milk/PBS/Tween-20 for 45min. The membrane was washed again and antibody-labeled proteins were detected by ECL (Amersham Pharmacia). For quantification, the LI-COR Odyssey system was employed, and the secondary antibody used was donkey anti-rabbit IRDye® 700DX at 1:5000 dilution (Li-COR Biosciences) in 1%milk/PBS/Tween-20. Membranes were incubated and washed in the same way as described before and scanned using the LI-COR system.

4. Preparation of Nuclei Extracts

Exponentially growing DT40 cells were counted and pelleted, washed in cold PBS, and ressuspended in Nuclei Buffer (10 mM Tris-Cl pH7.5, 10 mM NaCl, 2 mM $MgCl_2$ and protease inhibitor cocktail tablets) using 5 µl per $1x10^6$ cells. Cells were incubated for 10 min on ice, NP-40 was then added to a final concentration of 1% and followed by 5 min incubation. Nuclear extracts were pelleted by centrifugation for 1 min at 4°C and 5500 x g. After ressuspension in sample buffer, samples were sonicated 3x 10 sec and boiled for 5min before being loaded on to an SDS-PAGE gel.

5. Cell culture

Chicken DT40 cells were grown in RPMI 1640 medium supplemented with 5% (v/v) FBS (foetal bovine serum), 1% (v/v) chicken serum, 100 U/ml penicillin and 100 µg/ml streptomycin, at 39°C and 5% CO_2 in a humid incubator.

6. Transient transfection and generation of DT40 stable cell lines

To generate cells expressing transiently the system used was Nucleofector (Lonza, Cologne, Germany). Cells growing exponentially were pelleted and $10x10^6$ cells ressuspended in 10 ml of PBS. After centrifugation (1300 x g, 5 min), 5 µg of DNA and 100 µl of Nucleofector solution V were added to cells and immediately transferred to a cuvette which was placed inside the Nucleofector machine set with program B-030. Immediately the mixture was transferred to a pre-warmed flask with 10 ml of complete medium. Cells were incubated ON and visualized the following day.

Table 2. Stable cell lines constructed

Cell Line	Parental Cell Line	Construct Transfected	Selection Marker
SMC2:GFP-CENP-A	SMC2 KO	**SBP-GFP-linker*-CENP-A** (pEGFPC1, Clontech)	neomycin
:SMC2:Hec1mRFP	SMC2 KO	**Hec1-mRFP** (ggHec1)	puromycin
SMC2:Mad2-GFP	SMC2 KO	**Mad2-GFP** (ggMad2, gift from Dr.Tatsuo Fukagawa, NIG, Tokyo)	puromycin
SMC2:MCAK-GFP	SMC2 KO	**MCAK-GFP** (hsMCAK, gift from Dr. Jason Swedlow, Univ. Dundee)	hygromycin
Dronpa-CENP-A	Clone 18	**Dronpa-linker-CENP-A** (Dronpa C1, gift from Jennifer Lippincott-Schwartz, NIH)	puromycin
CENP-H:GFP-CENP-A	CENP-H KO	**SBP-GFP-linker-CENP-A** (pEGFPN1, Clontech)	puromycin
CENP-C:GFP-CENP-A	CENP-C KO	**SBP-GFP-linker-CENP-A** (pEGFPN1, Clontech)	hygromycin
CENP-N:GFP-CENP-A	CENP-N KO	**SBP-GFP-linker-CENP-A** (pEGFPN1, Clontech)	neomycin
CENP-W:GFP-CENP-A	CENP-W KO	**SBP-GFP-linker-CENP-A** (pEGFPN1, Clontech)	neomycin

* 17-amino acid linker

Stable cells lines were generated using electroporation. Exponentially growing $10x10^6$ cells were centrifuged (1300 x g, 5 min) and washed in 10 ml of Optimem. After another centrifugation, 20 µg of the DNA of interest and 2 µg of plasmid DNA containing a resistant marker were mixed with cells ressuspended in 500 µl of Optimem. The mixture was transferred to a cuvette (Bio-Rad Laboratories, Inc.) and incubated for 3 min on ice. Cells were electroporated at 300 mA and 950 µF (Gene Pulser Xcell Electroporation System, Bio-Rad) and ressuspended in 10 ml of complete media ON. The following day, the total volume was adjusted to 50 ml and the corresponding antibiotic was added according to the resistant marker used. Cells were plated in five 96 well plates using 100

µl media per each well. Plates were checked frequently for single clones per well and after 5-8 days clones were transferred to a 12 well plate with 500 µl of media without antibiotics. Cells were grown exponentially, and positive clones were selected either by FACS, microscopy, immunoblotting or immunostaining with specific antibodies (Table 2).

7. RNA interference

In order to deplete Hec1 a siRNA strategy was used: a 21-mer oligonucleotide (ccagacugaggaagaaauudtdt) covering bases 1404-1424 downstream of the start codon of Gallus gallus Hec1 cDNA was used. A 21-mer oligonucleotide (cguacgcggaauacuucgadtdt) with no significant homology to any known chicken mRNA in the databases was used as a control. The $SMC2^{ON/OFF}$ LacO CEN cell line was grown in the presence (or absence) of doxycycline for 8 h and then $10x10^6$ cells were washed in PBS, ressuspended in 100 µl of Solution V (Lonza, Cologne) with 10 µM of each small interfering RNA. After transferring to a cuvette, cells were transfected using the Nucleofector system (Amaxa, Cologne, Germany) and plated in complete medium plus (or minus) doxycycline. The experiments were analyzed between 26 and 30 h after repression.

8. Purification of CENP-C antibody

Affi-Prep Protein A matrix (Bio-Rad) was washed with 100 mM Tris-Cl, pH 8.0, followed by centrifugation for 5 min at 500 x g. The same volume of serum containing the antibody against ggCENP-C previously raised in the lab (WCE30b) was mixed with Protein A matrix and incubated for 1 h at 4°C in a rotator. To wash the antibody-matrix, the mixture was transferred to a column and 5x total volume 100 mM Tris-Cl pH 8.0 was added to the column, followed by a second wash with 5x total volume 100 mM Tris-Cl pH 8.0. Elution of a small fraction (1/5 of the initial volume each) was carried out with 100 mM glycine pH 3.0 into eppendorfs containing 1/10 of the volume of 1M Tris-Cl pH 8.0 to re-equilibrate the pH. The fractions were assayed for protein concentration using the BioRad Bradford assay, and samples where protein was present were mixed together. Affinity

purified antibody was tested for immunofluorescence at different conditions and dilutions.

9. Indirect Immunofluorescence Microscopy

Chicken DT40 cells were plated on polysine slides (VWR) for 20 min inside the tissue culture incubator. Slides were washed briefly in pre-warmed 1x PBS and fixed for 5 min in 4% (v/v) paraformaldehyde (Electron Microscopy Services) in warm 1xPBS. After permeabilization with 0.15% (v/v) Triton X-100 in 1xPBS, slides were incubated with 1% (v/v) BSA in PBS for 30 min at 37°C inside a humid chamber. Primary antibodies (Table 3) diluted in BSA/PBS were applied for 45-60min at 37°C in a humid chamber. Slides were washed 3 times for 5 min in PBS and incubated with appropriate secondary antibodies conjugated with FITC, Texas Red or Cy5 (1:200 (goat, Immunojackson) at 37°C for 30 min. After three washes with PBS, slides were mounted with coverslips (22x50 mm, thickness 1.5) using Vectashield with Dapi 1.5µg/ml (Vector Laboratories).

Table 3. Antibodies used for immunofluorescence (IF) and immunoblotting (IB)

ANTIBODY	Source	Species	Application and dilutions	Protocol
CENP-A	Fukagawa[a]	Rabbit	IF or IB– 1:2000	PFA and TEEN
H3K9me3	Upstate (07-523)	Rabbit	IF - 1:250	PFA and TEEN
H3K4me2	Upstate (07-030)	Rabbit	IF – 1:250	PFA and TEEN
H3T3ph	Abcam	Rabbit	IF – 1:1000	PFA and TEEN
CENP-H	Fukagawa[a]	Rabbit	IF – 1:200	PFA and TEEN
Hec1	Fukagawa[a]	Rabbit	IF – 1:200	PFA
SBP	**Clone 14**	Mouse	IB – 1:300	
α - Tubulin	SIGMA (B512)	Mouse	IF - 1:1000	PFA and MeOH
γ- Tubulin	SIGMA (GTU-88)	Mouse	IF - 1:1000	MeOH
PP1	Santa Cruz	Rabbit	IB – 1:300	
CENP-T	Fukagawa[a]	Rabbit	IF – 1:1000	PFA and TEEN
CENP-C	**WCE30b**	Rabbit	IF – 1:200	PFA and TEEN
SMC2	**997-3**	Rabbit	IB – 1:1000	
BubR1		Rabbit	IF – 1:500	PFA

a Tatsuo Fukagawa, National Institute of Genetics, Japan.
antibodies from the Earnshaw laboratory are indicated in **bold**.

Image sections were acquired using a microscope (IX-70; Olympus) with a charge-coupled device camera (CH350 or HQ; Photometrics) controlled by DeltaVision SoftWorx

(Applied Precision, LLC) and a 100× S Plan Apocromat NA 1.4 objective using a Sedat Quad filter set (Chroma Technology Corp). Image sections were deconvolved, and maximum projections were generated using SoftWorx. All files were saved as TIFF files and exported to Photoshop (Adobe) for final presentation.

10. Fluorescence In-situ hybridization

A 2kb BamHI fragment from pSV2X5 corresponding to DXZ1, (the large X chromosome-specific alpha satellite array), was labeled with biotin using the Bionick Labelling System (Invitrogen). Unincorporated nucleotides were removed by spin column centrifugation. The probes were ethanol-precipitated with salmon-sperm DNA and resuspended in 50% formamide/2xSSC/IO% dextran sulfate at 37°C. The probes were denatured at 96°C for 10 min and reannealed by incubating on ice. Twenty µl of the probe was added on top of cells previously attached to slides, and put in a heating block at 75°C for 5 min. Slides were incubated overnight at 39°C and washed the next morning in 0.1xSSC which had been pre-warmed to 60°C. The washes were repeated 2 x at 60°C for 5 min each. The last wash was completed using 4x SSC/0.1 % Tween-20. The biotin signal was detected with FITC-avidin using one round of amplification with anti-avidin antibody. The nuclei were then counterstained with DAPI.

11. Sample preparation for electron microscopy

DT40 cells were attached to concanavalin A–coated locator coverslips (EMS). The cells were fixed with 2.5% electron microscopy (EM) grade I glutaraldehyde in PHEM (25 mM HEPES, 10 mM EGTA, 60 mM PIPES, 2 mM $MgCl_2$, pH6.9), and in some cases, 1% Triton was added to the primary fixative to aid in visualizing kinetochore microtubules. Metaphase cells were identified by fluorescence light microscopy (Deltavision system described in section 9.), where z-stack images were acquired and located on the finder grid. Grid coverslips were sent to Bruce McEwen's laboratory (Wadsworth Center, Albany, USA) where they were processed by EM, and together with the grid location coordinates, cells were selected.

12. Time-lapse imaging

Coverslips (22x22 mm, 1.5) were coated with Concanavalin-A (10mg/ml filtered before used), washed thoroughly and dried under the UV. Cells were plated for 20min and assembled on a "rose chamber" with Leibovitz Media (media suitable to keep cells in CO_2-free environments) supplemented with 5% FBS (v/v), 1% (v/v) chicken serum, 100 U/ml penicillin and 100 µg/ml streptomycin. Alternatively, and in order to decrease spindle rotation, an agarose layer was placed on top of the cells. In this process, a solution of 0.02% (w/v) low-melting agarose was prepared in Leibovitz Media. After heating, the mixture was supplemented with 5% FBS and 1% chicken serum. The 170 µm agarose layer was then prepared by placing two 1.5 22x22 mm coverslips on each side of a slide, 300 µl of agarose solution was spread between the two coverslips and another slide was immediately placed over the top. After solidifying, these "sandwiched" layers were kept in a humid chamber at 4°C until use. The agarose layer was cut with a scalpel and gently placed on top of the cells. Finally, the coverslip was mounted in an open "rose chamber", more Leibovitz media was added on the top, and the rose chamber closed with a clean 22x22 mm coverslip.

Digital images were collected with a cooled CCD camera (Orca ER; Hamamatsu, Bridgewater, NJ) coupled to a Yokogawa spinning disk confocal unit (CSU10; Perkin Elmer, Norwalk, CT), which was attached to an inverted microscope (TE300; Nikon, Melville, NY) with a 100× 1.4 NA plan-Apochromatic differential interference contrast objective. Image acquisition and the microscope shutter were controlled by Metamorph software (Universal Imaging, West Chester, PA) on a PC computer. Stage temperature was maintained at ~37°C using an air curtain incubator (ASI 400; Nevtek, Burnsville, VA). Fluorescence images were acquired at 488 nm at a single focal plan with an exposure time of 1500 ms every 4s. For live cell imaging of $SMC2^{ON/OFF}$ CENPH-GFP cells the bin was set to 1x1, while for LacO CEN or LacO Arm the bin was 2x2. Movies were processed and saved as .mov files using Metamorph software.

13. Phage fixation and staining

Fifty µl of P1, T4 and Lambda phage were washed in SM Buffer (50 mM Tris-HCl pH7.5, 100 mM NaCl, 8 mM $MgSO_4$), pelleted after a short spin, and fixed for 5 min in 4% (v/v) PFA in 1xSM. Phage were washed again in SM and ressuspended in 30µl of Vectashield with 1.5µg/ml of Dapi for 20 min. 2 to 3 µl of this suspension were used to mount coverslips with previously fixed $SMC2^{OFF}$ cells expressing CENP-H-GFP or GFP-CENP-A.

14. Quantification of DNA using ImageProPlus

$SMC2^{OFF}$ CENP-H-GFP or GFP-CENP-A cells mixed with phage were visualized using the Deltavision controlled microscope described previously. Cells in metaphase were selected and fields of view 1024 x 1024 were acquired with several z-sections of 200nm. This ensured that phage were also acquired in the same image. After deconvolution, planes where pulled kinetochores could be observed were sum quick projected. Single planes where phages were observed were selected for each image acquired. All the images were saved as TIFF files.

For the phage images, the single TIFF file was opened in ImagePro Plus. Regions of interest (ROI) covering the phage area were selected by hand and the sum intensity value was annotated. Following this, the same ROI was moved between 5-10 pixels and the intensity was annotated as background. The intensity value then was determined by subtracting the background value from the sum value. The intensity values for all phage in each experiment were entered in GraphPad Prism (GraphPad Software, Inc. California, USA) where a XY graph was plotted and the best-fit linear regression calculated. This represented the linear standard of the amount of DNA versus intensity. For the $SMC2^{OFF}$ cells, separated TIFF files of the 488 and 528 nm channels were opened in ImagePro Plus (Media Cybernetics, Inc., Bethesda, USA). Using the 528 nm image, a ROI covering the area occupied by the pulled centromere was selected. This ROI was copied and loaded into the 488 nm file where the sum value of intensity was determined. Again, the background value was determined by moving the ROI 5-10 pixels away from the metaphase plate. The intensity of the Dapi channel was determined by subtracting the background. The

absolute amount of DNA was calculated according to the equation of the previously determined best-fit linear regression.

The line profile was drawn in ImageJ (Research National Institute of Mental Health, Bethesda, USA) values exported to Excel (Microsoft, Redmond, WA), and graphs of each channel superimposed.

15. Image Analysis and Kymographs

The movement of paired lacO:lacI-GFP integrations was followed using the Track Objects tool in Metamorph after image calibration; whenever any of the spots became out of focus, the time point was removed from the raw movie. After exporting the coordinates (x,y) of the LacI spots to Excel (Microsoft, Redmond, WA), the angle between a line drawn through both spots, and the horizontal axis, was calculated for each image in the stack. A custom-written program in MatLab (MathWorks, Natick, MA; created by J. Gatlin – MatLab Code 1.) was used to align and rotate the raw image sections based on the calculated angle and the position of one of the two LacI integrations. The aligned stack was then exported back to Metamorph where the Kymograph tool was used to build kymographs.

The measurements of the lacO integration in fixed samples were obtained using a microscope (Model IX-70; Olympus) controlled by DeltaVision Softworks (as decribed in Section 9.) and using the SoftWorks tool "Measure Distance." The cells were selected according to the following criteria: 1) perfectly aligned metaphase plates and 2) both lacO integrations were visible in the same focal plane. Fluorescence images were acquired at 488 nm on a single focal plane, and the measurements were determined.

The spindle pole separation measurements were carried out on cells immunostained for γ-tubulin, with DNA visualized using DAPI. Measurements were only considered when cells exhibited a clear metaphase plate, and both γ-tubulin stained poles were in the same focal plane. These selected cells were imaged in a single focal plane at 568 nm, and the distance was measured.

MatLab Code 1. Spindle Rotation

```
% SpindleRotation

% Written by J.C. Gatlin to align and rotate time-lapse images of spindles.
The program reads in a metamorph stack to be aligned and rotated.
% It gets the rotation angles for each image from an excel spreadsheet that
% includes rotation angles calculated from spindle pole positions obtained
% using the Metamorph track points/objects tool.
% This program uses functions from the DIPimage library (goto www.diplib.org
% to download)

clear all;
Stack = FNtiffread;
[D1,D2] = size(Stack);
[D3,D4] = size(Stack(1).data);
Angles = xlsread('TrackingDOX6',-1);
Pole1coords = xlsread('TrackingDOX6',-1);

% Creates a larger image in which the original image can be rotated without
% losing information.  This image is four times the original in size!

FillerMat = zeros(size(Stack(1).data));
FillerMat2 = cat(1,FillerMat,FillerMat);
for i = 1:D2;
    BigStack = cat(1,Stack(i).data,FillerMat);
    BiggestStack = cat(2,BigStack,FillerMat2);
    [D5 D6] =size(BiggestStack);

% Translates the left-most spindle pole in the original image to the middle
% of the larger image.  This is required because the rotation function of
% dip_image rotates around the image center, not the origin.

    xCoord = round(Pole1coords(i,1));
    yCoord = round(Pole1coords(i,2));
    xCenter = floor(D6/2+1);
    yCenter = floor(D5/2+1);
    xTrans = xCenter-xCoord;
    yTrans = yCenter-yCoord;
    se = translate(strel(1), [yTrans xTrans]);
    preRot = imdilate(BiggestStack,se);

% Rotates the each entire image around the center and then creates a stack
of smaller, cropped images displaying the horizontally aligned pole pair.

    Rotated = rotation(preRot,Angles(i));
    Dimenori = [D4 D3];
    Dimenrot =size(Rotated);
    RectXmin = floor (abs((Dimenrot(1,1)-Dimenori(1,1)))/2+1);
    RectYmin = floor (abs((Dimenrot(1,2)-Dimenori(1,2)))/2+1);
    RotatedCrop = dip_crop(Rotated,[RectXmin RectYmin], Dimenori);
    if (i<10);
        filename = ['SeqImages00',num2str(i),'.tif'];
        else if (i<100);
                filename = ['SeqImages0',num2str(i),'.tif'];
                else filename = ['SeqImages',num2str(i),'.tif'];
            end;
    end;
fileroot =['c:\Program Files\MATLAB\R2006b\work\',filename];
imwrite(uint16(RotatedCrop),fileroot,'Compression','none');
end;
```

16. Determination of number of CENP-H molecules per kinetochore

SMC2^{ON} and SMC2^{OFF} cells were plated in ConA-coated coverslips and after cells were fixed and mixed with budding yeast cells expressing GFP tagged Ndc80p at its own chromosomal locus. Image sections with 200 nm step size along the z-axis were acquired using a Nikon Eclipse-TE2000U with 1.4 NA, 100x DIC oil immersion objective. Emission was collected by the same objective and imaged by a cooled CCD Orca ER (Hamamatsu) camera after passing through a standard GFP filter set from Chroma. Image acquisition was controlled by Metamorph 6.0. Fluorescence images were acquired with an exposure time of 400 ms.

To determine fluorescence intensity of CENP-H-GFP of each kinetochore image intensities were integrated using a 5x5 pixel region after subtracting the background signal. The same procedure was used to quantify each cluster of budding yeast kinetochores, assuming 8 copies of Ndc80p at each of the 16 chromosomes. The absolute number of CENP-H-GFP per kinetochore was determined using Ndc80p as an internal reference. Fluorescence intensity was converted in number of molecules, knowing that each budding yeast kinetochore has 8 Ndc80 molecules.

17. Sample preparation for super-resolution microscopy

Cells expressing Dronpa-CENPA were plated on washed coverslips for 20min and washed with Dulbeco's PBS without Calcium or Magnesium (Invitrogen). Coverslips were then incubated in 1xTEEN (10xTEEN – 25 mM NaCl, 200 nM NaEDTA pH9.0, 1 mM Triethanolamine-HCl pH8.5) for 30 min. To produce chromatin shearing the Coverslips were carefully removed from the solution with forceps and the bottom part leant against 3MM filter paper, and immediately placed in 4% (v/v) PFA in TEEN where they were fixed for 5min. The Coverslips were blocked in 1% BSA (v/v) in D-PBS for 30 min at 37°C, and incubated with appropriate primary antibodies for 45-60 min. After 3 washes in D-PBS, coverslips were incubated for 30 min at 37˚C with appropriate secondary antibodies coupled to AlexaFluor 647 (1:200; Invitrogen), washed several more times, and kept ON at 4°C in D-PBS.

18. Super-resolution microscopy with single molecule sensitivity

Single-molecule fluorescence imaging was performed on a Nikon Eclipse TE2000 inverted microscope, equipped with a total internal reflection fluorescence (TIRF) oil-immersion objective (Apochromat, 60x, NA 1.49, Nikon). Excitation was provided by a 488 nm CW Ar+ laser (163-C, Spectra-Physics, 0.5 kW/cm2) or a 633-nm He/Ne CW laser (Coherent model #31-2140-000, 1 kW/cm2 at the sample) passing through appropriate bandpass filters (Chroma Technology). Pulses for dronpa photoactivation (2 Hz, 5 ms, 1 W/cm^2) were provided by a CW 405-nm laser (Cube, Coherent) passing through an electronic shutter (Newport), that in turn was controlled by a function generator (USB-6218, National Instruments). Widefield illumination was achieved by focusing the expanded and collimated laser beam onto the back-focal plane of the objective. The resulting illuminated area was roughly of about 60 µm in diameter. Emission was collected by the same objective and imaged by an Andor Luca (S) EMCCD (Electron Multiplying Charge Coupled Device) camera after passing through a dichroic mirror (z488rdc or z633rdc, Chroma Technology) and additional spectral filters (HQ500LP and HQ530/50, or HQ645LP and HQ700/75, Chroma Technology). Additional lenses resulted in a final pixel size of 74 nm. Integration time per frame was 100 ms, and the total number of frames collected was typically 500-1000. Two-color imaging of Dronpa and AlexaFluor 647 was performed sequentially. Chromatic shifts were corrected by localizing immobilized 0.1 µm Tetraspeck beads (Invitrogen) with both colors.

The movies were analyzed with an Igor Pro routine by fitting Gaussian functions to individual molecules and localizing their centre. Density super-resolution images were reconstructed by dividing each pixel into 4 subpixels and assigning each localization to a subpixel. The image brightness thus represents the density of localizations in a subpixel. The FWHM (full width at half maximum) values were estimated from line cross-sections of the fibers drawn with ImageJ by fitting a Gaussian function in GraphPad Prism. Similarly, a spatial resolution of 37 nm was estimated by multiple localizations of the same single molecule of AlexaFluor647 in the same conditions of the above experiments, and fitting a Gaussian function to its cross section in a density reconstructed image.

IV. CONDENSIN REGULATES THE STIFFNESS OF THE VERTEBRATE CENTROMERE

1. INTRODUCTION

Accurate chromosome segregation is essential to correctly transmit the genetic information to the next generation during the cell cycle. In mitosis, the replicated chromatin is condensed into rod-shaped structures: the chromosomes. The chromosomes are composed of two sister chromatids held together by cohesion at a specialised chromosomal region: the centromere. The centromeric region is also where the kinetochores assemble during mitosis. The centromere/kinetochore directs a series of key tasks in chromosome segregation: it is involved in sister chromatid cohesion and separation; it is the site where microtubules of the mitotic spindle attach; it monitors microtubule proper attachment by activating/deactivating the spindle assembly checkpoint; and it is the force generator to drive chromosome movement (Przewloka and Glover, 2009).

In order to obtain a correct distribution of the genetic material during cell division, the chromosomes need to achieve a special configuration during mitosis. The chromosomes have to align at the "metaphase plate" with the sister kinetochores attached to spindle fibers coming from opposite poles: this is called bi-orientation.

Chromosome alignment in metaphase is the result of an equilibrium of forces generated by the mitotic spindle, the chromosomes and the molecular effectors that mediate connections between kinetochores and microtubules. Kinetochores remain attached to microtubule tips even during their assembly and disassembly. This generates the back and forth movements of the sister kinetochores on the metaphase plate known as oscillations. At the metaphase plate, tension is generated because robust centromere chromatin linking sister kinetochores opposes the pulling forces of the spindle. When all chromosomes are oriented and under tension, the spindle checkpoint is inactivated and anaphase occurs.

The microtubule-based spindle machinery is well characterized at the biochemical and biophysical level. Mathematical and computational models of the spindle apparatus, based on experimental data, are able to describe the principles of the spindle assembly and its maintenance throughout mitosis (Cytrynbaum et al., 2003; Civelekoglu-Scholey et al., 2006; Mogilner et al., 2006; Pearson et al., 2006). On the other

hand, chromatin also has a determinant role in responding to spindle forces, especially at the centromeric region. However, the mechanical properties of centromere chromatin remain largely undefined.

Recently Bouck and Bloom demonstrated that nucleosomes have a role in the rest length of centromeric chromatin (i.e., the characteristic length of inner centromeric chromatin when is unloaded). Decreasing the density of nucleosomes interferes with centromeric chromatin's rest length (Bouck and Bloom, 2007). In their study, the levels of histone H3 and H4 were depleted in G1 phase yeast using a regulatable promoter and cells were examined in the following mitosis. In metaphase, the bipolar spindle was normal, however both spindle length and interkinetochore distance were increased. These increases were dependent on microtubule pulling forces (showed after depletion of two kinesin motors when a decrease in these lengths was observed). If chromatin is modeled as an elastic polymer that obeys Hooke's Law their study shows that once histones are depleted the chromatin rest length increases. However, no difference was observed in the spring constant (the characteristic value that defines the properties of an elastic material) that governs the chromatin elasticity.

Although chromatin was once thought to be a passive component of the mitotic apparatus, it is now thought to have an active role. Discovery of the elastic pericentromeric chromatin in the yeast spindle (Bouck and Bloom, 2007) suggests that mechanical alterations at the pericentromeric region, might also be involved in regulating chromosome segregation, microtubule dynamics and checkpoint function. Thus, it is important to define contributions of centromeric chromatin to spindle stability.

One of the aims of my work was to understand the function of the condensin complex specifically at the centromere during mitosis. Condensin I and II are pentameric protein complexes that share two of the subunits, and are among the most abundant non-histone components of mitotic chromosomes. Using a conditional knockout of SMC2 (a subunit present in both condensin I and II complexes) in chicken DT40 cells the Earnshaw lab has demonstrated that chromosomes can condense in the absence of condensin ($SMC2^{OFF}$) to a degree close to wild-type ($SMC2^{ON}$) (Vagnarelli et al., 2006). These chromosomes can align on the metaphase plate but anaphase segregation displays chromatin bridges that block cytokinesis.

This conditional knockout was used to analyse the behaviour of centromeres in metaphase in the absence of condensin ($SMC2^{OFF}$) (Ribeiro et al., 2009). By high-resolution live cell analysis of kinetochore behaviour in metaphase, I have shown that the centromeric chromatin is abnormally stretched in the absence of condensin. Kinetochores perform prominent excursions toward the poles, trailing behind a thin thread of chromatin. These excursions are reversible suggesting that the centromeric chromatin behaves like an elastic polymer.

Importantly, condensin is dispensable for the normal level of compaction (rest length) of centromeres in the absence of tension. If the centromeric chromatin is modelled as an elastic polymer, the absence of condensin decreases its stiffness (spring constant) by 50% when pulling forces are applied (i.e. microtubules attached to the kinetochores). I have also shown that condensin ATPase activity is an important regulator of centromere rigidity and function. By analysing mitotic progression of cells with or without condensin, I was able to assign a biological function to the lack of stiffness within the centromeric chromatin: weak centromeres lacking condensin delay anaphase onset by altering the timely silencing of the spindle assembly checkpoint.

The work in this chapter was done under close supervision of Dr. Paola Vagnarelli, so Dr. Paola Vagnarelli contributed to the work presented in the figures thoughout this chapter.

2. RESULTS

2.1 The inter-kinetochore distance is increased in condensin-depleted cells

The chicken DT40 is a B lymphocyte cell line that has been used in the laboratory as a model system to study vertebrate protein function by gene knockout. One essential advantage of this system is the high homologous recombination rate, which enables the ready generation of knockouts of essential genes (Buerstedde and Takeda, 1991; Sonoda et al., 1998). In the past, Dr. Damien Hudson in our laboratory generated a conditional knockout cell line for condensin I and II by targeting the single copy of the condensin subunit gene SMC2. The cells were kept alive by expressing the SMC2 cDNA under the control of a tetracycline-repressible promoter (Hudson et al., 2003). This enabled us to obtain SMC2-depleted cells ($SMC2^{OFF}$ cells) following the addition of the tetracycline analogue doxycycline, which shuts off expression of the "rescuing" cDNA. $SMC2^{OFF}$ cells are a useful tool for detailed study of both condensin I and II functions during specific stages of mitosis when analyzed in parallel with the same cell line in which SMC2 expression has not been repressed ($SMC2^{ON}$ cells).

Condensin depleted cells still condense chromosomes during mitosis, yet the chromosome arms only reach 60% of the normal condensation (Vagnarelli et al., 2006). During metaphase one of the most noticeable phenomena, in these cells, is the oscillation between sister kinetochores that occurs once microtubules bind to kinetochores. In metaphase of $SMC2^{OFF}$ fixed cells the interkinetochore distance (measured as the distance between CENP-H-GFP of sister kinetochores) is 1.4 greater than in $SMC2^{ON}$ metaphase cells (Fig. 1). However, if microtubules are depolymerized with colcemid, the distance between sister kinetochores in $SMC2^{OFF}$ cells is the same as that in cells expressing SMC2 (Fig. 1). These results reveal that condensin is not necessary to set the rest length of the centromeric region. However, once the microtubules attach to kinetochores and exert pulling forces, centromeres lacking condensin are unable to respond normally.

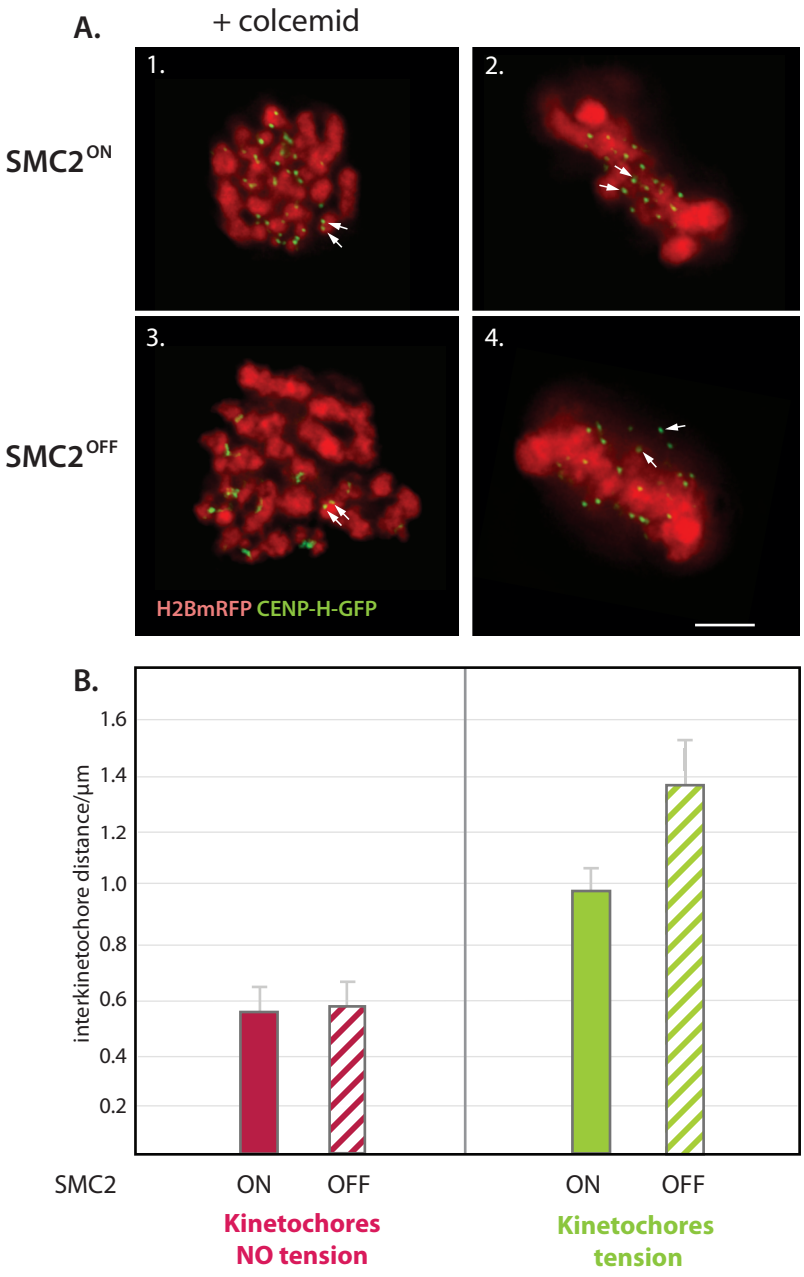

Figure 1 | Condensin affects interkinetochore distance in a microtubule dependent fashion. A. H2BmRFP:CENP-H-GFP SMC2$^{ON/OFF}$ cells, in the absence of microtubules (+colcemid) (1. and 3.) or in the presence of microtubules and aligned in metaphase (2. and 4.). Arrows indicate sister kinetochores. Scale bar 5 µm. **B.** Graph representing the distance between sister kinetochores in the four situations depicted in the images of panel A. (error bars represent s.d., n=100 for each of 3 independent experiments).

2.2 Live-cell imaging shows prominent excursions of kinetochores during metaphase in SMC2^{OFF} cells

To determine the types of deformation occurring in the centromeric region observed in the absence of condensin we carried out live cell imaging in SMC2^{OFF} cells. To observe kinetochore movements by live cell imaging, the parental SMC2 KO cell line was engineered by tagging the endogenous single copy of CENP-H gene with GFP so that it was expressed under control of its own promoter, thereby creating a fully functional tagged copy of this essential protein (from now on designated SMC2$^{ON/OFF}$-CENP-H-GFP) (Fukagawa et al., 2001; Vagnarelli et al., 2006). Live cell imaging was carried out using a spinning disk confocal microscope. Image acquisition conditions were determined to ensure minimum perturbation to the cells and preservation of the normal progression of mitosis. Examples of still images from the movie are shown in Fig. 2A. Condensin-depleted cells underwent abnormal centromeric oscillations during metaphase. Centromeres engaged in poleward movement appeared to pull out long "strings" of subjacent chromatin rather than moving the whole chromosome (Fig. 2B). To analyse more closely these differences we tracked the interkinetochore distances by selecting pairs of kinetochores that remained in the same focal plane for at least 90 sec. In control cells, the interkinetochore distance fluctuated within the narrow range of 0.4 to 0.8 μm (n=6). In SMC2^{OFF} cells the amplitude of oscillatory movements increased dramatically and ranged between 0.5 and 1.9 μm (n=5) (Fig. 2C).

These data show that centromere oscillations in condensin-depleted cells, although displaying a wider range of distances, can approach values observed in control SMC2^{ON} cells. Previous studies showed contradictory results concerning the reversibility/irreversibility of these movements in the presence/absence of bipolar attachment (Oliveira et al., 2005; Gerlich et al., 2006). While one study reported that when CAP-D2 subunit of condensin I was depleted in HeLa cells the sister kinetochores showed abnormal reverse stretch in the presence of microtubules (Gerlich et al., 2006). Another study stated that when condensin I subunit CAP-H is depleted by RNAi in *D. melanogaster* the deformations of chromatin after stretch were permanent and not reversible (Oliveira et al., 2005). Our results are in agreement with Gerlich *et al.* data where a reversible behaviour of centromeric chromatin in the absence of condensin is observed. Furthermore we can rule out the hypothesis that inner centromeric chromatin in chicken DT40 cells is permanently deformed in the absence of condesin.

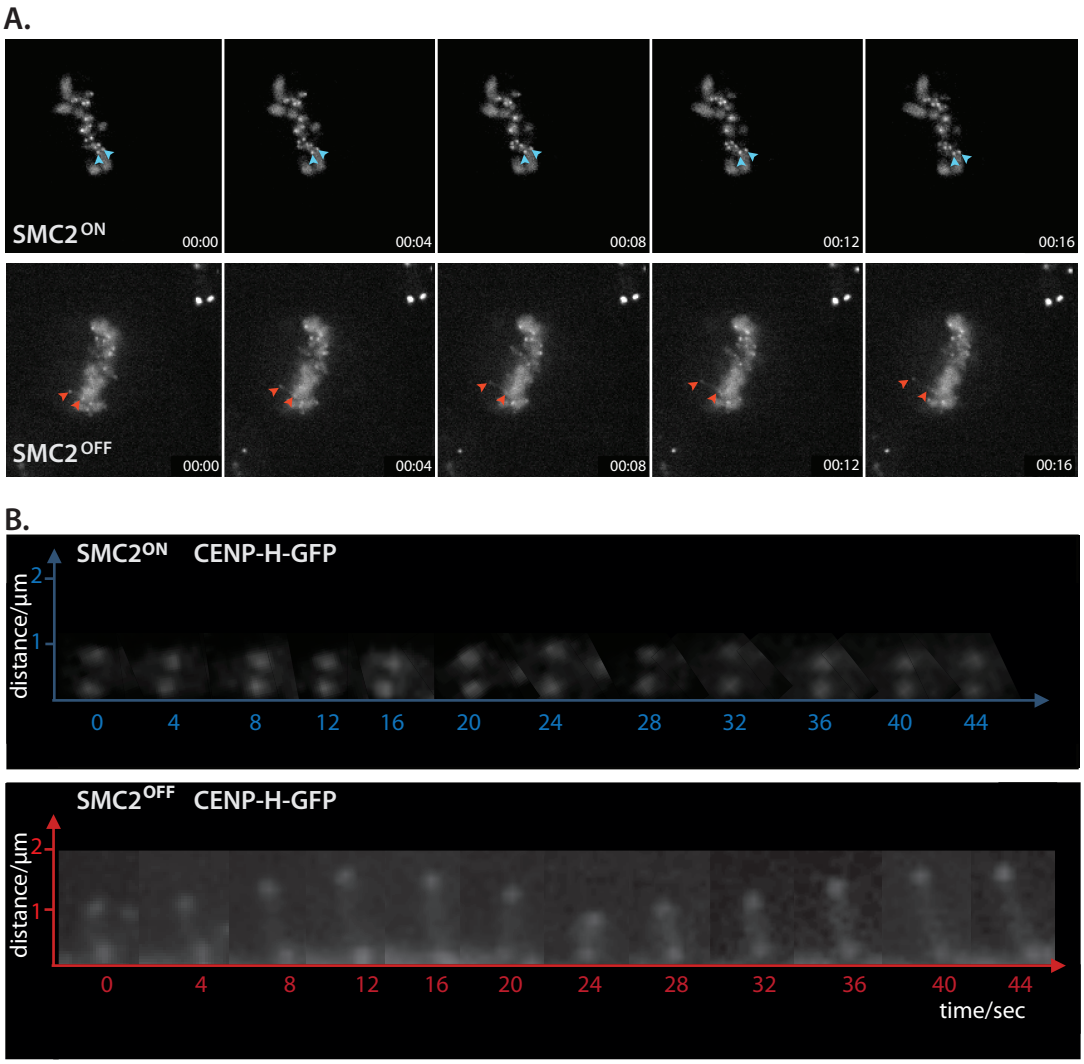

Figure 2 | Condensin depleted cells show abnormal inner centromeric movements. A. Still images from time-lapse movies of CENP-H-GFP cells in metaphase imaged every 4 sec. Arrowheads indicate sister kinetochore oscillations. **B.** Comparison between excursions undertaken by kinetochore pairs of SMC2^{ON} and SMC2^{OFF} cells. **C.** Examples of movements of kinetochores tracked distances obtained from *in vivo* analysis of SMC2^{ON} cells (blue lines, n=6) and SCM2^{OFF} cells (red lines, n=4).

2.3 Abnormal kinetochore movement is quenched in the presence of nocodazole

We have shown that the centromeric chromatin exhibits elastic behaviour in the absence of condensin such that centromeres return to their original position. This could happen because of normal oscillatory contractile and distension movements imposed by spindle microtubules (Shelby et al., 1996).

To further characterize the microtubule dependence of the abnormal kinetochore movement we carried out live cell analysis of the effect of the microtubule destabilizing drug nocodazole on kinetochore movements in the absence of condensin. $SMC2^{OFF}$-CENP-H-GFP cells were imaged under the microscope while nocodazole was added to the chamber (Fig. 3). Five minutes after the addition of nocodazole the long-range oscillations observed in $SMC2^{OFF}$ cells ceased and centromeres recompacted to similar levels as in control cells.

These results show that the removal of the pulling forces exerted by bipolar attachment allows sister centromeres of $SMC2^{OFF}$ cells to recover their normal rest length, indicating that these movements are reversible and microtubule-dependent.

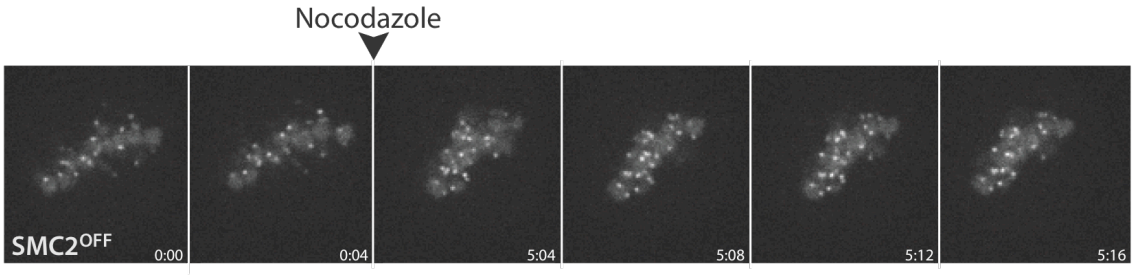

Figure 3 | Kinetochore excursions in condensin-depleted cells are microtubule dependent. Still images from live cell imaging of condensin depleted cells expressing CENP-H-GFP (every 4 sec). Arrow indicates time of addition of nocodazole to the cells. Imaging was resumed 5 min after nocodazole addition and shows that the abnormal kinetohores excursions cease.

2.4 LacO integration in the pericentromeric region of condensin-depleted chromosomes mimics kinetochore behaviour

Chicken DT40 cells have ~70 chromosomes. This means that in mitosis there are more than 140 kinetochores moving on the spindle. This large number of kinetochores was a limitation for further *in vivo* analysis of centromere behaviour in the absence of condensin. Dr. Paola Vagnarelli in our laboratory previously established a series of cell lines with LacO integrations into DT40 chromosomes. A DNA construct containing 256 copies of the lac operator (*E. coli LacO*) repeat together with a gene encoding dihydrofolate reductase (DHFR) was introduced into the SMC2 knockout cells. This array can be visualized with Lac repressor fused to GFP (Belmont and Straight, 1998; Vagnarelli et al., 2006). Several cell lines were obtained, one of which had a LacO:LacI integration in the pericentromeric region of a microchromosome (Fig. 4C CEN).

Live cell imaging was performed in similar conditions as for CENP-H-GFP SMC2$^{ON/OFF}$ cells. On average the LacO:LacI integration sites on sister chromatids in SMC2^{OFF} cells were further apart than they were in control SMC2^{ON} cells (Fig. 5C and D). Furthermore, monitoring the LacO:LacO-CEN integration revealed that the pericentromeric region underwent excursions resembling those of kinetochores in SMC2^{OFF} cells (Fig. 4B). Analysis of the LacO integrations showed that in the absence of condensin the pericentromeric oscillations fluctuated between -0.33 and 0.37 μm (n=7) whereas in control cells the oscillation values fell into the range between -0.19 and 0.12 μm (n=3) (Fig. 5C). Measurement of the distances between insertions in SMC2^{ON} metaphase cells yielded values within the relatively narrow range of 0.32 to 0.52 μm (n=3). In SMC2^{OFF} cells the distance between paired integrations fluctuated between a minimum of 0.45 and a maximum of 1.39 μm (n=7) (Fig. 5A). The stretching of inner centromere chromatin is manifested as sister kinetochore "breathing" when chromosomes are aligned and bipolar attached to microtubules. This phenomenon has been reported after insertion of reporter arrays adjacent to centromeres in budding yeast (Goshima and Yanagida, 2000; He et al., 2000; Tanaka et al., 2000; Pearson et al., 2001). However, this phenomenon has not previously been observed in vertebrate cells.

To simplify the analysis of the output data from *in vivo* imaging Dr. Jay Gatlin (Salmon's Lab, UNC, Chapel Hill) developed a MatLab code to analyze kinetochore movements. This code aligns and rotates the raw data from a movie and based on

calculated angles from tracking analysis aligns one of the two LacO:LacI integrations. After running the code, the aligned movies were exported back to Metamorph to prepare kymographs (graphical representations of spatial position over time in which the y axis represents time). In Figure 4B examples of kymographs are shown. The increase in amplitude of movements is easily observed of LacO-CEN in $SMC2^{OFF}$ cells compared to the kymograph of $SMC2^{ON}$ cells.

We then studied a second cell line with integration in the arm of a macrochromosome to verify if the abnormal oscillations were specific to the pericentromeric region of the chromosome (Fig. 4C ARM). We used the same live cell imaging conditions to analyse this integration. The kymograph of Figure 4B shows no oscillatory movements either in presence or absence of condensin (Fig. 5D). When comparing between $SMC2^{ON}$ and $SMC2^{OFF}$ cells it is important to notice that the distance in condensin-null cells is larger. This is due to the fact that chromatin compaction at non-centromeric loci in $SMC2^{OFF}$ cells is only 60% of that in $SMC2^{ON}$ cells (Vagnarelli et al., 2006).

To test if the movements of centromere-proximal integration were also dependent on microtubule attachment we treated LacO-CEN $SMC2^{OFF}$ cells with the microtubule stabilizing drug nocodazole. After selecting metaphase-aligned cells we started *in vivo* image acquisition. To add nocodazole (0.5 µg/ml) to the Rose Chamber we stopped recording and image acquisition was resumed after 5 minutes (Fig. 4B and Fig. 5F). The kymograph illustrates that 5 minutes after the addition of nocodazole the oscillations ceased. This indicates that the abnormal movement of a pericentromeric LacO array is microtubule dependent, as shown for kinetochores (Fig. 3).

In conclusion, our data show that we have developed an extremely simplified, yet powerful system to further study parameters involved in centromere stretching/compaction in the absence of condensin.

To explore the influence of microtubule binding by kinetochores on the abnormal metaphase oscillations observed in the absence of condensin, we depleted Hec1 with RNAi. Hec1 is part of the tetrameric complex Ndc80, which is a stable core component of the outer kinetochore plate essential for organizing microtubule attachment sites. Hec1 is also involved in the regulation of kinetochore microtubule plus-end dynamics and attachment stability (DeLuca et al., 2005; Deluca et al., 2006). Hec1 depletion was

performed in both SMC2^{ON} and SMC2^{OFF} cells bearing LacO-CEN using a specific RNAi oligo for chicken Hec1 protein and a control oligonucleotide. Cells were nucleofected 8 hours after doxycycline treatment (to initiate the depletion of condensin) and the *in vivo* analysis was done 20 hours later by plating cells on Concavalin-A treated coverslips. For each condition, twelve movies were made. To calculate the distances between the 2 LacI insertions we used the MetaMorph "Track Distances" tool (Fig. 5G). Some of the movies were also used to build kymographs (fig. 4B). The control oligonucleotide had no effect on the oscillation of LacO-CEN movements in SMC2^{OFF} cells. The depletion of Hec1 in SMC2^{ON} cells also did not alter the normal distances observed between LacO-CEN loci on sister chromatids. However, SMC2^{OFF} cells depleted of Hec1 showed metaphase oscillatory amplitudes similar to SMC2^{ON} cells. Thus, when kinetochore/microtubule binding stability is compromised, the abnormal metaphase stretching associated with condensin depletion ceases. These results show that microtubule attachment and dynamics at the kinetochore plate during metaphase are also important to drive the observed oscillations.

As mentioned above, previous studies of centromeric chromatin after RNAi depletion of condensin I gave contradictory results. While one study done in HeLa cells suggested that centromeric chromatin had elastic behaviour (Gerlich et al., 2006), data from another study using *Drosophila* cells proposes a plastic behaviour of the centromeric chromatin, such that stretching distortions were not reversed (Oliveira et al., 2005). One possible explanation for the conflicting results is that condensin might have different roles in different organisms. Still another reason that could explain the different result is the way the analysis was carried out: live cell imaging and fixed analysis, respectively. The data that I have presented thus far for chicken DT40 cells shows that centromeric chromatin in the absence of the condensin complex has an elastic behaviour, similar to that observed in HeLa cells. But there was still one hypothesis remaining to be ruled out that could explain the difference: Oliveira *et al.,* used the proteasome inhibitor MG132 throughout their study in order to block cells in metaphase. Centromeric chromatin of cells blocked in metaphase might lose its ability to go through the back and forth movements after a while and be permanently deformed. Alternatively, MG132 could have a secondary effect on the dynamic kinetochore excursions. To test these hypotheses we did live cell imaging of SMC2^{OFF} LacO-CEN cells after a two-hour treatment with MG132. As shown in the kymograph in Figure 4B (and graph Fig. 5E), there is no alteration in the oscillatory extensions observed when cells are blocked in metaphase. Thus, the plastic

deformation observed in the centromeric chromatin of *Drosophila* cells following condensin depletion cannot be a consequence of prolonged metaphase. It also cannot be explained as a side effect of MG132 treatment. Either different organisms have different roles for condensin at the pericentromeric chromatin or the analysis of fixed samples does not permit detection of the types of deformation undergone by this chromosomal region.

Overall these results show that LacO-CEN integrations are a useful tool to dissect the mechanical properties of pericentromeric chromatin. These studies also show that microtubule binding and dynamics govern the abnormal movement, independently of the amount of time spent in mitosis.

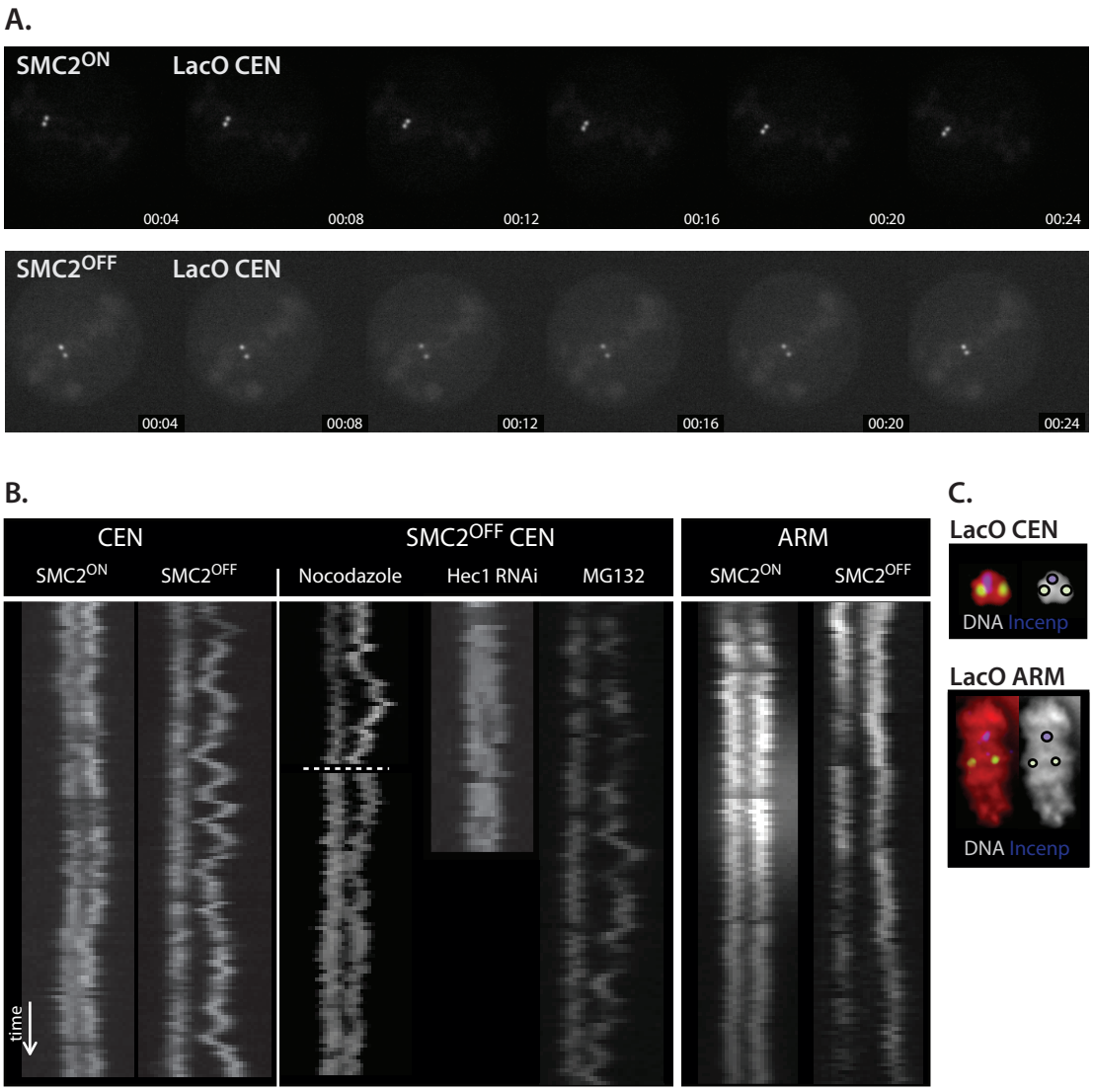

Figure 4 | LacO integration at a pericentromeric loci recapitulates kinetochore movements. A. Still images from movies of LacOCEN integration in SMC2^{ON} (top panel) and SMC2^{OFF} (bottom panel) cells, showing the normal and abnormal oscillations, respectively. **B.** Kymographs of the LacO array movements. In SMC2^{OFF} cells LacO integration at the pericentromeric chromatin undergoes excursions similar to those of sister kinetochores. These movements are abolished after nocodazole treatment (dotted line indicates time of addition) and Hec1 RNAi. LacO movements are not affected by treatment with the proteasome inhibitor MG132. In SMC2^{OFF} cells the LacO ARM integrations does not oscillate but exhibits an increased LacO spacing. **C.** INCENP immunostaining in the two different LacO cell lines under analysis. LacO CEN - LacO integration on a microchromosome in close proximity to the inner centromeric chromatin as detected by INCENP. LacO ARM - LacO integration on a macrochromosome where the inner centromeric region detected by INCENP is distant from the LacO:LacIGFP loci.

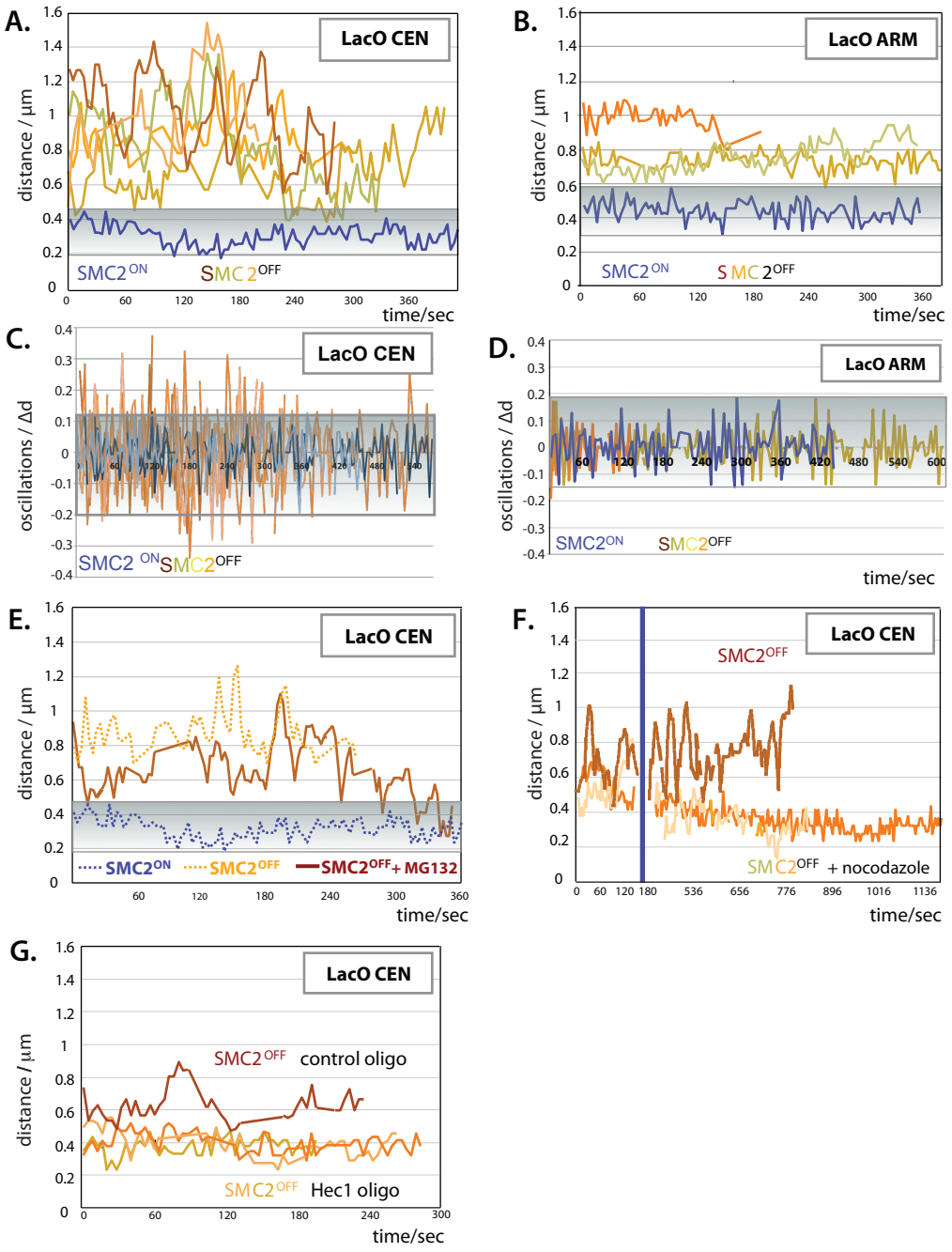

Figure 5 | Live cell imaging analysis of LacO integrations movements during metaphase under different conditions. LacO integration at the pericentromeric region of a microchromosome (LacO:CEN) (A,C,E,F and G) and the same integration at the arm of a macrochromosome (LacO:ARM) (B,D) in unperturbed SMC2^{ON} and SMC2^{OFF} cell lines and after treatment with MG132 (E), nocodazole (F) and Hec1 RNAi (G). The shaded area in A, B, C, D and E indicate the range of movements occurring in control SMC2^{ON} cells. **A. and C.** The amplitude of SMC2^{OFF}:LacO CEN oscillations (brown, grey, orange lines) is much wider than the ocillations observed in SMC2^{ON} cells (blue line). **B. and D.** The amplitude of SMC2^{OFF}:LacO ARM oscillations (brown, grey, orange lines) is within the range of the SMC2^{ON} (blue line). **E.** MG132 does not affect the extended movements of the LacO:CEN in the absence of condensin (brown line). **F.** Nocodazole treatment (blue bar indicates the time at which nocodazole was added to the culture) cease (pale brown and orange lines) the extended oscillatory movements of untreated SMC2^{OFF} cells (brown line). **G.** Hec1 RNAi (pale brown, orange and yellow lines), but not a control oligonucleotide (brown line), abolishes the extended movements of the LacO:CEN in the absence of condensin.

2.5 SMC2 ATPase mutant does not rescue the abnormal dynamic behaviour of LacO integration

One key to understanding the role of condensin at the centromeric chromatin is to ascertain whether the ATPase activity of the complex is essential to confer stiffness. A known strength of chicken DT40 cells is the ability to do complementation studies. Thus, it is possible to look at ATPase mutants of SMC2 homogenously expressed in a SMC2 depleted background. The SMC2 ATP hydrolysis mutant used (S1086R) has the ability to assemble the condensin complex and bind chromatin but does not rescue life (Hudson et al., 2008).

We prepared $SMC2^{ON}$ and $SMC2^{OFF}$ LacO-CEN stable cell lines expressing wild-type SMC2 or the above mentioned mutant. SBP-tagged cDNAs of wild-type ($SMC2^{WT}$) and SMC2 mutant ($SMC2^{S1086R}$) were expressed under the control of a 3.8 Kb fragment from the endogenous SMC2 promoter. We confirmed that cells expressing $SMC2^{WT}$ are able to rescue the $SMC2^{OFF}$ phenotype. To confirm that both cDNAs were expressed in the null background I analyzed RNA extracted from $SMC2^{ON}$ and $SMC2^{OFF}$ cells. TetO specific primers only amplify a fragment corresponding to the original tetO rescue construct in $SMC2^{ON}$ but not in $SMC2^{OFF}$ cells. Primers specific for the SMC2 coding region were used to verify that in $SMC2^{OFF}$ the inserted constructs were being expressed (Fig. 6B). To further test the presence of SBP-$SMC2^{WT}$ or SBP-$SMC2^{S1086R}$, protein extracts were prepared from $SMC2^{ON/OFF}$ cells and analysed by immunoblotting with antibodies against SMC2 or SBP (Fig. 6A). In $SMC2^{OFF}$ cells, as expected, only the SBP tagged protein was observed.

To test the effect of the ATPase mutant on the behaviour of centromeres, cells were treated with doxycycline to deplete SMC2, and after fixing the cells we measured the distance between LacO loci on sister chromatids in metaphase cells (Fig. 6A). Expression of wild-type SMC2 restored the distance between the 2 LacO-CEN integrations while the ATPase defective mutant was unable to rescue the distance (Fig. 6D). Based on these results it is possible to conclude that SMC2 ATPase activity is required for the normal elasticity of the pericentromeric chromatin.

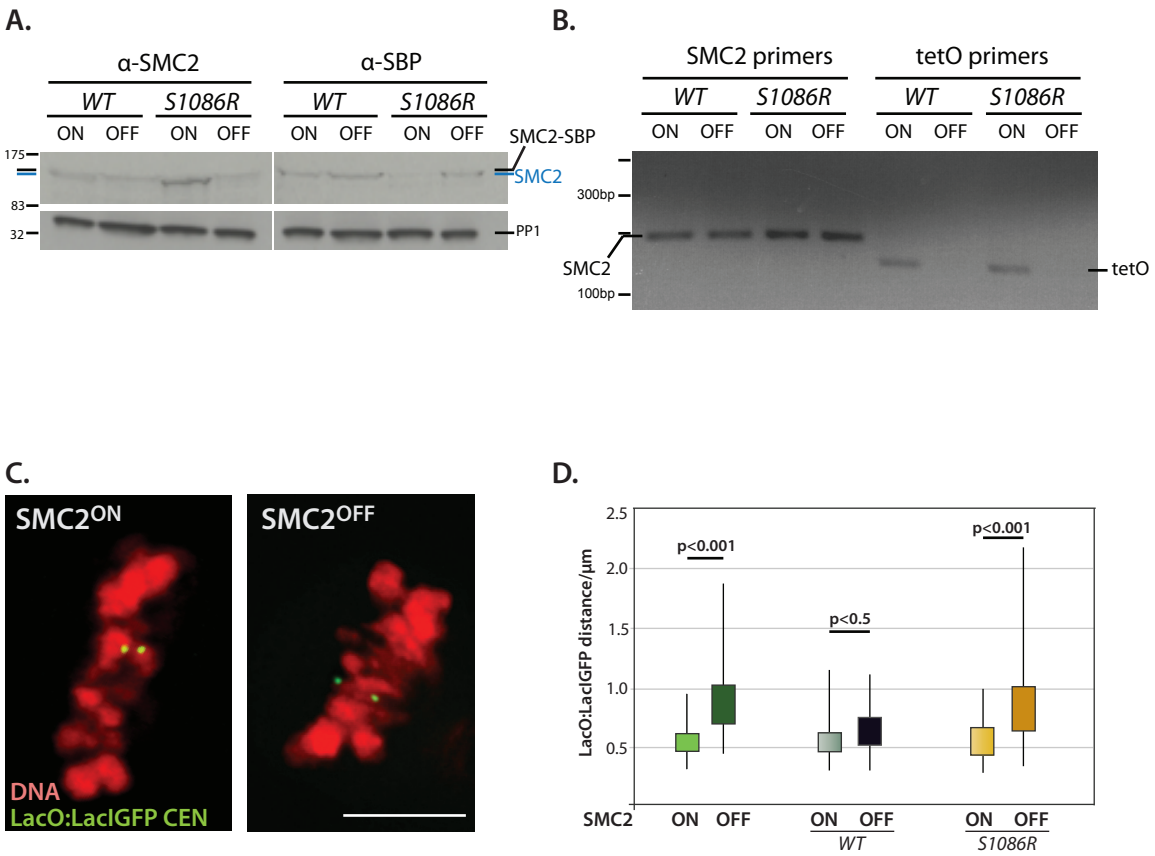

Figure 6 | SMC2 ATPase activity is required to confer stiffness at the inner centromeric chromatin. SMC2 KO:LacO CEN cell line was used to establish two derivative cell lines expressing either SMC2^{WT} or SMC2^{S1086R}. Both transgenes were driven by a fragment of the cloned endogenous SMC2 promoter, and were tagged with SBP to distinguish from the Dox-regulated SMC2 gene. Upon addition of Dox to the cultures, cells expressed only when the SBP-tagged SMC2. **A.** Western blot of SMC2^{ON} and SMC2^{OFF} cell lines expressing SMC2^{WT}:SBP and SMC2^{S1086R}:SBP showing the presence of the SBP-tagged SMC2 proteins after the repression of the Dox-regulated gene. **B.** RT-PCR from SMC2^{ON} and SMC2^{OFF} cell lines expressing SMC2^{WT}:SBP and SMC2^{S1086R}:SBP with oligo pairs specific either for the Dox-regulated gene or the SBP-tagged transgene. The Dox-regulated gene is not transcribed after 30 h of doxycycline treatment while the transcription of SBP tagged genes is unperturbed. **C.** SMC2^{ON} and SMC2^{OFF} cells in metaphase with LacI:GFP signals in the same focal plane (scale bar 5 µm). **D.** Distribution of distances between the LacI:GFP signals measured in cells with chromosomes aligned in the metaphase plate of both SMC2^{ON}:CEN and SMC2^{OFF}:CEN after incubation with 20 µM MG132. SMC2^{WT} restores the normal interlocus spacing distribution but the ATPase-deficient SMC2 point mutant (SMC2^{S1086R}) does not (n = 90; $p < 0.001$; non-parametric Mann-Whitney test).

2.6 Kinetochore structure and function is normal in the absence of condensin

Results thus far have shown that after condensin depletion, centromeres show increased oscillatory stretching during metaphase. This behaviour is reversible and microtubule dependent. These oscillatory movements are greatly exaggerated in the absence of SMC2 ATPase activity. In order to understand if condensin also plays a role in the specialized structure of the kinetochore a series of experiments were designed. A first approach was based on immunofluorescence using specific antibodies against kinetochore proteins. As a second approach, we looked at the localization of kinetochore proteins after establishing stable cell lines expressing GFP-tagged proteins. A third approach used serial-section electron microscopy to analyze kinetochore ultrastructure in the presence and absence of condensin.

Data from immunofluorescence staining with CENP-H antibody in a SMC2 KO cell line expressing GFP-CENP-A showed that both inner kinetochore proteins localize to discrete spots at kinetochores undergoing excursions in $SMC2^{OFF}$ metaphase cells (Fig. 7A,B). This result shows that condensin is not primarily involved in the structure of the inner kinetochore.

To look at proteins of the outer kinetochore/microtubule interface, we conducted immunofluorescence of $SMC2^{ON}$ and $SMC2^{OFF}$ cells with antibody to Hec1. Hec1, as previously described, is part of the outer kinetochore plate. Hec1 localizes distally to GFP-CENP-A both in $SMC2^{ON}$ and $SMC2^{OFF}$ cells. No mislocalization of Hec1 was observed in kinetochores undergoing excursions. This suggests that the microtubule/kinetochore interface is intact and the outer kinetochore plate is not deformed when kinetochores are stretched in $SMC2^{OFF}$ cells.

In order to analyse the structure of the pulled kinetochore by electron microscopy (EM) we established a collaboration with Bruce McEwen (Wadsworth Centre, Albany, NYC). Samples were prepared in our lab (described in Material and Methods section 11.) using gridded coverslips that allowed the exact determination of the coordinates of cells that should be analysed by serial section electron microscopy. $SMC2^{ON}$ and $SMC2^{OFF}$ cells aligned in metaphase were selected and annotated and z sections with 300 nm step-size were acquired using the Deltavision microscope (Fig. 8A). After electron microscopy image acquisition, a correlative image between LM and EM could be prepared (Fig. 8A', A''). This allows the determination of kinetochore localization with CENP-H-GFP and the

observation of the subjacent chromatin (H2BmRFP) (Dong et al., 2008). Furthermore, EM data provided further details about the ultrastructure of $SMC2^{OFF}$ stretched kinetochores allowing a comparison between the structure of $SMC2^{ON}$ and $SMC2^{OFF}$ kinetochores (Fig. 8B). Comparison of inner and outer kinetochore plates of pulled and non-pulled kinetochores did not show any detectable structural alteration in kinetochores depleted of condensin. Additionally, the number of microtubules bound per kinetochore was scored in $SMC2^{ON}$ and $SMC2^{OFF}$ cells by Yimin Dong in the McEwen lab and no alteration in the average number was observed. In both cases there are on average 4 microtubules bound per kinetochore (Fig. 8C). The range of microtubules observed (2-7 microtubules bound per kinetochore) might be due to intermediate states of attachment achieved during biorientation. This data allowed us to strengthen our conclusion that there is no overt defect in the structure or primary function of condensin-depleted kinetochores.

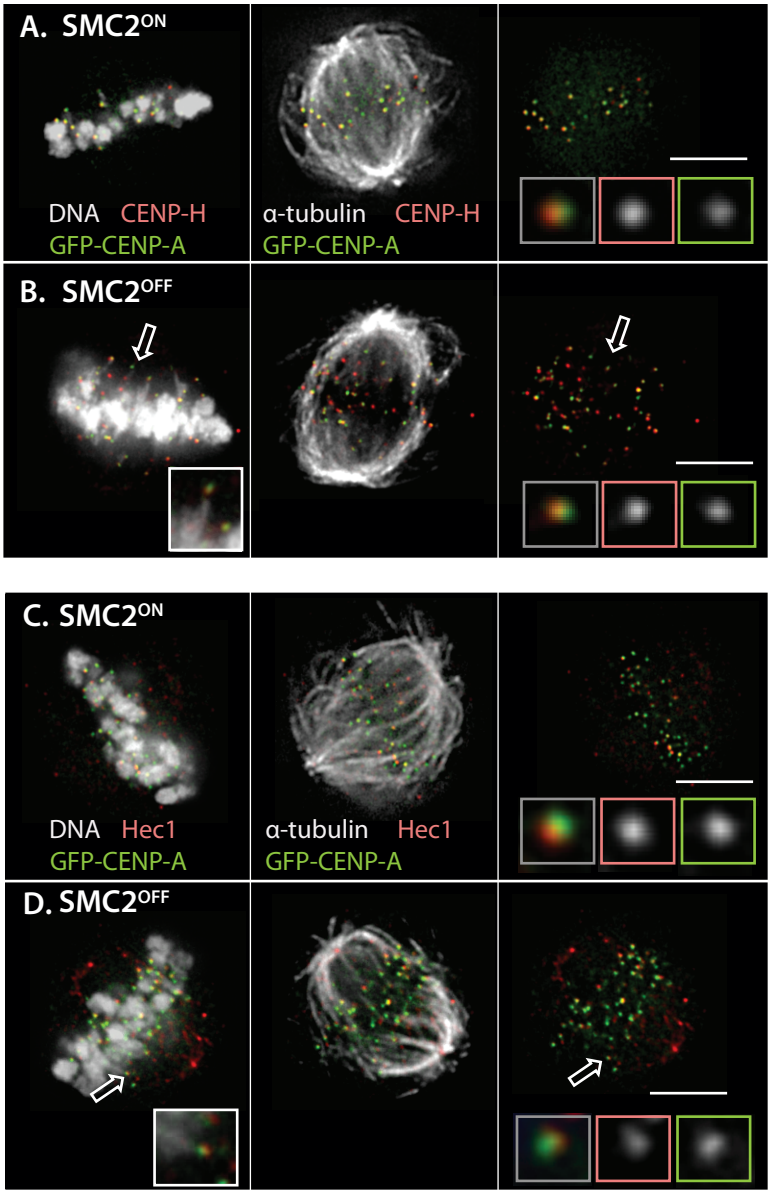

Figure 7 | Kinetochore structure is preserved in the absence of condensin. A and B. Relative localization of CENP-A and CENP-H-GFP in SMC2^{ON} (**A**) and SMC2^{OFF} (**B**) metaphases. Inset in B: kinetochore excursion (arrow) stained for CENP-H (red) and CENP-A-GFP (green). **C. and D.** Co-localization of Hec1 and GFP-CENP-A in SMC2^{ON} (**C**) and SMC2^{OFF} cells (**D**). Inset in D, kinetochore excursion (arrow) stained for Hec1 (red) and GFP-CENP-A (green) (Scale bar 5 μm). The data in this figure was contributed by Dr. Paola Vagnarelli.

A.

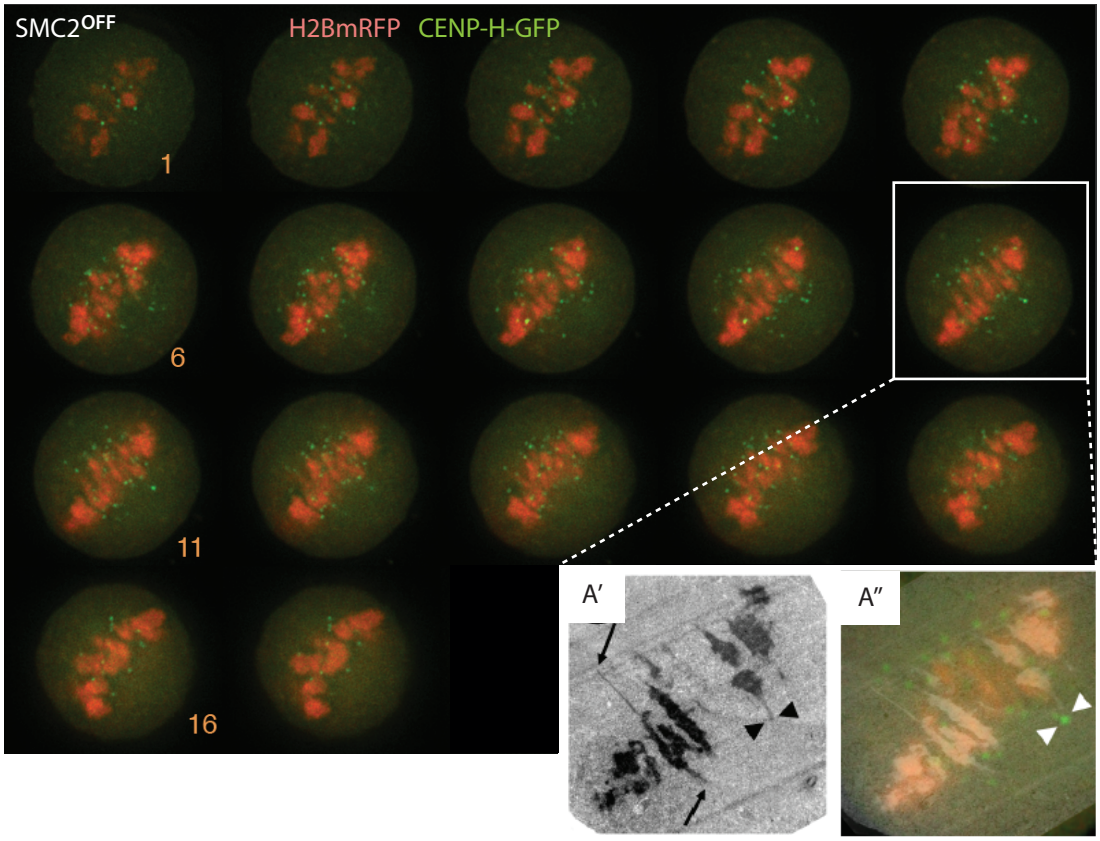

B.

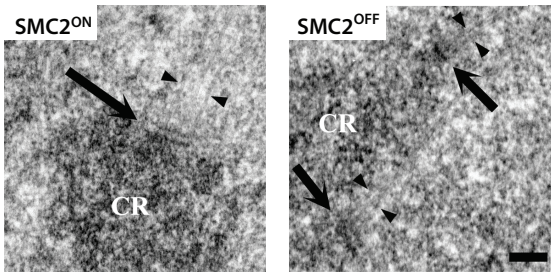

C.

	MTs per KT	range	number of KT	number of cells
SMC2^{ON}	4.3 ± 1.1	3 - 7	32	2
SMC2^{OFF}	4.3 ± 1.2	2 - 7	49	3

Figure 8 | Analysis of kinetochore structure of condensin-depleted cells using correlative light microscopy / electron microscopy and serial section EM analysis. A. Light microscopy z-section series of a SMC2^{OFF} cell at metaphase (200 nm z-sections from 1 to 17). EM selected serial section and correlation with light microscopy corresponding section (white square) (**A' and A"**). **B.** Example of a SMC2^{ON} cell: inner and outer kinetochore plates (arrow) and bound microtubules (MTs) (arrowheads). Example of a SMC2^{OFF} cell where two kinetochores can be observed, the outer plate (arrow) and attached MTs (arrowheads) of both kinetochores are indicated (scale bar 200 nm) **C.** The number of MTs per kinetochore is the same in SMC2^{ON} and SMC2^{OFF} cells. This numbers was determined from chromosomes aligned at metaphase in serial EM sections of SMC2^{ON} and SMC2^{OFF} cells. The data in this figure was contributed by Yimin Dong, Dr. Bruce McEwen and Dr. Paola Vagnarelli.

2.7 SMC2^{ON} and SMC2^{OFF} kinetochores have the same number of CENP-H molecules

It has been shown biochemically, that in the absence of condensin a large fraction of chromosome scaffold proteins is missing from mitotic chromosomes (Hudson et al., 2003) indicating that the condensin complex, rather than being fundamental for the generation of condensed mitotic chromosomes, has an essential role in conferring structural integrity to mitotic chromosomes (Gassmann et al., 2004).

To understand if condensin was affecting the levels of CENP-H protein at centromeres a quantitative approach experiment was designed in collaboration with Dr. Ajit Joglekar (Salmon's Lab, UNC, Chapel Hill).We have studied CENP-H because this protein can be tagged with GFP at the endogenous locus under control of its own promoter. This allows the quantification of endogenous levels of proteins, considering that the GFP-fluorescence intensity is a direct readout of the protein level (Wu and Pollard, 2005) We used fluorescence microscopy to quantify the copy number of centromeric core component CENP-H, in SMC2^{ON} and SMC2^{OFF} cells. As a standard we used a protein with known copy number - budding yeast Ndc80p-GFP.. Dr. Joglekar established previously an assay to count with molecular accuracy the components of the microtubule kinetochore attachment in budding yeast (Joglekar et al., 2006). *S. cerevisiae* has a well studied single kinetochore per microtubule attachment, 125 bp of centromeric DNA is wrapped around a single nucleosome containing a centromere-specific histone H3 variant (Meluh et al., 1998; Collins et al., 2004), named Cse4p (the homologue of vertebrate CENP-A). The centromeric DNA of each chromosome is bound to the plus-end of microtubules by eight Ndc80 protein complexes. Furthermore, the simplified geometry of budding yeast's spindle has practical advantages for fluorescence microscopy, i.e., the sister kinetochores of the 16 chromosomes become arranged into two distinct clusters in either side of the spindle equator during metaphase.

S. cerevisiae expressing Ndc80p tagged with GFP at its own chromosomal locus was mixed with SMC2^{ON} or SMC2^{OFF} cells (Fig. 9A). Image sections, with 200 nm separation between consecutive images along the z axis were acquired with a widefield microscope (described in section 16. of Material and Methods). The fluorescence of Ndc80p *S. cerevisiae* was used as an internal reference to convert the fluorescence intensity values into number of molecules, knowing that each budding yeast kinetochore has 8 Ndc80

molecules. These calculations revealed that there are 29 molecules of CENP-H at $SMC2^{ON}$ kinetochores and 31 molecules at $SMC2^{OFF}$ kinetochores (Fig. 9B).

Although there are differences in protein content between isolated $SMC2^{ON}$ and $SMC2^{OFF}$ chromosomes (Shinya Ohta, unpublished results), we have shown that at least one of the core components of the kinetochores, CENP-H, does not show any significant alteration in copy number when observed *in situ*. Together with localization evidence, these data suggest that neither inner nor outer kinetochore plate structures are affected in the absence of condensin.

A.

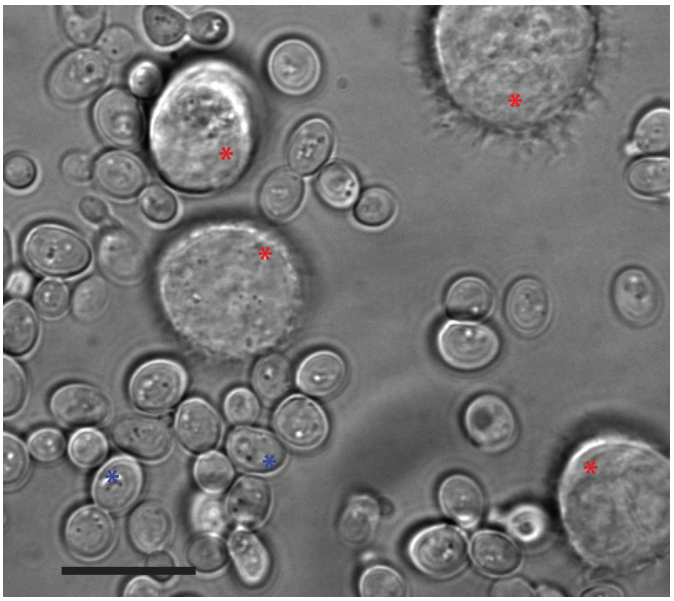

B.

	Average signal (AU)	Std. dev.	Ratio (CENPH / Ndc80)	Number of molecules per kinetochore
CENPH-GFP SMC2^{ON}	274	81	0.222	**29**
Ndc80p-GFP	1234	157		
CENPH-GFP SMC2^{OFF}	280	54	0.244	**31**
Ndc80p-GFP	1148	234		

Figure 9 | Absolute number of CENP-H molecules is conserved in SMC2^{ON} and SMC2^{OFF} kinetochores. A. Brightfield image of CENPH-GFP SMC2^{OFF} cells (red *) mixed with a *S. cerevisiae* strain expressing Ndc80p-GFP (blue *) (scale bar 5 µm). **B.** Table displaying the values of fluorescence intensity (and standard deviation) of CENP-H-GFP per kinetochore of SMC2^{ON}, SMC2^{OFF} as well as Ndc80p-GFP from *S. cerevisiae*. The absolute number of CENP-H molecules per kinetochore was determined using budding yeast Ndc80 as an internal reference. Fluorescence intensity was converted in number of molecules, knowing that each *S. cerevisiae* kinetochore has eight Ndc80 molecules (Joglekar, *et al.* 2006). The data in this figure was contributed by Dr. Ajit Joglekar.

2.8 Centromeric chromatin is an elastic component of the mitotic spindle and plays a role in setting the pole-to-pole distance in metaphase cells

The length stability of metaphase spindles suggests that spindle poles are under roughly equal and opposing forces. A simplified model of the forces that cooperate to establish the spindle steady-state during metaphase depicts three sources of active forces: inward forces generated by the minus-end microtubule sliding motors (such as kinesin-14) acting on interpolar microtubules; microtubule assembly/disassembly at the kinetochore; and outward forces developed by the pulling action of cortical dynein motors on the astral microtubules acting on the cell cortex (Mogilner et al., 2006). A fourth force, which has been regarded as passively reacting to the active forces, is the elastic stretching of the chromosomes (Inoue and Salmon, 1995). Recently, it has been shown that centromeric chromatin packaging might have an active role in opposing microtubule spindle forces (Bouck and Bloom, 2007). The authors reduced the density of histone H3 or H4 in G1 with a regulatable promoter. The analysis of the following mitosis showed that both spindle length and inter-kinetochore distances increased in yeast cells with fewer histones.

To measure the pole-to-pole distance, $SMC2^{ON}$ and $SMC2^{OFF}$ cells were stained with an antibody against one of the components of the centrosomes: γ-tubulin. The distances between poles were measured in metaphase cells in which both poles were on the same focal plane (Fig. 10A). In $SMC2^{ON}$ cells the average pole-to-pole distance is 6.9 μm (s.d. = 0.69 μm) while in $SMC2^{OFF}$ the average value is 7.6 μm (s.d. = 0.82 μm) (Fig. 10B). Thus, an increase in pole-to-pole distance in condensin-depleted cells accompanies the increase in interkinetochore distance.

As shown in section 2.2, the inner centromeric chromatin in the absence of condensin has an elastic behaviour. In a simplified system, chromatin can be modeled as a linear spring that obeys the Hooke's Law: $F = - k\Delta d$ (where force exerted by the spindle, F, is directly proportional to the distance stretched, Δd, and a spring constant k) (Gardner et al., 2005). There are two possibilities to explain the change in interkinetochore distance. On one hand chromatin rest length is increased (similar to what is observed when histone density decreases (Bouck and Bloom, 2007)). On the other hand, chromatin spring constant decreases in $SMC2^{OFF}$ cells. To understand what was altered in our system we determined the distance stretched (Δd) between sister kinetochores in the presence and

absence of condensin. The distance stretched was measured in two different ways. First, we measured the average distance in each of the live cell movies, and subtracted from it the rest length value calculated from the average distance in colcemid treated cells (Fig. 1A). Second, we determined Δd considering the maximum and minimum distances between sister kinetochores in each of the movies. In both cases the distance stretched was increased twofold in the absence of condensin. Based on several lines of evidence shown in previous sections that prove that $SMC2^{OFF}$ stretched kinetochores are structurally unperturbed it is possible to assume that there is little or no difference in the forces applied at kinetochores. Therefore, the difference in the average oscillation amplitude suggests that the spring constant is significantly altered in the absence of condensin (Fig. 10C). The ratio of k^{ON} / k^{OFF} implies a 54% or 50% decreased k^{OFF} (considering the average distance or the maximum-minimum distance, respectively). Interestingly, analysis of the movements of LacO centromere-proximal integration lead to determination of an identical spring constant value, with a decrease of 58% of k^{OFF} compared to wild-type cells. Furthermore, comparison of the spring constant of the LacO-ARM integration between $SMC2^{ON}$ and $SMC2^{OFF}$ cells showed a negligible decrease of 15% in $SMC2^{OFF}$ cells.

This demonstrated that the condensin complex sets the stiffness of centromeric chromatin. Together, these results show that changes in chromatin strength affect spindle length and not spindle stability, suggesting that inner centromeric chromatin exerts an inward force governing metaphase spindle length.

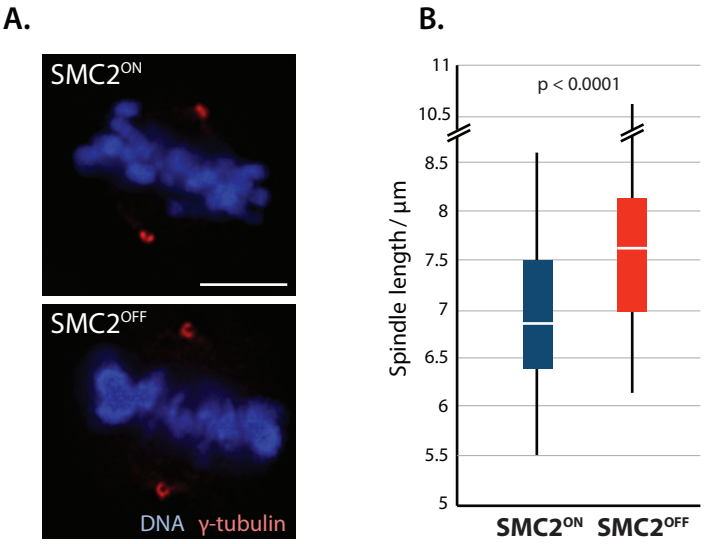

C.

	Δd (µm) Kinetochore		Δd lacO	Δd lacO
	average	max - min	CEN	ARM
$SMC2^{ON}$	0.24 ± 0.09	0.49 ± 0.13	0.29 ± 0.1	0.22 ± 0.04
$SMC2^{OFF}$	0.52 ± 0.26	0.98 ± 0.13	0.69 ± 0.15	0.26 ± 0.01
$\frac{\Delta d_{SMC2^{ON}}}{\Delta d_{SMC2^{OFF}}}$	**0.46**	**0.5**	**0.42**	**0.85**
k^{OFF} (1)	0.46 k^{ON}	0.5 k^{ON}	0.42 k^{ON}	0.85 k^{ON}

(1) **Linear Spring:** $F = -k\Delta d \Rightarrow F^{ON} = F^{OFF} \Rightarrow \Delta^{ON} / \Delta^{OFF} = k^{OFF} / k^{ON}$

Figure 10 | Condensin-depleted cells show an increased pole-to-pole distance and are less stiff in the inner centromeric region. A. Wild-type or condensin-depleted cells with chromosomes aligned in the metaphase plate stained for γ-tubulin were selected for measurements if both poles were on the same focal plane (scale bar 5 µm) **B.** Graph representing the measurement data of spindle length in $SMC^{ON/OFF}$ metaphases (3 independent experiments, n=110, p<0.0001 *t* test). **C.** Summary of the average (Δd) or maximum (Δdmax) interkinetochore or inter-locus distances in the presence and in the absence of condensin, as determined from live cell imaging. In the absence of condensin, the Δdmax values for the kinetochores and CEN integration are increased by 50 and 58%, respectively, when compared to wild-type cells. No significant changes are observed for the ARM integration. Assuming that pericentromeric chromatin behaves like a linear spring (where force exerted by the spindle, F is directly proportional to the distance stretched, Δd, and a spring constant, k), and postulating that forces are unaltered then the ratio between Δd is inversely proportional to the ratios between k. It is possible to conclude that there is a reduction in the inner centromeric stiffness in the absence of condensin.

2.9 The spindle assembly checkpoint is robust in SMC2^{OFF} cells

One clue to the potential significant biological role of the decrease of chromatin spring constant in the cell cycle progression of cells depleted of condensin arise from measurement of the mitotic index. Unperturbed SMC2^{OFF} cells had a higher mitotic index (7.7 ± 3.5%; average ± s.d.) compared to wild-type SMC2^{ON} cells (3.1 ± 1.2%) consistent with a mitotic delay (Fig. 11A). Thus, condensin-depleted cells accumulate in late prometaphase and metaphase before eventually entering anaphase (Fig. 11A).

Cells with compromised centromeric chromatin could have defects in the binding/anchoring or activation of proteins involved in the spindle assembly checkpoint (SAC). The SAC monitors defects in attachment of chromosomes to the mitotic spindle (Rieder et al., 1995) and the tension exerted on chromosomes by spindle forces in mitosis (Li and Nicklas, 1995; Nicklas et al., 1995; Stern and Murray, 2001). The purpose of this checkpoint is to block anaphase onset until all kinetochores achieve a proper bipolar attachment, ensuring the fidelity of chromosome segregation in mitosis (Murray, 1998; Musacchio and Salmon, 2007).

To analyse the robustness of the SAC classic experiments were conducted using microtubule drugs. To generate unattached kinetochores, cells were exposed to colcemid. This caused microtubule depolymerisation, such that no microtubules were bound to kinetochores. On the other hand, defects affecting tension rather than attachment were produced by the microtubule-stabilizing drug taxol. Importantly, in the presence of both drugs, SMC2^{OFF} cells showed an increase in mitotic index comparable to SMC2^{ON} cells (Fig. 11B and C).

These experiments clearly demonstrate that the SAC response is intact in SMC2^{OFF} cells. This implies that kinetochore proteins involved in the SAC are recruited and regulated in a timely manner in the absence of condensin.

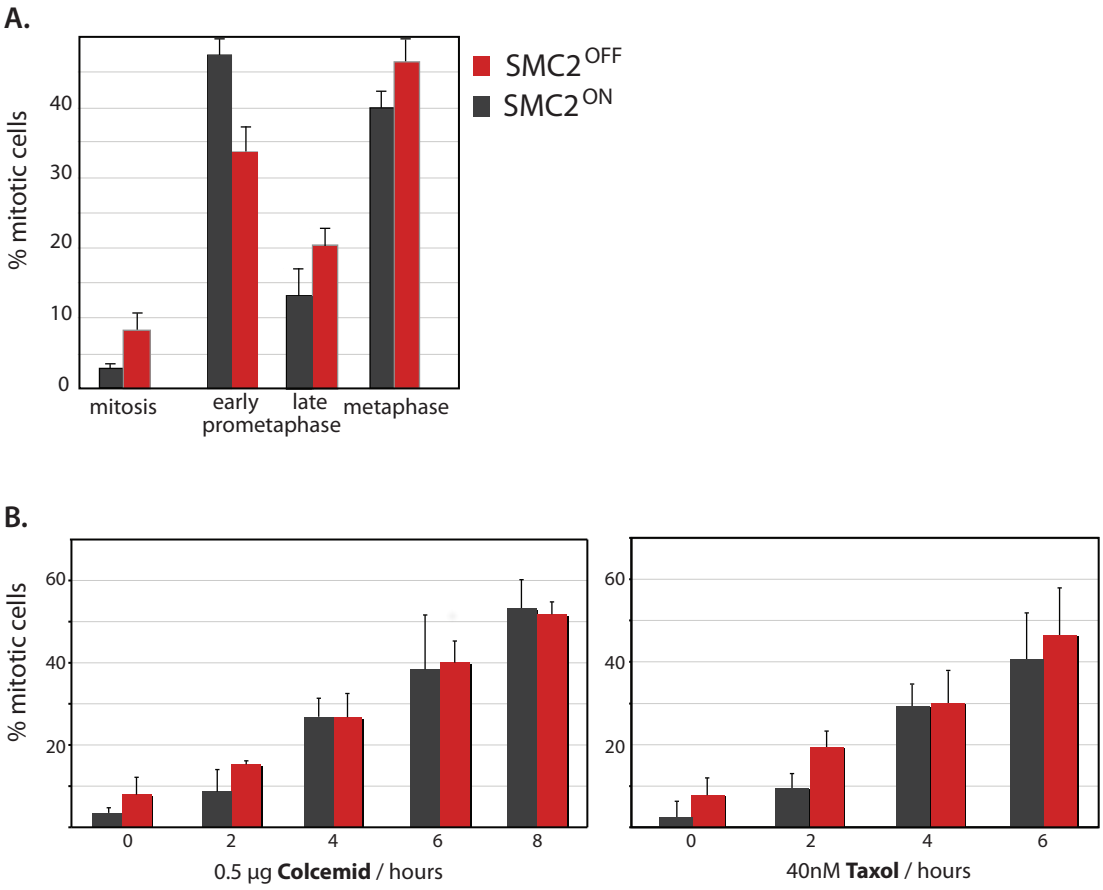

Figure 11 | Condensin-depleted cells have increased mitotic index and normal activation of the spindle assembly checkpoint. A. SMC2^{OFF} have increased mitotic index due to an accumulation in late prometaphase and metaphase mitotic stages (n = 500 in each of three experiments). However, cells can activate the spindle checkpoint normally in the presence of colcemid **B.** or taxol **C.** (n = 500 in each of three experiments).

2.10 Timely silencing of the spindle assembly checkpoint is compromised in condensin-depleted cells

The fact that SAC signaling is normal, together with the observed increase in mitotic index in SMC2^{OFF} cells indicates that this increase could be arising from a continued activation of the checkpoint. A daunting number of proteins are involved in activating and deactivating the SAC response. Two of the key proteins are Mad2 and the checkpoint kinase BubR1. BubR1 is directly involved in the wait-anaphase signal and is a marker for the outer kinetochore in chromosomes that have not yet achieved bipolar orientation (Jablonski et al., 1998). Mad2 accumulates at unattached kinetochores and levels are highly reduced as kinetochores fill more of their attachment sites with microtubules. This dynamic pattern of Mad2 localisation is interpreted as a readout of lack of attachment (Waters et al., 1998; Skoufias et al., 2001).

Besides generating the checkpoint signal, the kinetochore also captures and stabilizes/destabilizes microtubule attachments. One protein that is involved in destabilizing microtubule attachments is the mitotic centromere-associated kinesin (MCAK) which is negatively regulated by Aurora B phosphorylation. MCAK concentrates at centromeres and when dephosphorylated it becomes active and catalyses microtubule disassembly enabling the release of incorrect attachments, such as merotelic attachments (Andrews et al., 2004; Lan et al., 2004).

A stable SMC2$^{ON/OFF}$ cell line expressing MCAK:GFP was engineered. These cells were fixed and stained with CENP-H centromeric protein. In agreement with what is known, MCAK localized to some of the centromeres of metaphase cells with bioriented chromosomes, but there was no detectable localization of MCAK:GFP at stretched kinetochores of SMC2^{OFF} metaphase cells (Fig. 12B). There was no clear difference in BubR1 localization and/or amount in SMC2^{ON} and SMC2^{OFF} cells stained with specific antibody for BubR1. Furthermore, kinetochores undergoing excursions away from the metaphase plate do not recruit BubR1. This indicates that the pulled kinetochores are bipolarly attached and probably under tension (Fig. 12A). Mad2:GFP was also absent from pulled kinetochores in SMC2^{OFF} cells, indicating that these kinetochores were fully occupied with microtubules (Fig. 12A).

However, an increase in the number of SMC2^{OFF} cells with aligned metaphases having two or more Mad2:GFP-positive kinetochores was obvious (Fig. 12C and D).

This result was a clear indication that there was persistent activation of the checkpoint on kinetochores aligned on the metaphase plate in SMC2^{OFF} cells. However, kinetochores undergoing extended excursions have stable bipolar microtubule attachments.

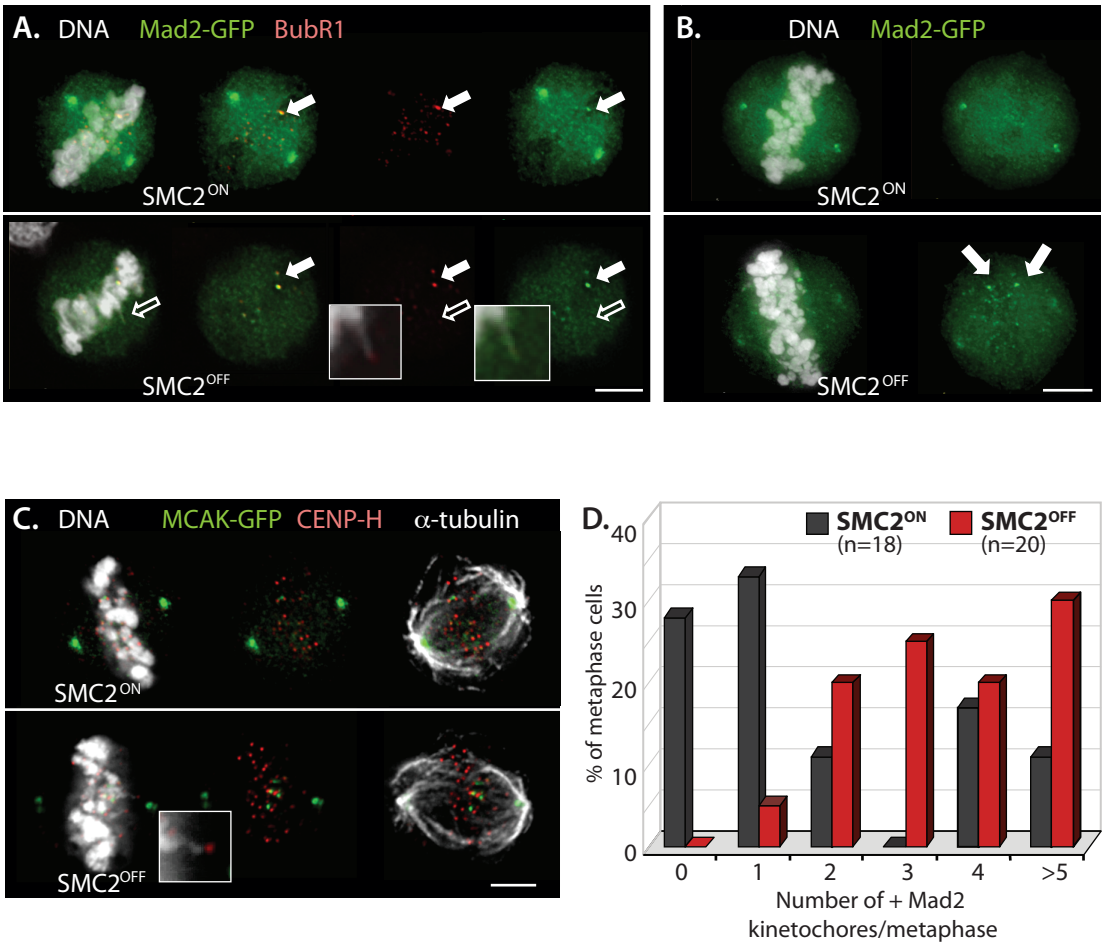

Figure 12 | SMC2^{OFF} cells exhibit persistent spindle checkpoint activation. A. Mad2 and BubR1 are not present in kinetochores of SMC2^{OFF} cells undergoing poleward excursions (empty arrow and inset). SMC2$^{ON/OFF}$ kinetochores where Mad2-GFP protein is present also have BubR1 detectable levels (filled arrows). **B.** SMC2$^{ON/OFF}$ cells in metaphase expressing Mad2-GFP. **C.** Kinetochores of SMC2^{OFF} cells engaged in poleward excursions do not have detectable levels of MCAK-GFP (inset and empty arrow). **D.** Quantification of Mad2-positive kinetochores per metaphase (scale bars 5 μm).

2.11 Chromosome segregation is normal in SMC2^{OFF} cells

Kinetochores of chromosomes bioriented in metaphase present a back-to-back orientation that ultimately helps to ensure a proper amphitelic attachment (Rieder and Salmon, 1998; Loncarek et al., 2007). In the absence of condensin, weak inner centromeric chromatin could be unable to maintain this configuration. If this was the case, an increase in syntelic and merotelic attachments would be observed, and ultimately would lead to an increase in chromosome missegregation (Cimini et al., 2002).

Altogether, the previous described data - *in vivo* live cell imaging of CENP-H labeled kinetochores and EM data argues against the likelihood of merotelic/syntelic attachment occurring in SMC2^{OFF} cells. However other assays to rule out missegregation defects were developed.

As previously mentioned, Dr. Paola Vagnarelli engineered a collection of eight different cell lines containing random insertions of a LacO array into chromosome arms. To score segregation of these loci we observed anaphase cells under the microscope. Observation of one spot in each segregating group of chromatids was scored as proper chromosome segregation. If the two spots were on the same side or if one of them was in the middle the cell was scored positive for missegregation (Fig. 13A). This quantification of loci segregation showed that there were no significant segregation defects in SMC2^{OFF} cells (Fig. 13B).

To increase the sensitivity of the assay a SMC2 KO cell line carrying a fragment of the human X chromosome was used. This short chromosomal fragment is impaired for segregation fidelity (Spence et al., 2002; Spence et al., 2006). In this case, a labeled probe was used to specifically detect the human chromosome (Fig. 13C). Chromosome segregation events were scored by preventing cells from completing cytokinesis with cytochalasin D. Thus, each chromosome segregation event generated a dikaryon with 2 sister nuclei in a common cytoplasm. This enabled the accurate scoring of the distribution of the human X mini-chromosome in both nuclei (1:1 correct segregation) or in only one of the nuclei (2:0 missegregation). Again, this assay revealed that condensin depletion was not affecting chromosome segregation.

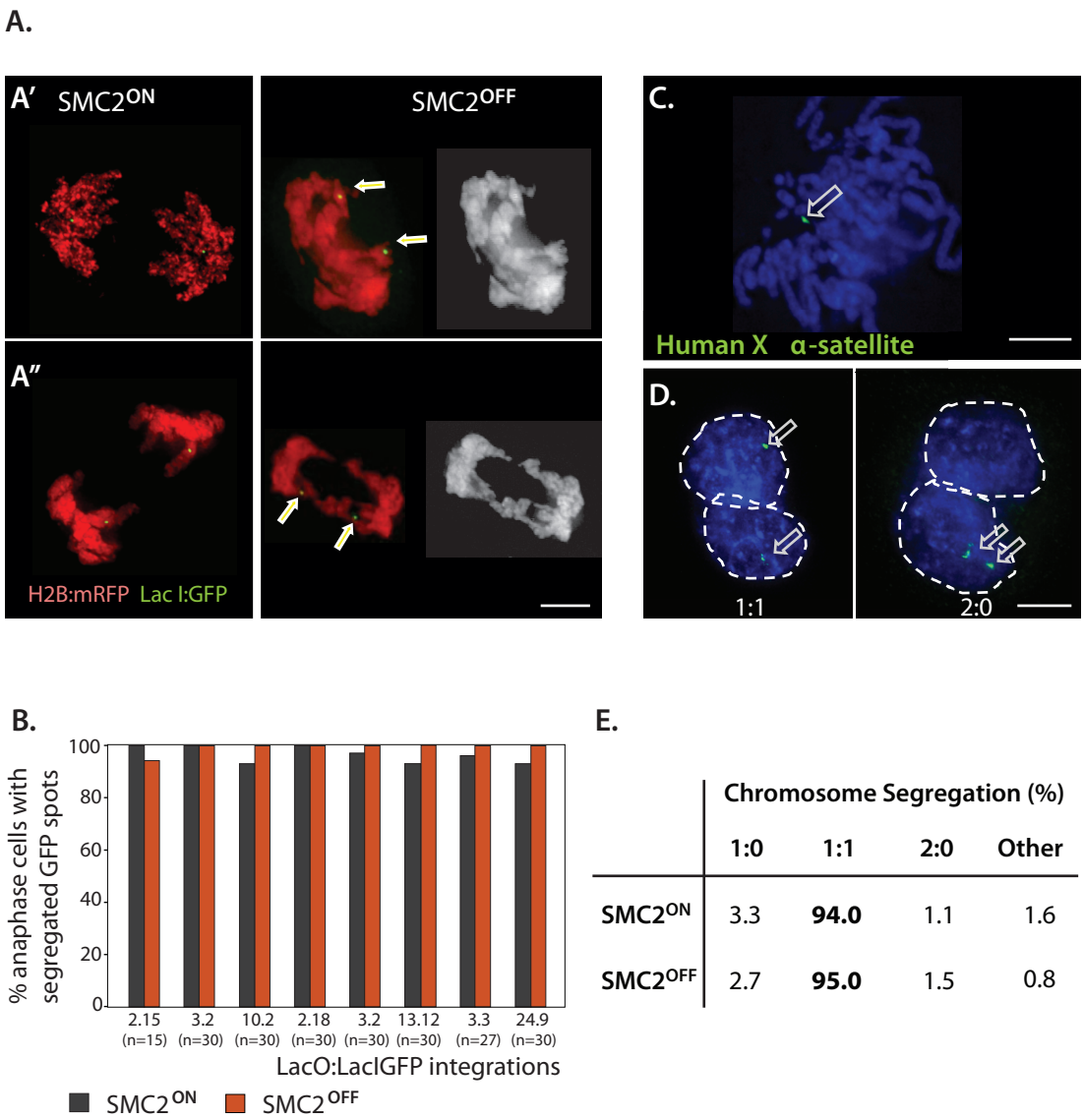

E.

	Chromosome Segregation (%)			
	1:0	**1:1**	**2:0**	**Other**
SMC2^{ON}	3.3	**94.0**	1.1	1.6
SMC2^{OFF}	2.7	**95.0**	1.5	0.8

Figure 13 | Condensin depleted cells have normal chromosome segregation. A. Anaphases of SMC2^{ON} and SMC2^{OFF} cells showing 1:1 segregation of the DHFR–LacO array in two different cell lines. The yellow arrows indicate the position of the integrated sequence visualised by LacI–GFP. **A′** Cells with integration on a micro-chromosome. **A″** Cells with integration on a macro-chromosome (scale bar 5μm). **B.** Quantification of the experiment shown in A. Anaphase segregation in eight different cell lines where normal levels of loci segregation was observed, in both SMC2^{ON} and SMC2^{OFF}cells. **C.** SMC2 KO cell line carrying a human minichromosome was used to test the missegregation frequency of this specific chromosome in the presence and absence of condensin. Chromosome spread hybridized with a chromosome X-specific α-satellite probe (empty arrow); **D.** Cells blocked with cytochalasin D showing two different types of segregation 1:1 and 2:0 (scale bar 5 μm). **E.** Quantification of the experiment shown in **D** (n=500 cells).

3. DISCUSSION

3.1 Kinetochores appear structurally normal and functional in SMC2^{OFF} cells

The possibility of generating a clonal cell population depleted of both condensin complexes allowed the detailed study of condensin's role in the centromeric chromatin of metaphase cells.

Kinetochores undergoing excursions in the absence of condensin are structurally intact as demonstrated by the following criteria: 1) CENP-H and CENP-A colocalize as discrete spots; 2) these spots are not distorted in kinetochores undergoing excursions; 3) loss of condensin had no effect on the number of CENP-H molecules per kinetochore; 4) localisation of Hec1 in the outer kinetochore plate relative to CENP-A was unchanged by condensin depletion; 5) Electron microscopy serial section analysis revealed normal plates, even in kinetochores undergoing excursions. Thus, neither the inner nor the outer kinetochore plates showed obvious structural alterations in the absence of condensin.

Moreover, several lines of evidence suggested that SMC2^{OFF} kinetochores are functional. Electron microscopy analysis revealed that on average the same number of microtubules is bound to kinetochores of SMC2^{ON} and SMC2^{OFF} metaphase chromosomes. Kinetochores of condensin-depleted chromosomes are able to bind the checkpoint proteins Mad2 and BubR1, and the cells have a robust SAC response to microtubule poisoning drugs. Finally, there was no increase in segregation defects in condensin-depleted cells.

In sum, these results suggest that vertebrate centromeres have a rigid component (CENP-A containing chromatin) that provides a robust platform for kinetochore assembly and microtubule interactions, coupled to a highly dynamic elastic component (the inner centromeric chromatin).

However, several studies have previously reported centromeric and/or kinetochore distortion in the absence of condensin. In *S. cerevisiae* (Yong-Gonzalez et al., 2007), condensin mutations leads to partial loss of Cse4 (the homologue of vertebrate CENP-A) . In human cells, depletion of different non-SMC subunits of either condensin I or II leads to an apparent distortion of CREST (calcinosis, raynaud's syndrome, esophageal dysmotility,

sclerodactyly, telangiectasia sera) or CENP-E by immunofluorescence analysis (Ono et al., 2003), although other studies failed to show any significant deformation of centromeric structure by live cell analysis (Gerlich et al., 2006). In *D. melanogaster*, condensin RNAi affects CID (CENP-A homologue) (Jager et al., 2005) while in *Xenopus*, condensin immunodepletion distorts the outer kinetochore marker CENP-E (Wignall et al., 2003). In holocentric chromosomes of *C. elegans*, RNAi depletion of condensin subunit SMC4 also affects the distribution of hcp3 (CENP-A homologue) (Hagstrom et al., 2002). More recently it has been reported that condensin in human cells has a pivotal role in CENP-A assembly and proper microtubule attachment (Samoshkin et al., 2009). The latter authors claim that SMC2 RNAi depletion in human HeLa cells results in a significant loss of CENP-A loading, leading to the appearance of a stretched CENP-A domain and an increase of merotelic attachments with consequent missegregation defects.

Overall, the contradictory results obtained might have at least three explanations. Considering the size of kinetochore and number of microtubules attached sites, human and chicken cells may exhibit structural differences. While human cells have 20-25 microtubule attachment sites per kinetochore (Rieder, 1982), chicken cells only have 3-5 sites. This four- to five- fold decrease in the number of attachment sites could render the chicken kinetochores less prone to be distorted, or to have less available microtubule sites for incorrect attachments. Another possible argument that reinforces the value of our data comes from *in vivo* versus fixed sample analysis. The analysis undertaken in this study as well the only other study where *in vivo* analysis was done (Gerlich et al., 2006) show in both cases that CENP-A structure is not dependent on condensin. This detail might be extremely important if consideration is taken to the fact that condensin-depleted cells are particularly sensitive to fixation conditions (Hudson et al., 2003).

Nonetheless, our data undoubtedly shows that condensin does not have a role in the structure or function of inner and outer kinetochores and as well it is not correlated with an increase in merotelic attachments in DT40 cells.

3.2 Microtubule dynamics and attachment affects SMC2^{OFF} oscillatory movements

In vivo high-temporal resolution imaging analysis of kinetochore movements in the absence of condensin revealed that the inner centromeric chromatin stretched easily and kinetochores moved up to ~2μm away from the metaphase plate. The kinetochore excursions trailed a thin string of chromatin without moving the whole chromosome. Overall, kinetochore movements were uncoordinated and reversible. The elasticity of these movements was a controversial question. One published study showed reversibility of chromatin movements, using live cell imaging after depletion of one non-SMC subunit in human cells (Gerlich et al., 2006). Another study involving *D. melanogaster* cells after RNAi depletion of condensin I suggested permanent deformation in analysis of fixed samples (Oliveira et al., 2005).

To study the factors that affected the abnormal oscillatory movements *in vivo* we analysed the effect of nocodazole. This revealed that stretched kinetochore movements during metaphase were microtubule dependent because interkinetochore distance returned to normal values 5 minutes after nocodazole addition to cells. Additional analyses were done on a simplified system using integrations of LacO arrays close to the centromeric region that were subsequently detected with LacI-GFP. This simplified system recapitulated kinetochore behaviour in SMC2^{ON} and SMC2^{OFF} cells and allowed a more detailed study, since instead of looking to 70 kinetochore pairs the analysis could focus on a single locus. This also had an extra advantage of analyzing the exact same locus independently of the experiment or observation. Similar "breathing" of pericentric regions was previously observed in wild type budding yeast for reporter arrays adjacent to centromeres (Goshima and Yanagida, 2000; He et al., 2000).

Kymographs prepared from the movies of LacO centromere-proximal integration showed the dynamic separation between these signals and their uncoordinated behaviour. Thus, this simplified system is an accurate reporter for kinetochore behaviour. As with kinetochores, the excursions were reversible and microtubule-dependent: they were abolished by nocodazole as well by Hec1 RNAi knockdown. The oscillatory movements were unaffected by a prolonged cell cycle block in metaphase, caused by the addition of MG132. In controls, a LacO array integrated on the arm of a macro-chromosome maintained a constant relative distance between sister chromatids during

metaphase. This distance was larger than that of controls because chromatin is 40% less compact in SMC2^{OFF} cells (Hudson et al., 2003; Vagnarelli et al., 2006).

The oscillatory movements of both kinetochores and LacO-CEN integrations of condensin-depleted chromosomes are affected by microtubule attachment and dynamics.

3.3 Condensin has a role in determining the stiffness of centromeric chromatin

Although depletion of condensin does not interfere with the structure of the kinetochore, it clearly affects the physical properties of inner centromeric chromatin. Mechanical properties of chromatin are similar to those of a simple or Hookean spring where $F = - k\Delta d$. In this equation, F is the force applied, k is the spring constant and Δd is the distance stretched; i.e., force is directly proportional to the extent that a spring is stretched. Since kinetochore and spindle structure is conserved, F_{MAX} was assumed to be equivalent in the presence and absence of condensin. The rest length of the spring, likely set by chromatin higher-order structure (Bouck and Bloom, 2007) is unchanged in absence of condensin. However, the average extent of excursions (Δd) in SMC2^{OFF} cells (0.52 μm, s.d. = 0.26 μm) was twofold greater than that observed in SMC2^{ON} cells (0.24 μm, s.d. = 0.09 μm). Thus, it is possible to conclude that the spring constant of centromeres lacking condensin is 0.46 that of wild type centromeres. Remarkably, when the same measurements were done for the LacO-CEN integration the same decrease in the spring constant was observed. The average extent of excursion for the LacO-CEN array in SMC2^{ON} and SMC2^{OFF} cells increased from 0.29 μm (s.d. = 0.1 μm) to 0.69 μm (s.d. = 0.15 μm) respectively. This corresponds to a decrease in the spring constant of cells lacking condensin to 0.42 that of wild type cells. In contrast, for the LacO-ARM integration, the spring constant of SMC2^{OFF} cells was essentially unchanged, at 0.85 that of SMC2^{ON} cells.

Force equilibrium within the metaphase spindle is reached when microtubules impose forces on the chromosomes via the kinetochore until centromeric chromatin is pulled far enough to counter-balance those microtubule forces. In condensin-depleted cells microtubule outward forces are still cancelled by weaker centromeric chromatin, just at an increased extension (Δd) (Fig. 14).

Previously it was shown that by lowering the histone H3 or H4 content of centromeric chromatin, the rest length of inner-centromeric chromatin was altered without changing the spring constant (Bouck and Bloom, 2007). Thus, my studies provide the first demonstration of a protein complex affecting the spring constant of centromeric chromatin.

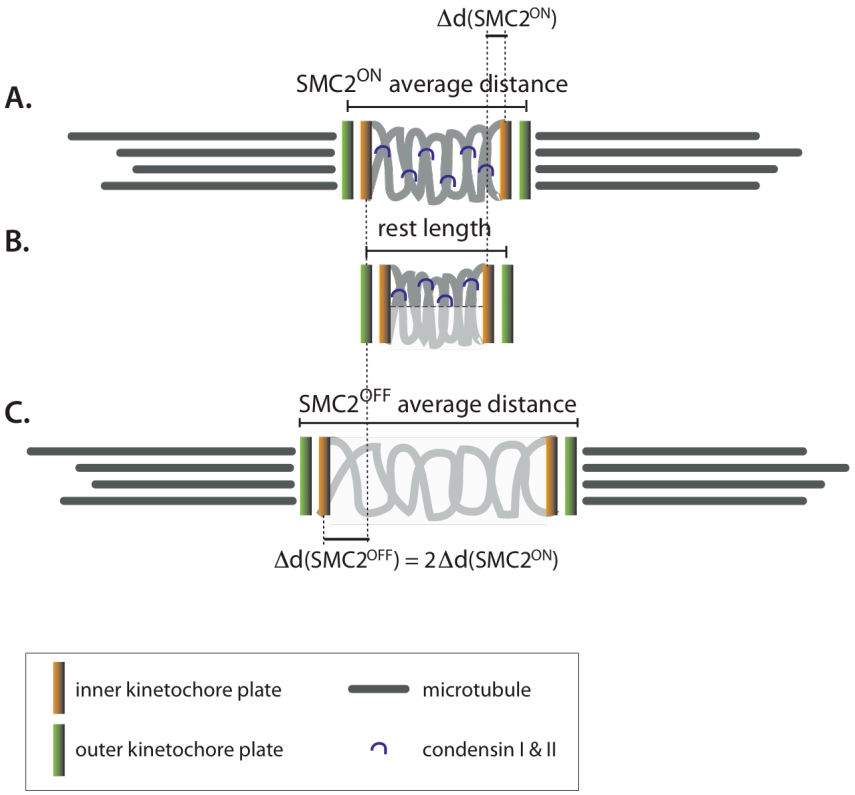

Figure 14 | Condensin sets inner centromeric stiffness in response to spindle forces. In mitosis, before microtubules attach chromatin rest length is set by chromatin higher order structure (**B**) which is independent of condensin. In normal cells, once microtubules attach (**A**) to sister kinetochores and form bipolar attachments, kinetochores oscillate in response to microtubule forces, showing an increase in interkinetochore distance ($\Delta d(SMC2^{ON})$). In the absence of condensin (**C**) the interkinetochore amplitude is increased by a factor of ~2, suggesting that the condensin complex sets the stiffness of pericentromeric chromatin in response to spindle forces.

3.4 Mitotic delay in condensin-depleted cells is caused by prolonged activation of the spindle assembly checkpoint

So far the work presented here demonstrates that condensin has a very specific role in conferring stiffness to centromeric chromatin. The next obvious question was to understand the biological importance of stiff chromatin for metaphase and/or mitotic progression.

Condensin-depleted cells do not show any increase in missegregation defects and retain an active spindle assembly checkpoint, but present a higher mitotic index. As previously discussed, condensin repression increases the spring constant of pericentric chromatin without changing the rest length that is possibly set by chromatin higher order structure. Furthermore, the number of Mad2 positive kinetochores is increased in metaphase cells. All together it is possible to postulate that chromatin has an active role in regulating microtubule attachment to kinetochores.

Recently published data (Maresca and Salmon, 2009; Uchida et al., 2009) showed that intrakinetochore rather than interkinetochore stretch is the key mechanism in silencing the spindle assembly checkpoint. Both studies showed that when microtubules attach in metaphase, inner and outer kinetochore plates undergo a physical stretch. This is both necessary and sufficient to silence the SAC. This implies that the SAC monitors rearrangements within the kinetochore rather than tension. Although this might seem to be in disagreement with our data, in fact several lines of evidence (Skibbens et al., 1993; Cassimeris et al., 1994; Skibbens and Salmon, 1997) demonstrated that tension controls the direction of kinetochore movement and predicted that tension regulates kinetochore directional instability. Furthermore it has also been demonstrated that kinetochore microtubule binding stability is dependent on tension (Nicklas and Koch, 1969; Nicklas and Ward, 1994). Even more strikingly, tension increases the number of kinetochore microtubules (King and Nicklas, 2000). From the experimental data above presented there are 2 possibilities to fit our model: (1) either condensin depleted centromeres interfere directly in intrakinetochore stretch, participating in this way in the SAC response; (2) or condensin-depleted centromeres that present high degrees of stretch might create a tension gradient within the spindle. In fact, although the SAC might be monitored at the kinetochore level, nevertheless tension might increase the probability of attaching microtubules with a consequent stabilization of kinetochore-microtubule attachment.

Clearly, kinetochores not under tension have an increased probability of losing microtubules with an obvious consequence of activating the SAC. Thus there is a degree of correlation between interkinetochore stretch and microtubule stability even if interkinetochore stretch might happen at low levels of tension.

Kinetochore movements are coupled to microtubule plus-end polymerization/depolymerization at kinetochores. One current model proposes that kinetochores sense both a spatial gradient that suppresses kinetochore microtubules (kMT) catastrophe near the poles and attachment site tension that promotes kMT rescue at higher degrees of chromatin stretch (Gardner et al., 2005). The catastrophe gradient does not result in complete depolymerization of kinetochore microtubules; instead the effects of the gradient are opposed by tension-dependent microtubule rescue. Assuming bioriented sister kinetochores, once microtubules depolymerize the force at kinetochore increases. This tension is predicted to result in a switch to microtubule growth. Furthermore, tension applied to kinetochores is known to promote their occupancy with microtubules (King and Nicklas, 2000). But how bioriented attachments are stabilized via tension has been a long-standing question.

Very recently Liu et al. (Liu et al., 2009) showed a mechanism linking both processes. Their study was performed using a fluorescence resonance energy transfer (FRET)-based sensors that allow a temporal and spatial *in vivo* study of phosphorylation (Fuller et al., 2008). They showed that microtubule stability is increased due to spatial separation of kinetochore substrates from Aurora B at the centromere. Aurora B kinase phosphorylation has an essential role in preventing the stabilization of microtubule attachment (Cheeseman et al., 2006; Deluca et al., 2006; Ciferri et al., 2008; Gestaut et al., 2008). Aurora B is tethered through INCENP to the centromere (Ruchaud et al., 2007) where a subset of Aurora B molecules located in the centromere-kinetochore interface can target its substrates. Thus, tension applied when spindle microtubules pull bi-oriented sister kinetochores in opposite directions, away from the inner centromere leads to dephosphorylation of kinetochore substrates. This in turn increases kinetochore affinity for microtubules and stabilizes attachments, leading to a consequent silencing of the SAC.

In this context the results described for stretched chromatin and the increased number of unattached kinetochores (as seen by increased number of Mad2 positive

kinetochores) observed in SMC2^{OFF} cells lead us to the propose the following model. Centromeres lacking functional condensin may create a gradient of tension within the spindle. This could cause kinetochores to release microtubules at intermediate degrees of centromere stretch (i.e. closer to the metaphase plate), resulting in an increased tendency for microtubules to detach from kinetochores, thereby promoting Mad2 binding (Waters et al., 1998).

Very recently, Jaqaman *et al.* demonstrated the existence of a coupling mechanism between oscillation speed and metaphase plate thickness: as chromosomes align in metaphase oscillation speed decreases (with a constant oscillation period) dictating the thickness of the plate. It is suggested that sister kinetochore linkage stiffness has a major role in setting metaphase plate (Jaqaman et al., 2010). Furthermore, this study showed that there is a correlation between sister kinetochore stiffness and oscillation speed. Interestingly, when condensin is depleted the sister linkage is compromised (as observed in our studies) and leads to an increase in speed oscillation without compromising the metaphase thickness. This suggests that there exists an adjusting mechanism of increasing the oscillation period. Considering these results would be interesting to do a systematic analysis of oscillation period and speed in our condensin-depleted cells and also in the SMC2 ATPase mutant cell line. Future detailed studies in the referred cell lines might help in understanding what is the mechanism behind the compensatory increased speed observed in condensin-depleted cells. Is the presence of the condensin complex even without ATPase activity enough to change the mechanical linkage, or is the ATPase activity required for oscillation of inner centromeric movements?

On the whole, the work discussed here demonstrates that chromatin, particularly in the inner centromeric region, should be regarded as an important mechanical element of the mitotic spindle.

V. A SUPER-RESOLUTION MAP OF THE VERTEBRATE CENTROMERE

1. INTRODUCTION

1.1 Centromere organization models

The centromere is a specialized region of the chromosome essential for various aspects of chromosome segregation during cell division. In mitosis, the centromeric chromatin specifies the assembly of the kinetochore, a multiprotein complex that mediates microtubule attachment, corrects improper attachments, and directs chromosome segregation. Understanding the structure, composition and folding of the centromeric region is fundamental to identify the minimal determinants for its function.

Although centromeres play a conserved role in chromosome architecture and genome stability, their underlying sequences are diverse within and between species. The unifying component of all centromeres is CENP-A (*S. pombe* cnp-1, *S. cerevisiae* cse4, *C. elegans* HCP-3, *D. melanogaster* CID), a 17 kDa protein first identified in serum from patients with scleroderma (Earnshaw and Rothfield, 1985), and subsequently shown to be a variant of histone H3 (Palmer and Margolis, 1987; Palmer et al., 1991; Sullivan et al., 1994). Even though CENP-A replaces one or both copies of H3 in centromeric nucleosomes, not every centromeric nucleosome contains CENP-A. An early study from Zinkowski *et al*, (Zinkowski et al., 1991) showed that in mechanically stretched chromosomes CENP antibodies stained blocks of chromatin interspersed with regions where staining was absent. Furthermore, it was later demonstrated that regions of CENP-A are interspersed with blocks of canonical H3 nucleosomes (Blower et al., 2002). This unique pattern first described in human and *Drosophila* centromeres, was later confirmed by observations in organisms from fission yeast to plants, or other types of centromeres, such as neocentromeres (Nagaki et al., 2004; Cam et al., 2005; Alonso et al., 2007).

Currently, there is one model for the point centromere folding: the intramolecular loop model and two other models for the folding/organization of regional centromeres: the repeat-subunit model and the looped or folded model (Fig. 1).

The intramolecular loop model for budding yeast *S. cerevisiae* centromere, which has only one CENP-A nucleosome, and one microtubule attachment per kinetochore is based in studies of intramolecular looping at the centromere (Yeh et al., 2008). This study proposes a cylindrical array of pericentromeric cohesin surrounding the mitotic spindle

after observations carried out *in vivo*. The state of pericentric DNA as mapped by chromatin conformation, indicated that pericentric chromatin is organized into an intramolecular loop stabilized by the cohesin organization (Fig. 1A). This work also proposes that the chromatin loops described could be the fundamental unit DNA loops in the mammalian kinetochores, i.e. the regional centromere would be a repeat of pericentric loops clustered together (Yeh et al., 2008; Bloom and Joglekar, 2010).

The repeat-subunit model is based on light microscopy and deconvolution observations of interphase centromeric fibers. In this model CENP-A nucleosomes are interspersed with H3 canonical nucleosomes (Blower et al., 2002). Interestingly, a similar arrangement of centromeric nucleosomes was observed at neocentromeres using a ChIP approach (Chueh et al., 2005): CENP-A peaks are interleaved with histone H3 suggesting that they represent a separate coil of the repeat-subunit model. In this model, each chromatin subdomain containing CENP-A is then folded into a helix where CENP-A regions are brought together into a continuous unit that defines the kinetochore inner plate. The canonical nucleosomes are placed inside the centromeric region, forming an "amphipathic" solenoid structure (Fig. 1B).

The third alternative model is based on serial sectioning EM analysis of CENP-A localization in centromeres and neocentromeres. At kinetochores, CENP-A occupies a compact domain stretching across two thirds of the length and one third of the width and height of the constriction. Therefore, the model proposes that the coiled centromeric chromatin is folded, or looped back upon itself, creating an unfoldable unit where CENP-A would occupy a very small and compact region (Marshall et al., 2008) (Fig. 1C).

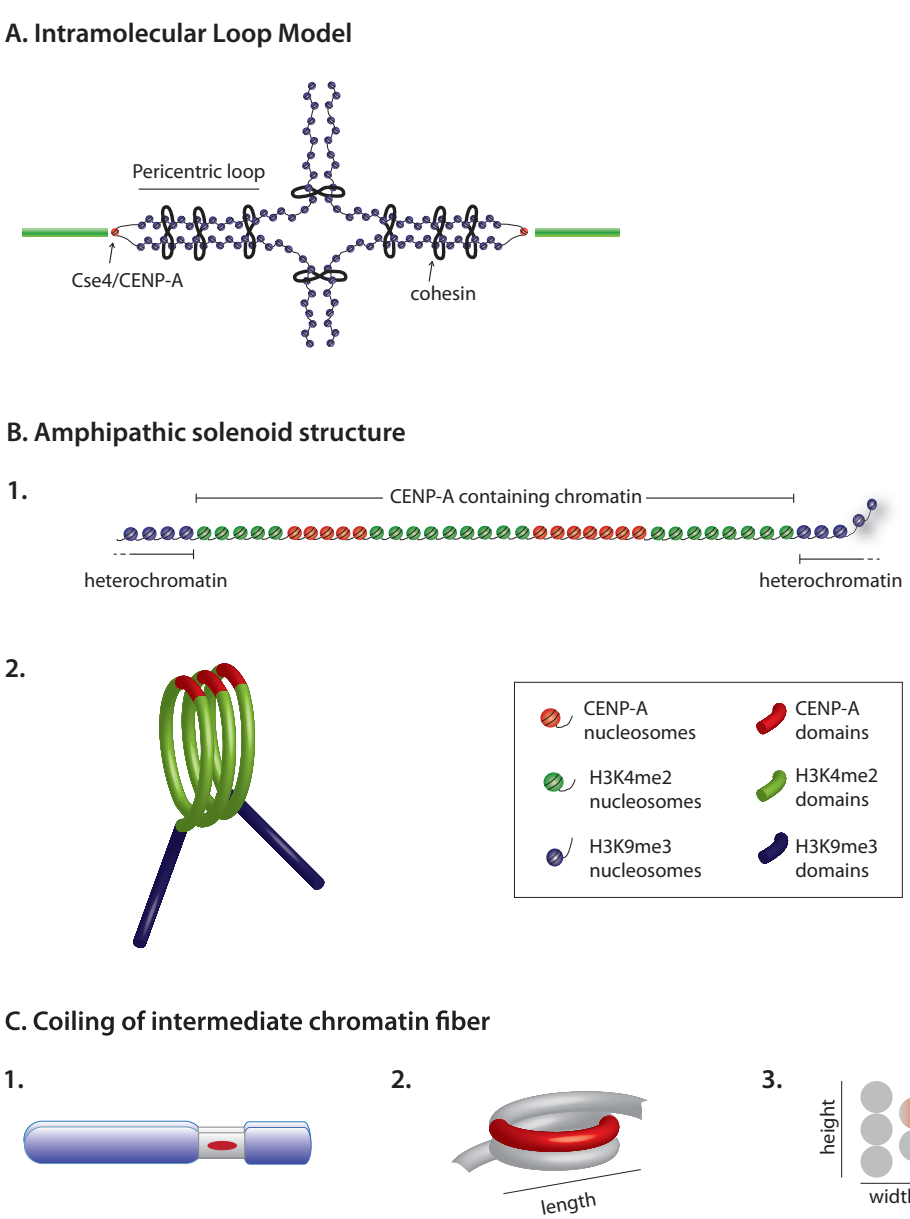

Figure 1 | Current models of centromeric chromatin organization.
A. Pericentric loop model. Model of budding yeast pericentric chromatin and centromere folding. Pericentric chromatin spans the distance between bioriented kinetochores, resulting in a cylindrical array within the mitotic spindle. This results in a cruciform configuration between sites of microtubule attachment and sister chromatid pairing. These loops of pericentric DNA together held by cohesin may provide the mechanical linkage between separated sister kinetochores (adapted from Yeh *et. al*, 2008)
B. Amphipatic solenoid structure. 1. Two dimensional chromatin fibers. Subdomains within the centromeric chromatin containing CENP-A nucleosomes (red) are interspersed with H3K4me2 domains (green) to form a domain of CENP-A containing chromatin, flanked by heterochromatin containing H3K9me3 nucleosomes (blue). **2.** At metaphase, when mitotic chromosomes condense, the interspersed CENP-A containing chromatin is organized in a amphipathic solenoid where the CENP-A subdomains face outwards interacting with outer kinetochore proteins. H3-containing nucleosomes are oriented inwards between the two sister chromatids (adapted from Schueler and Sullivan, 2006).
B. Coiling (or folding) of intermediate chromatin fiber. 1. Based on EM data only two thirds of the primary constriction is occupied by CENP-A (red). **2.** Coiling of the intermediate centromeric chromatin would result in a higher-order structure as shown in **3.** (adapted from Marshall *et. al*, 2008)

1.2 Single molecule super-resolution microscopy to study the organization of centromeric region

The models for centromeric chromatin folding and organization described above are based on light microscopy or EM analysis. High resolution analysis of the centromere by conventional microscopy has been restricted because of its intrinsic resolution. Resolution is limited by the wavelike character of light, which diffracts while passing through a lens and by the numerical aperture of the objective (Fig. 2); this limitation prevents objects spaced more closely than ~250 nm along the *x-y* axis and ~500 nm in the *z* axis from being distinguished from each other. EM has a much better spatial resolution, which can be as low as 2.4 Å. However, EM analysis of kinetochore components is limited by the constraints of preserving the structure and the availability of antibodies. Therefore, in order to understand the organization of the inner centromere and kinetochore we used the recently developed technique of super-resolution microscopy for analysis of the CENP-A containing region.

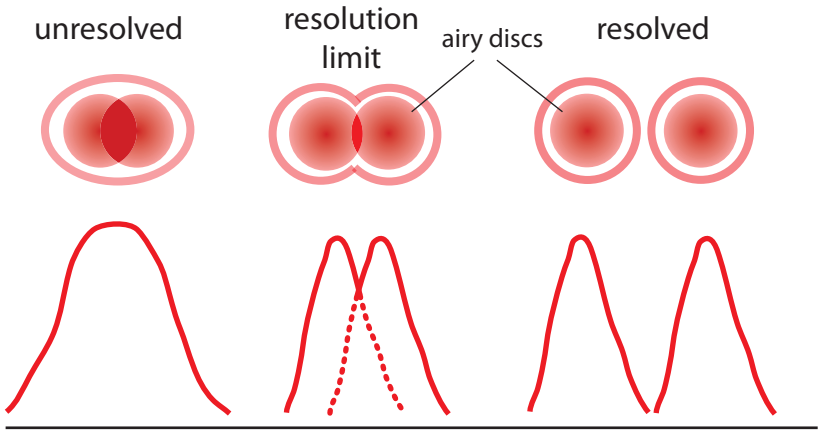

Figure 2 | Airy patterns and the limit of resolution. The limit of resolution is a measure of the ability of the objective lens to separate in the image adjacent details that are present in the object. The resolving power of an optical system is ultimately limited by diffraction by the aperture. Thus an optical system cannot form a perfect image of a point. When light from the various points of a specimen passes through the objective and an image is created, the various points in the specimen appear as small patterns in the image. These are known as Airy discs. The phenomenon is caused by diffraction of light as it passes through the circular aperture of the objective. Airy discs consist of small, concentric light and dark circles. The smaller the Airy discs projected by an objective in forming the image, the more detail of the specimen is discernible. Objective lenses of higher numerical aperture are capable of producing smaller Airy discs, and therefore can distinguish finer detail in the specimen. The limit at which two Airy discs can be resolved into separate entities is often called the Rayleigh criterion. This is when the first diffraction minimum of the image of one source point coincides with the maximum of another. The resolution is dependent on the objective numerical aperture (NA) and on the wavelength of the light that crosses the sample (λ): resolution = λ / 2x NA.

Recently, two distinct conceptual strategies have overcome light's diffraction barrier, allowing the analysis of biological structures at the super-resolution level. One strategy is a shaped illumination-based super-resolution method. This uses purely optical approaches to reduce the focal spot size, as in stimulated emission depletion (STED) fluorescence microscopy (Hell and Wichmann, 1994; Klar et al., 2000) and structured illumination microscopy (SIM) (Gustafsson, 2000). By modifying the excitation light pattern to yield a smaller excitation volume, STED and SIM can resolve structural details of biological specimens, down to ~30 nm in the *x-y* direction in the case of STED and ~100 nm in the case of SIM.

A second strategy for overcoming light's diffraction barrier is a probe-based super-resolution method. Its principle relies on the use of photoswitchable molecules to resolve dense populations of molecules with a resolution of tens of nm. This relies on stochastic fluorescence activation of a sparse subset of individual photoactivatable molecules; each single emitter can then be localized with nm accuracy by fitting a Gaussian function to its 2D intensity distribution. After image acquisition the fluorophores are bleached, and a new subset of fluorophores is stochastically activated. By performing several cycles (typically 1000s) of photoactivation, imaging, localization and bleaching, it is possible to computationally reconstruct a super-resolution image that consists of all the single-molecule positions of the fluorophores in the sample. This technique was independently developed by three groups and given the names photoactivated localization microscopy (PALM) (Betzig et al., 2006), fluorescence photoactivated localization microscopy (fPALM) (Hess et al., 2006), and stochastic optical reconstruction microscopy (STORM) (Rust et al., 2006). Whereas PALM/fPALM use photoactivatable or photoconvertible fluorescent proteins as probes, STORM uses synthetic fluorophores as probes. Probe-based super-resolution allows biological structures to be defined with 10s of nm accuracy, similar to the illumination-based super-resolution (Hell, 2009; Lippincott-Schwartz and Manley, 2009; Patterson et al., 2010).

Both illumination-based and probe-based super-resolution imaging approaches permit biologists to now visualize structures and processes within cells at or near to the molecular level. The order-of-magnitude improvement in spatial resolution achieved over previous light microscopy methods translates into an enormous potential for addressing several biological questions that require resolutions below 250 nm (Lippincott-Schwartz and Manley, 2009).

In parallel with the development of super-resolution imaging with single molecule sensitivity, several fluorescent proteins were discovered that fit the necessary requirements. The principal criterion that a fluorophore must exhibit is the ability of being photoactivatable (eg. PA-GFP), photoswitchable (eg. Dronpa), or photoconvertible (eg. tdEos) by a specific wavelength in order to control their emission over time. Other requirements include a very high brightness and contrast levels; these are essential to detect the highest possible number of photons per molecule before it photobleaches or reverts to a dark state. Aside from the fluorescent proteins, some synthetic organic dyes have also been used successfully because they display reversible photoswitching and irreversible photoactivation (the latter are also referred to as caged fluorophores). The main advantage of using synthetic fluorophores is their high brightness, excellent photostability, and improved contrast when compared to fluorescent proteins. Conventional fluorophores, like Cyanine and Alexa dyes, have now become commonly used in conjugation to primary or secondary antibody and usually in the presence of special buffers. Thus, their use is still limited to fixed sample examinations (Patterson et al., 2010).

For the studies described in this chapter I used the photoswitchable fluorophore dronpa to tag proteins of interest. To achieve dual color super-resolution I used secondary antibodies labeled with Alexa647 that in the presence of a proper buffer can cycle between dark-metastable and fluorescent states by irradiation at 633 nm (Folling et al., 2008; Heilemann et al., 2008; Steinhauer et al., 2008; van de Linde et al., 2008).

Alongside super-resolution with single molecule sensitivity we further developed an assay to artificially unfold the tight structure of the inner kinetochore domain. This method uses a low salt buffer lacking divalent cations (Earnshaw and Laemmli, 1983; Hudson et al., 2003). As we have recently shown, this causes the chromosomes to swell and chromatin higher-order structures to be lost, while preserving proteins attached to chromatin (Ribeiro et al., 2009).

By this approach, I was able to propose an alternative model for the folding and organization of the inner kinetochore domain.

2. RESULTS

2.1 Functional kinetochores of DT40 cells have on average 58 Kb of DNA

The distribution of kinetochore proteins within the DNA of neocentromeres has been mapped with high precision by chromatin immunoprecipitation (ChIP) (Alonso et al., 2003; Saffery et al., 2003; Capozzi et al., 2008). However, within the compact inner kinetochore structure it is not known how much additional DNA is included when the centromeric chromatin fiber folds to form the kinetochore. We have previously shown (Ribeiro et al., 2009) that the centromeres of condensin-depleted cells are fully functional whilst moving up to 2 μm away from the body of the chromosomes on the metaphase plate. This remarkable behaviour generates a very unique system to determine the amount of chromatin contained in a functional kinetochore *in vivo*. In order to obtain an absolute value of the DNA contained within the centromeric region I used, as reference points, three phages – T4, P1 and λ – with known amounts of DNA: 168, 90 and 48 kb, respectively. As a proof of principle the phage were fixed, stained with DAPI and images acquired from phages in separated slides. This analysis confirmed that it was possible to observe them and each represented a distinct but homogenous population. The 3 phages were then mixed to confirm that linear correlation between DNA amount and intensity could be observed (Fig. 3).

In order to quantify the amount of DNA in the kinetochore, I used the SMC2 KO cell lines expressing CENPH-GFP and GFP-CENP-A described in the previous chapter. These conditional cell lines were treated with doxycycline for 30 hours to deplete the condensin complexes. The 3 phages were fixed in PFA and resuspended in Vectashield with Dapi (1.5mg/ml); this mixture was used to mount the previously fixed cells (Fig. 4A). The cells and phage prepared in this way were used to acquire z-section images of $SMC2^{OFF}$ cells in metaphase and phages on a DeltaVision microscope system. By mixing both cells and phages we obtained an internal calibration for fluorescence intensity that provided an internal standard curve used to convert intensity into DNA amount in each set of experiments (Fig. 4C and D). TIFF files of all images (in separate channels) were transferred to ImageProPlus where the quantification was carried out. The quantification was done as described in the Material and Methods section. Compact CENP-A domains of functional SMC2-depleted kinetochores contained an average of 61 ± 24 Kb (average ± s.d., n=40) of

DNA while CENP-H domains contained 54 ± 21 Kb (average ± s.d., n=41) (Fig. 4C-F). The overall amount of DNA in a functional kinetochore of DT40 cells is 58 ± 23 kb (average ± s.d.) (Fig. 4F). Although there was no relevant difference between the average values determined for CENP-A and CENP-H domains, the interval of values obtained was very wide (ranging from 28 to 147 Kb).

To understand if the broad range of values determined for the amount of DNA at the kinetochore could be attributed to differences in kinetochore sizes, we further analysed the dimension of the outer kinetochore plates. In order to obtain this data we used the previously prepared EM serial sections of cells in metaphase (Chapter IV section 2.6). Our collaborators (Bruce McEwen and Yimin Dong) measured the length of outer kinetochore plates in the presence and absence of condensin. This analysis revealed, that kinetochores of wild type cells have an overall mean size of 145 ± 27 nm distributed into two Gaussian subpopulations with peaks centered at 126 ± 14 and 171 ± 9 nm (average ± s.d.; n=48) (Fig. 5). These measurements suggest that there may be more than one population of kinetochore sizes.

Although kinetochores of condensin-depleted cells appear structurally normal, they are slightly smaller in diameter than wild-type kinetochores. We observed that $SMC2^{OFF}$ kinetochore size distribution was fitted by a normal Gaussian centered at 106 ± 26 nm (average ± s.d.; n=49). A further indication that $SMC2^{OFF}$ kinetochores might be smaller came from an independent mass spectrometry analysis of isolated mitotic chromosomes. In these studies, loss of condensin correlates with a slight decrease of many centromere proteins (Shinya Ohta, unpublished data). However, $SMC2^{OFF}$ kinetochores are capable of directing chromosome alignment and anaphase segregation and therefore we postulate that they represent a "minimal" or "core" functional kinetochore.

Since wild-type kinetochores are about 1.3 x larger than $SMC2^{OFF}$ kinetochores, they would be expected to have about 1.3 x more DNA, and therefore about 1.3 x more nucleosomes. Based on the nucleosome spacing of 190 bp, as determined for DT40 cells (Jim Allan, personal communication), and according to the average amount of quantified DNA, a wild-type chicken kinetochore contains 415 ± 165 nucleosomes.

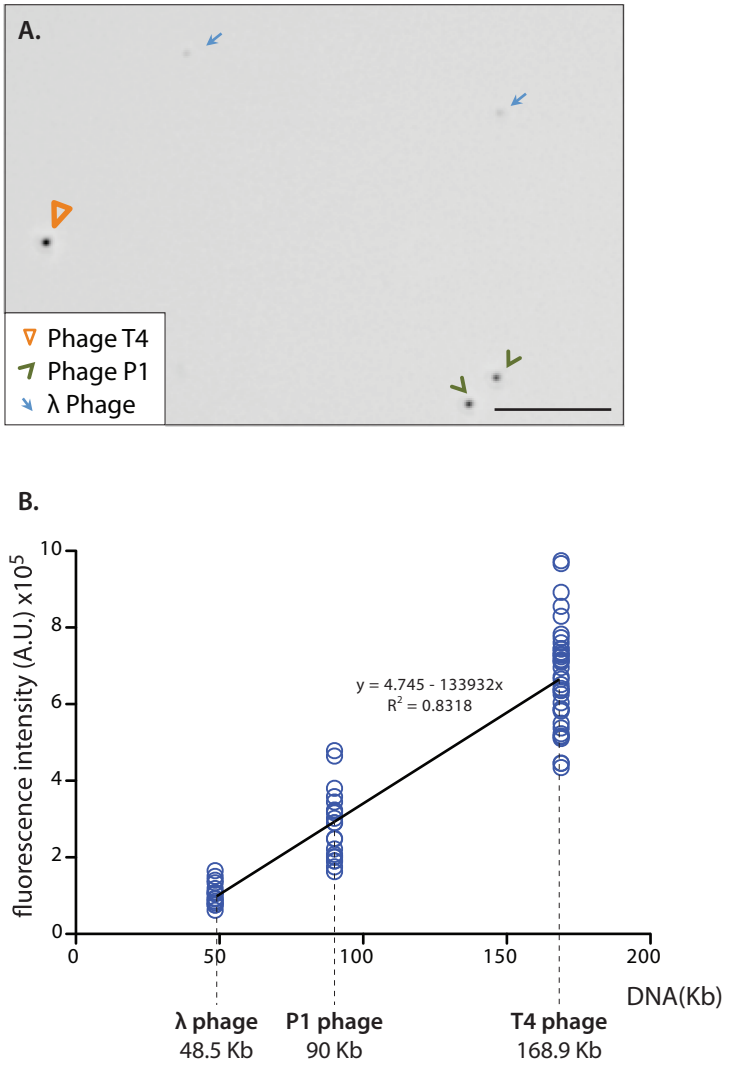

Figure 3 | Standard curve for determination of DNA amount based on fluorescence intensity. A. Inverted DAPI fluorescence image of a mixture of bacteriophages lambda, P1 and T4 in the same field of view (scale bar 5µm). **B.** Standard curve of fluorescence intensity (y axis) and DNA amount of bacteriophages lambda, P1 and T4 stained with DAPI (x axis).

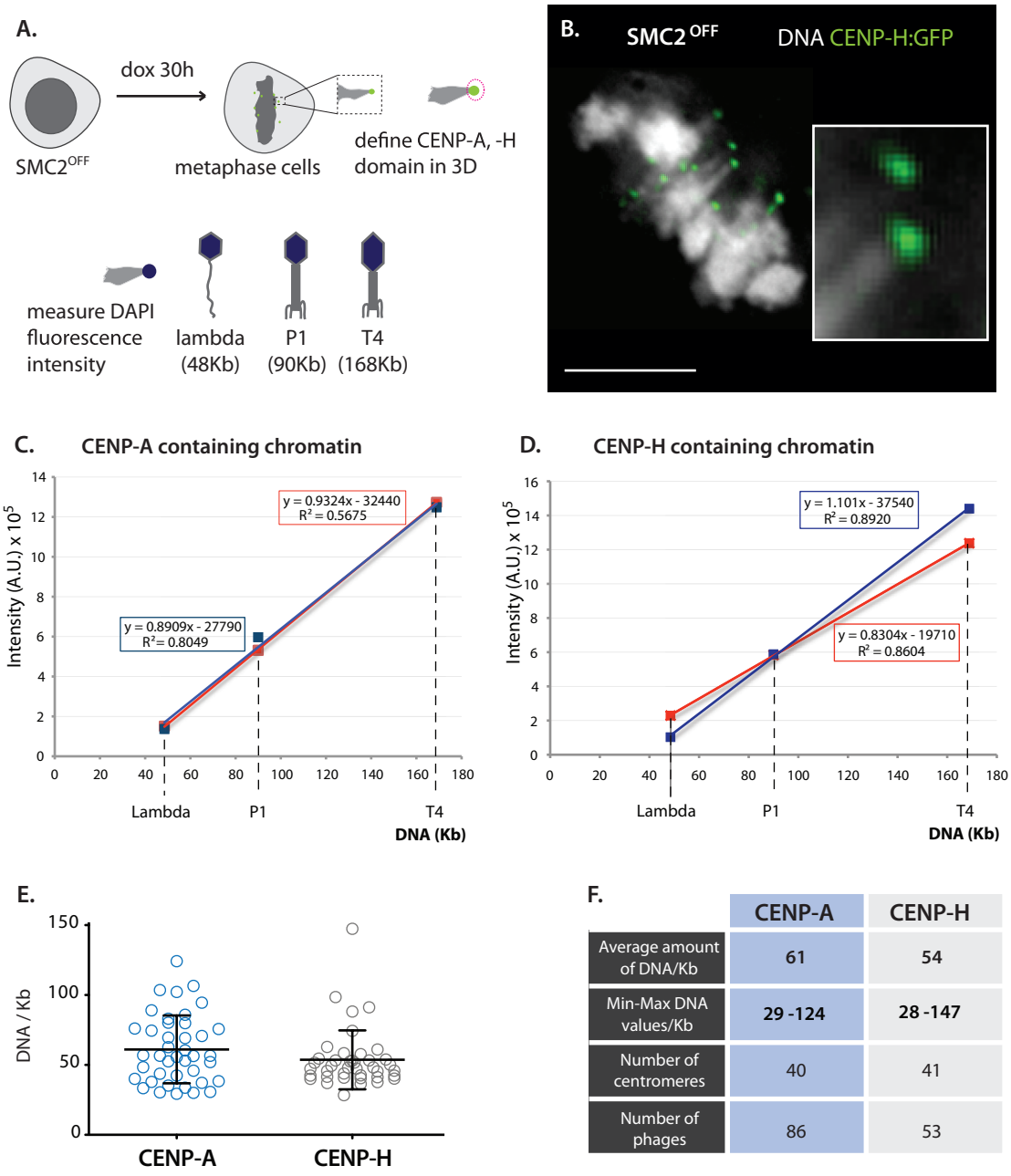

F.

	CENP-A	CENP-H
Average amount of DNA/Kb	61	54
Min-Max DNA values/Kb	29 -124	28 -147
Number of centromeres	40	41
Number of phages	86	53

Figure 4 |Quantification of DNA amount in a functional vertebrate kinetochore. A. Experimental procedure to measure kinetochore DNA content. **B.** Image of SMC2^{OFF} cell with several kinetochores undergoing "excursions". Inset shows two kinetochores marked with CENP-H-GFP with trailing chromatin (scale bar 5 µm). **C. and D.** Standard curves of the fluorescence intensity of DAPI-stained bacteriophages lambda, P1 and T4 mixed with SMC2^{OFF} cells expressing GFP-CENP-A (**C**) or CENP-H-GFP (**D**) used to convert fluorescence intensity into DNA amount **E.** Distribution of the amounts of DNA quantified for CENP-A and CENP-H area after plotting the values onto the standard curve obtained for the three internal reference bacteriophages (Graphs **C.** and **D.**). **F.** Values obtained from the quantification done in **E.**

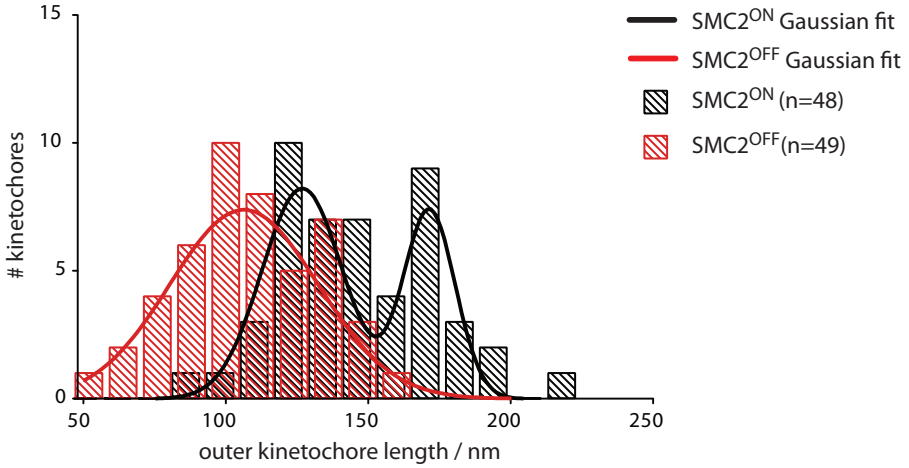

Figure 5 | Frequency of distribution of outer kinetochore size measured by EM.
The black solid line represents the best fit to bimodal Gaussian distribution centered at 127 ± 14 nm and 171 ± 9 nm for $SMC2^{ON}$ outer kinetochore diameter (average ± s.d.; n = 48). The red solid line represents the best fit to Gaussian distribution centered at 106 ± 26 nm for $SMC2^{OFF}$ outer kinetochore diameter (average ± s.d.; n = 49). The data in this figure was contributed by Yimin Dong and Dr. Bruce McEwen.

2.2 Map of inner centromeric chromatin

Centromeres are usually embedded in highly condensed heterochromatin and, as a result, the possibility to characterize the distribution of proteins in the underlying pericentromeric chromatin relative to the kinetochore *in vivo* has been very limited. The remarkable morphology of $SMC2^{OFF}$ pulled kinetochores allows them to be used as a system to analyse the organisation of the underlying distended pericentromeric region. Histones may present different modifications at their N-terminal tail. Histone modifications can either function by disrupting chromosomal contacts or by regulating non-histone protein interactions with chromatin. The two Histone modifications better characterized at the inner centromere/centromere region are di-methylated histone H3 at lysine 4 (H3K4me2) and tri-methylated histone H3 at lysine 9 (H3K9me3). While H3K4me2 is associated with activation of transcription, H3K9me3 is associated with repressed heterochromatin (Kouzarides, 2007). To characterize the chromatin adjacent to the kinetochore region, I immunostained condensin-depleted metaphase cells with antibodies against histone modifications known to be present within the centromeric and pericentromeric regions. Cells with chromosomes aligned in the metaphase plate with GFP-CENP-A-labeled centromeres were examined by indirect immunfuorescence and deconvolution microscopy (Fig. 6). H3K9me3 was present between sister kinetochores in $SMC2^{ON}$ cells (Fig. 6d) and fully occupied the extended pericentromeric region of pulled $SMC2^{OFF}$ cells, stretching out to the kinetochore (Fig. 6d'). In contrast, H3K4me2 only partially stained the pulled pericentromeric region, with a non-stained region consistently observed next to the kinetochores (Fig. 6a'). The inner centromeric protein, INCENP, which belongs to the well-characterized chromosomal passenger complex, occupies the whole extended pericentromeric region, as does the mitotic specific phosphorylation of threonine 3 on H3 (Dai et al., 2005) (Fig. 6b' and c'). It is worth noting that none of the histone modifications overlap significantly with CENP-A regions.

The enrichment of H3K9me3 and the lower levels of H3K4me2 adjacent to the CENP-A containing domain are in contradiction with what has been observed in human and *D. melanogaster* mitotic chromosomes (Sullivan and Karpen, 2004). These differences can be due to organism specificity, lack of sensitivity of microscopy tools or antibody accessibility.

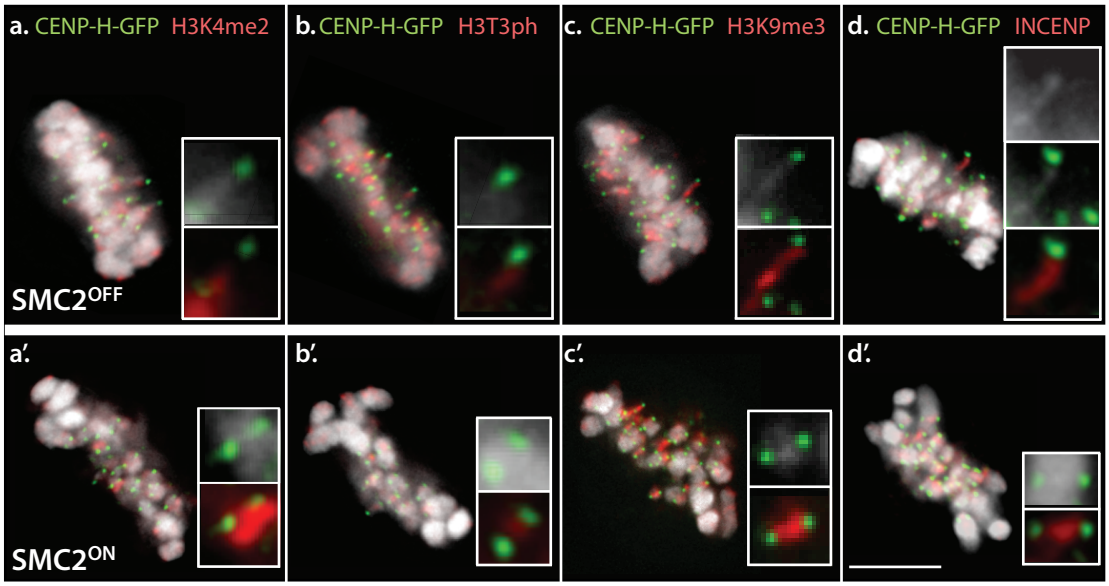

Figure 6 | Localization of histone modifications and INCENP on the extended inner centromeric chromatin of SMC2^{OFF} cells. SMC2^{OFF} (top panels) and SMC2^{ON} (bottom panels) metaphase cells expressing CENP-H-GFP and immunostained for **(a, a′)** H3K4me2, **(b, b′)** H3T3ph, **(c, c′)** H3K9me3 and **(d, d′)** INCENP (scale bar 5 µm).

2.3 The centromeric region unfolds to a higher extent in interphase than in mitotic cells

Information about protein localization within the inner domain of the kinetochore is essential to understand both its intrinsic composition and its overall organization. However, the tight structure of the centromere hampers protein localization. Few attempts have been made to build a detailed map of the localization of proteins in the kinetochore. For instance, Schittenhem *et al.* (Schittenhelm et al., 2007) determined by light microscopy the spatial organization of *Drosophila* kinetochores after analysis of kinetochores co-expressing combinations of mRFP/GFP tagged proteins. This study allowed a resolution of tens of nanometers and showed that CENP-C spreads in a polar orientation over a region between CENP-A and Mis12/Ndc-80 complexes. More recently, Wan *et al.* (Wan et al., 2009) used a fluorescent light microscopy-based method to measure the average separation between proteins labeled with two different fluorophores with nm accuracy within human metaphase kinetochores. This method revealed a detailed map of the relative localization of most outer kinetochore proteins to CENP-A. The measurements obtained allowed the conclusion that only CENP-C and CENP-A have compliant behaviour, i.e., both proteins oscillate when kinetochores move under tension. Furthermore, this study was complemented with the localization of the same subset of proteins when microtubules are not exerting forces in the kinetochore. The comparison of both showed selective inward movement of the Ndc80 complex implying that this complex might be bent, and that kinetochore undergoes through structural rearrangements. Although this is a comprehensive study of the outer kinetochore machinery, it still does not reveal how the inner kinetochore domain is organized.

In an attempt to acquire more details about the inner kinetochore region's organization, I stretched the centromeric region and looked at the distribution of both CCAN proteins and known histone modifications relative to tagged CENP-A.

In order to prepare fibers, I further developed a previously established assay (Earnshaw and Laemmli, 1983; Hudson et al., 2003; Ribeiro et al., 2009). This uses a low ionic-strength buffer (TEEN buffer – 2.5 mM NaCl, 20 nM NaEDTA pH9.0, 100 nM Triethanolamine-HCl pH8.5) containing EDTA in which the DNA negative charges are not fully neutralized. In this buffer, chromatin unfolds to beads-on-a-string nucleosomes, but kinetochore protein binding is retained (Ribeiro et al., 2009). Although interphase pre-

kinetochores are much more resistant to unfolding in this buffer than pericentromeric heterochromatin, longer incubations in TEEN buffer caused them to unravel, producing fibers in which separated blocks of CENP-A interspersed with non-CENP-A blocks (Fig. 7A). Interestingly, when these fibers were co-immunostained with antibodies specific for histone modifications (referred to in the previous section of this chapter), it became clear that H3K9me3 occupied the non-CENP-A subdomains (mean occupancy – defined as the percentage of the CENP-A-containing region occupied by H3K9me3 = 56%; s.d. 20%, n=11). Immunostaining for H3K4me2 was detected in the non-CENP-A blocks as well, but at lower levels than H3K9me3 (mean occupancy = 18%; s.d. 12%; n=9) (Fig 7A, 8A).

It has long been known that kinetochores undergo a structural maturation as cells enter mitosis (Roos, 1973), and indeed, mitotic kinetochores are considerably more resistant to unfolding in TEEN buffer than their interphase counterparts. When cells expressing GFP-CENP-A were blocked in prometaphase using colcemid, and then incubated for 30 min in TEEN buffer, fixed and processed for immunofluorescence, their kinetochores unfolded to a significantly lesser extent than their interphase counterparts (Fig. 7B, C). The average length of fibers (defined by the maximum extent of CENP-A staining) derived from mitotic centromeres was 1.12 ± 0.44 μm (mean ± s.d.; n=98), whereas the corresponding length for interphase was 2.47 ± 1.31 μm (mean ± s.d.; n=48) (Fig. 8B). It was clear that the maximum stretch achieved in mitotic kinetochores was lower than that attained during interphase. While mitotic kinetochores reached a maximum length of 3.58 μm, for interphase cells a maximum of 11μm was observed. Based on this fact, we defined a cut-off of 3 μm, so that the two populations could be clearly distinguished from one another. Under this criteria, only 5% of mitotic CENP-A stretched domains measured > 3 μm (all less than 5 μm), while 40% of interphase pre-kinetochores were in this category, with 12% being longer than 6 μm (Fig. 8B).

Therefore TEEN buffer can be used to reveal differences in the organization of interphase pre-kinetochores and mitotic (mature) kinetochores.

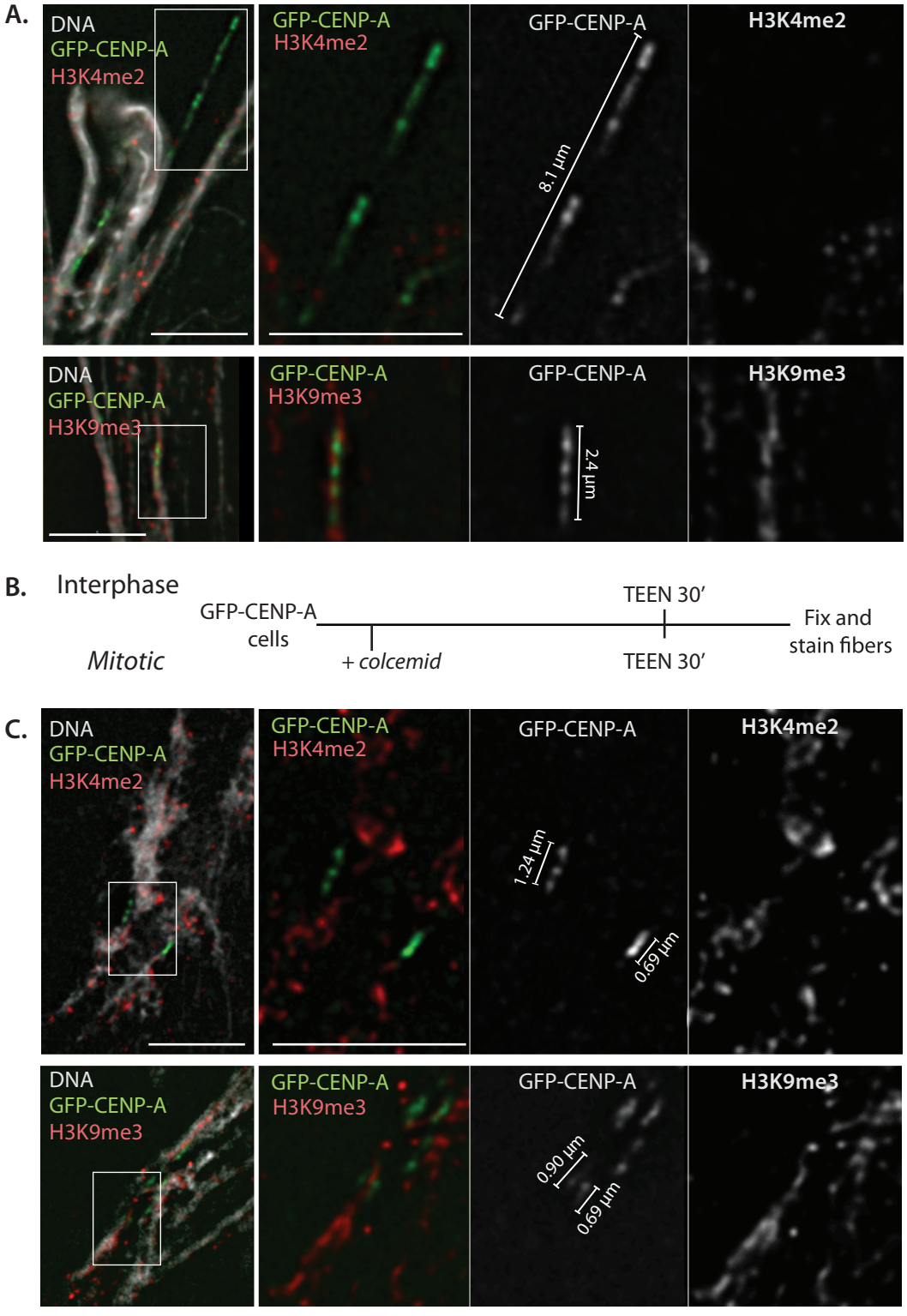

Figure 7 | Mitotic kinetochores and interphase pre-kinetochores behave differently when subjected to unfolding induced by TEEN buffer. A. Examples of interphase fibers immunostained for H3K9me3 and H3K4me2. Blocks of CENP-A on the unfolded chromatin fiber (green) are intercalated with blocks of H3K9me3 (bottom panels); H3K4me2 (top panels) is not present to the same extent. **B.** Experimental procedure for obtaining unfolded centromeric region of mitotic and interphase cells. **C.** Examples of mitotic fibers immunostained for H3K9me3 and H3K4me2 where CENP-A is present as a compact block. Neither H3K9me3 (bottom panels) nor H3K4me2 (top panels) are present in CENP-A regions (all scale bars 5 µm).

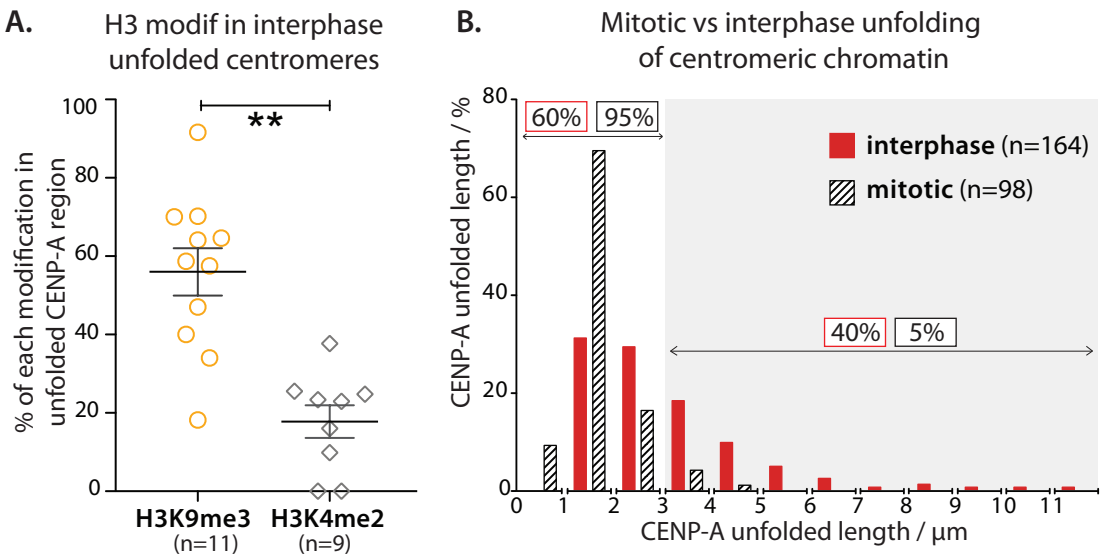

Figure 8 | Mitotic kinetochores are more stable than interphase pre-kinetochores when subjected to unfolding induced by TEEN buffer. A. Quantification of the percentage of the total length of the CENP-A-containing interphase fibers occupied by H3K9me3 (yellow) and H3K4me2 (grey). **B.** Distribution of CENP-A fiber lengths for interphase (red) and mitotic (black) cells. The grey shadow indicates the distribution of fibers longer than 3 µm (used to define a cut-off between the two populations).

2.4 Analysis of mitotic centromeric stretch in the absence of some CCAN proteins

I have shown that "mature" kinetochores are significantly more robust than interphase pre-kinetochores when exposed to TEEN buffer. This observation suggested that kinetochore maturation in mitosis could also involve the establishment of structural crosslinks. These crosslinks could occur either in the inner kinetochore domain, in the inner centromeric proximal chromatin, or in the outer kinetochore.

To test this hypothesis I analysed the behaviour of centromeric chromatin exposed to TEEN buffer in a series of DT40 knockout cell lines of individual CCAN proteins (such as CENP-C (Kwon et al., 2007), CENP-H (Fukagawa et al., 2001), CENP-N (Okada et al., 2006) and CENP–W (Hori et al., 2008)), as well as in the SMC2 knockout cell line.

All of these cell lines are conditional knockouts because the absence of the specific gene is lethal. Therefore, the cell lines are maintained by the expression of the cDNA using a tetracycline-repressible promoter. Addition of the tetracycline analogue, doxycycline, represses the cDNA transcription and allows the analyses of the phenotypes in the absence of each specific protein.

The different cell lines were treated with doxycycline for the recommended time (30 – 48 h), cells were then blocked in prometaphase by colcemid and the extent of CENP-A stretch (length of the unfolded CENP-A chromatin fiber) was measured after incubation in TEEN buffer.

Remarkably, no significant differences were observed for the maximal length of unfolded CENP-A containing mitotic chromatin in the absence of CENP-H, CENP-N or CENP-W (Fig. 9A, B). Using the 3 μm cut-off established above to distinguish between interphase and mitotic fibers, we observed CENP-A domains >3 μm in 8%, 5% and 8% of unfolded CENP-H^{ON}, CENP-N^{ON} and CENP-W^{ON} kinetochores, respectively. In the corresponding CENP-H^{OFF}, CENP-N^{OFF} and CENP-W^{OFF} kinetochores, we observed no increase in the maximal length of the CENP-A domains (4%, 0% and 8% >3μm, respectively). Thus, none of these proteins are essential for mitotic kinetochore structural integrity in this assay.

In contrast, the loss of CENP-C caused a striking de-stabilisation of the mitotic kinetochore in the TEEN assay (Fig. 10B). In this case, the population of fibers longer than 3 μm increased from 5% to 25% (Fig. 10A). The maximal lengths of CENP-A domains after

CENP-C depletion were much closer to the interphase kinetochore ones. Therefore, CENP-C is required for the stability of the mitotic inner kinetochore.

Depletion of condensin yielded an intermediate result in this unfolding assay. The number of extended CENP-A domains longer than 3 μm increased from 3% to 14%, however, domains longer than 6 μm were never observed (Fig. 9B). Thus, it appears that condensin could contribute to some extent to the structural integrity of the CENP-A containing region in mitosis.

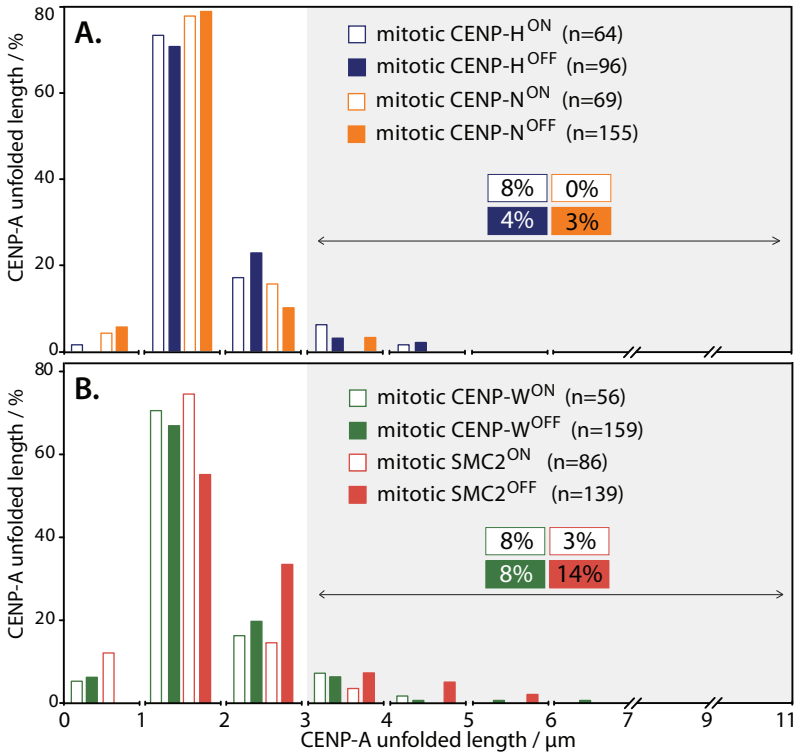

Figure 9 | CENP-H, CENP-N, CENP-W and the condensin complex have minor or no effect in the stability of mitotic kinetochores. A. Distribution of lengths of unfolded mitotic CENP-A chromatin fibers measured in the presence or absence of CENP-N (orange) or CENP-H (blue). **B.** Distribution of lengths of unfolded mitotic CENP-A chromatin fibers measured in the presence or absence of CENP-W (green) or SMC2 (pink).

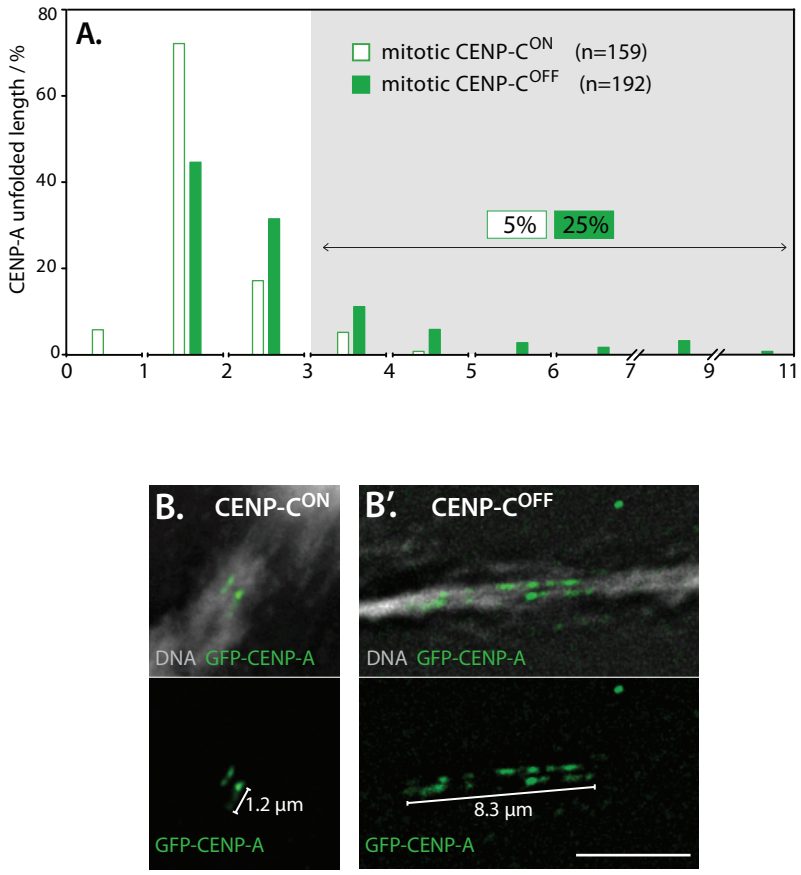

Figure 10 | CENP-C is essential to confer extra stability to mitotic kinetochores A. Distribution of unfolded CENP-A chromatin fibers from mitotic CENP-C^{ON} and CENP-C^{OFF} cells. **B.** In the absence of CENP-C (CENP-C^{OFF}) mitotic centromeres unravel to levels similar to those observed in interphase of wild type cells (scale bar 5 µm).

2.5 Characterization of interphase centromeric unfolded fibers

I next wanted to address the question of whether constitutive centromeric associated network (CCAN) proteins are bound to CENP-A or H3-containing chromatin blocks. To date, this type of analysis has been carried out by ChIP, and, using this assay, co-localization of CENP-C and CENP-H with CENP-A domains was observed in human neocentromeres (Alonso et al., 2007; Capozzi et al., 2008). All previous information available on the localization of histone modifications within the inner kinetochore domain come from either ChIP studies on human or mouse minor satellites (Peters et al., 2003; Lam et al., 2006) or from light microscopy immunofluorescence in stretched centromeres (Zinkowski et al., 1991) or extended fibers (Sullivan and Karpen, 2004).

Although previous studies mapped the distribution of ACA proteins along stretched centromeres, they were unable to map the distribution of other kinetochore proteins relative to CENP-A, either because lack of appropriate probes (Zinkowski et al., 1991), or because other kinetochore proteins were removed by the sample preparation procedure (Sullivan and Karpen, 2004).

We used interphase extended centromeric fibers obtained in TEEN to look at the localization of a subset of the CCAN proteins such as CENP-C, CENP-H and CENP-W. Centromeres from the GFP-CENP-A cell line were unfolded as described above and immunostained with a collection of CCAN-specific antibodies.

In figure 10 there are examples of images acquired using light microscopy followed by deconvolution. In shorter fibers with GFP-labeled CENP-A or CENP-H, all the CCAN proteins seem to colocalize with CENP-A (or CENP-H) (Fig. 11A). Likewise, in the example of a longer fiber (Fig. 11B), there appears to be co-localization between CENP-H (labeled with GFP) and CENP-T (detected by antibody).

Since the CCAN proteins are retained in the artificially unfolded fibers and they localize to CENP-A regions, we attempted to determine more accurately the relative localization of these proteins at higher spatial resolution.

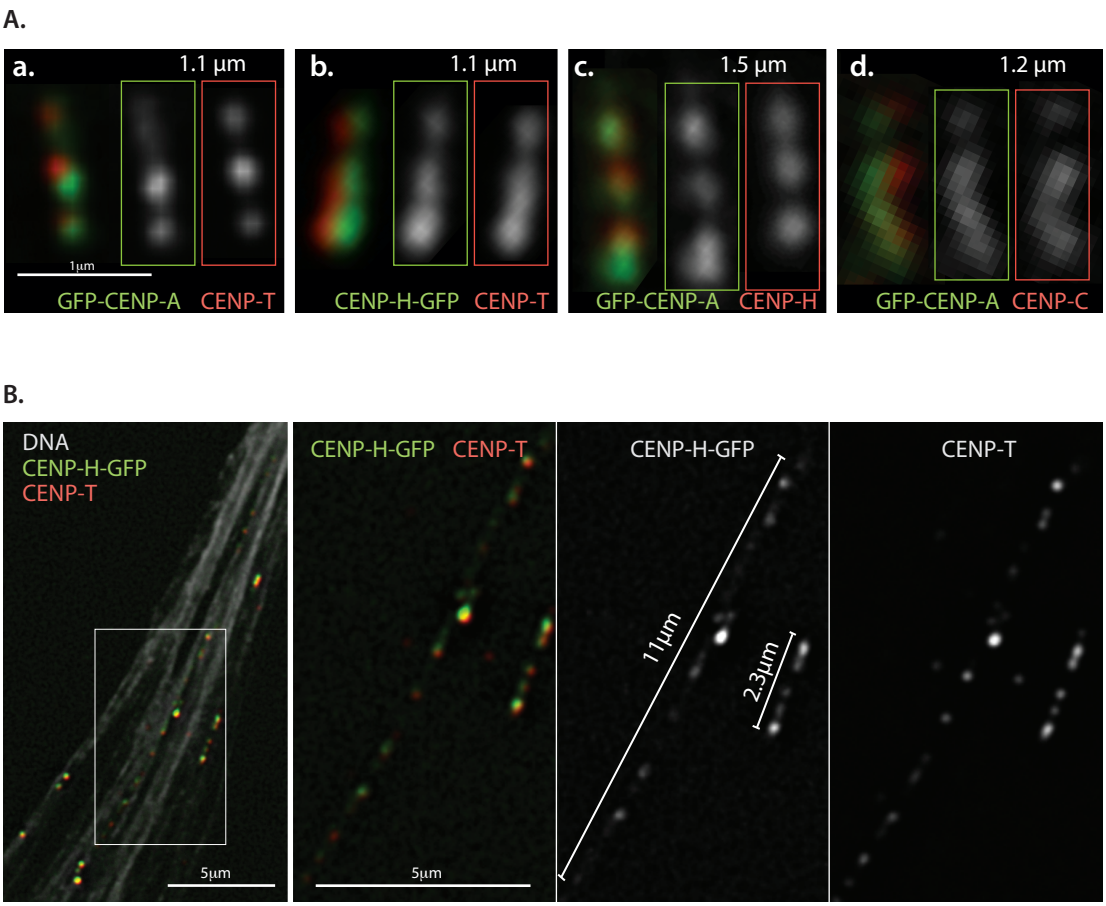

Figure 11 | Localization of CCAN proteins by deconvolution light microscopy on extended CENP-A containing regions from interphase cells. A. Examples of short fibers, length is indicated on top of each image**.** GFP-CENP-A (**a**) or CENP-H-GFP (**b**) immunostained with an antibody against CENP-T. GFP-CENP-A fibers immunostained with antibodies against CENP-H (**c**) and CENP-C (**d**). The two colored boxes indicate the separated channels for each image. Scale bar 1 µm. **B.** Example of a long fiber of CENP-H-GFP expressing cell line immunostained with CENP-T antibody. Inset shown for separate channels (scale bar 5 µm).

2.6 Use of super-resolution microscopy with single molecule sensitivity to characterize interphase centromeric fibers

To obtain a detailed map of the unfolded centromeric region, I decided to take advantage of super-resolution imaging. The advent of new microscopy techniques based on PALM and STORM, has lowered the resolution limit to tens of nm.

The method used is similar to (fluorescence) photoactivation-localisation microscopy (fPALM) (Betzig et al., 2006; Hess et al., 2006) and stochastic optical reconstruction microscopy (STORM) (Rust et al., 2006), which are both based on single-molecule detection of switchable fluorophores. Cycles of stochastic switching, detection and localization of single-molecules on a widefield microscope are used to reconstruct super-resolution images. Both provide single-molecule sensitivity with a spatial resolution of tens of nm.

PALM typically uses photoactivatable fluorescent proteins to achieve the temporal separation of the emission from different single molecules. For our experiments, we tagged CENP-A with the reversible fluorescent protein Dronpa, which photo-switches between dark and bright states upon illumination with 488 and 405 nm, respectively (Ando et al., 2004; Habuchi et al., 2005). Chromatin from cells stably expressing Dronpa-CENP-A was unfolded with TEEN buffer and immunostained for detection of different CCAN proteins using Alexa Fluor 647-labeled secondary antibodies. This synthetic fluorophore can spontaneously cycle between dark-metastable and fluorescent states by irradiation at 633 nm. The reaction is dependent on efficient oxygen removal and the addition of the triplet quencher (such as β-mercaptoethylamine) to generate a stable non-fluorescent state (Heilemann et al., 2008; Steinhauer et al., 2008; van de Linde et al., 2008). Using these tools, we constructed a two-colour super-resolution map of the stretched fibers by sequential imaging using 488-nm and 633-nm irradiation.

Several factors influence the spatial resolution achieved in a PALM experiment, namely the number of photons that we can detect from each fluorophore, the background of the image and the mechanical drift of the sample, among others. A common way to estimate the value of the spatial resolution is to localize several times the same single molecule (Fig. 12A), construct a density image that represents the probability to find that molecule in a certain area (Fig. 12B) and quantify the uncertainty in its position by fitting a gaussian function to a cross section of its localization density image

(Fig. 12C). The value of the full-width-at-half-maximum (FWHM) of the Gaussian function that we obtain, 37 nm in this case, is thus an estimation of our spatial resolution.

Next, to verify wether the Dronpa-CENP-A population that we observed corresponded to the majority of the endogenous CENP-A, we imaged Dronpa-CENP-A unfolded fibers immunostained with CENP-A antibody (Fig. 12D). This showed us that most of the endogenous CENP-A was in fact labeled with Dronpa.

After establishing the experimental conditions and estimating the spatial resolution given by the system, we looked at several of the CCAN proteins in 2-D fibers by super-resolution microscopy with single molecule sensitivity. After immunostaining Dronpa-CENP-A unfolded fibers with CENP-C, CENP-H and CENP-T specific antibodies we collected the data. This was then processed in order to localize individual molecules (Fig. 11). Reconstructed images show that CENP-C, CENP-H and CENP-T co-localize with CENP-A in fibers where the unfolding is not complete (Fig. 13A-C). However, when longer fibers are unfolded to reveal CENP-A subdomains we were able to observe a very interesting pattern. While CENP-C and CENP-H displayed a consistent localization with CENP-A subdomains (Fig. 13A', B'), CENP-T was reproducibly localized between CENP-A subdomains (Fig. 13C').

Interestingly, CENP-T localization is inconsistent with current centromere models, because they do not contemplate the presence of non-CENP-A chromatin domains in the outward face of the centromere, where the kinetochore assembles.

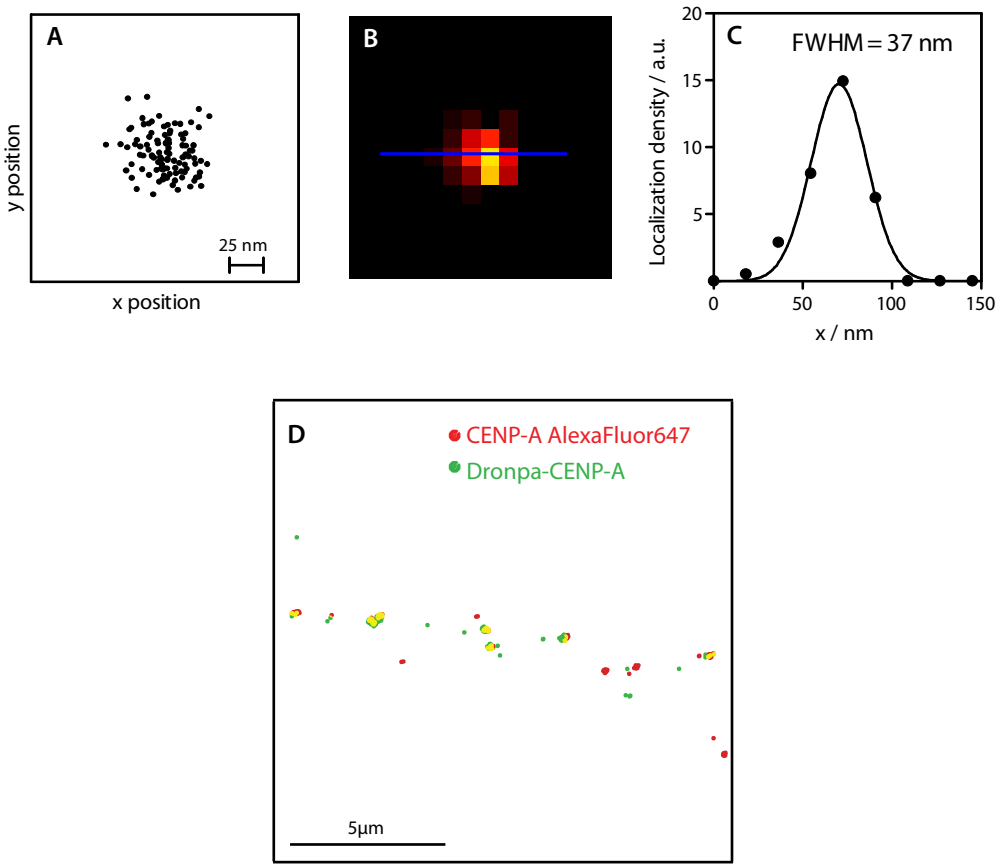

Figure 12 | Establishment of resolution and experimental conditions used in super-resolution imaging. A - C. Estimation of the spatial resolution achieved with super-resolution microscopy. **A.** Multiple localizations of the same molecule of AlexaFluor 647; **B.** Density image with line cross section; **C.** Gaussian fitting of the cross section drawn in B showing an estimate spatial resolution of 37 nm. **D.** Dronpa-CENP-A co-localization with CENP-A-Alexa 647. Dronpa-CENP-A cell line immunostained with a CENP-A antibody where the majority of CENP-A blocks show both labels. These experiments were done in collaboration with Dr. Cristina Flors.

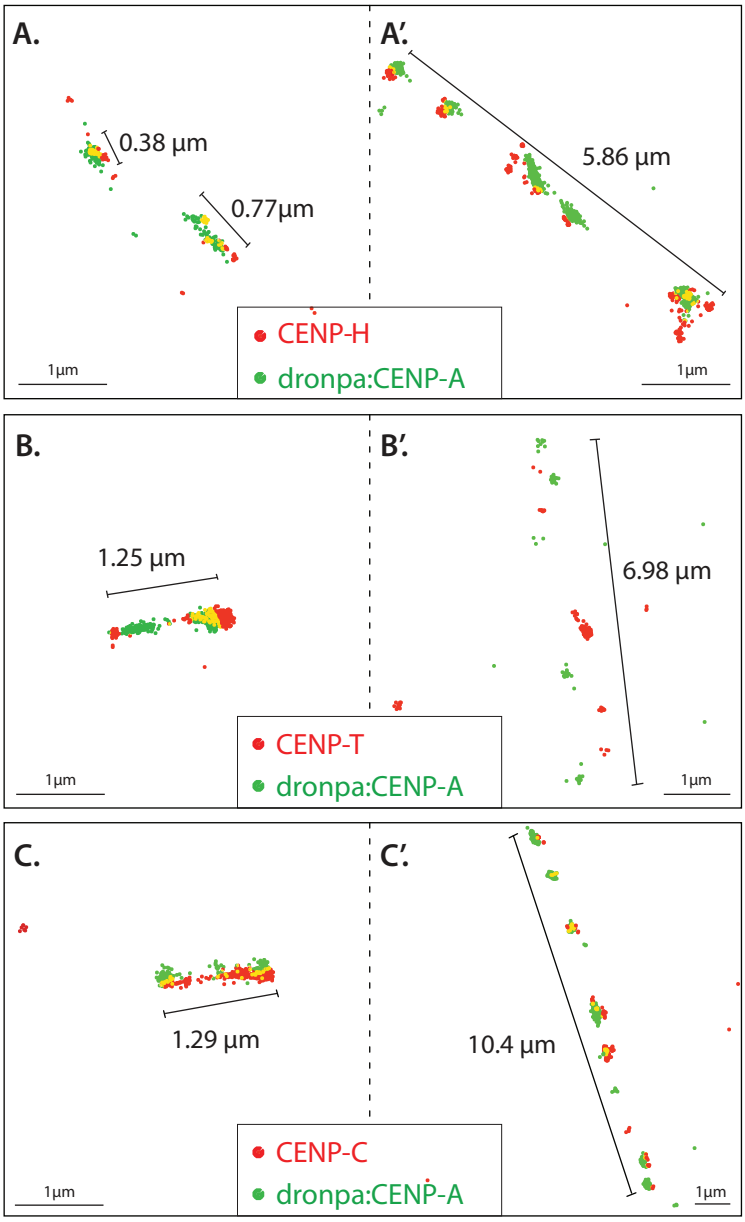

Figure 13 | Use of super-resolution microscopy with single molecule sensitivity to determine the localization of CCAN proteins in interphase CENP-A chromatin fibers. A. and A'. CENP-H (red dots) co-localizes with CENP-A (green dots) both in short (**A**) and more extended (**A'**) fibers. **B. and B'.** CENP-T (red dots) co-localizes with CENP-A (green dots) in short fibers (**B**). However in more extended fibers (**B'**), CENP-T is interspersed between CENP-A domains. **C. and C'.** CENP-C (red dots) co-localizes with CENP-A (green dots) both in short (**C**) and long (**C'**) fibers. CENP-C, CENP-H and CENP-T where detected with primary specific antibodies labeled with Alexa 647. These experiments were done in collaboration with Dr. Cristina Flors.

2.7 H3K9me3 is interspersed with CENP-A domains in interphase unfolded vertebrate centromere.

CENP-A containing chromatin domains are interspersed with blocks of non-CENP-A chromatin. Therefore, we wanted to characterize these non-CENP-A domains in terms of heterochromatin-associated modifications present in canonical histone H3.

Since some of our results obtained by deconvolution microscopy were not in agreement with the histone modifications patterns observed in stretched fibers of both human and *Drosophila* centromere (section 3 of current chapter), we wanted to use super-resolution microscopy to map heterochromatin-associated modifications more precisely along the centromeric chromatin fiber.

Figure 13 shows an extended centromeric region that stretches over 13 µm, as determined by the limits of the CENP-A domains. Alternating CENP-A and H3K9me3 chromatin blocks are readily apparent (Fig. 14A, A'). Super-resolution microscopy also detected H3K4me2 between CENP-A blocks, but while H3K9me3 was present as defined blocks, H3K4me2 showed a more scattered distribution (Fig. 14B, B'). In both examples there are chromatin regions unlabeled with either anti-H3K9me3 or anti-H3K4me2. These may contain either unmodified nucleosomes or nucleosomes bearing other modifications.

A rough estimation of the amount of CENP-A in the fiber in Figure 14A' can be obtained from the number of localizations (a total of 123 localizations). Assuming that on average each Dronpa molecule switches about 3-5 times (Flors et al., 2007), the number of *labeled* CENP-A molecules is about 25-40. This value, however, should be taken with caution, since Dronpa can switch up to 170 times (Habuchi et al., 2005). For this estimation, we also assume that most CENP-A in the fibers is labeled with Dronpa and that the amount of endogenous CENP-A is not significant (Fig. 12D).

The results here obtained lead us to conclude that H3K9me3 is definitely a histone modification present in CENP-A containing regions of DT40 cells. Furthermore, this modification is present at higher levels than the other modification studied, i.e. H3K4me2. These results are in disagreement with results published for other centromeres, where H3K9me3 was excluded and only H3K4me2 was observed (Sullivan and Karpen, 2004). These discrepancies could either reflect the existence of a differential organisation among

the centromeres from different species. Alternatively, the methods used in previous studies might not be sensitive enough for detection of low levels of antibody-labeled proteins. A corollary to this observation is that possibly these modifications are not relevant for centromere identity.

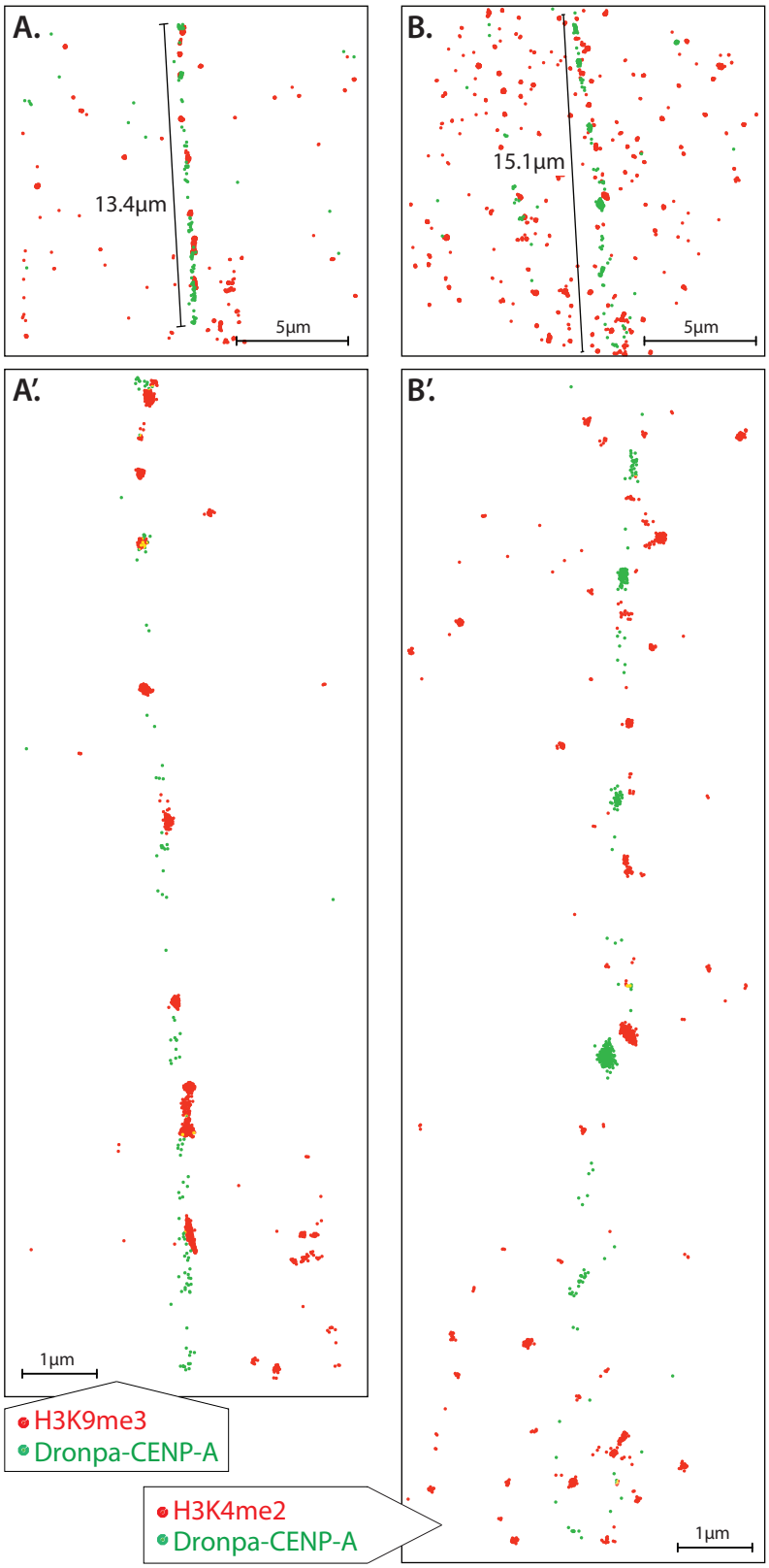

Figure 14 | Mapping histone modifications in interphase unfolded CENP-A containing region using super-resolution microscopy with single molecule sensitivity. A. Example of a long interphase fiber immunostained with an antibody against H3K9me3. This modification occupies chromatin blocks between CENP-A arrays. This is seen more clearly in the zoom in **A'. B.** Example of a long fiber immunostained with an antibody against H3K4me2. This modification is also detected between CENP-A arrays, but with a more diffuse distribution; zoom in **B'.** (Dronpa-CENP-A is represented as green dots and H3K9me3 or H3K4me2 labeled with Alexa 647 is represented as red dots. Each dot corresponds to a single molecule localization). These experiments were carried out in collaboration with Dr. Cristina Flors.

2.8 Evidence for the existence of two putative distinct chromatin structures in interphase chromatin extended fibers

Determination of the type of chromatin fiber structure present in centromeres has been hampered by ~ 250 nm resolution of common light microscopy systems. Since in our experimental system we gently unravel the chromatin fibers just making use of ionic strength, we considered that the width of the fibers obtained could be used to elucidate the forms of chromatin present in pre-kinetochores.

Therefore, we measured the FWHM (full-width at half maximum) of fibers where the labeled cluster was spatially isolated, and the appearance of a contiguous unit was unambiguous. We measured 53 fibers that were CENP-A tagged and 30 fibers with H3K9me3 labeling. Measurements of these fibers show a clear bimodal Gaussian distribution centered at 46 and 67 nm for CENP-A (Fig. 15A), and at 40 and 57 nm for H3K9me3 (Fig. 15B). Strikingly, the peaks in both measurements show a separation of 20 nm. If we take into consideration that the intrinsic error of our super-resolution measurements is 37 nm, these values of the distributions are consistent with the existence of 10 nm and 30 nm fibers.

Overall, it is tempting to suggest that the centromere is constituted by 30 nm fibers, which can be further unraveled to the level of 10 nm fibers. The width of these fibers are in agreement with the observed widths of 30-nm fiber obtained in *vitro* (Dorigo et al., 2004; Robinson et al., 2006) and the *in vivo* EM measurements (Marshall et al., 2008)

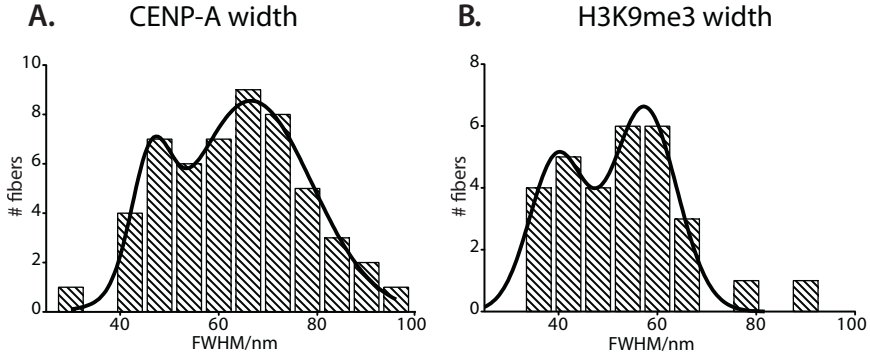

Figure 15 | Indication of the existence of two chromatin structures, the 10 and 30 nm fibers, in extended interphase fibers. A. Frequency distribution histogram of stretched fiber widths (FWHM - full width at half maximum) measured from super-resolution reconstructed images of (**A**) Dronpa-labeled CENP-A and (**B**) Alexa Fluor 647 labeled H3K9me3. The solid lines represent the best fit to bimodal Gaussian distributions centered at 46 and 67 nm for CENP-A (n = 53), and 40 and 57 nm for H3K9me3 (n=30). The data in this figure was contributed by Dr. Cristina Flors.

3. DISCUSSION

3.1 DNA content of a functional kinetochore

There are two critical aspects that today limit our understanding of the organization of regional centromeres. The first is the knowledge of the amount of DNA involved in the formation of the inner kinetochore domain structure together with its folding. The second concerns the interconnection between the architecture of the inner kinetochore domain and the outer kinetochore proteins that assemble in mitosis.

To address the first point I use the SMC2 conditional knockout cell line characterized in the previous chapter. As I have demonstrated (Chapter IV), in the absence of condensin kinetochores that are fully functional can move up to 2 μm away from the metaphase plate, allowing the resolution of the kinetochore from the underlying chromatin. Using this tool, I could define the thee-dimensional volumes occupied by CENP-A and CENP-H GFP-tagged proteins, and most importantly, quantify the amount of DNA contained within the kinetochore region. By using 3 different phages I first demonstrated that there is a linear relationship between DAPI fluorescence intensity and DNA amount. Then, the 3 different phages, containing known amounts of DNA, were used to establish a linear correlation and to convert the fluorescence intensity into amount of DNA of the kinetochores under analysis.

Based on these analyses I can estimate that the amount of DNA in DT40 kinetochores is 58 ± 23 Kb (average ± s.d., n=81). The observed range of DNA content could be due to the variation in size between kinetochores observed by electron microscopy. However I cannot rule out that the differences are related to the degree of stretching occurring at the particular kinetochore under analysis. Since kinetochores are pulled away from the primary constriction by random amounts up to 2 micron, the amount of pericentromeric chromatin immediately adjacent to the kinetochore may vary. Nevertheless, the amount of DNA that we detected in our study to be part of the kinetochore is much lower than that previously reported to participate in kinetochore structure (500 - 1500 Kb) (Blower et al., 2002) for human centromeres (0.5 – 7 Mb in size) (Willard, 1990; Rudd and Willard, 2004; Schueler and Sullivan, 2006). The amount of DNA in DT40 kinetochores reported here is much closer to the values determined by

chromatin immunoprecipitation (ChIP) for human neocentromeres, which ranges from 54 to 464 Kb (Lo et al., 2001a; Sumer et al., 2003; Chueh et al., 2005; Alonso et al., 2007; Capozzi et al., 2008). However, both ChIP and extended fiber studies (Sullivan and Karpen, 2004) cannot give information on the topology of chromatin fiber folding in the intact structure, as it is possible that other nearby chromatin fibers lacking CENP-A are incorporated during the folding of the compact kinetochore domain. Our results indicate that the inclusion of such external DNA in the structurally compact and functional kinetochore must be minimal at best.

Furthermore, the total number of nucleosomes, based on our quantification and considering that chicken cells have 191bp of DNA wrapped around each nucleosome (Jim Allan, personal communication) is 415 nucleosomes. From the estimated number of CENP-A molecules (25 to 40 molecules, i.e. 12 to 20 nucleosomes) we can establish that 3 to 10% of total centromere nucleosomes contain CENP-A in chicken DT40 centromeres. Bearing in mind that there are 4 – 7 microtubules per kinetochore, and 12 to 20 CENP-A nucleosomes, the relationship between the number of CENP-A nucleosomes and the number of microtubule attachments is 3:1 in these kinetochores.

Using the data obtained in this analysis and the data available from published studies in other organisms, we can try to establish if any kind of relationship exists either between the number of microtubules and the amount of DNA, or between the number of microtubules and the number of CENP-A nucleosomes (Fig. 16A). It is well established that, in budding yeast, 125 bp of DNA are wrapped around 1 CENP-A nucleosome, to which a single microtubule attaches (Fitzgerald-Hayes et al., 1982; Winey et al., 1995; Furuyama and Biggins, 2007). Beside the budding yeast point centromere, the fission yeast regional centromere is also well studied. In this case, CENP-A occupies an average of 10 Kb and there are 2 – 4 microtubule attachment sites (Ding et al., 1993; Partridge et al., 2000). However, the number of nucleosomes contained in this region is still controversial. In a recent study, it was postulated that fission yeast have 2 – 3 CENP-A nucleosomes (Joglekar et al., 2008); this number was calculated by counting the number of CENP-A:GFP proteins using a fluorescence ratio method. Assuming that the ratio DNA / CENP-A nucleosomes is a conserved parameter during evolution, and based on our calculation that 6.5% of the total amount of nucleosomes are CENP-A nucleosomes, this would give a theoretical number of 4 CENP-A nucleosomes for fission yeast centromere; this calculated value is remarkably similar to the published value (Joglekar et al., 2008)). Moreover, if we

plot the average values of the number of microtubules vs DNA amount and number of microtubules vs number of CENP-A nucleosomes for budding yeast, fission yeast and DT40 kinetochores we obtain, for both parameters, a relationship explained by a quadratic regression (Fig. 16A).

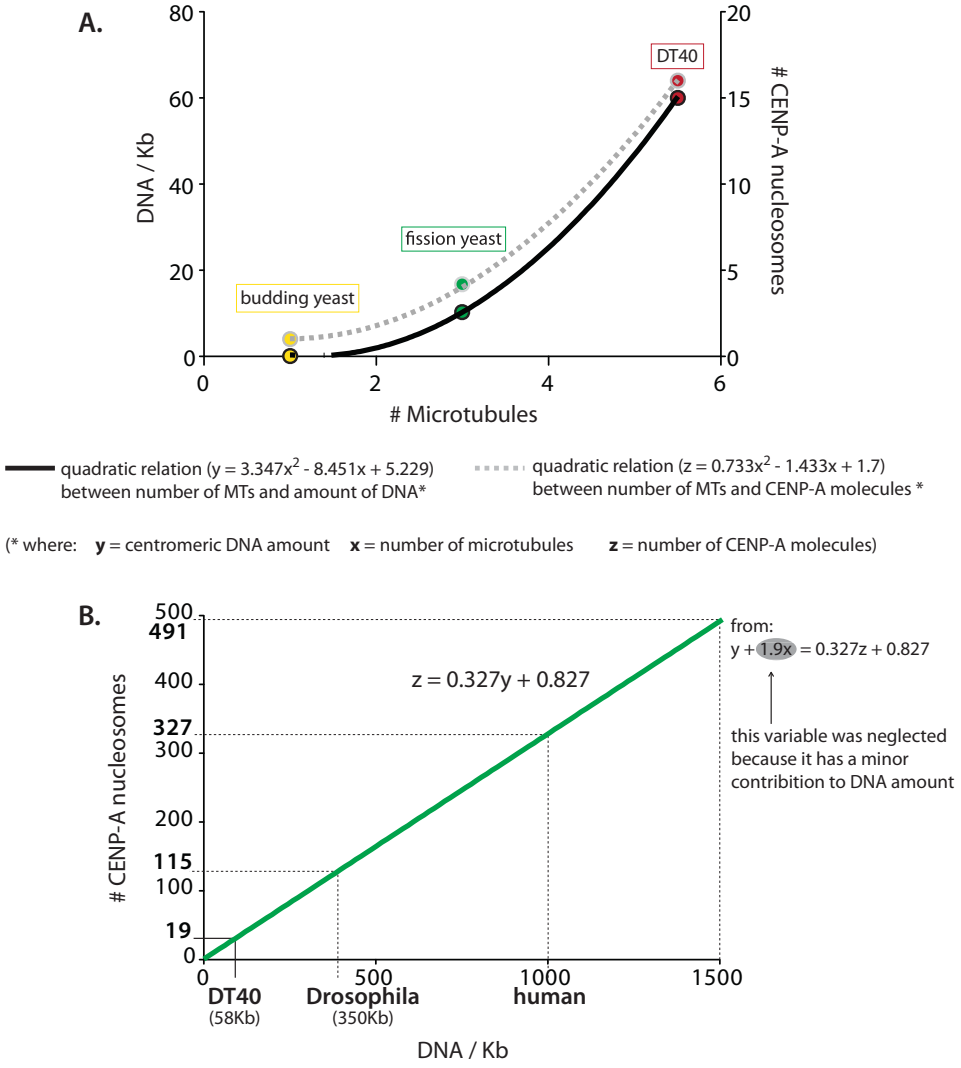

Figure 16 | Relation between number of CENP-A nucleosomes and number of microtubules, and between number of CENP-A nucleosomes and the DNA content of the inner kinetochore domain
A. Values calculated for DNA amount, number of microtubules (Chapter III) and number of CENP-A molecules for chicken DT40 kinetochores were plotted together with published values for budding and fission yeast. For fission yeast the number of CENP-A nucleosomes considered was based on the average % of CENP-A nucleosomes obtained for DT40 centromeres (i.e. 6.5% of total number of nucleosomes = 10 000 bp / 171 bp = 59 nucleosomes in total => 4 CENP-A nucleosomes). A quadratic relation was obtained for both comparisons defined by the equations shown. **B.** By deriving the equations obtained in A a multivariate equation was obtained with interdependence between the 3 considered variables. In order to simplify the relation, the number of microtubules was neglected assuming that it would have a minor contribution to the DNA amount values (its absence is more pronounced in lower DNA values). Dashed lines indicate the interpolated values for number of CENP-A containing nucleosomes based on known amounts of DNA

Using this regression we calculated the amount of DNA predicted to exist within in human kinetochores based on the known number of microtubules (20-25 microtubules (Rieder, 1982)). The value obtained, 1500 Kb, is very close to the estimated amount of CENP-A containing DNA – 500 to 1500 Kb (Blower et al., 2002). We further derived both equations and resolved them in order to identify the number of CENP-A molecules. To simplify, if we neglect the number of microtubules, assuming that this number would have a minor contribution to the amount of DNA, the equation is transformed into a linear regression between CENP-A nucleosomes and DNA amount. When plotting the known amount of DNA for different organisms, we can predict the number of CENP-A nucleosomes. The values correspond to a 5 – 6% occupancy of CENP-A containing nucleosomes at the inner centromeric region (Fig. 16B).

Using this equation, I calculate that in human centromeres, which are around 1000 Kb, there will be 327 CENP-A nucleosomes which represent 5% of the total number of nucleosomes. This value is vastly lower than the 15000 CENP-A containing nucleosomes in 2.5 Mb of chromatin proposed by Black et al. (Black et al., 2004). In the study, the value for CENP-A was calculated using protein extracts from cycling HeLa cells and was based on several assumptions: 1) the number of cells, 2) the average number of chromosomes and 3) the % of cell in each cell cycle phases using a ratio comparison by western blot.

Based on the relationship developed above (Fig. 16B), 2.5 Mb of chromatin would accommodate 818 CENP-A nucleosomes (5% of the total population). Interestingly, it has been shown that a decrease of at least 90% of CENP-A is enough to sustain a normal kinetochore function in HeLa cells (Liu et al., 2006). Although this was not extensively addressed in that study, it was suggested that human kinetochores might contain an excess of CENP-A nucleosomes. Hence, it is possible that the number predicted in our relation studies is the minimal number of CENP-A nucleosomes required for a functional centromere and that, in fact, human kinetochores have an excess of CENP-A. Nevertheless, with using the experimental setup here developed (centromeric chromatin unfolding and super-resolution microscopy) it would be possible to determine the number of CENP-A molecules present in HeLa kinetochores and extend this study to other organisms.

The results presented here are based on two different experimental approaches. One focuses on using light microscopy, where kinetochores can be resolved from the

underlying chromatin, enabling the quantification of DNA amount. The other is based on super-resolution microscopy with single molecule sensitivity and has allowed us to determine the absolute number of CENP-A molecules. The combination of the two techniques has proven to be extremely powerful for addressing questions previously technically unapproachable. In particular, the second approach, chromatin stretching together with super-resolution imaging, can be applied to the study of the centromeric chromatin in other organisms in order to obtain more information and more accurate numbers.

Attempts in identifying the critical parameters that could relate variables such as DNA amount, the number of CENP-A nucleosomes and microtubules are still very preliminary and should be taken with caution. Nonetheless, further work should be carried out to identify additional experimental-based relations between the variables derived above. The robustness of these correlations could be tested in the future once more experimentally based values are collected. If a correlation between the number of CENP-A nucleosomes and the amount of DNA packaged within the kinetochore is defined, it will be possible to conclusively settle a series of controversial debates in the field. At this point in time, however, key questions still remain unanswered. For instance, how important are each of the variables in kinetochore/centromere establishment (centromeric DNA, CENP-A nucleosomes and microtubules bound)? What is the minimal ratio of number of CENP-A nucleosomes/total number of nucleosomes necessary for a functional kinetochore? And finally what is the common (or not) architecture of the inner kinetochore domain?

Another unanswered, yet very interesting question, is what determines the number of microtubules bound per kinetochore. Is it dependent on kinetochore size? Or is it dependent upon spindle microtubules? I believe that the tools available in the Earnshaw lab could shed light on this question. As shown in the previous chapter, we have developed a DT40 cell line carrying a human X chromosome. Additionally, we have also engineered a cell line carrying a DT40 cell line carrying a CHO (Chinese hamster ovary) chromosome. Human chromosomes have a larger amount of centromeric DNA compared to the chicken one and CHO chromosomes are characterized by a big kinetochore. We know from our experiments that the segregation of the human X chromosome does not show any abnormality, so it would be interesting to know how

many microtubules bind these wider kinetochores: 4 - 7 microtubules, as seen with chicken chromosomes; or 20 - 25 microtubules, as observed at human kinetochores?

3.2 Mitotic (mature) kinetochores versus interphase pre-kinetochores – a role for CENP-C in kinetochore integrity

The discovery of anticentromere antibodies (ACA) in patient sera (Moroi et al., 1980) led to the finding that pre-kinetochores remain as locally condensed domains during interphase (Moroi et al., 1981). Early fluorescence and EM studies also revealed that the trilaminar kinetochore structure is only visible from late prophase until the end of mitosis, suggesting that the kinetochores go through cycles of assembly/disassembly at each cell division (Brenner et al., 1981; He and Brinkley, 1996). These pre-kinetochores undergo a program of structural (Roos, 1973) and biochemical (Liu et al., 2006) maturation as cells enter mitosis.

By unravelling centromeric chromatin fibers we could reveal some interesting differences in the organization of interphase pre-kinetochores and mitotic (mature) kinetochores. Mitotic kinetochores are more resistant to unfolding than their interphase counterparts. This suggests that one or more proteins that bind to kinetochores during the maturation process are possibly responsible for the crosslinks of CENP-A domains. Those crosslinks presumably confer upon kinetochores the structural rigidity required to withstand pulling forces within the mitotic spindle.

Currently more than 80 proteins, many of which are evolutionary conserved (Meraldi et al., 2006), are associated with the centromere-kinetochore complex in human cells (Cheeseman and Desai, 2008). While some of these proteins are constitutively associated with the centromere throughout the cell cycle, others are only transiently detected from late G2 to telophase. The assembly order and inter-dependency of several centromeric proteins does not follow a linear pathway: instead it appears to be extremely complex. An epistasis study of 20 kinetochore proteins proposed that the three major branches (immediately bellow CENP-A, which is on top of the hierarchy) are CENP-H/I/K, CENP-C and Aurora B (Liu et al., 2006). Each of these branches forms sub-branches that are interconnected to form a network. For instance, CENP-H, -I and -K are required for the localization of outer kinetochore proteins, including components of the SAC (spindle

assembly checkpoint), the microtubule binding protein Ndc80 complex and CENP-F (Fukagawa et al., 2001; Okada et al., 2006; Kwon et al., 2007). In vertebrates, CENP-C is upstream of most other kinetochore proteins, including the Mis12 complex, the plus end-directed microtubule motor CENP-E, some SAC components and the RZZ (Rod, Zw10 and Zwilch) complex (Liu et al., 2006; Kwon et al., 2007). The RZZ complex, in turn, recruits the minus-end directed motor dynein to kinetochores, which is involved in the activation/deactivation of SAC signaling (Karess, 2005).

Analysis of kinetochores from DT40 mutants has allowed us to show that mitotic kinetochore stabilization requires CENP-C, and that CENP-H, CENP-N or CENP-W play only minor roles in stabilizing mitotic kinetochores. This was surprising, since CENP-H is required for CENP-C accumulation at interphase pre-kinetochores, but not at mitotic kinetochores (Fukagawa et al., 2001; Kwon et al., 2007). Furthermore, the CENP-W/CENP-T complex associates with DNA in centromere regions, preferentially associating with histone H3 within CENP-A containing-region (Hori et al., 2008). In addition, CENP-N has been reported to bind to CENP-A nucleosomes (Carroll et al., 2009).Such a role for CENP-C in the stabilization of the mitotic kinetochore is consistent with several previous observations. The first indication came from experiments based on microinjection of anti-CENP-C coupled to electron microscopy analysis. These experiments showed that CENP-C determines the size of the kinetochore plate (Tomkiel et al., 1994). This finding was later confirmed by siRNA depletion of CENP-C (Liu et al., 2006), where EM also revealed discontinuous kinetochore plates, consistent with a role for CENP-C in the stability of CENP-A domains. The latter study identified CENP-C as a link in two or three sub-branches of the kinetochore assembly pathway (Liu et al., 2006). Looking carefully at the pathway where CENP-C is involved, we could predict that CENP-C could perform its scaffolding role by one (or more) of the following interactions with: 1) DNA (Sugimoto et al., 1994; Yang et al., 1996; Hori et al., 2008), 2) RNA (Du et al.; Wong et al., 2007) or 3) proteins such as CENP-L or Pcs1, as shown in fission yeast (Tanaka et al., 2009). It is also interesting to note that it has been proposed that CENP-C and CENP-T/CENP-W direct distinct pathways to connect the centromere with outer kinetochore assembly (Hori et al., 2008). So, our results are in agreement with such a distinct function of CENP-T/CENP-W and CENP-C within the kinetochore structure.

Interestingly, condensin also seems to have a role in kinetochore stabilization, although not to the same extent as CENP-C. It may be that, in the absence of physical

constraints provided by the underlying chromatin, the kinetochore loses stability. This implies that kinetochore stability could be enhanced by either the application of some force towards the surface of the chromosome, or that the underlying heterochromatin is necessary for plate stability. In prematurely condensed chromosomes, induced by cell fusion or caffeine treatment, it has been observed merging of the inner and outer kinetochore plates (Rattner and Wang, 1992; Wise and Brinkley, 1997). In both situations the underlying chromatin is probably under-condensed and this, in turn, could alter the relationship between the kinetochore and the underlying chromatin. Likewise, condensin's role in conferring stiffness to pericentromeric chromatin might have an impact on kinetochore stabilization, without altering the stepwise recruitment of outer kinetochore proteins.

On the light of published work would be interesting to define a role (if any) for Aurora B kinetochore stabilization. It has been observed by EM that in the absence of Aurora B, the distance between the inner kinetochore and the subjacent chromatin is decreased with no apparent perturbation of inner and outer kinetochore distances (Liu et al., 2006). It would be important to test the stability of mitotic kinetochore in the absence of the chromosomal protein complex with our assay. This can be done if GFP-tagged CENP-A is expressed in the INCENP knockout cell line, or using the Aurora B inhibitors such as ZM447439 (Gadea and Ruderman, 2005) or hesperadin. Three experimental outcomes are possible: 1) a major role in kinetochore stability, with fiber extension similar to the one observed in the absence of CENP-C; 2) minor role as observed for condensin-depleted cells; 3) no effect. A major role in kinetochore stability is possible but unlikely because CPC does not localize at the inner kinetochore. So, a milder effect is more likely to be observed and would indicate an indirect effect by activation/recruitment of some protein(s) dependent on Aurora B activity. And furthermore a support role could be ruled out in this scenario as there was never observed any increase in inner kinetochore distance in the absence of CPC proteins. Finally, if no effect is observed then would suggest that CPC proteins have no role in stabilizing inner kinetochore in DT40 cells.

Overall, our results demonstrate that interphase pre-kinetochores, and mature mitotic kinetochores, have intrinsic differences revealed by analysis of stretched centromeric chromatin. Moreover, extra kinetochore stabilization is conferred directly or indirectly by CENP-C.

3.3 Use of super-resolution microscopy to study the kinetochore

In this study, we applied super-resolution microscopy with single molecule sensitivity in an attempt to generate more accurate data on the localisation pattern of proteins relative to chromatin modifications within the inner kinetochore domain.

Several studies have addressed the same question using chromatin immunoprecipitation (ChIP) which is a powerful tool for identifying proteins association with specific regions of the genome. However, this technique does not provide any information about the relative distribution of the protein within a specific region once the chromatin fiber has folded into its mature three-dimensional structure.

Other studies, based on fluorescence microscopy, have measured with nm accuracy, the average separation between two kinetochore proteins along the inner-outer axis of human metaphase kinetochores either using specific antibodies (Wan et al., 2009), or fluorescently labeled proteins (Schittenhelm et al., 2007; Joglekar et al., 2009). This technique has provided detailed information about the relative localization of components of the outer-kinetochore, and some details about the inner kinetochore domain. For instance, one of the studies (Wan et al., 2009) has shown that only CENP-C (from more than 16 proteins analyzed) has the same compliant behaviour as CENP-A during metaphase oscillations, i.e., both CENP-A and CENP-C display flexibility, while all the other CCAN and outer kinetochore proteins remain stiff. However, because these measurements are done in the tightly packed kinetochore structure they do not provide information about the relative position of proteins along the chromatin fiber, therefore they are not suitable for predicting the folding and architecture of the inner kinetochore domain. Previous studies on stretched centromeric chromatin have attempted to map the distribution of kinetochore proteins, however, they failed to map the distribution of CENP-A relative to other kinetochore proteins, either because appropriate probes were not available (Zinkowski et al., 1991) or because other kinetochore proteins were not retained during sample preparation (Sullivan and Karpen, 2004).

I have localized H3K9me3 and H3K4me2 on extended centromere chromatin fibers using super-resolution microscopy. This involved immunostaining of unfolded kinetochores from cells expressing CENP-A tagged with the photoswitchable Dronpa with antibodies labeled with Alexa 647 against the referred histone modifications. These analyses showed that H3K9me3 was consistently present in blocks interspersed with

CENP-A domains, while H3K4me2 was seen at lower levels between CENP-A domains. These results further confirmed our observations made by deconvolution microscopy, particularly the presence of some heterochromatin-like histones modifications within the kinetochore.

I also examined, for the first time, the distribution of members of the constitutive centromere associated network (CCAN) relative to CENP-A along the chromatin fibers. CENP-C, CENP-H, CENP-I, CENP-K-U and CENP-W all co-immunoprecipitate with CENP-A following partial digestion of chromatin by micrococcal nuclease (Obuse et al., 2004a; Foltz et al., 2006); moreover, ChIP studies showed co-localization of CENP-C and CENP-H with discontinuous domains of CENP-A in human neocentromeres (Alonso et al., 2007; Capozzi et al., 2008). Of these proteins, only CENP-N has been shown to interact directly with CENP-A nucleosomes (Carroll et al., 2009). However, CENP-C, CENP-T and CENP-W co-immunoprecipitate with H3 nucleosomes after extensive nuclease digestion (Ando et al., 2002; Hori et al., 2008). This suggests that the two classes of nucleosomes must be closely apposed in the inner kinetochore. This prediction was confirmed by our data obtained by super-resolution light microscopy; in fact, CENP-C and CENP-H co-localized with CENP-A-rich subdomains in unfolded kinetochores. This suggests the presence of canonical H3 nucleosomes within the CENP-A-rich subdomains. In contrast, the distribution of CENP-T in highly unfolded pre-kinetochores overlaps with of the presence of H3K9me3 and H3K4me2 – containing nucleosomes.

Regarding the long fibers where the localization of histone modifications was studied (Fig. 13) it is worth noting that there are regions where both CENP-A and the histone modifications studied are absent. It is arguable that the empty spaces might correspond to spaces without any nucleosomes instead of what I postulated: nucleosomes with other histone modifications (or no modification at all) are present in empty spaces. In order to address this question I tried several antibodies for canonical histones but they did not show specific labelling. However, I believe that this question can be answer if a stable cell line expressing H2B-dronpa is engineered and super-resolution imaging of stretched fibers immunostained for CENP-A is carried out. Yet, it is important to highlight that we do not expect to achieve super-resolution with H2B-dronpa but only with CENP-A coupled to Alexa 647, because of the high levels of H2B present. Even so, this experimental set up should be enough to answer if nucleosomes totally cover the stretched fibers or if the fibers are fragmented.

3.4 Model for centromeric chromatin organization

The assay I developed to extend chromatin fibers but preserving some of the protein complexes associated with them, together with deconvolution and super-resolution microscopy, allowed me to propose an alternative model for inner kinetochore organization.

Current centromeric folding models propose that CENP-A and canonical H3 coexist in the same fiber but are sorted on different faces of an "amphipatic" helical arrangement, where CENP-A faces outward towards the kinetochore, and the H3-containing nucleosomes are embedded inwards towards the inner centromeric chromatin (Sullivan and Karpen, 2004; Schueler and Sullivan, 2006; Marshall et al., 2008). Overall, my data do not support the solenoid model because I show that H3 acts as an anchor for CENP-T in the outer kinetochore.

Based on my data, I propose an alternative model for kinetochore organization. The kinetochore contains a single continuous chromatin segment with alternating CENP-A and H3 domains flanked by heterochromatin. The data suggests a topology in which kinetochore chromatin folds into a planar sinusoidal patch, or boustrophedon (Greek ox–turning) (Fig. 17A). Other helical arrangements are possible, but this topology allows the kinetochore size to vary according to the number of microtubules bound with minimal perturbation of local packing. Each kinetochore could be composed of several patches stacked on top of one another as shown in Fig. 17. Such a kinetochore topology would be consistent with the poleward excursions observed in mitosis in condensin-depleted cells, with the layers held together by structural crosslinks dependent upon CENP-C. Moreover, it also explains why the unfolding of mitotic kinetochores is consistently lower, as the tight packaging of the layers is maintained by CENP-C crosslinks. On the other hand, when interphase centromeres unfold, the layers would unwind into a contiguous linear segment (Fig. 17E). In the model herein proposed, both CENP-A and H3 arrays face the external surface, enabling the binding of all CCAN proteins. CENP-C would bind to the more internal CENP-A blocks, crosslinking several layers. This would explain the mechanical coupling between CENP-A and CENP-C observed when kinetochores are under tension exerted by microtubules (Wan et al., 2009). The KMN network, after assembling in mitosis on top of the CCAN, binds microtubules and might confer stability to the kinetochore by crosslinking the CENP-C chromatin either directly or indirectly.

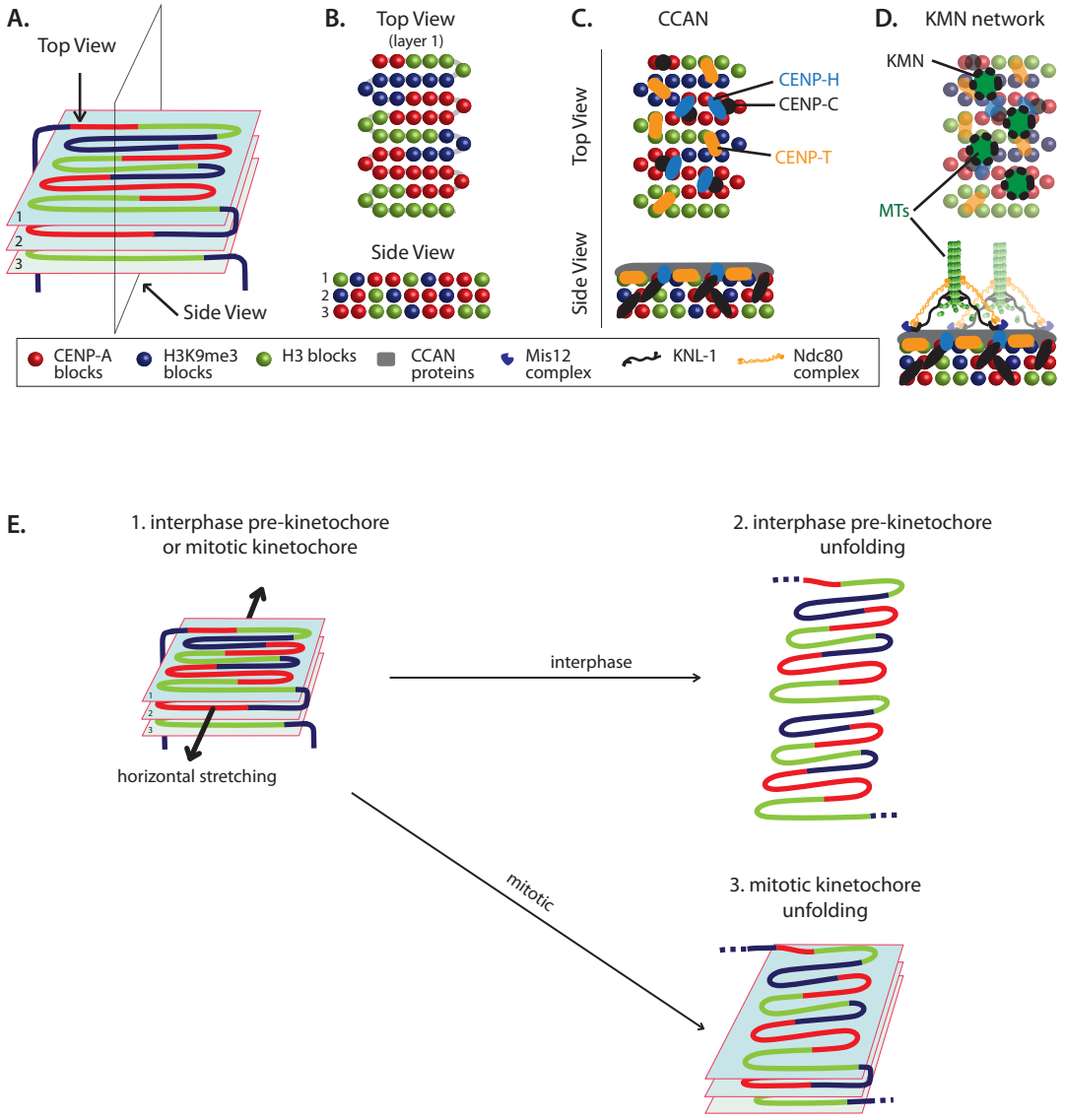

Figure 17 | Proposed "Boustrophedon" arrangement of mitotic kinetochore chromatin. A. A single continuous chromatin segment is arranged in a sinusoidal wave in a series of layers linked at both ends to heterochromatin (H3K9me3). CENP-A blocks (red) are interspersed with H3-containing nucleosomes lacking H3K9me3 (green) and nucleosomes containing H3K9me3 (blue). All domains are exposed to the outer face of the kinetochore. **B.** Top and side view as indicated in A. **C.** CCAN protein distribution in the kinetochore. CENP-H (light blue) and CENP-C (black) bind to CENP-A blocks. CENP-T (orange) binds exclusively to H3 blocks as observed by single molecule microscopy of extended fibers. CENP-C binds to more internal CENP-A blocks (crosslinking different layers) as observed by Wan *et. al.* 2009. **D.** The KMN network assembles in mitosis on top of the CCAN and binds microtubules. KMN binding may confer stability to the mitotic kinetochore by crosslinking the CENP-C either directly or indirectly. **E.** Different behaviour of interphase pre-kinetochores and mitotic kinetochores in the presence of TEEN buffer. **1.** Proposed folding model of the inner centromeric region highlighting the presumptive direction of stretching when cells are exposed to TEEN buffer. **2.** Interphase centromeric region folds to greater extents because layers are not crosslinked by CENP-C, and are then able to be arranjed in a single linear fiber. **3.** In mitosis, CENP-C crosslinks different layers and therefore confers extra stability to kinetochore.

VI. CONCLUSIONS

CONCLUSIONS

In the first part of this dissertation, I exploited the remarkable behaviour of kinetochores in cells lacking the condensin complex to conduct a detailed physical analysis of the inner centromere of mitotic chromosomes. When chromosomes are bioriented on the mitotic spindle, sister kinetochores come under tension and are pulled towards opposite spindle poles. Remarkably, in condensin-depleted cells, kinetochores under tension undergo excursions of over one micron out away from the surface of the chromosome while remaining structurally intact. Thus, kinetochores are axially elastic, behaving like a Hookean spring. The nature of this centromere "spring" has long fascinated biologists, but its constituents have eluded discovery. Using high-resolution spinning-disk confocal microscopy, I measured the stiffness of the spring by looking both at the behaviour of kinetochores and also at a synthetic chromosomal array inserted in pericentromeric heterochromatin. I have shown that the spring has a rest length set by the chromatin higher-order structure, but a stiffness determined by the condensin complex. My studies used a wide range of methods, including vertebrate cell genetics, “chemical genetics”, light and electron microscopy and *in vitro* methods to characterise the physical behaviour of kinetochores. The ability to rescue a genetic null mutation with wild-type but not mutant SMC2 (defective in ATPase function) allowed me to prove that the condensin-regulated centromere elasticity requires ATPase function and not just the presence of the complex. I further characterized the biological role of inner centromeric stiffness during cell cycle progression. I demonstrated that the loss of stiffness delays anaphase onset due to prolonged activation of the spindle checkpoint.

In the second part of this dissertation, I combined two different approaches to decipher the organization of the inner kinetochore domain. Firstly, I developed a gentle assay to unfold the centromeric region, and this revealed novel differences between interphase pre-kinetochores and mature mitotic kinetochores. Interphase pre-kinetochores can be unfolded to CENP-A blocks interspersed with enriched domains of H3K9me3 containing nucleosomes, while mitotic kinetochores are significantly more stable. Using a series of conditional knockouts of centromere associated network proteins (CCAN) I demonstrated a major role for CENP-C in stabilizing the mitotic kinetochore, whereas CENP-H, CENP-W, CENP–N and the condensin complex had minor or no effects.

Secondly, I used super-resolution microscopy with single molecule sensitivity to determine for the first time the relative position of histone modifications and CCAN components relative to CENP-A in unfolded pre-kinetochore fibers. I observed H3K9me3 enriched domains between CENP-A blocks, while H3K4me2 was present in lower amounts. Interestingly, I observed that CENP-C and CENP-H localize close to the CENP-A blocks whereas CENP-T is between them. This brings into question current accepted models of kinetochore organization where canonical H3 blocks have no place in the outward face of the inner kinetochore domain. Overall my data allowed me to propose a novel model where kinetochore chromatin is a single linear segment folded as a layered boustrophedon, with planar sinusoids containing interspersed CENP-A-rich and H3-rich subdomains oriented towards the outer kinetochore. In mitosis, a CENP-C-dependent mechanism crosslinks CENP-A blocks of different layers together. I foresee that this model and the methods I have developed will open new perspectives of looking at this fundamental region of the chromosome.

FINAL REMARKS AND FUTURE PERSPECTIVES

As demonstrated here, condensin has a role in the stiffness of the inner centromeric region that is clearly revealed by the exaggerated movements observed during metaphase oscillations of condensin-depleted chromosomes. In the light of what is now known about the involvement of the phosphorylation of kinetochore components by Aurora B on sister separation, it would be interesting to understand how the Aurora B activity gradient is set under conditions where the inter-kinetochore distance is increased. Furthermore, it was recently shown that metaphase plate thickness is governed by the reduced oscillation speed at a constant oscillation period and that both are fundamental for anaphase onset (Jaqaman et al., 2010). In the light of this novel study, it would be interesting to carry out a detailed analysis of the oscillation period and speed of kinetochore movements in condensin-depleted cells and cells carrying the SMC2 ATPase mutant. Alongside this study, a detailed analysis of Aurora B activity, and intrakinetochore distances (Maresca and Salmon, 2009; Uchida et al., 2009) might lead to a better understanding of the importance of the chromatin stiffness in microtubule dynamics and in the overall establishment of the metaphase plate.

Additionally, in the second part of the work the novel approaches developed: 1) centromeric chromatin unfolding under conditions where proteins remain associated and 2) super-resolution imaging, proved to be particularly informative to understand the inner kinetochore domain organization and architecture. I anticipate that both techniques can be applied to other organisms. Further improvements such as constructing *in vitro* nucleosome fibers by expressing the canonical histones and CENP-A followed by DNA assembly, that could be used as an internal reference, will allow the development of additional assays. For instance, it will be possible to accurately quantify the absolute number of CENP-A molecules in several organisms, and establish the role of CENP-A throughout evolution in the final kinetochore architecture. It should also be possible to determine the type of chromatin fibers present in unfolded centromeric fibers. Additionally, I also believe that it will be interesting to observe *in vivo* the unfolding of both heterochromatin and pre-kinetochore fibers. I predict that spinning-disk high-temporal resolution microscopy with further development of technical aspects, such as unfolding the centromere chromatin, will allow the visualization of such phenomena. In case this is possible, it would be extremely enlightening to further understand the packaging of chromatin within the inner kinetochore domain. Additionally, the minor role of the condensin complex in conferring stability to the mitotic kinetochore as observed by the longitudinal unfolding assay, might indicate a role of the inner centromeric chromatin in stabilizing the inner kinetochore plate. This could either be a structural role where the stiffness of the inner centromeric chromatin would have an impact in supporting the inner plate or, it could have a biological role, i.e., the condensin complex could be important to recruit other proteins involved in conferring stability to the inner plate.

In summary, the work presented in this dissertation provides a fundamental advance in the understanding of the centromere, a critical chromosomal substructure.

VII. APPENDIX

1. LIST OF FIGURES

II. INTRODUCTION

IV. CONDENSIN REGULATES THE STIFFNESS OF THE VERTEBRATE CENTROMERE

2. LIST OF ABBREVIATIONS

ACA	anti-centromere antibodies
APC/C	anaphase-promoting complex/cyclosome
Ar^+ laser	Argon-Ion Laser
ATP	adenosine triphosphate
bp	base pair(s)
BSA	bovine serum albumine
C. elegans	*Caenorhabditis elegans*
CAD	CENP-A distal
CCAN	centromere constitutive-associated network
CCD	charge coupled-device
cdc	cell-division cycle
cdk	cyclin-dependent kinase
cDNA	complementary DNA
CENP	centromere protein
ChIP	chromatin immunoprecipitation
Con-A	concanavalin A
CPC	chromosomal passenger complex
CREST	calcinosis, raynaud, esophageal dysmotility, sclerodactyly, telangiectasia
Cy	Cyanine
DAPI	4',6-diamidino-2-phenylindole, dihydrochloride
DNA	deoxyribonucleic acid
dNTPs	deoxyribonucleotide-5'-triphosphate
Drosophila	*Drosophila melanogaster*
DTT	1,4-dithiothreitol
E. coli	*Escherichia coli*
ECL	enhanced chemiluminescence
EDTA	ethylenediaminetetraacetic acid
eGFP	enhanced GFP
EGTA	ethylene glycol-bis-(β-aminoethyl ether)-N, N, N', N'-tetraacetic acid
EM	electron microscopy
EMCCD	electron multiplying charge coupled-device
FACS	flow analysis cell sorting

FBS	foetal bovine serum
FISH	fluorescence *in situ* hybridization
FITC	fluorescein isothiocyanate
FWHM	full width at half maximum
GFP	green fluorescent protein
GTP	guanosine triphosphate
H2A	histone 2A
H2B	histone 2B
H3	histone 3
H3K4me2	dimethylated histone H3 at Lysine 4
H3K9me3	Trimethylated histone H3 at Lysine 9
H3T3ph	phosphorylated histone 3 at Threonine 3
H4	histone 4
He/Ne laser	Helium-Neon laser
Hec1	highly expressed in cancer
HeLa	Henrietta Lacks
INCENP	inner centromeric protein
Kb	kilobases
KDa	kilo Dalton
KO	knockout
lacI	*E. coli* lac repressor protein
lacO	*E. coli* lac Operator
LB	Luria-Bertani
Mad	mitotic arrest deficient
MAPs	microtubule-associated proteins
MCAK	mitotic centromere-associated kinesin
MNase	micrococcal nuclease
mov	QuickTime file format
mRFP	monomeric red fluorescent protein
mRNA	messenger RNA
NAC	nucleosome-associated complex
Nde	nuclear distribution protein nudE
ON	overnight
P1	bacteriophage P1
PALM	photoactivated localization microscopy

PBS	phosphate-buffered saline
PCR	polymerase chain reaction
PFA	paraformaldehyde
PP1	protein phosphatase 1
PSF	point spread function
RNA	ribonucleic acid
RNAi	RNA interference
ROI	region of interest
RPMI	Roswell Park Memorial Institute medium
RT	room temperature
RT-PCR	reverse transcriptase polymerase chain reaction
S. cerevisiae	*Saccharomyces cerevisiae*
S. pombe	*Schizosaccharomyces pombe*
s.d.	standard deviation
SAC	spindle assembly checkpoint
SBP	strepatvidin binding protein
SDS	sodium dodecyl sulphate
SDS-PAGE	sodium dodecyl sulphate polyacrylamide gel electrophoresis
siRNA	small interfering RNA
$SMC2^{ON}$	SMC2 knockout cell line growing in the absence of doxycycline
$SMC2^{OFF}$	SMC2 knockout cell line growing in the presence of doxycycline
STED	stimulated emission depletion microscopy
STORM	stochastic optical reconstruction
T4	bacteriophage T4
tetO	tetracycline operator
tetR	tetracycline repressor
tiff	tagged image file format
TIRF	total internal reflection fluorescence
Tris	tris (hydroxymethyl)aminomethane
TRIzol	Total RNA Isolation reagent
wt	wild type
Xenopus	*Xenopus laevis*
λ	bacteriophage lambda

3. REFERENCES

Agudo, M., Abad, J.P., Molina, I., Losada, A., Ripoll, P., and Villasante, A. (2000). A dicentric chromosome of Drosophila melanogaster showing alternate centromere inactivation. Chromosoma *109*, 190-196.

Alexandrov, I.A., Mashkova, T.D., Akopian, T.A., Medvedev, L.I., Kisselev, L.L., Mitkevich, S.P., and Yurov, Y.B. (1991). Chromosome-specific alpha satellites: two distinct families on human chromosome 18. Genomics *11*, 15-23.

Alonso, A., Fritz, B., Hasson, D., Abrusan, G., Cheung, F., Yoda, K., Radlwimmer, B., Ladurner, A.G., and Warburton, P.E. (2007). Co-localization of CENP-C and CENP-H to discontinuous domains of CENP-A chromatin at human neocentromeres. Genome Biol *8*, R148.

Alonso, A., Mahmood, R., Li, S., Cheung, F., Yoda, K., and Warburton, P.E. (2003). Genomic microarray analysis reveals distinct locations for the CENP-A binding domains in three human chromosome 13q32 neocentromeres. Hum Mol Genet *12*, 2711-2721.

Amor, D.J., Kalitsis, P., Sumer, H., and Choo, K.H. (2004). Building the centromere: from foundation proteins to 3D organization. Trends Cell Biol *14*, 359-368.

Amos, L., and Klug, A. (1974). Arrangement of subunits in flagellar microtubules. J Cell Sci *14*, 523-549.

Ando, R., Mizuno, H., and Miyawaki, A. (2004). Regulated fast nucleocytoplasmic shuttling observed by reversible protein highlighting. Science *306*, 1370-1373.

Ando, S., Yang, H., Nozaki, N., Okazaki, T., and Yoda, K. (2002). CENP-A, -B, and -C chromatin complex that contains the I-type alpha-satellite array constitutes the prekinetochore in HeLa cells. Mol Cell Biol *22*, 2229-2241.

Andrews, P.D., Ovechkina, Y., Morrice, N., Wagenbach, M., Duncan, K., Wordeman, L., and Swedlow, J.R. (2004). Aurora B regulates MCAK at the mitotic centromere. Dev Cell *6*, 253-268.

Basto, R., Scaerou, F., Mische, S., Wojcik, E., Lefebvre, C., Gomes, R., Hays, T., and Karess, R. (2004). In vivo dynamics of the rough deal checkpoint protein during Drosophila mitosis. Curr Biol *14*, 56-61.

Bazett-Jones, D.P., Kimura, K., and Hirano, T. (2002). Efficient supercoiling of DNA by a single condensin complex as revealed by electron spectroscopic imaging. Mol Cell *9*, 1183-1190.

Belmont, A.S. (2002). Mitotic chromosome scaffold structure: New approaches to an old controversy. Proc Natl Acad Sci U S A *99*, 15855-15857.

Belmont, A.S., and Bruce, K. (1994). Visualization of G1 chromosomes: A folded, twisted, supercoiled chromonema model of interphase chromatid structure. J Cell Biol *127*, 287-302.

Belmont, A.S., Sedat, J.W., and Agard, D.A. (1987). A three-dimensional approach to mitotic chromosome structure: Evidence for a complex heirarchial organization. J Cell Biol *105*, 77-92.

Belmont, A.S., and Straight, A.F. (1998). In vivo visualization of chromosomes using lac operator-repressor binding. Trends Cell Biol *8*, 121-124.

Betzig, E., Patterson, G.H., Sougrat, R., Lindwasser, O.W., Olenych, S., Bonifacino, J.S., Davidson, M.W., Lippincott-Schwartz, J., and Hess, H.F. (2006). Imaging intracellular fluorescent proteins at nanometer resolution. Science *313*, 1642-1645.

Black, B.E., Foltz, D.R., Chakravarthy, S., Luger, K., Woods, V.L., Jr., and Cleveland, D.W. (2004). Structural determinants for generating centromeric chromatin. Nature *430*, 578-882.

Bloom, K., and Joglekar, A. (2010). Towards building a chromosome segregation machine. Nature *463*, 446-456.

Blower, M.D., Sullivan, B.A., and Karpen, G.H. (2002). Conserved organization of centromeric chromatin in flies and humans. Dev Cell *2*, 319-330.

Bouck, D.C., and Bloom, K. (2007). Pericentric chromatin is an elastic component of the mitotic spindle. Curr Biol *17*, 741-748.

Brenner, S., Pepper, D., Berns, M.W., Tan, E., and Brinkley, B.R. (1981). Kinetochore structure, duplication and distribution in mammalian cells: analysis by human autoantibodies from scleroderma patients. J Cell Biol *91*, 95-102.

Brinkley, B.R., and Stubblefield, E. (1966). The fine structure of the kinetochore of a mammalian cell in vitro. Chromosoma (Berl) *19*, 28-43.

Brinkley, B.R., Valdivia, M.M., Tousson, A., and Brenner, S.L. (1984). Compound kinetochores of the Indian muntjac: Evolution by linear fusion of unit kinetochores. Chromosoma (Berl) *91*, 1-11.

Brust-Mascher, I., and Scholey, J.M. (2002). Microtubule flux and sliding in mitotic spindles of Drosophila embryos. Mol Biol Cell *13*, 3967-3975.

Buerstedde, J.-M., and Takeda, S. (1991). Increased ratio of targeted to random integration after transfection of chicken B cell lines. Cell *67*, 179-188.

Cai, S., O'Connell, C.B., Khodjakov, A., and Walczak, C.E. (2009). Chromosome congression in the absence of kinetochore fibres. Nat Cell Biol *11*, 832-838.

Cam, H.P., Sugiyama, T., Chen, E.S., Chen, X., FitzGerald, P.C., and Grewal, S.I. (2005). Comprehensive analysis of heterochromatin- and RNAi-mediated epigenetic control of the fission yeast genome. Nat Genet *37*, 809-819.

Camahort, R., Li, B., Florens, L., Swanson, S.K., Washburn, M.P., and Gerton, J.L. (2007). Scm3 is essential to recruit the histone h3 variant cse4 to centromeres and to maintain a functional kinetochore. Mol Cell *26*, 853-865.

Camahort, R., Shivaraju, M., Mattingly, M., Li, B., Nakanishi, S., Zhu, D., Shilatifard, A., Workman, J.L., and Gerton, J.L. (2009). Cse4 is part of an octameric nucleosome in budding yeast. Mol Cell *35*, 794-805.

Capozzi, O., Purgato, S., Verdun di Cantogno, L., Grosso, E., Ciccone, R., Zuffardi, O., Della Valle, G., and Rocchi, M. (2008). Evolutionary and clinical neocentromeres: two faces of the same coin? Chromosoma *117*, 339-344.

Carazo-Salas, R.E., Gruss, O.J., Mattaj, I.W., and Karsenti, E. (2001). Ran-GTP coordinates regulation of microtubule nucleation and dynamics during mitotic-spindle assembly. Nat Cell Biol *3*, 228-234.

Carpenter, A.J., and Porter, A.C. (2004). Construction, characterization, and complementation of a conditional-lethal DNA topoisomerase IIalpha mutant human cell line. Mol Biol Cell *15*, 5700-5711.

Carroll, C.W., Silva, M.C., Godek, K.M., Jansen, L.E., and Straight, A.F. (2009). Centromere assembly requires the direct recognition of CENP-A nucleosomes by CENP-N. Nat Cell Biol *11*, 896-902.

Cassimeris, L., Rieder, C.L., and Salmon, E.D. (1994). Microtubule assembly and kinetochore directional instability in vertebrate monopolar spindles: implications for the mechanism of chromosome congression. J Cell Sci *107 (Pt 1)*, 285-297.

Chang, C.J., Goulding, S., Earnshaw, W.C., and Carmena, M. (2003). RNAi analysis reveals an unexpected role for topoisomerase II in chromosome arm congression to a metaphase plate. J Cell Sci *116*, 4715-4726.

Cheeseman, I.M., Chappie, J.S., Wilson-Kubalek, E.M., and Desai, A. (2006). The Conserved KMN Network Constitutes the Core Microtubule-Binding Site of the Kinetochore. Cell *127*, 983-997.

Cheeseman, I.M., and Desai, A. (2008). Molecular architecture of the kinetochore-microtubule interface. Nat Rev Mol Cell Biol *9*, 33-46.

Cheeseman, I.M., Hori, T., Fukagawa, T., and Desai, A. (2008). KNL1 and the CENP-H/I/K complex coordinately direct kinetochore assembly in vertebrates. Mol Biol Cell *19*, 587-594.

Cheeseman, I.M., Niessen, S., Anderson, S., Hyndman, F., Yates, J.R., Oegema, K., and Desai, A. (2004). A conserved protein network controls assembly of the outer kinetochore and its ability to sustain tension. Genes Dev *18*, 2255-2268.

Chen, R.H., Waters, J.C., Salmon, E.D., and Murray, A.W. (1996). Association of spindle assembly checkpoint component XMAD2 with unattached kinetochores. Science *274*, 242-246.

Choo, K.H.A. (2001). Domain organization at the centromere and neocentromere. Dev Cell *1*, 165-177.

Chueh, A.C., Wong, L.H., Wong, N., and Choo, K.H. (2005). Variable and hierarchical size distribution of L1-retroelement-enriched CENP-A clusters within a functional human neocentromere. Hum Mol Genet *14*, 85-93.

Ciferri, C., Pasqualato, S., Screpanti, E., Varetti, G., Santaguida, S., Dos Reis, G., Maiolica, A., Polka, J., De Luca, J.G., De Wulf, P., *et al.* (2008). Implications for kinetochore-microtubule attachment from the structure of an engineered Ndc80 complex. Cell *133*, 427-439.

Ciliberto, A., and Shah, J.V. (2009). A quantitative systems view of the spindle assembly checkpoint. EMBO J *28*, 2162-2173.

Cimini, D., Cameron, L.A., and Salmon, E.D. (2004). Anaphase spindle mechanics prevent mis-segregation of merotelically oriented chromosomes. Curr Biol *14*, 2149-2155.

Cimini, D., Fioravanti, D., Salmon, E.D., and Degrassi, F. (2002). Merotelic kinetochore orientation versus chromosome mono-orientation in the origin of lagging chromosomes in human primary cells. J Cell Sci *115*, 507-515.

Cimini, D., Wan, X., Hirel, C.B., and Salmon, E.D. (2006). Aurora kinase promotes turnover of kinetochore microtubules to reduce chromosome segregation errors. Curr Biol *16*, 1711-1718.

Ciosk, R., Zachariae, W., Michaelis, C., Shevchenko, A., and Nasmyth, K. (1998). An ESP1/PDS1 complex regulates loss of sister chromatid cohesion at the metaphase to anaphase transition in yeas. Cell *93*, 1067-1076.

Civelekoglu-Scholey, G., Sharp, D.J., Mogilner, A., and Scholey, J.M. (2006). Model of chromosome motility in Drosophila embryos: adaptation of a general mechanism for rapid mitosis. Biophys J *90*, 3966-3982.

Clarke, L. (1990). Centromeres of budding and fission yeasts. Trends Genet *6*, 150-154.

Clarke, L., Amstutz, H., Fishel, B., and Carbon, J. (1986). Analysis of centromeric DNA in the fission yeast Schizosaccharomyces pombe. Proc NatAcad Sci (USA) *83*, 8253-8257.

Clarke, L., and Carbon, J. (1980). Isolation of a yeast centromere and construction of functional small circular chromosomes. Nature *287*, 504-509.

Clarke, L., and Carbon, J. (1985). The structure and function of yeast centromeres. Ann Rev Genet *19*, 29-56.

Cleveland, D.W., Fischer, S.G., Kirschner, M.W., and Laemmli, U.K. (1977). Peptide mapping by limited proteolysis in sodium dodecyl sulfate and analysis by gel electrophoresis. J Biol Chem *252*, 1102-1106.

Coelho, P.A., Queiroz-Machado, J., and Sunkel, C.E. (2003). Condensin-dependent localisation of topoisomerase II to an axial chromosomal structure is required for sister chromatid resolution during mitosis. J Cell Sci *116*, 4763-4776.

Collins, K.A., Furuyama, S., and Biggins, S. (2004). Proteolysis contributes to the exclusive centromere localization of the yeast Cse4/CENP-A histone H3 variant. Curr Biol *14*, 1968-1972.

Cytrynbaum, E.N., Scholey, J.M., and Mogilner, A. (2003). A force balance model of early spindle pole separation in Drosophila embryos. Biophys J *84*, 757-769.

Dai, J., Sultan, S., Taylor, S.S., and Higgins, J.M. (2005). The kinase haspin is required for mitotic histone H3 Thr 3 phosphorylation and normal metaphase chromosome alignment. Genes Dev *19*, 472-488.

Dalal, Y., Furuyama, T., Vermaak, D., and Henikoff, S. (2007). Structure, dynamics, and evolution of centromeric nucleosomes. Proc Natl Acad Sci USA *104*, 15974-15981.

De Brabander, M., Geuens, G., Nuydens, R., Willebrords, R., Aerts, F., and De Mey, J. (1986). Microtubule dynamics during the cell cycle: the effects of taxol and nocodazole on the microtubule system of Pt K2 cells at different stages of the mitotic cycle. Int Rev Cytol *101*, 215-274.

De Wulf, P., McAinsh, A.D., and Sorger, P.K. (2003). Hierarchical assembly of the budding yeast kinetochore from multiple subcomplexes. Genes Dev *17*, 2902-2921.

DeLuca, J.G., Dong, Y., Hergert, P., Strauss, J., Hickey, J.M., Salmon, E.D., and McEwen, B.F. (2005). Hec1 and nuf2 are core components of the kinetochore outer plate essential for organizing microtubule attachment sites. Mol BiolCell *16*, 519-531.

Deluca, J.G., Gall, W.E., Ciferri, C., Cimini, D., Musacchio, A., and Salmon, E.D. (2006). Kinetochore microtubule dynamics and attachment stability are regulated by hec1. Cell *127*, 969-982.

Desai, A., Maddox, P.S., Mitchison, T.J., and Salmon, E.D. (1998). Anaphase A chromosome movement and poleward spindle microtubule flux occur At similar rates in Xenopus extract spindles. J Cell Biol *141*, 703-713.

Desai, A., and Mitchison, T.J. (1997). Microtubule polymerization dynamics. Annu Rev Cell Dev Biol *13*, 83-117.

Desai, A., Rybina, S., Muller-Reichert, T., Shevchenko, A., Hyman, A., and Oegema, K. (2003). KNL-1 directs assembly of the microtubule-binding interface of the kinetochore in C. elegans. Genes Dev *17*, 2421-2435.

Ding, R., McDonald, K.L., and McIntosh, J.R. (1993). Three-dimentional reconstruction and analysis of mitotic spindles from the yeast Schizosaccharomyces pombe. J Cell Biol *120*, 141-151.

Dong, Y., Vagnarelli, P., Meng, X., Ribeiro, S.A., Earnshaw, W., and McEwen, B.F. (2008). Localizing Kinetochores in Condensin Deficient DT40 Cells Using Same Cell Correlative Confocal Light Microscopy/Electron Tomography. Microscopy and Microanalysis *14 (suppl. 2)*, 1070-1071

Dong, Y., Vanden Beldt, K.J., Meng, X., Khodjakov, A., and McEwen, B.F. (2007). The outer plate in vertebrate kinetochores is a flexible network with multiple microtubule interactions. Nat Cell Biol *9*, 516-522.

Dorigo, B., Schalch, T., Kulangara, A., Duda, S., Schroeder, R.R., and Richmond, T.J. (2004). Nucleosome arrays reveal the two-start organization of the chromatin fiber. Science *306*, 1571-1573.

Du, Y., Topp, C.N., and Dawe, R.K. DNA Binding of Centromere Protein C (CENPC) Is Stabilized by Single-Stranded RNA. PLoS Genet *6*, e1000835.

Dunleavy, E.M., Roche, D., Tagami, H., Lacoste, N., Ray-Gallet, D., Nakamura, Y., Daigo, Y., Nakatani, Y., and Almouzni-Pettinotti, G. (2009). HJURP is a cell-cycle-dependent maintenance and deposition factor of CENP-A at centromeres. Cell *137*, 485-497.

Earnshaw, W.C., Bernat, R.L., Cooke, C.A., and Rothfield, N.F. (1991). Role of the centromere/ kinetochore in cell cycle control. Cold Spring Harbor Symp Quant Biol *56*, 675-685.

Earnshaw, W.C., Bordwell, B., Marino, C., and Rothfield, N. (1986). Three human chromosomal autoantigens are recognized by sera from patients with anti-centromere antibodies. J Clin Invest *77*, 426-430.

Earnshaw, W.C., Halligan, B., Cooke, C.A., Heck, M.M., and Liu, L.F. (1985). Topoisomerase II is a structural component of mitotic chromosome scaffolds. J Cell Biol *100*, 1706-1715.

Earnshaw, W.C., and Heck, M.M. (1985). Localization of topoisomerase II in mitotic chromosomes. J Cell Biol *100*, 1716-1725.

Earnshaw, W.C., and Laemmli, U.K. (1983). Architecture of metaphase chromosomes and chromosome scaffolds. JCell Biol *96*, 84-93.

Earnshaw, W.C., and Migeon, B. (1985). A family of centromere proteins is absent from the latent centromere of a stable isodicentric chromosome. Chromosoma (Berl) *92*, 290-296.

Earnshaw, W.C., Ratrie, H., and Stetten, G. (1989). Visualization of centromere proteins CENP-B and CENP-C on a stable dicentric chromosome in cytological spreads. Chromosoma (Berl) *98*, 1-12.

Earnshaw, W.C., and Rothfield, N. (1985). Identification of a family of human centromere proteins using autoimmune sera from patients with scleroderma. Chromosoma (Berl) *91*, 313-321.

Earnshaw, W.C., Sullivan, K.F., Machlin, P.S., Cooke, C.A., Kaiser, D.A., Pollard, T.D., Rothfield, N.F., and Cleveland, D.W. (1987). Molecular cloning of cDNA for CENP-B, the major human centromere autoantigen. JCell Biol *104*, 817-829.

Euskirchen, G.M. (2002). Nnf1p, Dsn1p, Mtw1p, and Nsl1p: a new group of proteins important for chromosome segregation in Saccharomyces cerevisiae. Eukaryot Cell *1*, 229-240.

Evans, T., Rosenthal, E.T., Youngblom, J., Distel, D., and Hunt, T. (1983). Cyclin: a protein specified by maternal mRNA in sea urchin eggs that is destroyed at each cleavage division. Cell *33*, 389-396.

Fang, G., Yu, H., and Kirschner, M.W. (1998). Direct binding of CDC20 protein family members activates the anaphase-promoting complex in mitosis and G1. Mol Cell *2*, 163-171.

Fitzgerald-Hayes, M., Clarke, L., and Carbon, J. (1982). Nucleotide sequence comparisons and functional analysis of yeast centromere DNAs. Cell *29*, 235-244.

Flors, C., Hotta, J., Uji-i, H., Dedecker, P., Ando, R., Mizuno, H., Miyawaki, A., and Hofkens, J. (2007). A stroboscopic approach for fast photoactivation-localization microscopy with Dronpa mutants. J Am Chem Soc *129*, 13970-13977.

Folling, J., Bossi, M., Bock, H., Medda, R., Wurm, C.A., Hein, B., Jakobs, S., Eggeling, C., and Hell, S.W. (2008). Fluorescence nanoscopy by ground-state depletion and single-molecule return. Nat Methods *5*, 943-945.

Foltz, D.R., Jansen, L.E., Bailey, A.O., Yates, J.R., 3rd, Bassett, E.A., Wood, S., Black, B.E., and Cleveland, D.W. (2009). Centromere-specific assembly of CENP-a nucleosomes is mediated by HJURP. Cell *137*, 472-484.

Foltz, D.R., Jansen, L.E., Black, B.E., Bailey, A.O., Yates, J.R., and Cleveland, D.W. (2006). The human CENP-A centromeric nucleosome-associated complex. Nat Cell Biol.

Fujita, Y., Hayashi, T., Kiyomitsu, T., Toyoda, Y., Kokubu, A., Obuse, C., and Yanagida, M. (2007). Priming of centromere for CENP-A recruitment by human hMis18alpha, hMis18beta, and M18BP1. Dev Cell *12*, 17-30.

Fukagawa, T., Mikami, Y., Nishihashi, A., Regnier, V., Haraguchi, T., Hiraoka, Y., Sugata, N., Todokoro, K., Brown, W., and Ikemura, T. (2001). CENP-H, a constitutive centromere component, is required for centromere targeting of CENP-C in vertebrate cells. Embo J *20*, 4603-4617.

Fuller, B.G., Lampson, M.A., Foley, E.A., Rosasco-Nitcher, S., Le, K.V., Tobelmann, P., Brautigan, D.L., Stukenberg, P.T., and Kapoor, T.M. (2008). Midzone activation of aurora B in anaphase produces an intracellular phosphorylation gradient. Nature *453*, 1132-1136.

Furuyama, S., and Biggins, S. (2007). Centromere identity is specified by a single centromeric nucleosome in budding yeast. Proc Natl Acad Sci U S A *104*, 14706-14711.

Furuyama, T., and Henikoff, S. (2009). Centromeric nucleosomes induce positive DNA supercoils. Cell *138*, 104-113.

Gadea, B.B., and Ruderman, J.V. (2005). Aurora kinase inhibitor ZM447439 blocks chromosome-induced spindle assembly, the completion of chromosome condensation, and the establishment of the spindle integrity checkpoint in Xenopus egg extracts. Mol Biol Cell *16*, 1305-1318.

Gardner, M.K., Pearson, C.G., Sprague, B.L., Zarzar, T.R., Bloom, K., Salmon, E.D., and Odde, D.J. (2005). Tension-dependent regulation of microtubule dynamics at kinetochores can explain metaphase congression in yeast. Mol Biol Cell *16*, 3764-3775.

Gasser, S.M., and Laemmli, U.K. (1986). The organisation of chromatin loops: characterization of a scaffold attachment site. EMBO J *5*, 511-518.

Gassmann, R., Vagnarelli, P., Hudson, D., and Earnshaw, W.C. (2004). Mitotic chromosome formation and the condensin paradox. Exp Cell Res *296*, 35-42.

Gerlich, D., Hirota, T., Koch, B., Peters, J.M., and Ellenberg, J. (2006). Condensin I stabilizes chromosomes mechanically through a dynamic interaction in live cells. Curr Biol *16*, 333-344.

Gestaut, D.R., Graczyk, B., Cooper, J., Widlund, P.O., Zelter, A., Wordeman, L., Asbury, C.L., and Davis, T.N. (2008). Phosphoregulation and depolymerization-driven movement of the Dam1 complex do not require ring formation. Nat Cell Biol *10*, 407-414.

Gimenez-Abian, J.F., Clarke, D.J., Mullinger, A.M., Downes, C.S., and Johnson, R.T. (1995). A postprophase topoisomerase II-dependent chromatid core separation step in the formation of metaphase chromosomes. J Cell Biol *131*, 7-17.

Glotzer, M., Murray, A.W., and Kirschner, M.W. (1991). Cyclin is degraded by the ubiquitin pathway. Nature *349*, 132-138.

Gonczy, P., Echeverri, C., Oegema, K., Coulson, A., Jones, S.J., Copley, R.R., Duperon, J., Oegema, J., Brehm, M., Cassin, E.*, et al.* (2000). Functional genomic analysis of cell division in C. elegans using RNAi of genes on chromosome III. Nature *408*, 331-336.

Gorbsky, G.J., and Ricketts, W.A. (1993). Differential expression of a phosphoepitope at the kinetochores of moving chromosomes. J Cell Biol *122*, 1311-1321.

Goshima, G., Kiyomitsu, T., Yoda, K., and Yanagida, M. (2003). Human centromere chromatin protein hMis12, essential for equal segregation, is independent of CENP-A loading pathway. J Cell Biol *160*, 25-39.

Goshima, G., Mayer, M., Zhang, N., Stuurman, N., and Vale, R.D. (2008). Augmin: a protein complex required for centrosome-independent microtubule generation within the spindle. J Cell Biol *181*, 421-429.

Goshima, G., and Yanagida, M. (2000). Establishing biorientation occurs with precocious separation of the sister kinetochores, but not the arms, in the early spindle of budding yeast. Cell *100*, 619-633.

Gustafsson, M.G. (2000). Surpassing the lateral resolution limit by a factor of two using structured illumination microscopy. J Microsc *198*, 82-87.

Haaf, T., Matera, A.G., Wienberg, J., and Ward, D.C. (1995). Presence and abundance of CENP-B box sequences in great ape subsets of primate-specific alpha-satellite DNA. J Mol Evol *41*, 487-491.

Habuchi, S., Ando, R., Dedecker, P., Verheijen, W., Mizuno, H., Miyawaki, A., and Hofkens, J. (2005). Reversible single-molecule photoswitching in the GFP-like fluorescent protein Dronpa. Proc Natl Acad Sci USA *102*, 9511-9516.

Hadwiger, J.A., Wittenbrg, C., Mendenhall, M.D., and Reed, S.I. (1989). The Saccharomyces cerevisiae CKS1 gene, a homolog of the Schizosaccharomyces pombe suc1+ gene, encodes a subunit of the Cdc28 protein kinase complex. Mol Cell Biol *9*, 2034-2041.

Hagstrom, K.A., Holmes, V.F., Cozzarelli, N.R., and Meyer, B.J. (2002). C. elegans condensin promotes mitotic chromosome architecture, centromere organization, and sister chromatid segregation during mitosis and meiosis. Genes Dev *16*, 729-742.

Hauf, S., Cole, R.W., LaTerra, S., Zimmer, C., Schnapp, G., Walter, R., Heckel, A., van Meel, J., Rieder, C.L., and Peters, J.M. (2003). The small molecule Hesperadin reveals a role for Aurora B in correcting kinetochore-microtubule attachment and in maintaining the spindle assembly checkpoint. J Cell Biol *161*, 281-294.

Hayashi, T., Fujita, Y., Iwasaki, O., Adachi, Y., Takahashi, K., and Yanagida, M. (2004). Mis16 and Mis18 are required for CENP-A loading and histone deacetylation at centromeres. Cell *118*, 715-729.

Hayden, J.H., Bowser, S.S., and Rieder, C.L. (1990). Kinetochores capture astral microtubules during chromosome attachment to the mitotic spindle: direct visualization in live newt lung cells. J Cell Biol *111*, 1039-1045.

He, D., and Brinkley, B.R. (1996). Structure and dynamic organization of centromeres/prekinetochores in the nucleus of mammalian cells. J Cell Sci *109 (Pt 11)*, 2693-2704.

He, X., Asthana, S., and Sorger, P.K. (2000). Transient sister chromatid separation and elastic deformation of chromosomes during mitosis in budding yeast. Cell *101*, 763-775.

Heald, R., Tournebize, R., Blank, T., Sandaltzopoulos, R., Becker, P., Hyman, A., and Karsenti, E. (1996). Self-organization of microtubules into bipolar spindles around artificial chromosomes in Xenopus egg extracts. Nature *382*, 420-425.

Heilemann, M., van de Linde, S., Schuttpelz, M., Kasper, R., Seefeldt, B., Mukherjee, A., Tinnefeld, P., and Sauer, M. (2008). Subdiffraction-resolution fluorescence imaging with conventional fluorescent probes. Angew Chem Int Ed Engl *47*, 6172-6176.

Hell, S.W. (2009). Microscopy and its focal switch. Nat Methods *6*, 24-32.

Hell, S.W., and Wichmann, J. (1994). Breaking the diffraction resolution limit by stimulated emission: stimulated-emission-depletion fluorescence microscopy. Opt Lett *19*, 780-782.

Hershko, A., and Ciechanover, A. (1998). The ubiquitin system. Annu Rev Biochem *67*, 425-479.

Hess, S.T., Girirajan, T.P., and Mason, M.D. (2006). Ultra-high resolution imaging by fluorescence photoactivation localization microscopy. Biophys J *91*, 4258-4272.

Hirano, T. (2002). The ABCs of SMC proteins: two-armed ATPases for chromosome condensation, cohesion, and repair. Genes Dev *16*, 399-414.

Hirano, T. (2006). At the heart of the chromosome: SMC proteins in action. Nat Rev Mol Cell Biol *7*, 311-322.

Hirano, T., and Mitchison, T.J. (1993). Topoisomerase II does not play a scaffolding role in the organization of mitotic chromosomes assembled in Xenopus egg extracts. J Cell Biol *120*, 601-612.

Hirano, T., and Mitchison, T.J. (1994). A heterodimeric coiled-coil protein required for mitotic chromosome condensation in vitro. Cell *79*, 449-458.

Hirota, T., Gerlich, D., Koch, B., Ellenberg, J., and Peters, J.M. (2004). Distinct functions of condensin I and II in mitotic chromosome assembly. J Cell Sci *117*, 6435-6445.

Holm, C. (1994). Coming undone: how to untangle a chromosome. Cell *77*, 955-957.

Holm, C., Stearns, T., and Botstein, D. (1989). DNA topoisomerase II must act at mitosis to prevent nondisjunction and chromosome breakage. Mol Cell Biol *9*, 159-168.

Hori, T., Amano, M., Suzuki, A., Backer, C.B., Welburn, J.P., Dong, Y., McEwen, B.F., Shang, W.H., Suzuki, E., Okawa, K.*, et al.* (2008). CCAN makes multiple contacts with centromeric DNA to provide distinct pathways to the outer kinetochore. Cell *135*, 1039-1052.

Hori, T., Haraguchi, T., Hiraoka, Y., Kimura, H., and Fukagawa, T. (2003). Dynamic behavior of Nuf2-Hec1 complex that localizes to the centrosome and centromere and is essential for mitotic progression in vertebrate cells. J Cell Sci *116*, 3347-3362.

Howell, B.J., McEwen, B.F., Canman, J.C., Hoffman, D.B., Farrar, E.M., Rieder, C.L., and Salmon, E.D. (2001). Cytoplasmic dynein/dynactin drives kinetochore protein transport to the spindle poles and has a role in mitotic spindle checkpoint inactivation. J Cell Biol *155*, 1159-1172.

Howman, E.V., Fowler, K.J., Newson, A.J., Redward, S., MacDonald, A.C., Kalitsis, P., and Choo, K.H. (2000). Early disruption of centromeric chromatin organization in centromere protein A (Cenpa) null mice. Proc Natl Acad Sci USA *97*, 1148-1153.

Hoyt, M.A., Totis, L., and Roberts, B.T. (1991). S. cerevisiae genes required for cell cycle arrest in response to loss of microtubule function. Cell *66*, 507-517.

Hudson, D., Fowler, K.J., Earle, E., Saffery, R., Kalitsis, P., Trowell, H., Hill, J., Wreford, N.G., de Kretser, D.M., Cancilla, M.R.*, et al.* (1998). Centromere protein B null mice are mitotically and meiotically normal but have lower body and testis weights. J Cell Biol *141*, 309-319.

Hudson, D.F., Ohta, S., Freisinger, T., Macisaac, F., Sennels, L., Alves, F., Lai, F., Kerr, A., Rappsilber, J., and Earnshaw, W.C. (2008). Molecular and genetic analysis of condensin function in vertebrate cells. Mol Biol Cell *19*, 3070-3079.

Hudson, D.F., Vagnarelli, P., Gassmann, R., and Earnshaw, W.C. (2003). Condensin is required for nonhistone protein assembly and structural integrity of vertebrate mitotic chromosomes. Dev Cell *5*, 323-336.

Ikeno, M., Masumoto, H., and Okazaki, T. (1994). Distribution of CENP-B boxes reflected in CREST centromere antigenic sites on long-range alpha-satellite DNA arrays of human chromosome 21. Hum Mol Genet *3*, 1245-1257.

Inoue, S., and Salmon, E.D. (1995). Force generation by microtubule assembly/disassembly in mitosis and related movements. Mol Biol Cell *6*, 1619-1640.

Irniger, S., Piatti, S., Michaelis, C., and Nasmyth, K. (1995). Genes involved in sister chromatid separation are needed for B-type cyclin proteolysis in budding yeast. Cell *81*, 269-278.

Izuta, H., Ikeno, M., Suzuki, N., Tomonaga, T., Nozaki, N., Obuse, C., Kisu, Y., Goshima, N., Nomura, F., Nomura, N.*, et al.* (2006). Comprehensive analysis of the ICEN (Interphase Centromere Complex) components enriched in the CENP-A chromatin of human cells. Genes Cells *11*, 673-684.

Jablonski, S.A., Chan, G.K.T., Cooke, C.A., Earnshaw, W.C., and Yen, T.J. (1998). The hBUB1 and hBUBR1 kinases sequentially assemble onto kinetochores during prophase with hBUBR1 concentrating at the kinetochore plates in mitosis. Chromosoma *107*, 386-396.

Jager, H., Rauch, M., and Heidmann, S. (2005). The Drosophila melanogaster condensin subunit Cap-G interacts with the centromere-specific histone H3 variant CID. Chromosoma *113*, 350-361.

Jansen, L.E., Black, B.E., Foltz, D.R., and Cleveland, D.W. (2007). Propagation of centromeric chromatin requires exit from mitosis. J Cell Biol *176*, 795-805.

Jaqaman, K., King, E.W., Amaro, A.C., Winter, J.R., Dorn, J.F., Elliot, H.L., Mchedlishili, N., McClelland, S.E., Porter, A.C., Posch, M.*, et al.* (2010). Kinetochore alignment within the metaphase plate is regulated by centromere stiffness and microtubule depolymerases. J Cell Biol.

Joglekar, A.P., Bloom, K., and Salmon, E.D. (2009). In vivo protein architecture of the eukaryotic kinetochore with nanometer scale accuracy. Curr Biol *19*, 694-699.

Joglekar, A.P., Bloom, K.S., and Salmon, E. (2010). Mechanisms of force generation by end-on kinetochore-microtubule attachments. Curr Opin Cell Biol.

Joglekar, A.P., Bouck, D., Finley, K., Liu, X., Wan, Y., Berman, J., He, X., Salmon, E.D., and Bloom, K.S. (2008). Molecular architecture of the kinetochore-microtubule attachment site is conserved between point and regional centromeres. J Cell Biol *181*, 587-594.

Joglekar, A.P., Bouck, D.C., Molk, J.N., Bloom, K.S., and Salmon, E.D. (2006). Molecular architecture of a kinetochore-microtubule attachment site. Nat Cell Biol *8*, 581-585.

Jokelainen, P.T. (1967). The ultrastructure and spatial organization of the metaphase kinetochore in mitotic rat cells. J Ultras Res *19*, 19-44.

Kapoor, M., Montes de Oca Luna, R., Liu, G., Lozano, G., Cummings, C., Mancini, M., Ouspenski, I., Brinkley, B.R., and May, G.S. (1998). The cenpB gene is not essential in mice. Chromosoma *107*, 570-576.

Kapoor, T.M., Lampson, M.A., Hergert, P., Cameron, L., Cimini, D., Salmon, E.D., McEwen, B.F., and Khodjakov, A. (2006). Chromosomes can congress to the metaphase plate before biorientation. Science *311*, 388-391.

Karess, R. (2005). Rod-Zw10-Zwilch: a key player in the spindle checkpoint. Trends Cell Biol *15*, 386-392.

Kelly, A.E., and Funabiki, H. (2009). Correcting aberrant kinetochore microtubule attachments: an Aurora B-centric view. Curr Opin Cell Biol *21*, 51-58.

Khodjakov, A., Cole, R.W., McEwen, B.F., Buttle, K.F., and Rieder, C.L. (1997). Chromosome fragments possessing only one kinetochore can congress to the spindle equator. J Cell Biol *136*, 229-240.

Khodjakov, A., and Rieder, C.L. (2009). The nature of cell-cycle checkpoints: facts and fallacies. J Biol *8*, 88.

Kimura, K., and Hirano, T. (1997). ATP-dependent positive supercoiling of DNA by 13S condensin: a biochemical implication for chromosome condensation. Cell *90*, 625-634.

Kimura, K., Rybenkov, V.V., Crisona, N.J., Hirano, T., and Cozzarelli, N.R. (1999). 13S condensin actively reconfigures DNA by introducing global positive writhe: implications for chromosome condensation. Cell *98*, 239-248.

King, J.M., and Nicklas, R.B. (2000). Tension on chromosomes increases the number of kinetochore microtubules but only within limits. J Cell Sci *113 Pt 21*, 3815-3823.

King, R.W., Peters, J.M., Tugendreich, S., Rolfe, M., Hieter, P., and Kirschner, M.W. (1995). A 20S complex containing CDC27 and CDC16 catalyzes the mitosis-specific conjugation of ubiquitin to cyclin B. Cell *81*, 279-288.

Kirschner, M., and Mitchison, T. (1986). Beyond self-assembly: from microtubules to morphogenesis. Cell *45*, 329-342.

Kiyomitsu, T., Obuse, C., and Yanagida, M. (2007). Human Blinkin/AF15q14 is required for chromosome alignment and the mitotic checkpoint through direct interaction with Bub1 and BubR1. Dev Cell *13*, 663-676.

Klar, T.A., Jakobs, S., Dyba, M., Egner, A., and Hell, S.W. (2000). Fluorescence microscopy with diffraction resolution barrier broken by stimulated emission. Proc Natl Acad Sci U S A *97*, 8206-8210.

Kline, S.L., Cheeseman, I.M., Hori, T., Fukagawa, T., and Desai, A. (2006). The human Mis12 complex is required for kinetochore assembly and proper chromosome segregation. J Cell Biol *173*, 9-17.

Kline-Smith, S.L., Sandall, S., and Desai, A. (2005). Kinetochore-spindle microtubule interactions during mitosis. Curr Opin Cell Biol *17*, 35-46.

Kouzarides, T. (2007). Chromatin modifications and their function. Cell *128*, 693-705.

Kwon, M.S., Hori, T., Okada, M., and Fukagawa, T. (2007). CENP-C is involved in chromosome segregation, mitotic checkpoint function, and kinetochore assembly. Mol Biol Cell *18*, 2155-2168.

Laemmli, U.K., Cheng, S.M., Adolph, K.W., Paulson, J.R., Brown, J.A., and Baumbach, W.R. (1978). Metaphase chromosome structure: the role of nonhistone proteins. Cold Spring Harbor Sym Quant Biol *423*, 351-360.

Lam, A.L., Boivin, C.D., Bonney, C.F., Rudd, M.K., and Sullivan, B.A. (2006). Human centromeric chromatin is a dynamic chromosomal domain that can spread over noncentromeric DNA. Proc Natl Acad Sci U SA *103*, 4186-4191.

Lan, W., Zhang, X., Kline-Smith, S.L., Rosasco, S.E., Barrett-Wilt, G.A., Shabanowitz, J., Hunt, D.F., Walczak, C.E., and Stukenberg, P.T. (2004). Aurora B phosphorylates centromeric MCAK and regulates its localization and microtubule depolymerization activity. Curr Biol *14*, 273-286.

Lewis, C.D., and Laemmli, U.K. (1982). Higher order metaphase chromosome structure: evidence for metalloprotein interactions. Cell *29*, 171-181.

Li, R., and Murray, A.W. (1991). Feedback control of mitosis in budding yeast. Cell *66*, 519-531.

Li, X., and Nicklas, R.B. (1995). Mitotic forces control a cell-cycle checkpoint. Nature *373*, 630-632.

Li , Y., and Benezra, R. (1996). Identification of a human mitotic checkpoint gene: hsMAD2. Science *274*, 246-248.

Lippincott-Schwartz, J., and Manley, S. (2009). Putting super-resolution fluorescence microscopy to work. Nat Methods *6*, 21-23.

Liu, D., Vader, G., Vromans, M.J., Lampson, M.A., and Lens, S.M. (2009). Sensing chromosome bi-orientation by spatial separation of aurora B kinase from kinetochore substrates. Science *323*, 1350-1353.

Liu, S.T., Hittle, J.C., Jablonski, S.A., Campbell, M.S., Yoda, K., and Yen, T.J. (2003). Human CENP-I specifies localization of CENP-F, MAD1 and MAD2 to kinetochores and is essential for mitosis. Nat Cell Biol *5*, 341-345.

Liu, S.T., Rattner, J.B., Jablonski, S.A., and Yen, T.J. (2006). Mapping the assembly pathways that specify formation of the trilaminar kinetochore plates in human cells. J Cell Biol *175*, 41-53.

Lo, A.W., Craig, J.M., Saffery, R., Kalitsis, P., Irvine, D.V., Earle, E., Magliano, D.J., and Choo, K.H. (2001a). A 330 kb CENP-A binding domain and altered replication timing at a human neocentromere. Embo J *20*, 2087-2096.

Lo, A.W., Magliano, D.J., Sibson, M.C., Kalitsis, P., Craig, J.M., and Choo, K.H. (2001b). A novel chromatin immunoprecipitation and array (CIA) analysis identifies a 460-kb CENP-A-binding neocentromere DNA. Genome Res *11*, 448-457.

Lohka, M., Hayes, M.K., and Maller, J.L. (1988). Purification of maturation-promoting factor, an intracellular regulator of early mitotic events. Proc Nat Acad Sci (USA) *85*, 3009-3013.

Loncarek, J., Kisurina-Evgenieva, O., Vinogradova, T., Hergert, P., La Terra, S., Kapoor, T.M., and Khodjakov, A. (2007). The centromere geometry essential for keeping mitosis error free is controlled by spindle forces. Nature *450*, 745-749.

Luger, K., Mader, A.W., Richmond, R.K., Sargent, D.F., and Richmond, T.J. (1997). Crystal structure of the nucleosome core particle at 2.8 A resolution. Nature *389*, 251-260.

Maddox, P., Straight, A., Coughlin, P., Mitchison, T.J., and Salmon, E.D. (2003). Direct observation of microtubule dynamics at kinetochores in Xenopus extract spindles: implications for spindle mechanics. J Cell Biol *162*, 377-382.

Maddox, P.S., Hyndman, F., Monen, J., Oegema, K., and Desai, A. (2007). Functional genomics identifies a Myb domain-containing protein family required for assembly of CENP-A chromatin. J Cell Biol *176*, 757-763.

Maddox, P.S., Oegema, K., Desai, A., and Cheeseman, I.M. (2004). "Holo"er than thou: chromosome segregation and kinetochore function in C. elegans. Chromosome Res *12*, 641-653.

Maresca, T.J., Groen, A.C., Gatlin, J.C., Ohi, R., Mitchison, T.J., and Salmon, E.D. (2009). Spindle assembly in the absence of a RanGTP gradient requires localized CPC activity. Curr Biol *19*, 1210-1215.

Maresca, T.J., and Salmon, E.D. (2009). Intrakinetochore stretch is associated with changes in kinetochore phosphorylation and spindle assembly checkpoint activity. J Cell Biol *184*, 373-381.

Marshall, O.J., Marshall, A.T., and Choo, K.H. (2008). Three-dimensional localization of CENP-A suggests a complex higher order structure of centromeric chromatin. J Cell Biol *183*, 1193-1202.

Masumoto, H., Masukata, H., Muro, Y., Nozaki, N., and Okazaki, T. (1989). A human centromere antigen (CENP-B) interacts with a short specific sequence in alphoid DNA, a human centromeric satellite. J Cell Biol *109*, 1963-1973.

McAinsh, A.D., Meraldi, P., Draviam, V.M., Toso, A., and Sorger, P.K. (2006). The human kinetochore proteins Nnf1R and Mcm21R are required for accurate chromosome segregation. EMBO J *25*, 4033-4049.

McAinsh, A.D., Tytell, J.D., and Sorger, P.K. (2003). Structure, function, and regulation of budding yeast kinetochores. Annu Rev Cell Dev Biol *19*, 519-539.

McClelland, S.E., Borusu, S., Amaro, A.C., Winter, J.R., Belwal, M., McAinsh, A.D., and Meraldi, P. (2007). The CENP-A NAC/CAD kinetochore complex controls chromosome congression and spindle bipolarity. EMBO J *26*, 5033-5047.

McEwen, B.F., Hsieh, C.E., Mattheyses, A.L., and Rieder, C.L. (1998). A new look at kinetochore structure in vertebrate somatic cells using high pressure freezing and freeze substitution. Chromosoma (Berl) *107*, 366-375.

Meireles, A.M., Fisher, K.H., Colombie, N., Wakefield, J.G., and Ohkura, H. (2009). Wac: a new Augmin subunit required for chromosome alignment but not for acentrosomal microtubule assembly in female meiosis. J Cell Biol *184*, 777-784.

Melby, T.E., Ciampaglio, C.N., Briscoe, G., and Erickson, H.P. (1998). The symmetrical structure of structural maintenance of chromosomes (SMC) and MukB proteins: long, antiparallel coiled coils, folded at a flexible hinge. J Cell Biol *142*, 1595-1604.

Meluh, P.B., Yang, P., Glowczewski, L., Koshland, D., and Smith, M.M. (1998). Cse4p is a component of the core centromere of Saccharomyces cerevisiae. Cell *94*, 607-613.

Meraldi, P., McAinsh, A.D., Rheinbay, E., and Sorger, P.K. (2006). Phylogenetic and structural analysis of centromeric DNA and kinetochore proteins. Genome Biol *7*, R23.

Merdes, A., and De Mey, J. (1990). The mechanism of kinetochore-spindle attachment and polewards movement analyzed in PtK2 cells at the prophase-prometaphase transition. Eur J Cell Biol *53*, 313-325.

Merry, D.W., Pathak, S., Hsu, T.C., and Brinkley, B.R. (1985). Anti-kinetochore antibodies: use as probes for inactive centromeres. Am J Hum Genet *37*, 425-430.

Mikami, Y., Hori, T., Kimura, H., and Fukagawa, T. (2005). The functional region of CENP-H interacts with the Nuf2 complex that localizes to centromere during mitosis. Mol Cell Biol *25*, 1958-1970.

Minoshima, Y., Hori, T., Okada, M., Kimura, H., Haraguchi, T., Hiraoka, Y., Bao, Y.C., Kawashima, T., Kitamura, T., and Fukagawa, T. (2005). The constitutive centromere component CENP-50 is required for recovery from spindle damage. Mol Cell Biol *25*, 10315-10328.

Mirkovitch, J., M. Mirault, and Laemmli, U. (1984). Organization of the higher-order chromatin loop: specific DNA attachment sites on nuclear scaffold. Cell *39*, 223-232.

Mitchison, T., and Kirschner, M. (1984). Dynamic instability of microtubule growth. Nature *312*, 237-242.

Mitchison, T.J., and Salmon, E.D. (1992). Poleward kinetochore fiber movement occurs during both metaphase and anaphase-A in newt lung cell mitosis. J Cell Biol *119*, 569-582.

Mizuguchi, G., Xiao, H., Wisniewski, J., Smith, M.M., and Wu, C. (2007). Nonhistone Scm3 and histones CenH3-H4 assemble the core of centromere-specific nucleosomes. Cell *129*, 1153-1164.

Mogilner, A., Wollman, R., Civelekoglu-Scholey, G., and Scholey, J. (2006). Modeling mitosis. Trends Cell Biol *16*, 88-96.

Moroi, Y., Hartman, A.L., Nakane, P.K., and Tan, E.M. (1981). Distribution of kinetochore (centromere) antigen in mammalian cell nuclei. J Cell Biol *90*, 254-259.

Moroi, Y., Peebles, C., Fritzler, M.J., Steigerwald, J., and Tan, E.M. (1980). Autoantibody to centromere (kinetochore) in scleroderma sera. Proc Nat Acad Sci (USA) *77*, 1627-1631.

Murray, A., and Hunt, T. (1993). The Cell Cycle (New York, Oxford University Press).

Murray, A.W. (1998). How to compact DNA. Science *282*, 425, 427.

Musacchio, A., and Salmon, E.D. (2007). The spindle-assembly checkpoint in space and time. Nat Rev Mol Cell Biol *8*, 379-393.

Nagaki, K., Cheng, Z., Ouyang, S., Talbert, P.B., Kim, M., Jones, K.M., Henikoff, S., Buell, C.R., and Jiang, J. (2004). Sequencing of a rice centromere uncovers active genes. Nat Genet *36*, 138-145.

Nakaseko, Y., Adachi, Y., Funahashi, S., Niwa, O., and Yanagida, M. (1986). Chromosome walking shows a highly homologous repetitive sequence present in all the centromere regions of fission yeast. The EMBO J *5*, 1011-1021.

Nash, R., Tokiwa, G., Anand, S., Erickson, K., and Futcher, A.B. (1988). The WHI1+ gene of Saccharomyces cerevisiae tethers cell division to cell size and is a cyclin homolog. The EMBO J *7*, 4335-4346.

Nasmyth, K., and Haering, C.H. (2009). Cohesin: its roles and mechanisms. Annu Rev Genet *43*, 525-558.

Nekrasov, V.S., Smith, M.A., Peak-Chew, S., and Kilmartin, J.V. (2003). Interactions between centromere complexes in Saccharomyces cerevisiae. Mol Biol Cell *14*, 4931-4946.

Neuwald, A.F., and Hirano, T. (2000). HEAT repeats associated with condensins, cohesins, and other complexes involved in chromosome-related functions. Genome Res *10*, 1445-1452.

Nicklas, R.B., and Koch, C.A. (1969). Chromosome micromanipulation. 3. Spindle fiber tension and the reorientation of mal-oriented chromosomes. J Cell Biol *43*, 40-50.

Nicklas, R.B., and Ward, S.C. (1994). Elements of error correction in mitosis: microtubule capture, release, and tension. J Cell Biol *126*, 1241-1253.

Nicklas, R.B., Wards, S.C., and Gorbsky, G.J. (1995). Kinetochore chemistry is sensitive to tension and may link mitotic forces for a cell cycle checkpoint. J Cell Biol *130*, 929-939.

Nicklas, R.B., Waters, J.C., Salmon, E.D., and Ward, S.C. (2001). Checkpoint signals in grasshopper meiosis are sensitive to microtubule attachment, but tension is still essential. J Cell Sci *114*, 4173-4183.

Nishihashi, A., Haraguchi, T., Hiraoka, Y., Ikemura, T., Regnier, V., Dodson, H., Earnshaw, W.C., and Fukagawa, T. (2002). CENP-I is essential for centromere function in vertebrate cells. Dev Cell *2*, 463-476.

O'Connell, C.B., and Khodjakov, A.L. (2007). Cooperative mechanisms of mitotic spindle formation. J Cell Sci *120*, 1717-1722.

Obuse, C., Iwasaki, O., Kiyomitsu, T., Goshima, G., Toyoda, Y., and Yanagida, M. (2004a). A conserved Mis12 centromere complex is linked to heterochromatic HP1 and outer kinetochore protein Zwint-1. Nat Cell Biol *6*, 1135-1141.

Obuse, C., Yang, H., Nozaki, N., Goto, S., Okazaki, T., and Yoda, K. (2004b). Proteomics analysis of the centromere complex from HeLa interphase cells: UV-damaged DNA binding protein 1 (DDB-1) is a component of the CEN-complex, while BMI-1 is transiently co-localized with the centromeric region in interphase. Genes Cells *9*, 105-120.

Oegema, K., Desai, A., Rybina, S., Kirkham, M., and Hyman, A.A. (2001). Functional Analysis of Kinetochore Assembly in Caenorhabditis elegans. J Cell Biol *153*, 1209-1226.

Ohi, R., Sapra, T., Howard, J., and Mitchison, T.J. (2004). Differentiation of cytoplasmic and meiotic spindle assembly MCAK functions by Aurora B-dependent phosphorylation. Mol Biol Cell *15*, 2895-2906.

Okada, M., Cheeseman, I.M., Hori, T., Okawa, K., McLeod, I.X., Yates, J.R., Desai, A., and Fukagawa, T. (2006). The CENP-H-I complex is required for the efficient incorporation of newly synthesized CENP-A into centromeres. Nat Cell Biol.

Okada, T., Ohzeki, J., Nakano, M., Yoda, K., Brinkley, W.R., Larionov, V., and Masumoto, H. (2007). CENP-B controls centromere formation depending on the chromatin context. Cell *131*, 1287-1300.

Oliveira, R.A., Coelho, P.A., and Sunkel, C.E. (2005). The condensin I subunit Barren/CAP-H is essential for the structural integrity of centromeric heterochromatin during mitosis. Mol Cell Biol *25*, 8971-8984.

Ono, T., Fang, Y., Spector, D.L., and Hirano, T. (2004). Spatial and temporal regulation of Condensins I and II in mitotic chromosome assembly in human cells. Mol Biol Cell *15*, 3296-3308.

Ono, T., Losada, A., Hirano, M., Myers, M.P., Neuwald, A.F., and Hirano, T. (2003). Differential Contributions of Condensin I and Condensin II to Mitotic Chromosome Architecture in Vertebrate Cells. Cell *115*, 109-121.

Painter, R.B., and Young, B.R. (1980). Radiosensitivity in ataxia-telangiectasia: a new explanation. Proc Natl Acad Sci U S A *77*, 7315-7317.

Palmer, D.K., and Margolis, R.L. (1987). A 17-kD centromere protein (CENP-A) copurifies with nucleosome core particles and with histones. J Cell Biol *104*, 805-815.

Palmer, D.K., O'Day, K., Le Trong, H., Charbonneau, H., and Margolis, R.L. (1991). Purification of the centromeric protein CENP-A and demonstration that it is a centromere specific histone. Proc Nat Acad Sci (USA) *88*, 3734-3738.

Palmer, D.K., O'Day, K., and Margolis, R.L. (1989). Biochemical analysis of CENP-A, a centromeric protein with histone-like properties. Prog Clin Biol Res *318*, 61-72.

Partridge, J.F., Borgstrom, B., and Allshire, R.C. (2000). Distinct protein interaction domains and protein spreading in a complex centromere. Genes Dev *14*, 783-791.

Patterson, G., Davidson, M., Manley, S., and Lippincott-Schwartz, J. (2010). Superresolution Imaging using Single-Molecule Localization. Annu Rev Phys Chem.

Paulson, J.R., and Laemmli, U.K. (1977). The structure of histone-depleted chromosomes. Cell *12*, 817-828.

Pearson, C.G., Gardner, M.K., Paliulis, L.V., Salmon, E.D., Odde, D.J., and Bloom, K. (2006). Measuring nanometer scale gradients in spindle microtubule dynamics using model convolution microscopy. Mol Biol Cell *17*, 4069-4079.

Pearson, C.G., Maddox, P.S., Salmon, E.D., and Bloom, K. (2001). Budding yeast chromosome structure and dynamics during mitosis. J Cell Biol *152*, 1255-1266.

Perez-Castro, A.V., Shamanski, F.L., Meneses, J.J., Lovato, T.L., Vogel, K.G., Moyzis, R.K., and Pedersen, R. (1998). Centromeric Protein B null mice are viable with no apparent abnormalities. Dev Biol *201*, 135-143.

Perpelescu, M., Nozaki, N., Obuse, C., Yang, H., and Yoda, K. (2009). Active establishment of centromeric CENP-A chromatin by RSF complex. J Cell Biol *185*, 397-407.

Peters, A.H., Kubicek, S., Mechtler, K., O'Sullivan, R.J., Derijck, A.A., Perez-Burgos, L., Kohlmaier, A., Opravil, S., Tachibana, M., Shinkai, Y., *et al.* (2003). Partitioning and plasticity of repressive histone methylation states in mammalian chromatin. Mol Cell *12*, 1577-1589.

Peters, J.M. (2006). The anaphase promoting complex/cyclosome: a machine designed to destroy. Nat Rev Mol Cell Biol *7*, 644-656.

Pidoux, A.L., and Allshire, R.C. (2004). Kinetochore and heterochromatin domains of the fission yeast centromere. Chromosome Res *12*, 521-534.

Pinsky, B.A., and Biggins, S. (2005). The spindle checkpoint: tension versus attachment. Trends Cell Biol *15*, 486-493.

Pinsky, B.A., Kung, C., Shokat, K.M., and Biggins, S. (2006). The Ipl1-Aurora protein kinase activates the spindle checkpoint by creating unattached kinetochores. Nat Cell Biol *8*, 78-83.

Pluta, A.F., Mackay, A.M., Ainsztein, A.M., Goldberg, I.G., and Earnshaw, W.C. (1995). The centromere: Hub of chromosomal activities. Science *270*, 1591-1594.

Poirier, M., Eroglu, S., Chatenay, D., and Marko, J.F. (2000). Reversible and irreversible unfolding of mitotic newt chromosomes by applied force. Mol Biol Cell *11*, 269-276.

Poirier, M.G., and Marko, J.F. (2002). Mitotic chromosomes are chromatin networks without a mechanically contiguous protein scaffold. Proc Natl Acad Sci USA *99*, 15393-15397.

Pollard, T.D., and Earnshaw, W. (2007). Cell Biology, 2nd Edition edn (Elsevier).

Prades, C., Laurent, A.M., Puechberty, J., Yurov, Y., and Roizes, G. (1996). SINE and LINE within human centromeres. J Mol Evol *42*, 37-43.

Przewloka, M.R., and Glover, D.M. (2009). The kinetochore and the centromere: a working long distance relationship. Annu Rev Genet *43*, 439-465.

Rattner, J.B., and Wang, T. (1992). Kinetochore formation and behaviour following premature chromosome condensation. J Cell Sci *103 (Pt 4)*, 1039-1045.

Regnier, V., Vagnarelli, P., Fukagawa, T., Zerjal, T., Burns, E., Trouche, D., Earnshaw, W., and Brown, W. (2005). CENP-A is required for accurate chromosome segregation and sustained kinetochore association of BubR1. Mol Cell Biol *25*, 3967-3981.

Ribeiro, S.A., Gatlin, J.C., Dong, Y., Joglekar, A., Cameron, L., Hudson, D.F., Farr, C.J., McEwen, B.F., Salmon, E.D., Earnshaw, W.C., *et al.* (2009). Condensin regulates the stiffness of vertebrate centromeres. Mol Biol Cell *20*, 2371-2380.

Rieder, C.L. (1982). The formation, structure and composition of the mammalian kinetochore and kinetochore fiber. Int Rev Cytol *79*, 1-58.

Rieder, C.L. (1990). Formation of the astral mitotic spindle: Ultrastructural basis for the centrosome-kinetochore interaction. Electron Microsc Rev *3*, 269-300.

Rieder, C.L., and Alexander, S.P. (1990). Kinetochores are transported poleward along a single astral microtubule during chromosome attachment to the spindle in newt lung cells. J Cell Biol *110*, 81-95.

Rieder, C.L., Cole, R.W., Khodjakov, A., and Sluder, G. (1995). The checkpoint delaying anaphase in response to chromosome malorientation is mediated by an inhibitory signal produced by unattached kinetochores. J Cell Biol *130*, 941-948.

Rieder, C.L., and Salmon, E.D. (1994). Motile kinetochores and polar ejection forces dictate chromosome position on the vertebrate mitotic spindle. J Cell Biol *124*, 223-233.

Rieder, C.L., and Salmon, E.D. (1998). The vertebrate cell kinetochore and its roles during mitosis. Trends Cell Biol *8*, 310-318.

Rieder, C.L., Schultz, A., Cole, R., and Sluder, G. (1994). Anaphase onset in vertebrate somatic cells is controlled by a checkpoint that monitors sister kinetochore attachment to the spindle. J Cell Biol *127*, 1301-1310.

Ris, H., and Witt, P.L. (1981). Structure of the mammalian kinetochore. Chromosoma (Berl) *82*, 153-170.

Robinson, P.J., Fairall, L., Huynh, V.A., and Rhodes, D. (2006). EM measurements define the dimensions of the "30-nm" chromatin fiber: evidence for a compact, interdigitated structure. Proc Natl Acad Sci U S A *103*, 6506-6511.

Roos, U.P. (1973). Light and electron microscopy of rat kangaroo cells in mitosis. II. Kinetochore structure and function. Chromosoma (Berl) *41*, 195-220.

Ruchaud, S., Carmena, M., and Earnshaw, W.C. (2007). Chromosomal passengers: conducting cell division. Nat Rev Mol Cell Biol *8*, 798-812.

Rudd, M.K., and Willard, H.F. (2004). Analysis of the centromeric regions of the human genome assembly. Trends Genet *20*, 529-533.

Rust, M.J., Bates, M., and Zhuang, X. (2006). Sub-diffraction-limit imaging by stochastic optical reconstruction microscopy (STORM). Nat Methods *3*, 793-795.

Saffery, R., Sumer, H., Hassan, S., Wong, L.H., Craig, J.M., Todokoro, K., Anderson, M., Stafford, A., and Choo, K.H. (2003). Transcription within a Functional Human Centromere. Mol Cell *12*, 509-516.

Saitoh, H., Tomkiel, J.E., Cooke, C.A., Ratrie, H.R., Maurer, M., Rothfield, N.F., and Earnshaw, W.C. (1992). CENP-C, an autoantigen in scleroderma, is a component of the human inner kinetochore plate. Cell *70*, 115-125.

Saitoh, N., Goldberg, I., Wood, E., and Earnshaw, W., C. (1994). ScII: an abundant chromosome scaffold protein is a member of a family of putative ATPases with an unusual predicted tertiary structure. J Cell Biol *127*, 303-318.

Saka, Y., Sutani, T., Yamashita, Y., Saitoh, S., Takeuchi, M., Nakaseko, Y., and Yanagida, M. (1994). Fission yeast cut3 and cut14, members of the ubiquitous protein family, are required for chromosome condensation and segregation in mitosis. The EMBO J *13*, 4938-4952.

Sakai, A., Hizume, K., Sutani, T., Takeyasu, K., and Yanagida, M. (2003). Condensin but not cohesin SMC heterodimer induces DNA reannealing through protein-protein assembly. Embo J *22*, 2764-2775.

Samoshkin, A., Arnaoutov, A., Jansen, L.E., Ouspenski, I., Dye, L., Karpova, T., McNally, J., Dasso, M., Cleveland, D.W., and Strunnikov, A. (2009). Human condensin function is essential for centromeric chromatin assembly and proper sister kinetochore orientation. PLoS One *4*, e6831.

Santaguida, S., and Musacchio, A. (2009). The life and miracles of kinetochores. EMBO J *28*, 2511-2531.

Schaar, B.T., Chan, G.K., Maddox, P., Salmon, E.D., and Yen, T.J. (1997). CENP-E function at kinetochores is essential for chromosome alignment. J Cell Biol *139*, 1373-1382.

Schittenhelm, R.B., Heeger, S., Althoff, F., Walter, A., Heidmann, S., Mechtler, K., and Lehner, C.F. (2007). Spatial organization of a ubiquitous eukaryotic kinetochore protein network in Drosophila chromosomes. Chromosoma *116*, 385-402.

Schleiffer, A., Kaitna, S., Maurer-Stroh, S., Glotzer, M., Nasmyth, K., and Eisenhaber, F. (2003). Kleisins: a superfamily of bacterial and eukaryotic SMC protein partners. Mol Cell *11*, 571-575.

Schueler, M.G., and Sullivan, B.A. (2006). Structural and Functional Dynamics of Human Centromeric Chromatin. Annu Rev Genomics Hum Genet *7*, 301-313.

Schuh, M., Lehner, C.F., and Heidmann, S. (2007). Incorporation of Drosophila CID/CENP-A and CENP-C into centromeres during early embryonic anaphase. Curr Biol *17*, 237-243.

Sedat, J., and Manuelidis, L. (1978). A direct approach to the structure of eukaryotic chromosomes. Cold Spring Harbor Symp Quant Biol *42*, 331-350.

Shelby, R.D., Hahn, K.M., and Sullivan, K.F. (1996). Dynamic elastic behavior of alpha-satellite DNA domains visualized in-situ in living human-cells. J Cell Biol *135*, 545-557.

Shelby, R.D., Vafa, O., and Sullivan, K.F. (1997). Assembly of CENP-A into centromeric chromatin requires a cooperative array of nucleosomal DNA contact sites. J Cell Biol *136*, 501-513.

Skibbens, R.V., Rieder, C.L., and Salmon, E.D. (1995). Kinetochore motility after severing between sister centromeres using laser microsurgery: evidence that kinetochore directional instability and position is regulated by tension. J Cell Sci *108 (Pt 7)*, 2537-2548.

Skibbens, R.V., and Salmon, E.D. (1997). Micromanipulation of chromosomes in mitotic vertebrate tissue cells: tension controls the state of kinetochore movement. Exp Cell Res *235*, 314-324.

Skibbens, R.V., Skeen, V.P., and Salmon, E.D. (1993). Directional instability of kinetochore motility during chromosome congression and segregation in mitotic newt lung cells: a push-pull mechanism. J Cell Biol *122*, 859-875.

Skoufias, D.A., Andreassen, P.R., Lacroix, F.B., Wilson, L., and Margolis, R.L. (2001). Mammalian mad2 and bub1/bubR1 recognize distinct spindle-attachment and kinetochore-tension checkpoints. Proc Natl Acad Sci U S A *98*, 4492-4497.

Skoufias, D.A., DeBonis, S., Saoudi, Y., Lebeau, L., Crevel, I., Cross, R., Wade, R.H., Hackney, D., and Kozielski, F. (2006). S-trityl-L-cysteine is a reversible, tight binding inhibitor of the human kinesin Eg5 that specifically blocks mitotic progression. J Biol Chem *281*, 17559-17569.

Sluder, G. (1979). Role of spindle microtubules in the control of cell cycle timing. J Cell Biol *80*, 674-691.

Sluder, G., and Begg, D.A. (1983). Control mechanisms of the cell cycle: role of the spatial arrangement of spindle components in the timing of mitotic events. J Cell Biol *97*, 877-886.

Sonoda, E., Sasaki, M.S., Buerstedde, J.-M., Bezzubova, O., Shinohara, A., Ogawa, H., Takata, M., Yamaguchi-Iwai, Y., and Takeda, S. (1998). Rad51-deficient vertebrate cells accumulate chromosomal breaks prior to cell death. EMBO J *17*, 598-608.

Spence, J.M., Critcher, R., Ebersole, T.A., Valdivia, M.M., Earnshaw, W.C., Fukagawa, T., and Farr, C.J. (2002). Co-localization of centromere activity, proteins and topoisomerase II within a subdomain of the major human X alpha-satellite array. Embo J *21*, 5269-5280.

Spence, J.M., Mills, W., Mann, K., Huxley, C., and Farr, C.J. (2006). Increased missegregation and chromosome loss with decreasing chromosome size in vertebrate cells. Chromosoma *115*, 60-74.

Starr, D.A., Williams, B.C., Hays, T.S., and Goldberg, M.L. (1998). ZW10 helps recruit dynactin and dynein to the kinetochore. J Cell Biol *142*, 763-774.

Steffensen, S., Coelho, P.A., Cobbe, N., Vass, S., Costa, M., Hassan, B., Prokopenko, S.N., Hugo Bellen, H., Heck, M.M.S., and Sunkel, C.E. (2001). A role for Drosophila SMC4 in the resolution of sister chromatids in mitosis. Curr Biol *11*, 295-307.

Steinhauer, C., Forthmann, C., Vogelsang, J., and Tinnefeld, P. (2008). Superresolution microscopy on the basis of engineered dark states. J Am Chem Soc *130*, 16840-16841.

Stern, B.M., and Murray, A.W. (2001). Lack of tension at kinetochores activates the spindle checkpoint in budding yeast. Curr Biol *11*, 1462-1467.

Stoler, S., Rogers, K., Weitze, S., Morey, L., Fitzgerald-Hayes, M., and Baker, R.E. (2007). Scm3, an essential Saccharomyces cerevisiae centromere protein required for G2/M progression and Cse4 localization. Proc Natl Acad Sci U S A *104*, 10571-10576.

Stray, J.E., and Lindsley, J.E. (2003). Biochemical analysis of the yeast condensin Smc2/4 complex: an ATPase that promotes knotting of circular DNA. J Biol Chem *278*, 26238-26248.

Sudakin, V., Ganoth, D., Dahan, A., Heller, H., Hershko, J., Luca, F.C., Ruderman, J.V., and Hershko, A. (1995). The cyclosome, a large complex containing cyclin-selective ubiquitin ligase activity, targets cyclins for destruction at the end of mitosis. Mol Biol Cell *6*, 185-197.

Sugimoto, K., Yata, H., Muro, Y., and Himeno, M. (1994). Human centromere protein C (CENP-C) is a DNA-binding protein which possess a novel DNA-binding motif. J Biochem *116*, 877-881.

Sullivan, B.A., Blower, M.D., and Karpen, G.H. (2001). Determining centromere identity: cyclical stories and forking paths. Nat Rev Genet *2*, 584-596.

Sullivan, B.A., and Karpen, G.H. (2004). Centromeric chromatin exhibits a histone modification pattern that is distinct from both euchromatin and heterochromatin. Nat Struct Mol Biol *11*, 1076-1083.

Sullivan, B.A., and Schwartz, S. (1995). Identification of centromeric antigens in dicentric Robertsonian translocations: CENP-C and CENP-E are necessary components of functional centromeres. Hum Mol Genet *4*, 2189-2197.

Sullivan, K.F., Hechenberger, M., and Masri, K. (1994). Human CENP-A contains a histone H3 related histone fold domain that is required for targeting to the centromere. J Cell Biol *127*, 581-192.

Sumer, H., Craig, J.M., Sibson, M., and Choo, K.H. (2003). A rapid method of genomic array analysis of scaffold/matrix attachment regions (S/MARs) identifies a 2.5-Mb region of enhanced scaffold/matrix attachment at a human neocentromere. Genome Res *13*, 1737-1743.

Sutani, T., and Yanagida, M. (1997). DNA renaturation activity of the SMC complex implicated in chromosome condensation. Nature *388*, 798-801.

Swedlow, J.R., and Hirano, T. (2003). The making of the mitotic chromosome: modern insights into classical questions. Mol Cell *11*, 557-569.

Tanaka, K., Chang, H.L., Kagami, A., and Watanabe, Y. (2009). CENP-C functions as a scaffold for effectors with essential kinetochore functions in mitosis and meiosis. Dev Cell *17*, 334-343.

Tanaka, T., Fuchs, J., Loidl, J., and Nasmyth, K. (2000). Cohesin ensures bipolar attachment of microtubules to sister centromeres and resists their precocious separation. Nat Cell Biol *2*, 492-499.

Tanaka, T.U., and Desai, A. (2008). Kinetochore-microtubule interactions: the means to the end. Curr Opin Cell Biol *20*, 53-63.

Tanaka, T.U., Rachidi, N., Janke, C., Pereira, G., Galova, M., Schiebel, E., Stark, M.J., and Nasmyth, K. (2002). Evidence that the Ipl1-Sli15 (Aurora kinase-INCENP) complex promotes chromosome bi-orientation by altering kinetochore-spindle pole connections. Cell *108*, 317-329.

Telzer, B.R., Moses, M.J., and Rosenbaum, J.L. (1975). Assembly of microtubules onto kinetochores of isolated mitotic chromosomes of HeLa cells. Proc Natl Acad Sci U S A *72*, 4023-4027.

Tomkiel, J.E., Cooke, C.A., Saitoh, H., Bernat, R.L., and Earnshaw, W.C. (1994). CENP-C is required for maintaining proper kinetochore size and for a timely transition to anaphase. J Cell Biol *125*, 531-545.

Uchida, K.S., Takagaki, K., Kumada, K., Hirayama, Y., Noda, T., and Hirota, T. (2009). Kinetochore stretching inactivates the spindle assembly checkpoint. J Cell Biol *184*, 383-390.

Uemura, T., Ohkura, H., Adachi, Y., Morino, K., Shiozaki, K., and Yanagida, M. (1987). DNA topoisomerase II is required for condensation and separation of mitotic chromosomes in S. pombe. Cell *50*, 917-925.

Uhlmann, F., Lottspeich, F., and Nasmyth, K. (1999). Sister-chromatid separation at anaphase onset is promoted by cleavage of the cohesin subunit Scc1. Nature *400*, 37-42.

Vagnarelli, P., Hudson, D.F., Ribeiro, S.A., Trinkle-Mulcahy, L., Spence, J.M., Lai, F., Farr, C.J., Lamond, A.I., and Earnshaw, W.C. (2006). Condensin and Repo-Man-PP1 co-operate in the regulation of chromosome architecture during mitosis. Nat Cell Biol *8*, 1133-1142.

Vale, R.D. (2003). The molecular motor toolbox for intracellular transport. Cell *112*, 467-480.

van de Linde, S., Sauer, M., and Heilemann, M. (2008). Subdiffraction-resolution fluorescence imaging of proteins in the mitochondrial inner membrane with photoswitchable fluorophores. J Struct Biol *164*, 250-254.

Visintin, R., Prinz, S., and Amon, A. (1997). CDC20 and CDH1: a family of substrate-specific activators of APC-dependent proteolysis. Science *278*, 460-463.

Vorobjev, I.A., and Chentsov, Y.S. (1980). The ultrastructure of centriole in mammalian tissue culture cells. Cell Biol Int Rep *4*, 1037-1044.

Voullaire, L.E., Slater, H.R., Petrovic, V., and Choo, K.H. (1993). A functional marker centromere with no detectible alpha-satellite, satellite III, or CENP-B protein: activation of a latent centromere? Am J Hum Genet *52*, 1153-1163.

Walczak, C.E., Cai, S., and Khodjakov, A. (2010). Mechanisms of chromosome behaviour during mitosis. Nat Rev Mol Cell Biol *11*, 91-102.

Wan, X., O'Quinn, R.P., Pierce, H.L., Joglekar, A.P., Gall, W.E., DeLuca, J.G., Carroll, C.W., Liu, S.T., Yen, T.J., McEwen, B.F., *et al.* (2009). Protein architecture of the human kinetochore microtubule attachment site. Cell *137*, 672-684.

Wang, H.W., Long, S., Ciferri, C., Westermann, S., Drubin, D., Barnes, G., and Nogales, E. (2008). Architecture and flexibility of the yeast Ndc80 kinetochore complex. J Mol Biol *383*, 894-903.

Wang, L., and Eastmond, D.A. (2002). Catalytic inhibitors of topoisomerase II are DNA-damaging agents: induction of chromosomal damage by merbarone and ICRF-187. Environ Mol Mutagen *39*, 348-356.

Warburton, P.E. (2004). Chromosomal dynamics of human neocentromere formation. Chromosome Res *12*, 617-626.

Warburton, P.E., Cooke, C., Bourassa, S., Vafa, O., Sullivan, B.A., Stetten, G., Gimelli, G., Warburton, D., Tyler-Smith, C., Sullivan, K.F., *et al.* (1997). Immunolocalization of CENP-A suggests a distinct nucleosome structure at the inner kinetochore plate of active centromeres. Curr Biol *7*, 901-904.

Waters, J.C., Chen, R.H., Murray, A.W., and Salmon, E.D. (1998). Localization of Mad2 to kinetochores depends on microtubule attachment, not tension. J Cell Biol *141*, 1181-1191.

Wei, B., Bu, H., Chen, H.J., Zhang, H.Y., and Li, X.J. (2006). [Clinicopathologic study of solid papillary carcinoma of breast]. Zhonghua Bing Li Xue Za Zhi *35*, 589-593.

Weinert, T.A., and Hartwell, L.H. (1988). The RAD9 gene controls the cell cycle response to DNA damage in Saccharomyces cerevisiae. Science *241*, 317-322.

Westermann, S., Drubin, D.G., and Barnes, G. (2007). Structures and functions of yeast kinetochore complexes. Annu Rev Biochem *76*, 563-591.

Wignall, S.M., Deehan, R., Maresca, T.J., and Heald, R. (2003). The condensin complex is required for proper spindle assembly and chromosome segregation in Xenopus egg extracts. J Cell Biol *161*, 1041-1051.

Wignall, S.M., and Villeneuve, A.M. (2009). Lateral microtubule bundles promote chromosome alignment during acentrosomal oocyte meiosis. Nat Cell Biol *11*, 839-844.

Wilde, A., Lizarraga, S.B., Zhang, L., Wiese, C., Gliksman, N.R., Walczak, C.E., and Zheng, Y. (2001). Ran stimulates spindle assembly by altering microtubule dynamics and the balance of motor activities. Nat Cell Biol *3*, 221-227.

Willard, H.F. (1990). Centromeres of mammalian chromosomes. Trends Genet *6*, 410 - 416.

Williams, B.C., Murphy, T.D., Goldberg, M.L., and Karpen, G.H. (1998). Neocentromere activity of structurally acentric mini-chromosomes in Drosophila. Nature Genet *18*, 30-37.

Winey, M., Mamay, C.L., O'Toole, E.T., Mastronarde, D.N., Giddings, T.H., Jr., McDonald, K.L., and McIntosh, J.R. (1995). Three-dimensional ultrastructural analysis of the Saccharomyces cerevisiae mitotic spindle. J Cell Biol *129*, 1601-1615.

Wise, D.A., and Brinkley, B.R. (1997). Mitosis in cells with unreplicated genomes (MUGs): Spindle assembly and behavior of centromere fragments. Cell Motil Cytoskel *36*, 291-302.

Witt, P.L., Ris, H., and Borisy, G.G. (1980). Origin of kinetochore microtubules in Chinese hamster ovary cells. Chromosoma *81*, 483-505.

Wojcik, E., Basto, R., Serr, M., Scaerou, F., Karess, R., and Hays, T. (2001). Kinetochore dynein: its dynamics and role in the transport of the Rough deal checkpoint protein. Nat Cell Biol *3*, 1001-1007.

Wong, L.H., Brettingham-Moore, K.H., Chan, L., Quach, J.M., Anderson, M.A., Northrop, E.L., Hannan, R., Saffery, R., Shaw, M.L., Williams, E., *et al.* (2007). Centromere RNA is a key component for the assembly of nucleoproteins at the nucleolus and centromere. Genome Res *17*, 1146-1160.

Wood, K.W., Sakowicz, R., Goldstein, L.S.B., and Cleveland, D.W. (1997). CENP-E is a plus end-directed kinetochore motor required for metaphase chromosome alignment. Cell *91*, 357-366.

Wu, J.Q., and Pollard, T.D. (2005). Counting cytokinesis proteins globally and locally in fission yeast. Science *310*, 310-314.

Yang, C.H., Tomkiel, J., Saitoh, H., Johnson, D.H., and Earnshaw, W.C. (1996). Identification of overlapping DNA-binding and centromere-targeting domains in the human kinetochore protein CENP-C. Mol Cell Biol *16*, 3576-3586.

Yang, Z., Tulu, U.S., Wadsworth, P., and Rieder, C.L. (2007). Kinetochore dynein is required for chromosome motion and congression independent of the spindle checkpoint. Curr Biol *17*, 973-980.

Yeh, E., Haase, J., Paliulis, L.V., Joglekar, A., Bond, L., Bouck, D., Salmon, E.D., and Bloom, K.S. (2008). Pericentric chromatin is organized into an intramolecular loop in mitosis. Curr Biol *18*, 81-90.

Yen, T.J., Compton, D.A., Earnshaw, W.C., and Cleveland, D.W. (1991). CENP-E, a human centromere associated protein released from chromosomes at the onset of anaphase. EMBO J *10*, 1245-1254.

Yoda, K., Ando, S., Morishita, S., Houmura, K., Hashimoto, K., Takeyasu, K., and Okazaki, T. (2000). Human centromere protein A (CENP-A) can replace histone H3 in nucleosome reconstitution in vitro. Proc Natl Acad Sci U S A *97*, 7266-7271.

Yong-Gonzalez, V., Wang, B.D., Butylin, P., Ouspenski, I., and Strunnikov, A. (2007). Condensin function at centromere chromatin facilitates proper kinetochore tension and ensures correct mitotic segregation of sister chromatids. Genes Cells *12*, 1075-1090.

Yoshimura, S.H., Hizume, K., Murakami, A., Sutani, T., Takeyasu, K., and Yanagida, M. (2002). Condensin architecture and interaction with DNA: regulatory non-SMC subunits bind to the head of SMC heterodimer. Curr Biol *12*, 508-513.

Zatsepina, O.V., Polyakov, V.Y., and CHentsov, Y.S. (1983). Chromonema and chromomere. Structural units of mitotic chromosomes. Chromosoma (Berl) *88*, 91-97.

Zheng, Y., Wong, M.L., Alberts, B., and Mitchison, T. (1995). Nucleation of microtubule assembly by a gamma-tubulin-containing ring complex. Nature *378*, 578-583.

Zinkowski, R.P., Meyne, J., and Brinkley, B.R. (1991). The centromere-kinetochore complex: a repeat subunit model. J Cell Biol *113*, 1091-1110.

Zou, H., McGarry, T.J., Bernal, T., and Kirschner, M.W. (1999). Identification of a vertebrate sister-chromatid separation inhibitor involved in transformation and tumorigenesis [see comments]. Science *285*, 418-422.